Unravelling adaptive evolution in response to changing salinities in a tripartite species interaction

Henry Göhlich

Unravelling adaptive evolution in response to changing salinities a tripartite species interaction

Dissertation

zur Erlangung des akademischen Grades eines Doktors der Naturwissenschaften

Doctor rerum naturalium

an der
Mathematisch-Naturwissenschaftlichen Fakultät
der
Christian-Albrechts-Universität zu Kiel
durchgeführt in der
Pipefish Group
am
GEOMAR | Helmholtz-Zentrum für Ozeanforschung Kiel

vorgelegt von

Henry Göhlich

Kiel, Dezember 2020

Gutachter: Dr. Olivia Roth
Gutachter: Prof. Dr. Hinrich Schulenburg
Tag der Disputation: 18.02.2021
Zum Druck genehmigt: Ja

SUMMARY

Over a long time, marine organism have adapted to their biotic and abiotic environment. Currently, anthropogenic induced climate change is rapidly altering the environment with unpredictable consequences for marine ecosystems. To predict how organisms will cope with those changes in a future ocean, research mainly focused on exposing individual species to elevated water temperatures and ocean acidification scenarios. In the Baltic Sea, a decrease in salinity due to increased rainfall is predicted to be an additional stressor for marine life. However, the impact of low salinity levels on marine organisms has been ignored. By studying the interaction between a filamentous phage and an opportunistic bacterium (*Vibrio alginolyticus*) as well as the interaction between *V. alginolyticus* and the pipefish *Syngnathus typhle*, this thesis provides empirical data on the ecological and coevolutionary consequences of altered salinity levels on species interactions. Filamentous phages can infect and integrate in the genome of *Vibrio* bacteria. Whether filamentous phages are detrimental or beneficial for the bacterium depends not only on the costs they are causing for the bacterium, but also on the additional genes they are carrying and the environment. The genes introduced by the phage can provide the bacterium with additional properties which help the bacterium to infect marine animals. The results of chapter I, show that filamentous phages predominantly infect *Vibrio* bacteria within one clade. Infections and thus potential transfer of genes across bacterial clades occur at lower frequencies. In chapter II, I showed that reduced salinity levels made the bacteria more susceptible for phage infections, which may result in an increased transfer of genes between bacteria and facilitate the spread of virulence and antibiotic resistant genes in the future Baltic Sea. In chapter III, I used an evolution experiment to find out that *Vibrio* bacteria can quickly become resistant against filamentous phages and that resistance evolution is delayed a low salinity level. At low salinity levels, phage-infected bacteria persisted longer in the populations compared to coevolving populations at high salinity levels suggesting that phage-infected bacteria are more competitive in predicted salinity conditions. In chapter IV, I investigated how the pipefish *S. typhle* copes with reduced salinity levels and the associated shift in the microbial community. By taking advantage of the natural salinity gradient of the Baltic Sea, I investigated the role of genetic adaptation, transgenerational plasticity, developmental plasticity and their interactions in responding towards a shift in biotic and abiotic conditions. Pipefish males collected at high salinity and exposed to low salinity levels in the lab were infected by a fungus in the brood pouch, which points out that rapid salinity changes can

impair the immune system resulting in a higher susceptibility to ambient pathogens. Gene expression analysis, survival measurements of juveniles and resistance to a fungus infection suggest that pipefish collected at low salinity are locally adapted but retain the phenotypic plasticity to cope with ancestral salinity levels and associated pathogens.

This PhD thesis provides evidence that a rapid salinity reduction in the Baltic Sea has negative effects on individual organisms ranging from microbes to teleost fish. The negative impact of an altered environment can be amplified by an additional organism. On evolutionary time scales changing environmental conditions in combination with threatening biotic species can be overcome via resistance evolution and local adaptation to salinity conditions. The results suggest that conclusions drawn from single species studies fail to capture fundamental interactions between organisms which constrains our ability to predict the future of any species in a rapidly changing ocean.

ZUSAMMENFASSUNG

Über eine lange Zeit haben sich Meeresorganismen an ihre biotische und abiotische Umwelt angepasst. Gegenwärtig verändert sich die Umwelt rapide, durch den Menschen verursachten Klimawandel mit unvorhersehbaren Folgen für marine Ökosysteme. Um vorherzusagen, wie Organismen mit diesen Veränderungen in einem zukünftigen Ozean zurechtkommen werden, konzentrierte sich die Forschung bisher hauptsächlich darauf, einzelne Arten erhöhten Wassertemperaturen und Szenarien der Ozeanversauerung auszusetzen. In der Ostsee wird eine Abnahme des Salzgehalts aufgrund erhöhter Niederschläge als zusätzlicher Stressor für die Meeresbewohner vorhergesagt. Die Auswirkungen eines niedrigen Salzgehalts auf Meeresorganismen wurden jedoch bisher ignoriert. Durch die Untersuchung der Interaktion zwischen einem filamentösen Phagen und einem opportunistischen Bakterium (*Vibrio alginolyticus*) sowie der Interaktion zwischen *V. alginolyticus* und der Grasnadel *Syngnathus typhle* liefert diese Arbeit empirische Daten zu den ökologischen und evolutionären Folgen veränderter Salzgehalte auf die Interaktionen der Arten. Filamentöse Phagen können *Vibrio* Bakterien infizieren und sich in deren Genom einbauen. Ob filamentöse Phagen für das Bakterium schädlich oder vorteilhaft sind, hängt nicht nur von den Kosten ab, die sie für das Bakterium verursachen, sondern auch von den zusätzlichen Genen, die sie tragen und von der Umwelt. Die durch den Phagen eingebrachten Gene können dem Bakterium zusätzliche Eigenschaften verleihen, die dem Bakterium helfen, Meerestiere zu infizieren. Die Ergebnisse aus Kapitel I zeigen, dass filamentöse Phagen überwiegend Vib*rio* Bakterien innerhalb einer Gruppe infizieren. Infektionen und damit ein möglicher Gentransfer über Bakterienstämme hinweg treten mit geringerer Häufigkeit auf. In Kapitel II habe ich gezeigt, dass ein reduzierter Salzgehalt die Bakterien anfälliger für Phageninfektionen macht, was zu einem verstärkten Gentransfer zwischen den Bakterien führen und die Ausbreitung von Virulenzgenen in der zukünftigen Ostsee erleichtern könnte. In Kapitel III habe ich ein Evolutionsexperiment durchgeführt und herausgefunden, dass *Vibrio* Bakterien schnell gegen filamentöse Phagen resistent werden können und dass die Resistenzevolution bei einem niedrigen Salzgehalt verzögert wird. Bei niedrigem Salzgehalt bleiben phagen-infizierte Bakterien länger in den Populationen im Vergleich zu ko-evolvierenden Populationen bei hohem Salzgehalt. Das deutet darauf hin, dass phageninfizierte Bakterien in vorhergesagten Salzgehaltsbedingungen konkurrenzfähiger sind. In Kapitel IV untersuchte ich, wie die

Grasnadel *S. typhle* mit reduziertem Salzgehalt und der damit verbundenen Veränderung der mikrobiellen Gemeinschaft zurechtkommt. Unter Ausnutzung des natürlichen Salzgehaltsgradienten der Ostsee untersuchte ich die Rolle der genetischen Anpassung, der transgenerationalen Plastizität, der Entwicklungsplastizität und ihrer Wechselwirkungen bei der Reaktion auf eine Veränderung der biotischen und abiotischen Bedingungen. Die der Grasnadel, die bei hohem Salzgehalt gesammelt und im Labor niedrigen Salzgehalten ausgesetzt wurden, wurden im Brutbeutel mit einem Pilz infiziert. Das weist darauf hin, dass schnelle Salzgehaltsänderungen das Immunsystem beeinträchtigen können, was zu einer höheren Anfälligkeit für Krankheitserreger aus der Umgebung führt. Genexpressionsanalysen, Überlebensmessungen der Jungfische und die Resistenz gegen eine Pilzinfektion deuten darauf hin, dass Grasnadeln, die bei niedrigem Salzgehalt gesammelt werden, lokal angepasst sind, aber die phänotypische Plastizität behalten, um mit dem angestammten Salzgehalt und den dort vorhandenen Krankheitserregern zurechtzukommen.

Diese Doktorarbeit liefert Belege, dass eine rasche Verringerung des Salzgehalts in der Ostsee negative Auswirkungen auf einzelne Organismen hat, von Mikroben bis hin zu echten Knochenfischen. Die negativen Auswirkungen einer veränderten Umwelt können durch einen zusätzlichen Organismus verstärkt werden. Auf evolutionären Zeitskalen können veränderte Umweltbedingungen in Kombination mit bedrohlichen Arten durch Resistenzevolution und lokale Anpassung an die Salzgehaltsbedingungen überwunden werden. Die Ergebnisse deuten darauf hin, dass Schlussfolgerungen, die aus Studien mit einzelnen Arten gezogen werden, grundlegenden Interaktionen zwischen Organismen nicht erfassen. Das begrenzt unsere Fähigkeit, die Zukunft der einzelnen Art in einem sich schnell verändernden Ozean vorherzusagen.

TABLE OF CONTENT

1 | INTRODUCTION

1.1 | The infinite game of coevolution

Since the emergence of the first living creatures in form of simple unicellular organisms on our planet about 3.7 billion years ago (Ohtomo, Kakegawa et al. 2014, Nutman, Bennett et al. 2016), species are constantly interacting with each other (Hutchinson 1959). These interactions strongly shape the ecology and evolution of each of the interacting species and are an important driver of biodiversity in all branches of the tree of life (Laine 2009, Thompson 2009, Ratzke, Barrere et al. 2020). Species interactions range from beneficial for both players (mutualistic species interactions) over detrimental for one organism and beneficial for the other (antagonistic, e.g. host-parasite and prey-predator systems) or detrimental for both (competition) (Vermeij 1994, Thompson 1999). Each of these relationships has different ecological and evolutionary consequences.

In host-parasite interactions, predator-prey systems or species competing for the same resources, reciprocal selection can lead to coevolution, when adaptation of one species changes the selection acting on the other and vice versa (Janzen 1980,

Glossary

Mutualism: Cooperation between two species, where the benefits outweigh the costs of the interaction for each of organism.

Parasitism: Interaction between species, where one organism exploits the other.

Symbiont: An organism, which closely interacts with another species, regardless of costs and benefits, is considered as symbiont.

Pathogen: Organism causing a disease in another organism.

Opportunistic pathogen: Infections organism that usually does not harm the host (commersal). When the host's resistance is low and/or the environmental conditions favor the microorganism, it can cause harm to the host.

Holobiont: Ecological unit, which is comprised of a host organism (e.g. animal) and the associated microbiom, including bacteria and viruses.

Virulence: Detrimental effects of a pathogen on the host, which are related to reduced fitness.

Bacteriophage (phage): Virus that infects bacteria

Temperate phage: Phage that is able to integrate in the genome of a bacterium and is transmitted horizontally.

Red Queen dynamics: Species constantly need to evolve to retain fitness in the presence of a co-evolving, antagonistic species.

Red King dynamics: Slow evolving species gain a larger share of benefits in a species interaction

PSU: Practical salinity unit; dimensionless unit for the conductivity of water. One PSU is roughly equivalent to 1 g of NaCl per liter water.

Nuismer, Gomulkiewicz et al. 2010). Reciprocal selection can drive distinct evolutionary dynamics in both interacting species (Woolhouse, Webster et al. 2002). Those coevolutionary dynamics are somewhere on the continuum between two extreme forms, referred to as arms race and fluctuating selection dynamics (Agrawal and Lively 2002, Woolhouse, Webster et al. 2002, Gandon, Buckling et al. 2008, Engelstadter 2015). Both types of coevolution have contrasting effects on biodiversity.

In arms race dynamics, an existing genotype is continuously replaced by a novel one, leading to increased fitness in the presence of the contemporary counterplayer and an increase in allele frequency (recurrent selective sweep of alleles). For example, in a host-parasite system, a de novo mutation or an existing allele results in a more efficient defense mechanism of the host against a specific parasite (Buckling and Rainey 2002, Retel, Kowallik et al. 2019). The increased fitness of host individuals carrying this allele leads to a rise in allele frequency until counter-adaptation allows the parasite to overcome, tolerate or escape the evolved host defense system (Buckling and Rainey 2002). The strong evolutionary influence of arms race dynamics is visible in the heritable signatures of contemporary genomes (Ebert and Fields 2020). In nature, we find plenty of examples for arms race dynamics, e.g. skinks (Scinicidae) and newts (Pleurodelinae) increase their level of toxins against predatory snakes (Serpentes), which counter adapt by enhanced toxin tolerance (Feldman, Durso et al. 2016, Hague, Toledo et al. 2018, Hague, Stokes et al. 2020), diatoms evolved protective architecture, material properties and secondary metabolites against specializing zooplanktonic predators (Hamm, Merkel et al. 2003, Lauritano, Carotenuto et al. 2012, Assmy, Smetacek et al. 2013), and the evolution of the human immune system counteracts novel surface proteins displayed by the malaria causing parasite *Plasmodium* (Jeffares, Pain et al. 2007, Sundararaman, Plenderleith et al. 2016). Humans are also fighting medical arms races against antibiotic resistance evolving bacteria, when developing new antibiotics and antibiotic treatments (Smith and Romesberg 2007, Hede 2014, Kim, Lieberman et al. 2014, Roemhild, Barbosa et al. 2015), or against an ever evolving influenza virus by developing variants of vaccines (Xue, Moncla et al. 2018, Francis, King et al. 2019, Xue and Bloom 2020).

Arguably, the oldest arms race on the planet is the billion-year-old and ongoing coevolution between viruses and all other cellular life forms (Forterre and Prangishvili 2009, Koonin and Dolja 2013). The high mutation rates in bacteriophage genomes, high abundances of phage particles in any given environment, extreme rapid turnover of phage

particles and bacteria (Fuhrman 1999), and strong selection on the bacterial host all positively influence the rate at which coevolution unfolds. (Middelboe, Hagström et al. 2001, Buckling and Rainey 2002, Retel, Markle et al. 2019). This makes the arms race between phages and bacteria especially conspicuous, and resulted in an impressive number of bacterial defense mechanisms and counter adaptations of phages to circumvent these defense mechanisms (Labrie, Samson et al. 2010, Stern and Sorek 2011, Dy, Richter et al. 2014, Hampton, Watson et al. 2020). In contrast to the characteristic cycle of adaptation and counteradaptation in arms race dynamics, fluctuating selection dynamics are characterized by oscillations in genotype frequencies (Levin 1988).

In fluctuating selection regimes, the direction and intensity of natural selection depends on the relative frequency of genotypes (Levin 1988). Stabilizing or negative frequency-dependent selection occurs, when a low frequency of a genotype results in increased fitness. For example, a phage evolves increased infectivity to a common bacteria genotype. This gives a fitness advantage to rare resistant bacterial genotypes, which consequently can rise in frequency (Gandon, Buckling et al. 2008). In this way, negative frequency dependent selection results in the maintenance of several genotypes in both interacting species (Betts, Kaltz et al. 2014). Negative frequency dependent host-parasite interactions were observed in study systems across the tree of life, including natural populations of the perennial herb *Linum marginale* and its fungal pathogen *Melampsora lini* (Thrall, Laine et al. 2012), the water flea *Daphnia magna* and its bacterial endoparasite *Pasteuria ramosa* (Decaestecker, Gaba et al. 2007), as well as various bacteria and lytic phages (Hall, Scanlan et al. 2011, Pascua, Hall et al. 2014).

In antagonistic species interactions, an adaptation against a counterplayer results in decreased fitness of the counterplayer. This is in contrast to mutualist species interactions, where both species benefit from each other's presence, and adaptation of one would also may increase the fitness of the other. "*Mutualism are best viewed as reciprocally exploitative interactions that provide net benefits for both partners*" (Bronstein 2001). Interacting species exchange goods or services and thereby provide the partners with additional traits. Cooperation allows new levels of organization, enables specialization, and the colonization of new ecological niches resulting in increased biological diversity (Jones, Lawton et al. 1996). In contrast to antagonistic relationships, where fast evolution and the Red Queen dynamics are predominant and result in higher fitness, slow evolving organisms (Red King

dynamics) are suggested to gain a disproportionate share of benefits in mutualistic relationships (Bergstrom and Lachmann 2003, Gao, Li et al. 2015)

From the game theoretic perspective, organisms in a mutualistic relationship are in an "Iterated Prisoner's Dilemma", i.e. in every encounter both players can either choose to cooperate or defect to increase their own fitness (Axelrod and Hamilton 1981, Killingback and Doebeli 2002, Antonovics, Bergmann et al. 2015). How to overcome the "Prisoner's Dilemma" has been investigated by scientist from various fields, including biologists, sociologist and economists (Herre, Knowlton et al. 1999, Raihani and Bshary 2011, West, El Mouden et al. 2011, Lewis and Dumbrell 2013, Antonovics, Bergmann et al. 2015, Bravetti and Padilla 2018) and led to several concepts trying to explain aspects in the evolution and maintenance of mutualistic relationships (Doebeli and Knowlton 1998, Nowak 2006, Gao, Li et al. 2015, Shibasaki 2019). For example, reciprocity selection theory suggests that cooperation evolves when the partners choose a strategy that increases the fitness of both interacting species (Trivers 1971, Bronstein 2001). Kin selection theory proposes that parasites and symbionts benefit from reducing their virulence or costs when they are predominantly transmitted vertically, due to sharing genes with the associated host organism (Bull, Molineux et al. 1991, Frank 1992, Yamamura 1993, Frank 1994, Ryan 2007, Buckling and Brockhurst 2008) and the sanction theory comprises that hosts punish exploiters or cheaters to maintain a functioning mutualistic relationship (Boyd and Richerson 1992, Kiers and van der Heijden 2006, Wong, Buston et al. 2007, Jensen 2010, Garcia and Traulsen 2019). Despite the comprehensive theoretical and empirical work making predictions or hypotheses about the link between focal species' behavior/strategies and the resulting coevolutionary dynamics, there is no general concept explaining the evolution of mutualism.

Several theoretical and empirical studies show that mutualism can evolve from parasitic relationships, including interactions with plants and viruses (Hamelin, Hilker et al. 2017), bacteria and phages (Bull, Molineux et al. 1991, Shapiro, Williams et al. 2016, Shapiro and Turner 2018), termites and flagellated gut protists (Nalepa 2020), various arthropods and endosymbiotic bacteria of the genus *Wolbachia* (Fenn and Blaxter 2006, Weeks, Turelli et al. 2007, Bordenstein, Paraskevopoulos et al. 2009, Zug and Hammerstein 2015), as well as proteobacteria and eukaryotic hosts (Sachs, Skophammer et al. 2014), e.g. the plant pathogen *Ralstonia solanacearum* and legume plants (Marchetti, Capela et al. 2010, Capela, Marchetti et al. 2017). Breakdowns of mutualisms (Sachs and Simms 2006) and even the

transition in the opposite direction, from mutualism to parasitism, are also possible (Redman, Dunigan et al. 2001, Brown, Creed et al. 2012, Murata, Nakano et al. 2019), suggesting that species interactions along the parasitism-mutualism-continuum are dynamic and modulated by the biotic and abiotic environment (Chamberlain, Bronstein et al. 2014, Harcombe, Betts et al. 2016) as well as the genome and transcriptome of the interacting species (Herrera, Schuster et al. 2020).

1.2 | Opportunistic pathogens play a different game

In the last decades, we gained and conceptualized a lot of knowledge about evolutionary dynamics of obligate parasites (Wolinska and King 2009, Papkou, Gokhale et al. 2016, Ebert and Fields 2020) and requirements for mutualistic interactions (Doebeli and Knowlton 1998, Bronstein 2009, Leigh 2010, Leeksl, dos Santos et al. 2019, Wein, Romero Picazo et al. 2019, Chomicki, Kiers et al. 2020). In recent years, the holobiont concept has revolutionized animal biology with implications for the evolution, ecology and physiology of both animal hosts and their associated microorganisms (McFall-Ngai, Hadfield et al. 2013). However, these concepts may not be directly applicable for opportunistic parasites, which spend most of their lifecycle outside the host. Both environments, outside and inside the host, select for distinct traits and alter the evolution of virulence in opportunistic pathogens (Friman, Hiltunen et al. 2011, Brown, Cornforth et al. 2012). The divergent selective environments can have a significant effect on the evolution of virulence in opportunistic pathogens (Friman, Hiltunen et al. 2011, Brown, Cornforth et al. 2012). Outside the host, opportunistic pathogens are under selection by the abiotic environment, predators, parasites and competitors for resources (Brown, Cornforth et al. 2012). Inside the host, they are under selection by the host's immune system (Cobey 2014) and by interactions with the present microbiota (Vonaesch, Anderson et al. 2018). The selections results in the evolution of bacterial virulence factors, such as adhesins or flagella to attach to the host tissue or enzymes causing damage to host cells (Kao, Lin et al. 2014, Kao, Sheu et al. 2016, Gao, Howden et al. 2018). Virulence factors are often encoded on pathogenic islands, which can be transferred horizontally by microorganisms via conjugative transposons (Waskito, Yih-Wu et al. 2018). This exchange of genetic material between phylogenetically distant opportunistic pathogens allows them to quickly acquire mechanisms to cope with the host

immune system (Hacker and Kaper 2000, Dobrindt, Hochhut et al. 2004, Brzuszkiewicz, Bruggemann et al. 2006). Consequently, the immune system of host organisms quickly needs to react and adapt to opportunistic pathogens (Cooper and Alder 2006, Flajnik and Kasahara 2010, Roth, Keller et al. 2012, Roth, Beemelmanns et al. 2018).

1.3 | Filamentous phages are game changers

The outcome of infections may not only be mediated by the two interacting species but also by additional interactions with other organisms. For example, bacteriophages can influence bacterial virulence in two ways. On the one hand, lethal infections by phages result in the selection of phage resistant bacterial strains (Middelboe, Hagström et al. 2001, Buckling and Rainey 2002). Bacterial resistance against phages can come at the cost of reduced bacterial virulence, as shown for *Serratia* (Flyg, Kenne et al. 1980), *Bacillus* (Heierson, Sidén et al. 1986), *Salmonella* (Santander and Robeson 2007), and *Vibrio* (Wendling, Piecyk et al. 2017) due to reduced growth or motility (Leon and Bastias 2015). Growth and motility are both shaping virulence towards the host in an infection; bacterial motility helps to colonize suitable niches within the host (Josenhans and Suerbaum 2002, Kao, Lin et al. 2014), and fast growth allows to quickly proliferate inside the host (Frank 1996). On the other hand, temperate phages may integrate as prophages into the bacterial genome and provide beneficial genes for opportunistic pathogens (Brussow, Canchaya et al. 2004, Ilyina 2015). In fact, many common human diseases induced by bacteria, e.g. Cholera, Diphtheria, Scarlet fewer or cystic fibrosis are indirectly triggered or favored by a temperate phage (Waldor and Mekalanos 1996, Tinsley, Bille et al. 2006, Ilyina 2015). Two well-studied examples of temperate phages are the filamentous phages (Box 2) CTXΦ and VGJΦ mediating the virulence in the bacterium *Vibrio cholera* (Waldor and Mekalanos 1996, Faruque and Mekalanos 2012). Every year *Vibrio cholera* causes 1.3 to 4.0 million diarrheal infections worldwide and the death of 21.000 to 143.000 humans (Ali, Nelson et al. 2015). In recent years, we gained a lot of epidemiological data about the Cholera disease (Ali, Nelson et al. 2015) and other *Vibrio* related diseases (Box 2) in aquatic organisms (Baker-Austin, Oliver et al. 2018), as well as detailed insights in the genomic architecture and molecular mechanisms of *Vibrio* and their associated filamentous phages (Faruque and Mekalanos 2012, Das 2014, Chibani, Hertel et al. 2019, Chibani, Roth et al. 2020). However, we lack empirical studies unravelling co-evolutionary dynamics between *Vibrio* and

filamentous phages. This limits our understanding in the spread of virulence genes and how this dynamic is affected in light of ongoing climate change.

Box 2: Study organisms

Broad-nosed pipefish, the work horse of the pipefish group

The broad-nosed pipefish *Syngnathus typhle* is native to seagrass meadows in the north-eastern Atlantic Ocean ranging from Norway to southern Portugal and is present also in the Baltic and the Mediterranean Sea (Gurkan and Taskavak 2007, Rispoli and Wilson 2008, Wilson and Veraguth 2010, Roth, Keller et al. 2012). *S. typhle* is part of an exclusive group of species exhibiting male pregnancy, which evolved only once in the animal kingdom in the order of the Syngnathiformes (Stolting and Wilson 2007, Whittington and Friesen 2020). The evolution of male pregnancy may have been facilitated by modifications of the adaptive immune system, in particular by the loss of genes in the major histocompatibility complex pathway II (Roth, Solbakken et al. 2020). Despite the lack of one arm of the immune system, the pipefish successfully copes with the vast and diverse array of microbes in our oceans and is home to a diverse community of bacteria of the genus *Vibrio spp*. While most of them are harmless to pipefish, some strains, e.g. in the clades of *V. alginolyticus*, *V. splendidus* and *V. harveyi,* are responsible for major disease outbreaks in members of the Syngnathiformes (Balcázar, Lee et al. 2010, Xie, Bu et al. 2020).

Vibrio bacteria

Vibrio bacteria are ubiquitous in the marine environment (Baker-Austin, Oliver et al. 2018). *Vibrio spp*. occur at a continuum from opportunistic pathogens (Baker-Austin, Oliver et al. 2018) to symbiotic partners (Heath-Heckman, Peyer et al. 2013) and free-living populations (Oberbeckmann, Wichels et al. 2011). Pathogenic *Vibrio* are multi host parasites that can infect various host species from several key groups, including bivalves (Wendling, Fabritzek et al. 2017), crustaceans (Sullivan and Neigel 2018), corals (Bourne, Iida et al. 2008, Kimes, Grim et al. 2012, Weynberg, Voolstra et al. 2015), fish (Ina-Salwany, Al-saari et al. 2019) and humans (Ali, Nelson et al. 2015). Empirical evidence suggests that multi-host pathogens have an impaired ability to specialize on local host species. Indeed, Pacific oyster and pipefish have been shown to be locally adapted to *Vibrio* populations (Roth, Keller et al. 2012, Wendling, Fabritzek et al. 2017). The pathogenicity of *Vibrio* is complex, modulated by environmental parameters (Wendling, Batista et al. 2014, Baker-Austin, Trinanes et al. 2017), and affected by the presence of vibriophages (Tan, Gram et al. 2014), especially filamentous phages providing beneficial genes (Davis and Waldor 2003, Faruque and Mekalanos 2012).

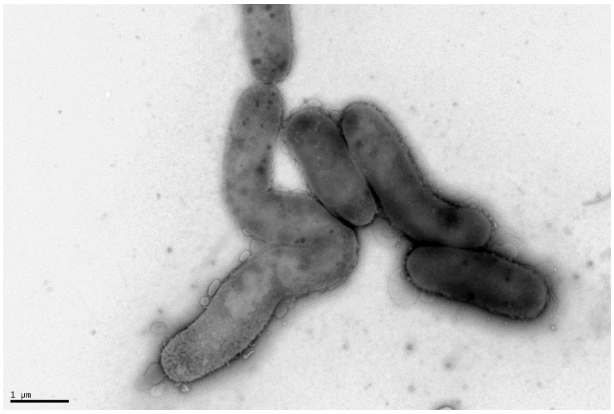

Filamentous phages

Filamentous phages have successfully invaded most microbial communities in ecosystems around the world (Roux, Krupovic et al. 2019). Their success story is based on the low costs associated with chronic infections, i.e. phages are released through the cell wall without killing the bacterial cell (Russel 1995, Rakonjac, Feng et al. 1999), and on their potential to transfer beneficial genes to their bacterial host (Ilyina 2015, Hay and Lithgow 2019). Filamentous phages are especially present in the genomes of *Vibrio spp*. strains from clinical and marine isolates (Chakraborty, Mukhopadhyay et al. 2000, Wendling, Piecyk et al. 2017, Castillo, Kauffman et al. 2018, Chibani, Hertel et al. 2019), where they provide virulence genes enabling pathogenic strains to successfully invade eukaryotic hosts (Faruque and Mekalanos 2012, Ilyina 2015).

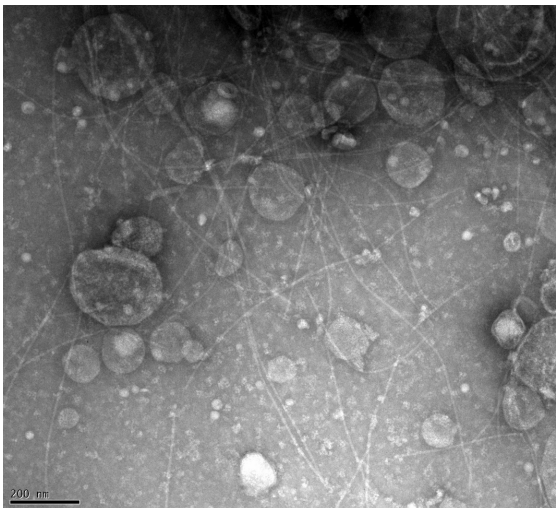

1.4 | How the environment changes the game of coevolution

Outbreaks of opportunistic diseases are often linked to environmental factors, such as rising temperatures. On the one hand, microorganisms proliferate faster at elevated temperatures and increase the expression of virulence, both can result in higher virulence, as shown for example in *Shigella* species (Maurelli and Sansonetti 1988), *Legionella* bacteria (Mauchline, James et al. 1994) and bacteria of the genus *Vibrio* (Kimes, Grim et al. 2012, Lages, Balado et al. 2019). On the other hand, high temperatures result in trade-offs inhibiting the activation of the host immune system leaving eukaryotic host more vulnerable to diseases (Landis, Kalbe et al. 2012).

A concept describing the interactions between the environment, host and pathogen is the environment–host–pathogen triangle or disease triangle (Stevens 1960). It suggests that the outbreak of a disease depends on all three components, the genotype of the host (G) and of the pathogen (G) as well as the environment (E) (gene x gene x environment, GxGxE). This concept has been applied and adjusted for many host-pathogen interactions (Scholthof 2007, Bruno 2015, James, Toledo et al. 2015, Chappelka and Grulke 2016, Aung, Jiang et al. 2018, Bart 2019) demonstrating that the environment affects host resistance, costs of resistance, pathogen infectivity, pathogen latency, transmission and virulence (Mitchell et al. 2005; Fels and Kaltz 2006; Laine 2007; Vale et al. 2008). For example, infections with allopatric *Vibrio* bacteria result in higher oyster larvae mortality compared to infections with sympatric *Vibrio* strains (GxG). Additionally, larvae mortality following *Vibrio* infection is higher at lower temperature, suggesting a GxGxE interaction (Wendling, Fabritzek et al. 2017). The effect of the environment was also shown for resistance evolution in the plant pathogenic bacterium *Pseudomonas syringae*, which quickly evolved resistance against lytic phages in high nutrient liquid culture (*in vitro*) but not on a tomato leaf (*in vivo*) (Hernandez and Koskella 2019).

In the same way antagonistic interactions are shaped by the environment, the costs and benefits in a mutualistic relationship can be shifted. For example, prolonged rises in seawater temperature result in the loss of endosymbiotic zooxanthellae in corals, leading to the disruption of this mutualistic species interaction, known as coral bleaching (Hoegh-Guldberg 1999). In contrast, additional genes introduced by temperate phages into bacterial genomes may only be beneficial in a specific environmental setting, e.g. virulence genes during infection of eukaryotic hosts (Waldor and Mekalanos 1996, Davies, Winstanley et al. 2016) or antibiotic resistance genes in the presence of antibiotics (Wendling, Refardt et

al. 2020). For opportunistic pathogens such as *Vibrio spp*., environmental changes may be especially relevant because alterations in the environment can affect the costs and benefits of a filamentous phage in the bacterial genome. This may turn filamentous phages from mutualists (cost < benefits) into parasites (costs > benefits) or vice versa. Hence, the environment may select for *Vibrio* strains with or without phages carrying pathogenic islands. This ultimately affects the fitness of *Vibrio* and the virulence for their eukaryotic hosts, such as the pipefish *Syngnathus typhle* (Box 2).

1.5 | Salinity changes in the future ocean and their effect on marine organisms

Currently, human activities and anthropogenic climate change rapidly alter the environment for organisms in every ecosystem of our planet, including our oceans (Solomon, Plattner et al. 2009). Whereas most climate change studies focused on the effect of rising sea surface temperatures and ocean acidification (i.e. shifts in the ocean carbonate chemistry)(Anthony, Kline et al. 2008, Atkinson and Cuet 2008, Kurihara 2008, Hofmann, Barry et al. 2010, Crozier and Hutchings 2014, Cole, Parker et al. 2016, Cattano, Claudet et al. 2018), the effect of salinity changes on marine species and their interactions has only recently gained increased attention (Kukkaro and Bamford 2009, Birrer, Reusch et al. 2012, Dayma, Raval et al. 2015, Poirier, Listmann et al. 2017). This constitutes a serious gap because climate change models predict a shift in surface salinity around the globe. A decrease in salinity is predicted in polar regions due to the meltdown of polar icecaps and in coastal regions due to increased precipitation (Gibson & Najjar 2000; Loder et al 2015). In

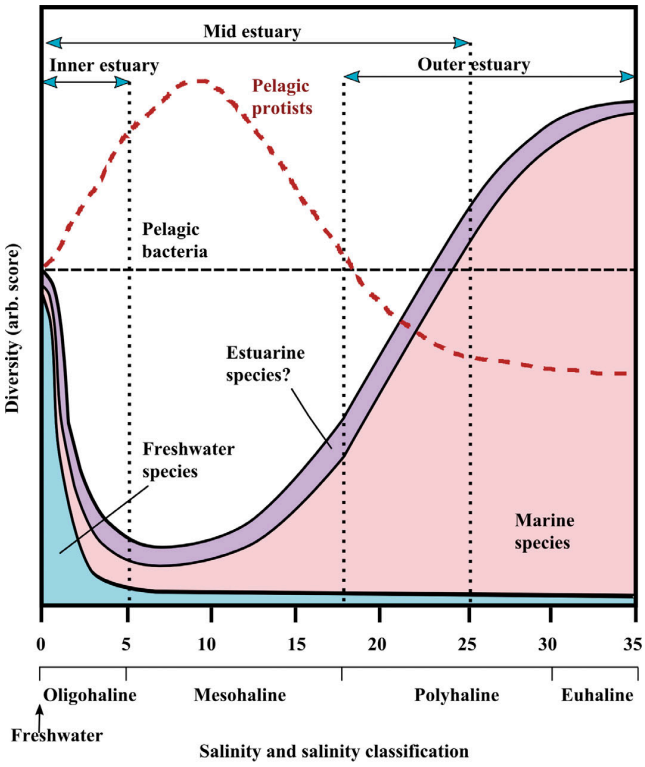

Figure 1: Diversity variation patterns along a salinity gradient. This graph summarizes the findings and concepts of several studies investigating the effect of salinity on the biodiversity of macrobenthic organisms, pelagic bacteria and pelagic protists (Vidal-Dura, Burke et al. 2018).

tropical regions, global warming is predicted to increase evaporation resulting in increased salinity levels (Boyer 2005, Friedman et al 2017).

Salinity is an important environmental component for any aquatic organism due to the high cost of osmoregulation (Holliday and Blaxter 1960, Muthiga and Szmant 1987, Morgan and Iwama 1991, Rivera-Ingraham, Nommick et al. 2016, Rivera-Ingraham and Lignot 2017). The cell membranes of microorganism and most metazoans are readily permeable for water and provide a more stringent barrier for most organic solutes and inorganic ions. Consequently, a change in salinity in the ambient water of organisms results in water flowing in or out of the cell, which ultimately affects cell size, pressure and intracellular solute concentration. Maintaining intracellular homeostasis is essential for enzyme functioning and transport mechanisms via the cell membrane. These ion regulation mechanisms can account for up to 30% of the total energy budget of a cell (Rolfe and Brown 1997). Therefore, it is not surprising that salinity affects genetic and phenotypic diversity and the distribution of many taxonomic and functional groups (Figure 1; Cognetti and Maltagliati 2000, Johannesson and Andre 2006, Vidal-Dura, Burke et al. 2018), including benthic and pelagic bacteria (Herlemann, Labrenz et al. 2011, Oberbeckmann, Wichels et al. 2011, Herlemann, Woelk et al. 2014, Pavloudi, Kristoffersen et al. 2017, Vidal-Dura, Burke et al. 2018) and their associated viral communities (Allen, McCrow et al. 2017), phytoplankton (Wasmund, Zalewski et al. 1999), zooplankton (Helenius, Leskinen et al. 2017), planktonic protists (Skarlato and Telesh 2017), benthic macro- (Whitfield, Elliott et al. 2012) and meiofauna (Broman, Raymond et al. 2019), as well as fish (Albaret, Simier et al. 2004, Barletta, Barletta-Bergan et al. 2005, Frelat, Orio et al. 2018).

Previous studies have shown that organisms are able to locally adapted to present salinity conditions, including fish (DeFaveri and Merila 2014, Hasan, DeFaveri et al. 2017, Leder, Andr et al. 2020). Adaptation to salinity may be facilitated via changes in nucleotide sequence (Leder, Andr et al. 2020) as well as by epigenetic marks such as DNA methylation patterns (Heckwolf, Meyer et al. 2020) which can be induced by the environment and transferred to the offspring (transgenerational plasticity). Acclimation to salinity variations are possible by phenotypic responses but are restricted due to energetic trade-offs (DeWitt, Sih et al. 1998). Whereas the individual process are well studied the interaction of genetic adaptation, transgenerational plasticity and phenotypic plasticity is far less understood (Kelly 2019). For example, the question whether genetically adapted organisms retain a sufficient phenotypic plasticity to cope with further changing environmental conditions.

In summary, salinity clearly affects the physiology, morphology and life-history traits of most aquatic organisms. Therefore, changing salinity conditions will most likely affect species interactions on ecological and evolutionary time scales as well as the composition of food webs and ecosystems (Johannesson, Le Moan et al. 2020).

1.6 | The Baltic Sea as a time machine for coastal environmental change

The Baltic Sea is a semi-enclosed water body characterized by a relatively stable salinity gradient making it ideal to address ecological and evolutionary questions (Johannesson, Le Moan et al. 2020). Due to its semi-enclosed, shallow morphology there is little water exchange with the open ocean. Hence, the salinity gradient ranges from about 30 PSU near the entrance in Northern Denmark to almost freshwater conditions in the innermost areas around Finland (Omstedt and Nohr 2004). Surrounded by nine industrialised countries, the Baltic Sea is undergoing levels of warming, acidification, deoxygenation and eutrophication that most coastal regions will only face in the future, making it an ideal study system to assess the impact of humans on ecosystems (Reusch, Dierking et al. 2018). Current climate models predict that salinity levels may drop by 3 to 5 PSU in the central and marginal parts of the Baltic Sea by the end of the century, which corresponds to a decrease of up to 50% (Firgue 2; Meier, Kjellstrom et al. 2006, Meier, Andersson et al. 2012, Andersson, Meier et al. 2015, Schimanke and Meier 2016). The salinity decrease is suggested to result from increased precipitation and river discharge in the northern parts of the Baltic Sea. Considering this fast environmental change, the reduced genetic diversity due to isolation (Johannesson and Andre 2006, Johannesson, Le Moan et

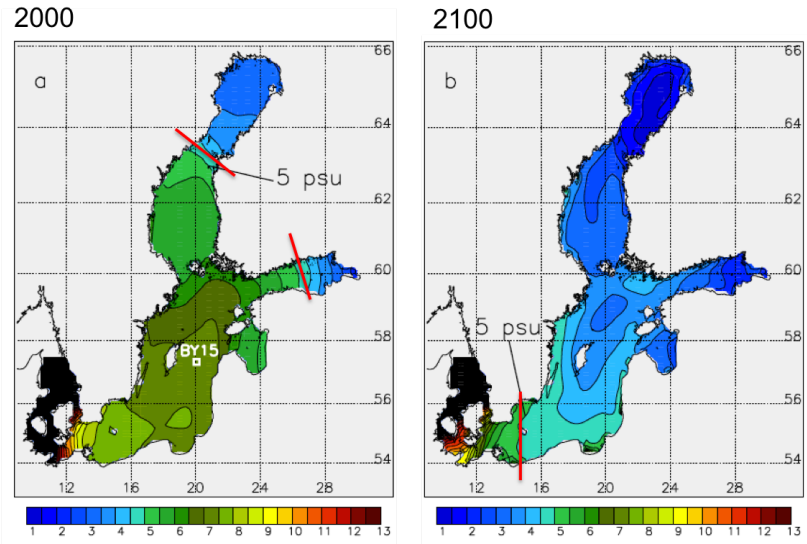

Figure 2: Predicted decrease of surface salinity in the Baltic Sea (adapted from Meier, Kjellstrom et al. 2006). Current surface salinity levels (left map) are predicted to decrease due to increased precipitation and river discharge in the northern parts of the Baltic Sea. Colours represent the salinity on a scale from 0 to 13 PSU.

al. 2020) and the strong impact of salinity on an organisms' metabolism and species distributions, the Baltic Sea is an ideal study system to investigate the salinity changes on species interactions.

1.7 | The aim of this dissertation and thesis outline

In the last decades, we gained deep understanding of the dynamics, drivers and mechanisms of coevolutionary adaptation in model organisms (Northfield and Ives 2013, Ebert and Fields 2020), as well as of the responses of organisms to climate change (Reusch 2014, Calosi, De Wit et al. 2016). The aim of this thesis was to provide insights into two topics where our understanding is still limited: (I) coevolutionary adaptation of non-model organisms in a tripartite study system and (II) the integration of salinity as a neglected environmental factor in a changing future ocean.

In my PhD, I used phage-bacteria infection assays, experimental evolution, whole genome sequencing, mathematical modelling and a controlled infection experiment accompanied with target gene expression, immune and mortality measurements to study the effect of predicted salinity changes in a tripartite system comprised of filamentous phages, the opportunistic pathogen *Vibrio* bacteria and the pipefish *Syngnathus typhle*. The thesis comprises four Chapters:

Chapter I

The structure of temperate phage - bacteria infection networks changes with the phylogenetic distance of the host bacteria

Wendling CC, Goehlich H, Roth O (2018). *Biology Letters* 14: 20180320.

In the first chapter, we used *Vibrio strains* from different clades and their derived temperate phages to investigate the potential of these phages to transfer genetic material across the phylogenetic tree of *Vibrio*. Therefore, we measured the pairwise infectivity of phages and bacteria to create two phage-bacteria infection networks, with either highly or lowly related strains and estimated the relative probability of phage infections within and across clades. We expected that lytic phage infections predominately occur within clades and at lower frequency across clades.

Chapter II

Filamentous phages reduce bacterial growth in low salinity

Goehlich H, Roth O, Wendling CC (2018). *Royal Society Open Science* 6:191669.

In the second chapter, we used 32 *Vibrio alginolyticus* strains and their derived filamentous phages to investigate how the predicted decrease of salinity in the Baltic Sea affects the relative cost of filamentous phage infections imposed on their bacterial hosts. Therefore, we created three networks of pairwise phage-bacteria infection with experimental salinity levels of 15, 10 and 7 PSU to assess phage infectivity and the cost of phage infections on bacterial growth at reduced salinity levels.

Chapter III

Low salinity slows down resistance evolution of Vibrio alginolyticus

Goehlich H, Roth O, Sieber M, Trübenbach K, Chibani, CM, Liesegang H, Rajkov J, Wendling CC. *Draft manuscript*

In the third chapter, we used an evolution experiment with one *Vibrio alginolyticus* strain and a filamentous phage to study how reduced and fluctuating salinity levels affect population dynamics in a coevolving phage bacteria population. Furthermore, we investigated the effect of salinity on bacterial resistance evolution and the prevalence of phage infected clones in microbial populations. Whole genome sequencing allowed us to identify the mutation responsible for resistance evolution and the presence of the phages integrated in the bacterial genome. A mathematical model provided additionally information about the drivers of observed populations dynamics and the differences in the speed of resistance evolution at different salinity regimes.

Chapter IV

Pipefish locally adapted to low salinity in the Baltic Sea retain phenotypic plasticity to cope with ancestral salinity levels

Goehlich H, Sartorris L, Wagner KS, Wendling CC, Roth O (2021) *Frontiers in Ecology & Evolution*

In the fourth chapter, we took advantage of the natural salinity gradient of the Baltic Sea to investigate the ability of *Syngnathus typhle* to adapt to low salinity conditions. Therefore, we collected pipefish at three sampling sites categorized as high salinity (14 - 17 PSU) and three sample sites categorized as low salinity (7 - 11 PSU) and placed them in a common garden setting in the laboratory. Exposing the offspring generation to the salinity level of their parents and to the contrasting salinity level allowed us to study the contribution of genetic adaptation, transgenerational plasticity, developmental plasticity and their interactions on the ability of pipefish to cope with changing salinity levels. Furthermore, we injected pipefish offspring with a *Vibrio alginolyticus* strain evolved at 15 and 7 PSU to test the effect of salinity on the virulence of this local opportunistic pathogen and on the fish's immune system.

2 | CHAPTER I

The structure of temperate phage-bacteria infection networks change with the phylogenetic distance of the host bacteria

Carolin C. Wendling[1,2], Henry Goehlich[1], Olivia Roth[1],

Published in *Royal Society Biology Letters.* 2018; 14; DOI: 10.1098/rsbl.2018.0320

[1] Parental Investment and Immune Dynamics, Marine Evolutionary Ecology, GEOMAR Helmholtz Centre for Ocean Research, Kiel, Germany
[2] current address: Institute of Integrative Biology, ETH Zürich, Zürich, Switzerland

Keywords

Vibrio, temperate phages, infection networks

2.1 | Abstract

With their ability to integrate into the bacterial chromosome and thereby transfer virulence or drug-resistance genes across bacterial species, temperate phages play a key role in bacterial evolution. Thus, it is paramount to understand who infects whom to be able to predict the movement of DNA across the prokaryotic world and ultimately the emergence of novel (drug-resistant) pathogens.

We empirically investigated lytic infection patterns among *Vibrio* spp. from distinct phylogenetic clades and their derived temperate phages. We found that across distantly related clades, infections occur preferentially within modules of the same clade. However, when the genetic distance of the host bacteria decreases, these clade-specific infections disappear. This indicates that the structure of temperate phage-bacteria infection networks changes with the phylogenetic distance of the host bacteria.

2.2 | Introduction

Bacteriophages are shaping bacterial populations and community structures. Whereas lytic phages are parasitic, temperate phages can be either mutualistic or parasitic (Harrison and Brockhurst 2017). Upon infection they either lyse the cell, or integrate into the bacterial chromosome as prophages. In particular, temperate phages can horizontally transfer genes encoding for antibiotic resistance or virulence factors among bacteria, which critically alters their hosts phenotype (Fineran, Petty et al. 2009).

While we have insights into infection patterns between bacteria and lytic phages (Flores, Meyer et al. 2011, Flores, Valverde et al. 2013, Kauffman, Hussain et al. 2018) our understanding of infection patterns between bacteria and temperate phages is still incomplete. Quantifying which temperate phages infect which bacteria is fundamental to understand how prophage-mediated horizontal gene transfer scales up to influence bacterial communities.

The family *Vibrionaceae* contains the greatest number of reported phage-host systems for the marine environment (Moebus 1987) with an estimated prevalence of 100% for temperate phages (Wendling, Piecyk et al. 2017). Thus, the genus *Vibrio,* which consists of 14 defined clades covering 58 species (Sawabe, Ogura et al. 2013), is ideal to investigate infection patterns between temperate phages and bacteria across different phylogenetic scales.

In a previous phage-bacteria infection network (PBIN) we observed that temperate phages isolated from *V. alginolyticus* could only infect bacteria from the same clade but not from a foreign clade (Wendling, Piecyk et al. 2017). However, that PBIN defined a pattern of relatively low taxonomic scales as it encompassed only two clades, which differed significantly in their sample sizes. If genetic differences between distinct phylogenetic groups of *Vibrio* limit the exchange of phages, we would expect a modular network, with nested patterns within each phylogenetic group once the number of different clades is increased (Flores, Meyer et al. 2011, Flores, Valverde et al. 2013). We therefore hypothesized that lytic infections by temperate vibriophages occur preferentially within but not across clades and tested this hypothesis on two different phylogenetic scales by empirically generating two PBINs that differ in the genetic distance of the tested bacteria.

2.3 | Methods

2.3.1 | Study organisms

We generated two three-fold replicated PBINs using bacteria of the genus *Vibrio* and their derived temperate phages Table S1 and S2). One network contained strains from low related *Vibrio* clades, with a maximum genetic distance of 0.04 (Fig. 1a) and their derived temperate phages and is called low relatedness network (LRN). In contrast, the genetic distance of the second network is about one order of magnitude shorter (genetic distance = 0.005, Fig. 1c). This network contained three different members of the *splendidus-like* clade and is called high relatedness network (HRN). Isolation and genotyping of all strains has been described elsewhere (Roth, Keller et al. 2012, Wendling, Batista et al. 2014, Wendling and Wegner 2015, Schade, Raupach et al. 2016).

2.3.2 | Bacterial resistance/phage infectivity

Resistance/ infectivity was measured by determining the reduction in bacterial growth rate (RBG) imposed by the phage, adapted from (Poullain, Gandon et al. 2008); for details see (S1).

2.3.3 | Statistical analysis

Phylogenetic analyses were performed as described in (Wendling, Piecyk et al. 2017); for details see (S1).

Network analysis: Infection data were processed in the form of binary matrices. The same analysis pipeline was used for both networks. Statistics were performed in R 3.1.2. We first confirmed that the three technical replicates were not significantly different using a Mantel test. Subsequent nestedness and modularity analysis was performed on a consensus matrix (positive infection: infection occurs at least in two replicates) using the packages: *bipartite*, *Falcon*, and *lpbrim* (Dormann, Gruber et al. 2008, Beckett, Boulton et al. 2014). For each phage, we performed a correlation between the genetic distance of its original hosts and the genetic distances of the hosts it could infect; for details see (S4).

Predicted Probabilities: Based on each network, we estimated the probability for every phage to infect a strain from the same clade as the phages host bacterium or a foreign clade, using a logistic regression with infection success as dependent variable and clade as independent variable. The complete model was analyzed using a glm and an analysis of deviance for which we assumed deviance change to be approximately χ^2 distributed. Null results (i.e. bacteria not infected by any phage respectively phages not able to infect any bacterium) were included in the analysis. Based on these obtained predicted probabilities (PP), we calculated the probability to infect a bacterium from the same relative to a foreign clade, according to the following formula: $(PP(Same) - PP(Foreign))/PP(Foreign)$. We used the same analysis to predict the probability for each bacterium to be infected by a phage, from the same relative to a foreign clade.

2.4 | Results

2.4.1 | Network structure

Genetic distances and infection patterns differed significantly between both networks. The LRN has a modular structure (Qbib = 0.62), with four distinct modules, out of which three could be assigned to either the *alginolyticus*, *splendidus* or *fischeri* clade (Fig. 1a and 1b). In support of this, the genetic distance of a phages host bacterium and the bacteria, which this phage can infect are significantly correlated (r^2 = 0.73, $t_{(df=196)}$ = 15.02, p<0.001, Fig. S4a). This indicates that phages, which were derived from a specific clade, are more likely to infect bacteria from the same than from distantly related clades. Module 4 contained strains from different clades, which are susceptible to various phages irrespective of their clade origin indicating that infections of distantly related *Vibrios* are possible but not very common.

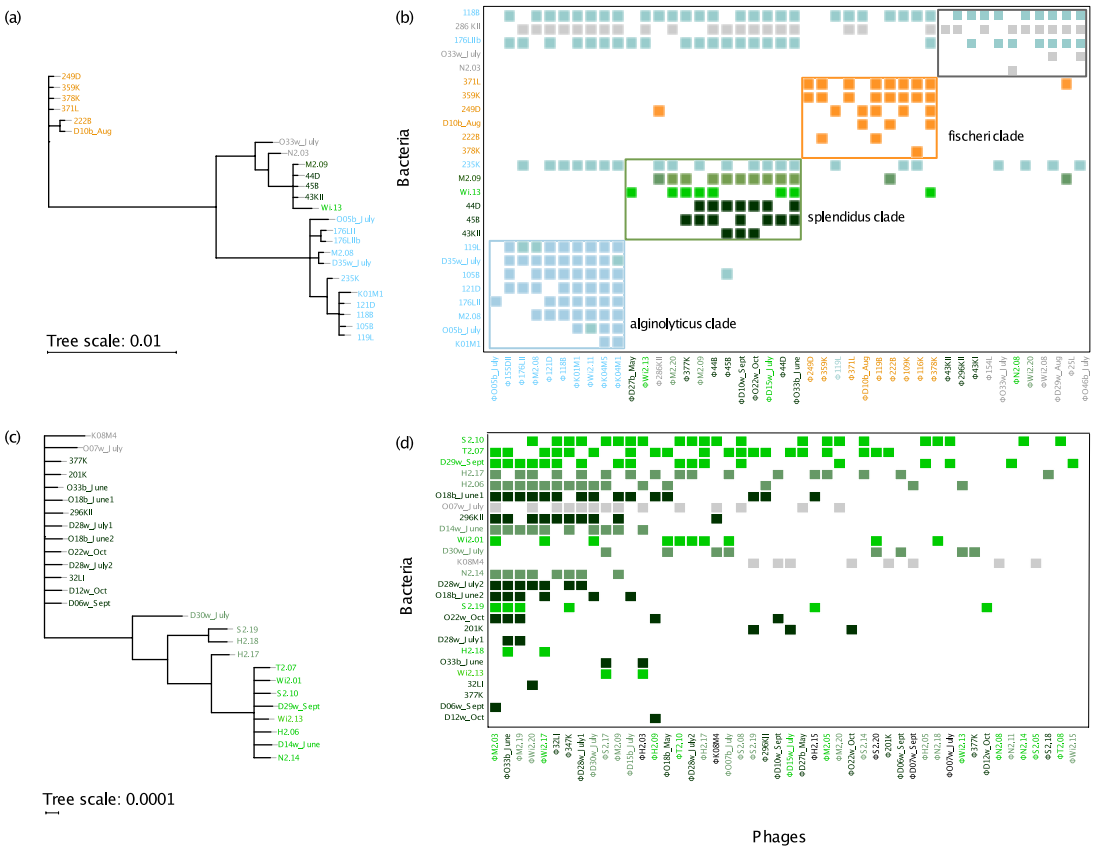

Figure 1: Bayesian phylogenetic trees of the LRN (a) and the HRN (c). Modular and nested display of the LRN (b) and HRN (d). Rows and columns represent bacteria and phages. Shown are only strains, which are susceptible to at least one phage infection, and phages, which could at least infect one bacterium. Colored squares indicate infection success. Colors correspond to the clade of the hosts that are infected by a particular phage. *Alginolyticus* clade: blue, Fischeri clade: orange, *Splendidus*-like clades in different shades of green: V. *splendidus*: dark green, V. *crassostreae*: mossy green, V. *cyclitrophicus*: neon green, other clades with < 3 strains per clade: grey.

2.4.2 | Relative infection/ resistance probability

Across distinct phylogenetic clades, i.e. the LRN the probability for a bacterium to be infected by a phage is higher when this bacterium belongs to the same phylogenetic clade as the phage's original host (Fig. 2). Similarly, phages are more likely to infect bacteria from the same clade as their original host, relative to bacteria from distantly related clades. However, at smaller phylogenetic scales (i.e. in the HRN) this pattern disappears.

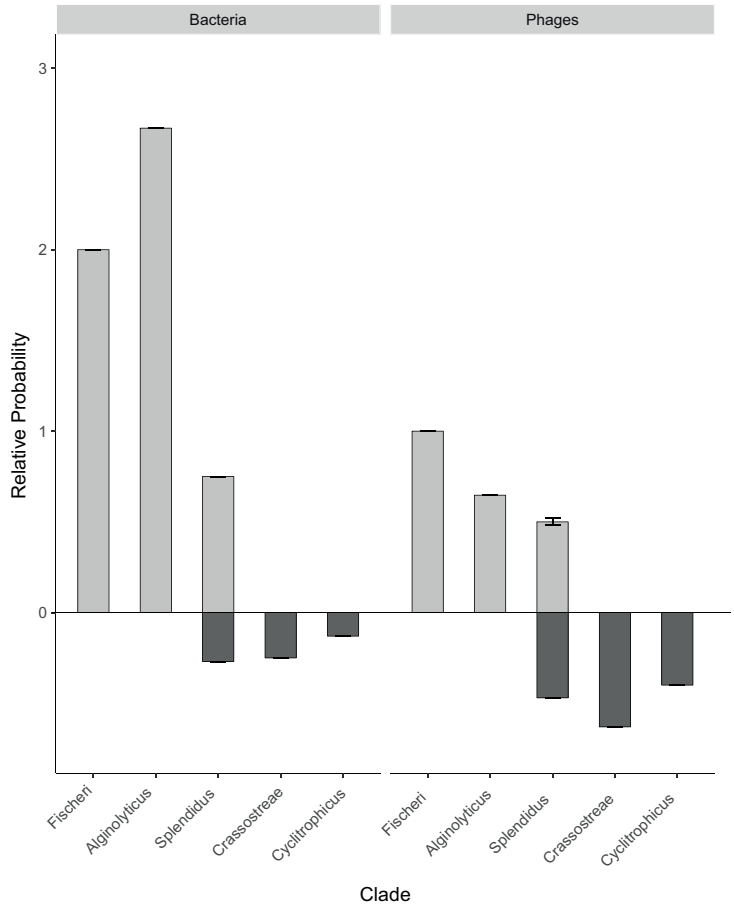

Figure 2: Probability to be infected by a phage from the same relative to a phage from a distantly related clade (left). Probability to infect a bacterium from the same relative to a bacterium from a distantly related clade (right). Values of rP > 0: more infections by same, Values of rP < 0: more infections by foreign. Light grey: LRN, dark grey: HRN.

Table 1: Nestedness statistics for the LRN, HRN and the three clade-specific modules of the LRN. * indicates significant networks

Network	Matrix connectance	Matrix fill	NODF nestedness score	p-value	Normalized temperature
HRN*	0.064	337	35.82	0.001	2.02
LRN	0.004	124	18.38	0.053	1.11
Alginolyticus Module*	0.68	54	85.7	0.001	1.38
Splendidus Module	0.54	42	42.16	0.91	0.83
Fischeri Module	0.43	26	49.17	0.08	1.22

2.5 | Discussion

Based on two PBINs, which differ in the genetic distance of the original hosts, we tested the hypothesis that lytic infections by temperate vibriophages occur preferentially within than across phylogenetic clades. While we observed clade-specific modularity in the LRN, the structure of the HRN is significantly nested. This suggests that the structure of PBINs changes with the phylogenetic distance of the host bacteria and confirms our hypothesis that temperate phages are more likely to infect bacteria from the same clade as their original host, relative to bacteria from distantly related clades.

Clade specific modularity suggests that either non-host resistance (Antonovics, Boots et al. 2013) or diversifying coevolutionary induced selection (Flores, Meyer et al. 2011) resulted in largely independent *Vibrio*/phage communities across the *Vibrio* phylogeny where genetic differences may limit the exchange of temperate phages between clades. In contrast, nested structures observed within the *Alginolyticus* (Wendling, Piecyk et al. 2017) and *Splendidus*-like clades (present study) are considered to be a result of gene for gene coevolution (Lenski and Levin 1985). Under this scenario, bacteria gain resistance to recently evolved phages by new mutations, thereby maintaining resistance to ancestral phages. Similarly, new mutations lead to phage host range expansion without losing the ability to infect ancestral bacteria.

Although temperate phages preferentially infect bacteria which belong to the same clade as their original host, we also observed that infections of distantly related bacteria are possible but not very common. This pattern was mainly driven by four strains (Fig. 1b). These strains were highly susceptible to most of the phages irrespective from which original host the phages were isolated. In contrast, we could not identify a single phage with an

equally broad
host-range. We thus speculate that the observed resistance/susceptibility pattern is driven by divergent bacterial resistance mechanisms than by phage-host range. Future studies, which identify resistance as well as infectivity mechanisms, are needed.

Phages are not only important in shaping bacterial community composition, they also play a pivotal role in bacterial evolution through the movement of important genes among bacteria (Fineran, Petty et al. 2009). It becomes increasingly clear that this phage-mediated DNA transfer can occur across distantly related bacteria and even the apparently highly conserved 16S rRNA gene was found within the genome of a broad host range transducing phage (Beumer and Robinson 2005). It is thus paramount to better understand phage host range and bacterial resistance to predict possible phage-driven horizontal gene transfer events across bacterial species, and thus the emergence of new (drug-resistant) pathogens.

Acknowledgments

We thank the group of Mathias Wegner for providing several *Vibrio* strains and Kim-Sara Wagner for laboratory support.

Funding

This study was supported by two grants of the Deutsche Forschungsgemeinschaft: WE 5822/1-1 and the Cluster of Excellence 80 “The Future Ocean” given to CCW and OR.

Ethical statement

No ethical approval was required.

Conflict of interest

We have no competing interests.

Author contribution

CCW and OR gained funding; CCW devised the study; CCW and HG conducted the experiments; CCW and OR interpreted the data; CCW analyzed the data and drafted the manuscript; all authors contributed to the manuscript, agree to be held accountable for the content therein and approved the final version of the manuscript.

Data archiving

Data are available from PANGAEA https://doi.org/10.1594/PANGAEA.889653

Electronic supplement is available at the publisher’s homepage:
https://royalsocietypublishing.org/doi/full/10.1098/rsbl.2018.0320

3 | CHAPTER II

Filamentous phages reduce bacterial growth in low salinities

Henry Goehlich[1], Olivia Roth[1], Carolin C. Wendling[1,2]

Published in *Royal Society Open Science.* 2018;1-13; DOI: 10.1098/rsos.191669

[1] Parental Investment and Immune Dynamics, Marine Evolutionary Ecology, GEOMAR Helmholtz Centre for Ocean Research, Kiel, Germany
[2] current address: Institute of Integrative Biology, ETH Zürich, Zürich, Switzerland

Keywords:

Phage-bacteria infection network, *Vibrio*, filamentous phages, salinity changes

3.1 | Abstract

Being non-lytic, filamentous phages can replicate at high frequencies and often carry virulence factors, which are important in the evolution and emergence of novel pathogens. However, their net-effect on bacterial fitness remains unknown. To understand the ecology and evolution between filamentous phages and their hosts, it is important to understand (1) fitness effects of a filamentous phages on their hosts, and (2) how these effects depend on the environment.

To determine how the net-effect on bacterial fitness by filamentous phages changes across environments, we constructed phage-bacterium infection networks at ambient 15 practical salinity units (PSU) and stressful salinities (11 & 7 PSU) using the marine bacterium, *Vibrio alginolyticus* and its derived filamentous phages as model system.
We observed no significant difference in network structure at 15 PSU and 11 PSU. However, at 7 PSU phages significantly reduced bacterial growth changing network structure. This pattern was mainly driven by a significant increase in bacterial susceptibility.

Our findings suggest that filamentous phages decrease bacterial growth, an indirect measure of fitness at stress-full environmental conditions, which might impact bacterial communities, alter horizontal gene transfer events and possibly favor the emergence of novel pathogens in environmental *Vibrios*.

3.2 | Introduction

Bacteriophages are highly abundant in the oceans with profound implications on bacterial ecology and evolution (Rohwer and Thurber 2009). Phages increase bacterial population diversity (Buckling and Rainey 2002, Brockhurst, Buckling et al. 2005), affect bacterial competition (Koskella, Lin et al. 2012), mediate horizontal gene transfer (Brown-Jaque, Calero-Caceres et al. 2015, Hall, Brockhurst et al. 2017) and play a major role in the marine nutrient cycle (Wilhelm and Suttle 1999). Identifying who infects whom, and how phages can change the fitness of their host, is crucial to predict phage-mediated impacts on microbial communities.

Phage-bacterium infection networks (PBIN) are ideal to identify phage host range, bacterial resistance and their co-evolutionary dynamics(Weitz, Poisot et al. 2013). Previous studies focused mainly on infection networks between bacteria and lytic phages (Flores, Meyer et al. 2011, Flores, Valverde et al. 2013, Kauffman, Hussain et al. 2018). In contrast, infection networks between bacteria and temperate or filamentous phages, are just beginning to be explored (Wendling, Piecyk et al. 2017, Wendling, Goehlich et al. 2018).

Being non-lytic, filamentous phages constitute an antithesis to the classical view of head-and-tail killer phages (Rakonjac, Bennett et al. 2011, Rakonjac 2012). Filamentous phages do not form classical host-parasite relationships with their hosts, but have evolved to keep the balance between their own reproduction and host survival (Rakonjac 2012). Thus, the net effect on bacterial fitness imposed by filamentous phages varies, depending on ecological and evolutionary factors. For instance, high-efficiency-replicating phages like Ff of *E. coli* that do not bring any benefit to their host, seem to be more parasitic than low-efficiency-replicating phages, which contribute to bacterial virulence through accessory virulence genes, for instance CTX-phage of *Vibrio cholerae* (Rakonjac 2012, Rakonjac, Russel et al. 2017).

Bacteria of the genus *Vibrio* harbor a diverse repertoire of filamentous phages, which play an important role in the evolution and emergence of novel pathogens (Weynberg, Voolstra et al. 2015, Castillo, Kauffman et al. 2018). The host-range of filamentous vibriophages is correlated to the phylogenetic distance of the phage's host bacterium and all other bacteria, which they are able to infect (Wendling, Goehlich et al. 2018). But, even if isolated from closely related host bacteria the host range of filamentous phages can differ significantly among individual phages (Wendling, Piecyk et al. 2017).

Crucially, studies on lytic phages revealed that phage host-range is rarely a binary trait and that it is important to take the abiotic environment into consideration to infer the underlying ecological and evolutionary dynamics (Koskella and Meaden 2013). Abiotic factors can influence the phage infection and replication process: for instance, a reduction in salinity can alter the adsorption rates of various phages onto their bacterial host, which changes infection outcomes between bacteria and phages (Kukkaro and Bamford 2009). Thus, in the light of phage-driven emergence of novel *Vibrio* pathogens we set out to investigate, whether and in which direction abiotic factors, in particular salinity, affect the structure of filamentous PBINs.

Marine bacteria of the genus *Vibrio* are present along the coast of the Baltic Sea (Eiler, Johansson et al. 2006, Roth, Keller et al. 2012) and their abundance, genetic composition and virulence are related to environmental factors, including temperature and salinity (Eiler, Johansson et al. 2006, Dayma, Raval et al. 2015, Poirier, Listmann et al. 2017). Characteristic for this habitat is a salinity gradient ranging from almost freshwater in the North and East to nearly fully marine conditions at the transition to the North Sea (Herlemann, Labrenz et al. 2011). By the end of the century the average salinity in the Baltic Sea is predicted to drop by approximately 4 practical salinity units (PSU) as a result of global climate change(Meier, Kjellstrom et al. 2006). Thus, the Baltic Sea represents a natural time machine for the future coastal ocean (Reusch, Dierking et al. 2018) making it an ideal ecosystem to study the effect of environmental change on species interactions.
In this study we investigated how reduced salinities influence the interaction between bacteria and filamentous phages using an established model system, i.e. the marine bacterium *Vibrio alginolyticus* and filamentous phages thereof. We measured reduction in bacterial growth imposed by filamentous phages at ambient salinity and at two different reduced salinities and compared networks from the different salinities to identify the drivers causing the different network structures.

3.3 | Methods

3.3.1 | Bacterial isolation

All *Vibrio alginolyticus* strains were isolated from nine healthy broad-nosed pipefish (*Syngnathus typhle*) caught in the Kiel Fjord (ambient salinity of 15 practical salinity units (PSU)) (Roth, Keller et al. 2012). For the present study, we selected a subset of 32 out of 75 previously characterized bacterial strains comprising three different phage-susceptibility categories (Wendling, Piecyk et al. 2017): two highly susceptible, 28 intermediate susceptible and three resistant strains, as well as their derived filamentous phages, to investigate whether the phage-bacterium infection network (PBIN) changes with different salinities. We chose three different salinity levels: current ambient salinity conditions in the Kiel Fjord region (15 PSU), predicted average salinity conditions (11 PSU) and potential temporary salinity conditions at the end of the century (7 PSU) (Meier, Kjellstrom et al. 2006, Bock and Lieberum 2017).

3.3.2 | Phage-bacterium infection assay

Phage extraction: Filamentous phages were obtained from the supernatant of bacterial cultures during exponential phase. To control for variations in phage-production across salinities, we decided to extract all phages at 15 PSU and only perform the infection assays at the three different salinities. All *Vibrio* strains were revived form cryo cultures in liquid Medium101 (Medium101: 0.5% (w/v) peptone, 0.3% (w/v) meat extract, 1.5% (w/v) NaCl in MilliQ water) overnight at 25°C and constant shaking at 180 rpm. Subsequently, overnight cultures were diluted 1:100 and grown for 7h in 15 ml Falcon tubes with 4 ml Medium101 at 25°C and 180 rpm. Afterwards, bacterial cultures were centrifuged at 6000 g for 10 min resulting in a bacterial pellet and suspended phages in the supernatant. Phage-containing supernatant was filtered (pore size: 0.20 μm) to remove all bacteria and ten-fold diluted in TM buffer (modified from Sen & Ghosh, 2005: 50% (v/v) 20 mM $MgCl_2$, 50% (v/v) 50 mM Tris-HCl, pH 7.5).

The presence of active filamentous phages in these supernatants has been confirmed in an earlier study (Wendling, Goehlich et al. 2018). To re-confirm the presence of phages in the current study we performed spot assays on a highly susceptible host strain K01M1, as described in (Wendling, Piecyk et al. 2017). In addition, a subset of nine strains has been fully sequenced, which revealed the presence of 1-2 different filamentous phages per strain (Wendling, Piecyk et al. 2017). Based on these observations, we are confident that the supernatants in the present study contain filamentous phages.

Reduction in bacterial growth assay: We measured the reduction in bacterial growth (RBG) imposed by the phage in liquid culture (Poullain, Gandon et al. 2008) for more than 9000 possible phage-bacteria interactions (32 phages x 32 bacteria x 3 salinities x 3 replicates) with media and growth-time adjusted to the Baltic vibriophagessystem (Wendling, Goehlich et al. 2018). To do so, overnight cultures of all bacterial strains (grown at 15 PSU) were diluted 1:10 in their respective Medium101 at 7 PSU, 11 PSU or 15 PSU and incubated with constant shaking at 180 rpm and 25°C for 1.5h (15 & 11 PSU) or 2h (7 PSU) respectively, to achieve similar starting optical densities (OD600) ranging between 0.104 and 0.125. We added 15 μl of bacteria in the log phase (concentration: $5*10^6$ cells/ml) to transparent, flat-bottom 96-well microtiter (NunclonTM) plates containing 120 μl Medium101 with the respective salinity and either 15 μl TM Buffer containing phage lysate (with a 10-1 dilution of the original phage-containing supernatant) or 15 μl TM Buffer only as control. We

measured bacterial optical density at 600 nm (OD600) using an automated plate reader (at the beginning (t = 0h) and after 18 hours (t = 18h) of static incubation at 25°C. The reduction in bacterial growth imposed by phage i on strain j, was calculated according to the following formula:

$$RBGij = \frac{OD600\ (t = 18h) - OD600\ (t = 0h)\ [ij]}{OD600\ (t = 18h) - OD600\ (t = 0h)\ [Control\ j]}$$

The calculation for the threshold of infection was adapted from Poullain (2008) and revealed a bimodal histogram of all RBG values with a local minimum at RBG = 0.82 for our *Vibrio* system (Wendling, Goehlich et al. 2018). We thus concluded that RBG values lower than 0.82 indicate a significant reduction in bacterial growth imposed by the phage and thus a successful infection, which has a negative impact on bacterial fitness. RBG values higher than 0.82 do not necessarily indicate the absence of an infection at, but they indicate that the phage does not have a negative impact on bacterial fitness.

Due to handling errors during the RBG assay, we had to remove three phages (ΦK09K2, ΦK09K3 and ΦK10K4) from the analysis.

3.3.3 | Bacterial growth rates and phage production

Bacterial growth rates: We measured bacterial growth at each salinity to assess potential correlations between growth rates and phage infections by means of 24h growth curves. Growth curves were obtained for each strain at each salinity using 96 well plates. In brief, overnight cultures of each strain were diluted 1:100 with medium 101 containing the respective salinity (7, 11 or 15 PSU) and 200 μl of these dilutions were transferred to a 96-well plate. Optical density was measured in triplicates at 600 nm every 15 min over 24h using an automated plate reader.

Phage production: To assess whether salinity influences the phage production of resident phages, we measured the amount of plaque forming units relative to colony forming units (PFU/CFU) for each strain. CFU was measured by plating 100 μl of overnight cultures onto TCBS agar plates, and the number of colonies was counted after overnight incubation at 25°C. PFU was measured by small-scale PEG precipitation of the same overnight cultures

used for quantifying CFU because quantification via standard spot assays was not possible as we mostly observed opaque zonas of reduced growth. Thus, we used spectrometry to quantify phage prevalence which uses the constant relationship between the length of viral DNA and the amount of the major coat protein VIII of filamentous phages, which, together, are the main contributors of the absorption spectrum in the UV range (http://www.abdesignlabs.com/technical-resources/bacteriophage-spectrophotometry). The amount of phage particles per ml can be calculated according to the following formula:

$$phages/ml = \frac{(OD269 - OD320) * 6e16}{bp}$$

where OD269 and OD320 stand for optical density at 269 and 320 nm and bp stands for number of base pairs per phage. After centrifuging 1500 μl of the phage containing overnight culture at 13,000 g for 2 min, 1200 μl of the supernatant was mixed with 300 μl PEG/NaCl 5x and incubated on ice for 30 min. Afterwards phage particles were pelleted by two rounds of centrifugation at 13,000 g for 2 min, resuspended in 120 μl TBS 1x and incubated on ice. After one hour, the suspension was cleaned by centrifugation at 13,000 g for 1 min and absorbance was measured at 269 and 320 nm.

3.4 | Statistical analysis

3.4.1 | Network analysis

After confirming that all three technical replicates per salinity did not differ significantly (Mantel test; Monte-Carlo test observation based on 9999 permutations: $p < 0.001$), we created a consensus matrix for each salinity (positive infection: infection occurs at least in two replicates, Electronic supplement S1). We performed network analyses for each consensus matrix based on the Falcon interactive mode (Beckett, Boulton et al. 2014) and the bipartite package (Dormann and Strauss 2014) using nested measures based on overlap and decreasing fill (NODF) and the SS null model (Almeida-Neto, Guimaraes et al. 2008). Analysis of nestedness can be sensitive to the inclusion of empty rows and columns, we thus performed the analysis again after removing all empty rows and columns of each network.

The impact of salinity on network connectance and fill, the number of infecting phages and the number of susceptible bacteria was analyzed using a linear model for each of these parameters with salinity as fixed effect.

3.4.2 | Bacterial growth rates

We used the grofit package (Kahm, Hasenbrink et al. 2010) to calculate growth rates (μ) from 24h growth curves. To determine differences in growth rates between different salinities and strains, we used a linear mixed-effect model (package: lme4) (Bates, Machler et al. 2015) with salinity and strain as fixed factors and the day of measurement as random effect.

3.4.3 | Correlation of phage infections with bacterial growth rates

We used ggscatter (package: ggpubr) to test for a correlation between growth rate at 7 PSU relative to 15 PSU and the number of phages causing infections at 7 PSU in a single bacterial strain. We further tested for correlations between the number of phages causing infections in a single bacterial strain and the respective growth rates at 7 PSU, 11 PSU and 15 PSU.

3.4.4 | Production of resident phages

To determine whether resident phages of each strain produce different amounts of phages in the different salinities we performed a paired t-test between PFU/CFU at 7 PSU and PFU/CFU at 15 PSU.

3.5 | Results & Discussion

3.5.1 | Filamentous phages reduce bacterial growth at low salinities

Based on three-times-replicated phage-bacteria infection networks (PBIN, Figure 1), we compared network structures of filamentous PBINs across three different salinities, relevant for the Kiel Fjord region: current average salinity with 15 practical salinity units (PSU), current annual minimum salinity and predicted average salinity by the end the of the century (11 PSU) as well as predicted short term minimum salinity by 2100 (7 PSU). One limitation of the present study is that we cannot infer cryptic infections, i.e. infections, which do not reduce bacterial growth. Thus, we only consider instances, where infections are harmful for the bacterium, as in reducing its growth rate by more than 20% as true infections.

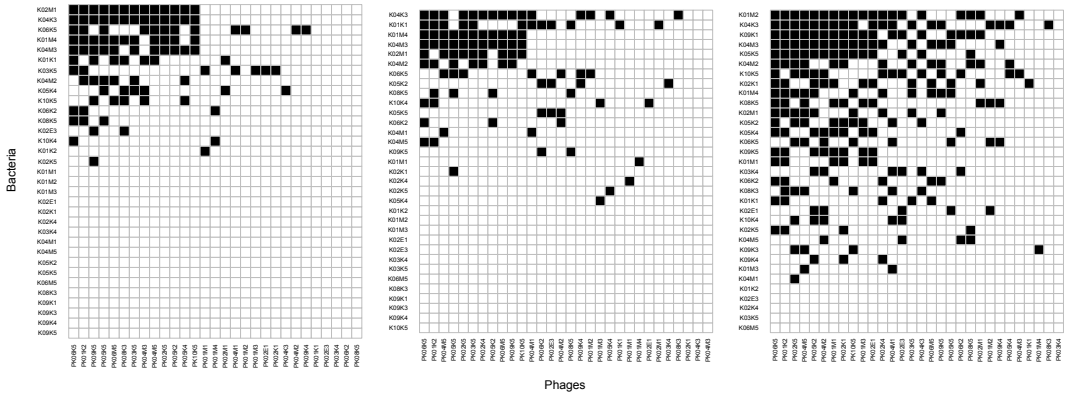

Figure 1: Phage– bacteria infection network (PBIN) of the consensus matrices.
Rows: bacteria, columns: phages, black cells:successful infection. 15 PSU (left), 11 PSU (middle) and 7 PSU (right).

All PBINs showed a significant nested structure based on overlap and decreasing fill (NODF, Table 1) with highest nestedness at 7 PSU (51.22) followed by 15 PSU (41.9), and lowest nestedness at 11 PSU (29.8) suggesting that the nested structure remains consistent irrespective of the salinity level. We did not find a difference in nestedness measures after excluding empty rows and columns from the analysis, confirming that all three networks are truly nested, which was previously observed in filamentous PBINs containing closely related *Vibrio* strains (Wendling, Piecyk et al. 2017, Wendling, Goehlich et al. 2018).

Table 1: Network statistics at 15, 11 and 7 PSU. Nestedness based on overlap and decreasing fill (NODF: 100 = perfectly nested and 0 = zero nestedness), nT: normalized temperature, indicating the deviation from the null model (< 1 observed network is less nested than expected). Connectance: ratio of the number of successful infections relative to all possible interactions between phages and bacteria. Fill: total amount of successful infections.

Salinity (PSU)	NODF	nT	Z-score	p-value	Connectance	Susceptible bacteria	Infecting phages	Fill
15	41.88	1.54	7.24	0.001	0.11	16	24	103
11	29.8	1.59	7.7	0.001	0.10	20	27	101
07	51.22	1.65	14.73	0.001	0.25	28	29	246

Network parameters were similar for the 11 and 15 PSU networks but changed significantly at 7 PSU (Figure 2, Table 2). This indicates that unlike a gradual increase, a certain salinity threshold is required to cause this significant reduction in bacterial growth in the presence of filamentous phages (Table 2).

The number of phages able to at least infect one bacterium did not differ among all three salinities. Instead, the number of bacteria susceptible to at least one phage infection almost doubled from 15 PSU to 7 PSU (Figure 2). Thus, the observed reduction in bacterial growth at 7 PSU seems to be mainly driven by increased bacterial susceptibility rather than phage infectivity.

Table 2: Linear model for selected network parameters: C: network connectance, F: network fill, P: number of infecting phages, B: number of susceptible bacteria. Shown are comparisons for 11 PSU and 7 PSU relative 15 PSU (Intercept).

		Estimate	Standard error	t-value	p (>t)
C	Intercept	0.13	0.01	18.52	1.60e-06 ***
	11 PSU	-0.02	0.01	-1.64	0.15
	7 PSU	0.15	0.01	14.40	7.02e-06 ***
F	Intercept	130.00	6.97	18.66	1.53e-06 ***
	11 PSU	-14.67	9.85	-1.49	0.19
	7 PSU	139.33	9.85	14.14	7.80e-06 ***
P	Intercept	28.33	0.64	44.39	8.75e-09 ***
	11 PSU	-0.33	0.90	-0.37	0.73
	7 PSU	0.33	0.90	0.37	0.73
B	Intercept	19.00	0.61	31.22	7.17e-08 ***
	11 PSU	2.00	0.86	2.32	0.06
	7 PSU	10.67	0.86	12.39	1.68e-05 ***

The aim of this study was to determine how salinity changes the impact of filamentous phages on bacterial growth and thus ultimately bacterial fitness and the network structure of a filamentous PBINs. In the future, the underlying molecular mechanisms, which could explain the observed decrease in bacterial growth at 7 PSU, should be identified. Thus, we can only speculate, that various parameters, for instance differences in phage adsorption rates (salinity can affect the adsorption to the bacterial cell wall in both directions (Kukkaro and Bamford 2009, Flores, Meyer et al. 2011, Zemb, Manefield et al. 2013, Mei, He et al. 2015, Silva-Valenzuela and Camilli 2019) can cause the observed change in network structure in the present study.

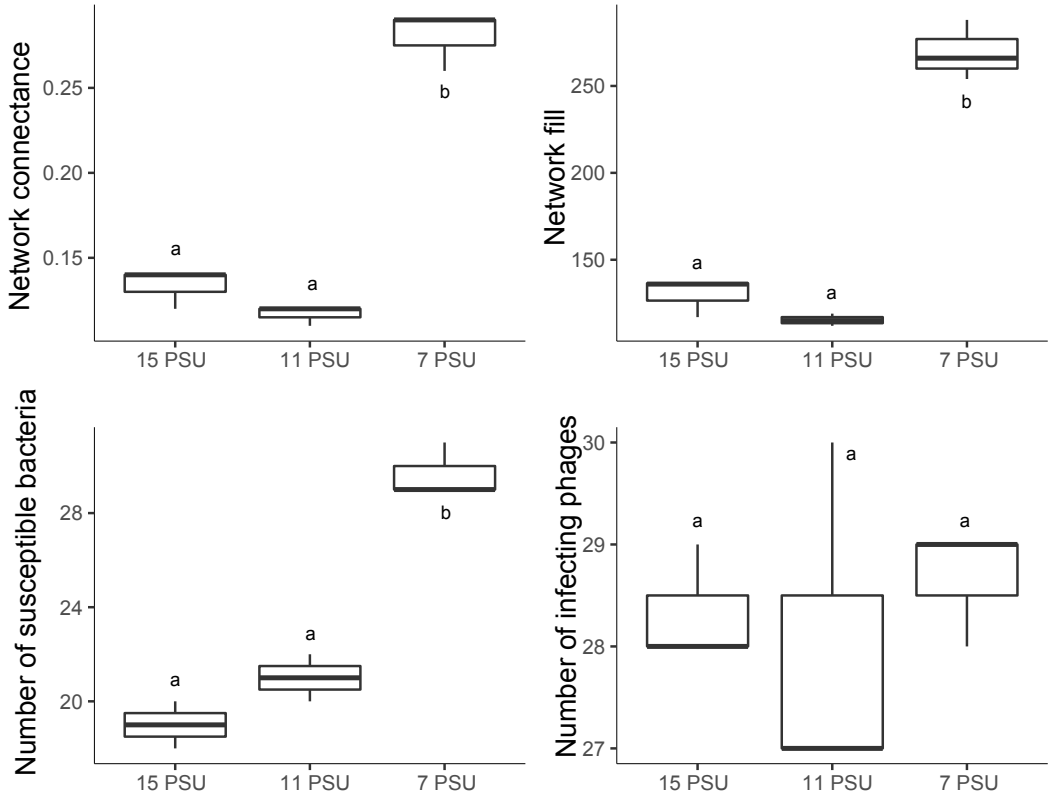

Figure 2: Comparison of selected network parameters at 15, 11 and 7 PSU.
(a) network connectance, (b) network fill, (c) number of susceptible bacteria, (d) number of infecting phages. Significant differences are indicated by small letters.

Reduced salinities represent a stress-full condition for *V. alginolyticus* and result in a reduction in growth rate (μ) by up to 50% relative to ambient conditions ($\chi^2_{(2)} = 2641.2$, $p < 0.001$) and overall prolonged growth (Electronic supplement S2). This negative impact on bacterial growth parameters could have influenced the infection outcome at low salinities in several ways. It is for instance possible that the prolonged growth at 7 PSU might increase the time window for phage infection at low salinities. Future studies would have to compare the number of phage infections at selected timepoints during 24 hours at all three salinities. Furthermore, it is possible that resident filamentous phages produce at a higher frequency at 7 PSU, which is costly for the bacterial host and will thus result in reduced growth rates. However, we did not find a significant difference in phage production between 7 and 15 PSU salinities (paired t-test: $t_{(32)} = 1.16$, $p = 0.255$, Electronic supplement S3) and can thus exclude that reduced growth at 7 PSU is a direct consequence of costly phage production. Lastly, we tested whether the reduction in growth alone is explaining the increased number of phage infections at 7 PSU. To do so, we determined whether those bacterial strains, that experienced a strong reduction in growth at 7 PSU relative to 15 PSU are driving the

increased number of successful phage infections at 7 PSU. In contrast to this expectation, strain-specific reduction of growth rate at 7 PSU relative to 15 PSU was not an indicator for the observed increase in successful phage infections ($r = 0.065$, $p = 0.52$, Electronic supplement S4). Furthermore, there was no correlation between the number of phage infections per strain and strain-specific growth rate at the three salinity levels (Electronic supplement S5), which differed significantly between strains ($\chi^2_{(32)} = 477.8$, $p < 0.001$). This indicates that reduced bacterial growth alone at 7 PSU is not an indicator for the observed increase in successful infections.

3.5.2 | Ecological and evolutionary implications

We show that filamentous phages significantly decrease bacterial growth at low salinities, a pattern which is predominantly driven by increased bacterial susceptibility rather than increased phage infectivity. According to the present data, we do not expect an increase in successful infections of *Vibrios* by filamentous phages in response to the predicted reduction of the average salinity concentration from 15 PSU to 11 PSU in the Kiel Fjord by the end of the century (Meier, Kjellstrom et al. 2006). However, due to saltwater inflow events from the North Sea, rainfall and river runoffs, salinity concentrations in the coastal area of the southern Baltic Sea usually fluctuate by five units above and below the average salinity level, which can result in rapid salinity drops down to 7 PSU and below (Bock and Lieberum 2017). To this end, these temporal low salinity events may result in an increase in filamentous phage infections, which can have various consequences at population and community levels. For instance, if these infecting phages carry virulence genes, which is common for filamentous vibriophages (Weynberg, Voolstra et al. 2015, Castillo, Kauffman et al. 2018), new pathogenic *Vibrios* will possibly emerge in response to decreasing salinities. To study these long-term interactions between *Vibrios* and filamentous phages at different environmental conditions, future work should focus on how abiotic parameters influence the interaction of filamentous phages and *Vibrio* bacteria on evolutionary time scales. It might be possible, that bacteria will adapt to counter these negative effects resulting from increasing phage pressure at low salinities. Overall, our results confirm that species interactions are strongly shaped by the environment and that it is paramount to integrate abiotic factors when studying them.

Acknowledgments

We thank Angela Stippkugel and Kim-Sara Wagner for their support in the laboratory. This project was funded by a DFG grant [WE 5822/ 1-1] within the priority programme SPP1819 given to CCW and OR. We thank all anonymous reviewers for valuable comments on the manuscript and the International Max Planck Research Schools for career and financial support of HG.

Funding

This study was supported by two grants of the Deutsche Forschungsgemeinschaft: WE 5822/1-1 and the Cluster of Excellence 80 "The Future Ocean" given to CCW and OR.

Ethical statement

No ethical approval was required.

Conflict of interest

We have no competing interests.

Author contribution

CCW, OR and HG designed the study. HG performed the experiments, analyzed the data and wrote the first draft. CCW, HG and OR wrote the final version.

Data archiving

Data were deposited at PANGAEA. https://doi.pangaea.de/10.1594/PANGAEA.906121

3.6 | Supplement

S1: Unsorted consensus matrices

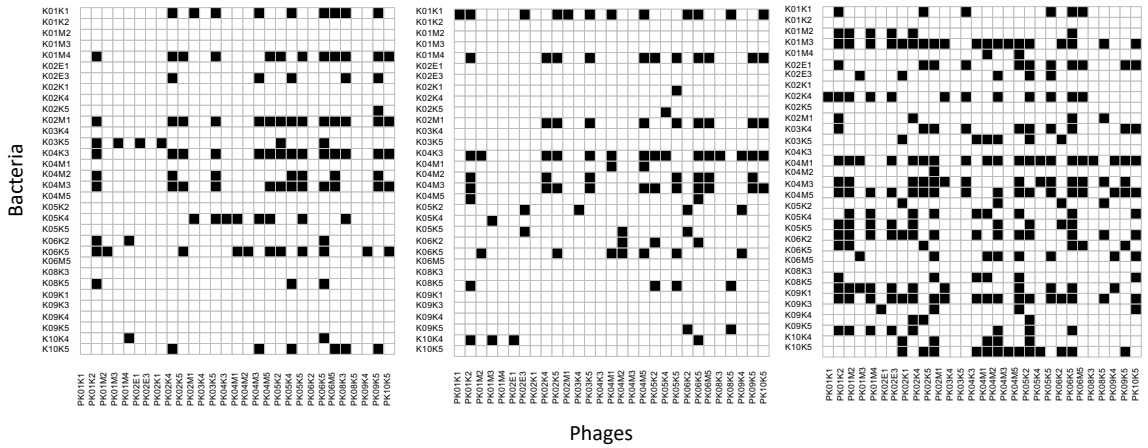

Figure S1: Unsorted consensus matrices per salinity (left: 15 PSU, middle: 11 PSU and right: 7 PSU). Rows represent bacteria and columns represent phages. Black cells indicate infection success in at least 2 out of the three replicates.

S2: 24h-Growth curves of each strain

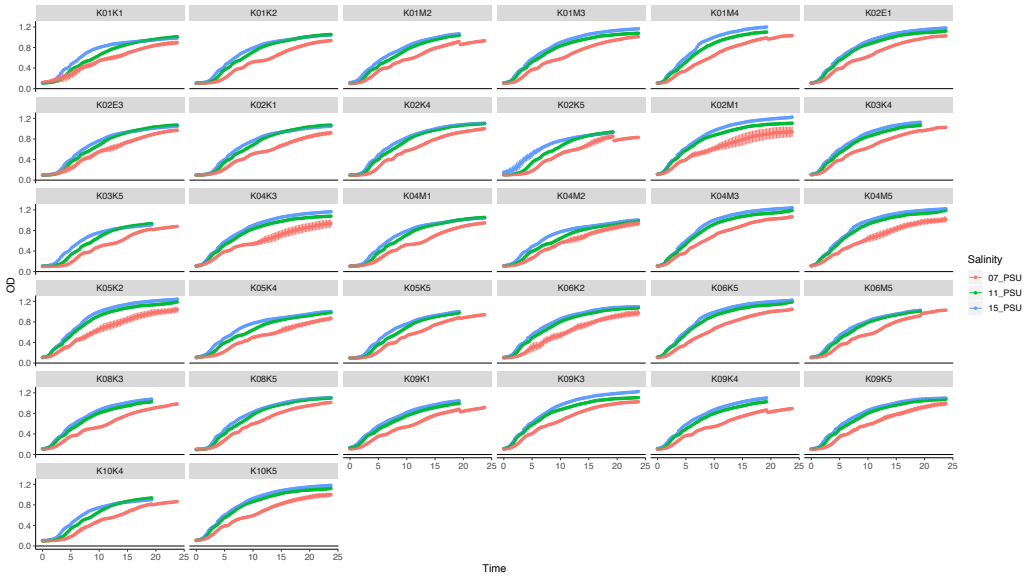

Figure S2: 24-hour growth curves per strain and salinity (red: 7 PSU, green: 11 PSU and blue: 15 PSU). Shown are mean and standard-error (n=3). OD was measured at 600nm using an automated plate-reader.

S3: production of resident phages

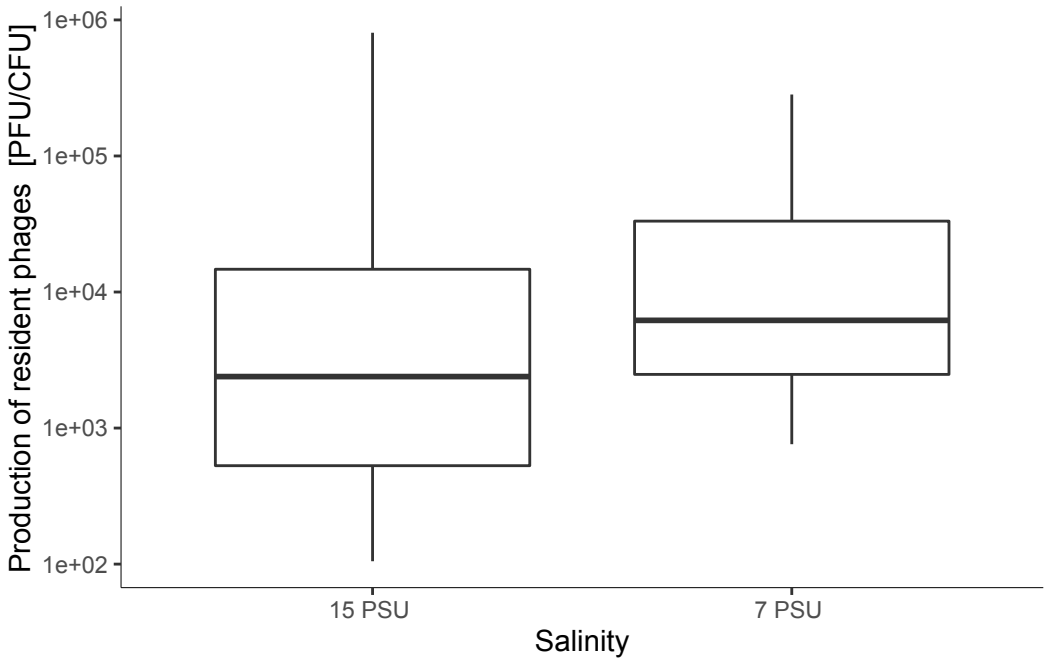

Figure S3: Production of resident phages Plaque forming units to Cell forming units [PFU/CFU] at 15 PSU (left) and 7 PSU (right).

S4: Bacterial growth rate at 7 relative to 15 PSU

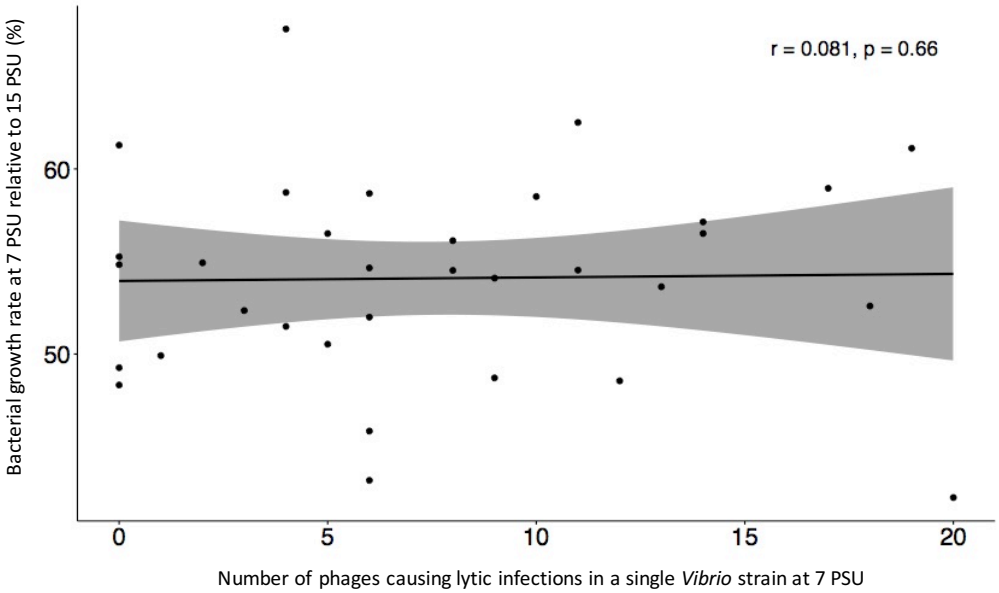

Figure S4: Regression between number of phages causing successful infections in a single *Vibrio* strain at 7 PSU and bacterial growth rate at 7 PSU

S5: Bacterial growth versus the number of phages causing infections

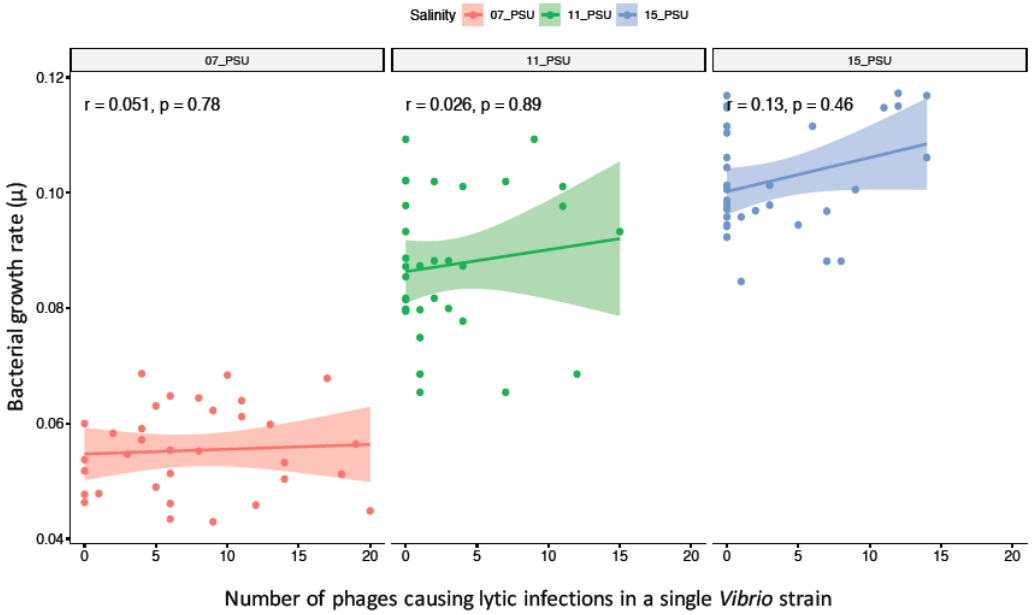

Figure S5: Regression between number of phages causing successful infections in a single *Vibrio* strain and growth rate of the respective strains at different salinities.

4 | CHAPTER III

Low salinity slows down resistance evolution of *Vibrio alginolyticus* against a filamentous phage

Henry Goehlich[1,4], Olivia Roth[1], Michael Sieber[2], Cynthia M. Chibani[3], Jelena Rajkov[1], Katja Trübenbach[1], Heiko Liesegang[4], Carolin C. Wendling[1,4]

Manuscript in draft

[1] Parental Investment and Immune Dynamics, Marine Evolutionary Ecology, GEOMAR Helmholtz Centre for Ocean Research, Kiel, Germany

[2] Max Planck Institute for Evolutionary Biology, August-Thienemann-Str. 2, 24306 Plön, Germany

[3] Georg-August University Göttingen, Department of Genomic and Applied Microbiology, Grisebachstr. 8, 37077 Göttingen, Germany

[4] current address: ETH Zürich, Institute of Integrative Biology, Universitätsstraße 16, 8092 Zürich, Switzerland

current address: Universität Kiel, Department of Microbiology, Am Botanischen Garten 1-9, 24118 Kiel, Germany

Keywords
Vibrio, filamentous phages, salinity, climate change, Baltic Sea, resistance evolution, Inoviridae, Experimental evolution

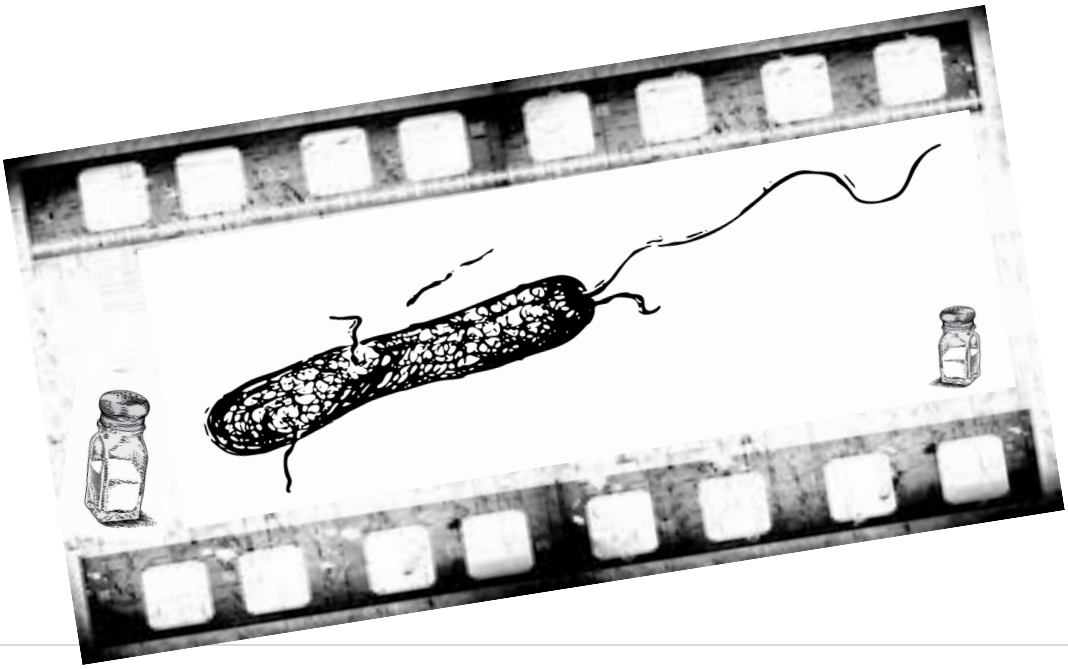

4.1 | Abstract

Bacteriophages, viruses that infect bacteria, are one of the strongest forces shaping bacterial ecology and evolution. However, not all phages are lethal. Filamentous phages for instance, can release phage progeny without killing their bacterial host and some can even provide their bacterial host with accessory genes. We expect costs (phage production) and benefits (accessory genes) associated with the carriage of filamentous phages to vary with environmental conditions because of, for example, environment-dependent phage production rate or environment-dependent benefits of the accessory genes. However, our understanding of how these costs and benefits is limited. Here, we combined experimental evolution and mathematical modelling of a co-evolving marine *Vibrio alginolyticus* – filamentous phage interaction to show that reduced salinity, which significantly impairs bacterial growth and phage reproduction, slows down phage resistance evolution. At reduced salinity, bacteria carrying the co-evolving phage remained twice as long in the bacterial population before being outcompeted by phage-resistant mutants. Our deterministic model suggests that the delayed presence of phage-infected clones and resistance evolution is driven by a lower bacterial growth rate at 7 PSU, which in turn reduces the encounter rate of phage and bacteria. Reduced absolute growth rates at low salinity and relaxed costs of phage carriage (i.e. reduced phage production) result in a prolonged presence of phage infected bacterial clones. These results suggest that environmental parameters, which reduce the costs of carrying a filamentous phage might increase the prevalence of filamentous phages in bacterial populations, even if they do not carry any known accessory genes.

4.2 | Introduction

Bacteriophages are viruses that infect bacteria and archea. Whereas lytic phages kill their bacterial host to reproduce, filamentous phages coexist episomally in infected cells or integrate as prophages into the bacterial chromosome (Reviewed in Hobbs and Abedon 2016). Depending on the life-style and reproduction strategy of a phage, costs and benefits of a phage infection can vary. While, lytic phages are parasites that provide no benefits to individual bacteria cells, filamentous phages of the family *Inoviridae* are known for their

cooperative lifestyle and were considered as “masters of a microbial sharing economy” (Reviewed in Hay and Lithgow, 2019). They have a self-interest to maintain or increase bacterial fitness to ultimately enhance their chance of survival and reproduction. A unique characteristic of filamentous phages are chronic infections, i.e. phages are released through the cell wall without killing the bacteria (Russel 1995, Rakonjac, Feng et al. 1999). Hypothesized to have evolved independently from classical head and tail phages, the strategy of filamentous phages has been so successful that they are present in most ecosystems and associated with various taxa of bacteria and archaea (Roux, Krupovic et al. 2019).

Part of their success story is the introduction of beneficial genes into the bacterial genome increasing bacterial fitness. For example, phage-encoded virulence genes can turn harmless bacteria into virulent pathogens. This phage-induced bacterial transformation, called lysogenic conversion, is best described for *Vibrio cholerae* and the vibriophagesCTXΦ (Waldor and Mekalanos 1996, Das 2014, Ilyina 2015). However, not all benefits associated with filamentous phages are as obvious as described above and many are potentially only relevant in specific environmental conditions. While superinfections with mutants of Pf4Φ cause death through lysis of individual *Pseudomonas aeruginosa* cells, the released virions in turn increase bacterial persistence in cystic fibrosis patients by contributing to biofilm formation which ultimately enhances virulence and antibiotic resistance (Webb, Lau et al. 2004, Rice, Tan et al. 2009, Secor, Michaels et al. 2017, Burgener, Sweere et al. 2019).

The costs associated with filamentous phages for the bacterial host include the replication of both the phage and phage-encoded proteins, which are necessary for phage secretion. The additional produced molecules may result in reduced bacterial growth rates (Ahmad, Askora et al. 2014) or in the inhibition of bacterial RNA expression (Horabin and Webster 1986). Some bacterial hosts are also at risk of death (Kuo, Chiang et al. 1994, Kuo, Yang et al. 2000) resulting from an imbalance in toxins and antitoxins, when toxin-antitoxin systems are removed with the phage (Webb, Lau et al. 2004, Rice, Tan et al. 2009, Roux, Krupovic et al. 2019, Li, Liu et al. 2020) or because of reduced membrane integrity due to phage encoded transmembrane proteins resulting in the loss of the membrane potential and impeded nutrient uptake (Horabin and Webster 1988). Taken together, filamentous phages may only increase host fitness, when the benefits outweigh the costs of phage infection,

which is the case in niche-adaptation such as to eukaryotic hosts (Bille, Meyer et al. 2017) or to extreme environments (Yu, Chen et al. 2015).

While co-evolutionary dynamics between lytic phages and bacteria have been intensively studied (Buckling and Rainey 2002, Brockhurst, Morgan et al. 2003, Brockhurst, Buckling et al. 2005, Gomez and Buckling 2011, Koskella, Lin et al. 2012, Scanlan and Buckling 2012), co-evolution between bacteria and filamentous phages has received less attention. Moreover, studies revealing which environmental conditions select for, as opposed to against, carriage of filamentous phages are rare and focus on the model organism *E. coli* (Bull, Molineux et al. 1991, Shapiro, Williams et al. 2016, Shapiro and Turner 2018). Similar to bacteria-lytic phage interactions, which are modulated by the environment (Brockhurst, Morgan et al. 2003, Gomez and Buckling 2011, Harrison, Laine et al. 2013, Wright, Brockhurst et al. 2016, Hernandez and Koskella 2019), we predict that environmental conditions will affect the net-fitness effect of filamentous phages on their bacterial host and in turn change population and co-evolutionary dynamics.

Salinity is an environmental factor strongly affecting the composition of microbial communities (Herlemann, Lundin et al. 2016, Hu, Karlson et al. 2016) and the fitness of individual bacteria, including *Vibrio* (Goehlich, Roth et al. 2019). Climate change scenarios predict a salinity drop by up to 5 PSU (Practical Salinity Unit) for the Baltic Sea until the end of the century (Meier, Kjellstrom et al. 2006). In addition, salinity fluctuations on shorter timescales, e.g. between 20 and 9 PSU in the entrance of the Kiel fjord, are imposed by river run offs, rainfall and water inflow from the North Sea (Girjatowicz and Swiatek 2016, Bock and Lieberum 2017). Salinity changes do not only affect growth**,** physiology and the expression of motility and virulence factors in *Vibrios* (Reviewed in Hase and Barquera 2001), they also modulate interactions with bacterial host organisms (Dayma, Raval et al. 2015, Poirier, Listmann et al. 2017) and phages (Goehlich, Roth et al. 2019, Silva-Valenzuela and Camilli 2019). In a previous study, we observed that at reduced salinity levels *V. alginolyticus* bacteria were more susceptible to filamentous phages or that the cost imposed by the phage were higher for the bacterium (Goehlich, Roth et al. 2019). A shift in cost and benefits of infecting phages may alter the trajectory of resistance evolution and the prevalence of phage-infected clones in co-evolving phage bacteria populations.

To assess whether changing environmental conditions influence co-evolutionary dynamics between filamentous phages and their host bacteria we performed a serial transfer

experiment at different salinity levels using the marine bacterium *V. alginolyticus* strain K01M1 and an extrachromosomal filamentous vibriophagesVALGΦ8 (Chibani, Hertel et al. 2019). We additionally modelled the co-evolutionary interactions using a parameterized model. This allowed us to determine the main parameters that influenced the salinity-depended changes in the co-evolutionary trajectories.

4.3 | Material and Methods

4.3.1 | Study organisms

Vibrio alginolyticus strain K01M1 (Gene bank accession number: CP017889.1, CP017890.1) and *V. alginolyticus* strain K04M1 harbouring filamentous vibriophagesVALGΦ8 (MN690600) were isolated from healthy pipefish (Roth, Keller et al. 2012) and characterised by whole genome sequencing (Chibani, Roth et al. 2020). The *V. alginolyticus* strain K01M1 harbours a resident filamentous vibriophagesVALGΦ6 which replicates at a lower frequency in comparison to vibriophagesVALGΦ8 (Chibani, Hertel et al. 2019).

4.3.2 | Evolution experiment

We induced vibriophagesVALGΦ8 in overnight cultures (ONCs) of K04M1 by adding mitomycin C (Sigma) with a final concentration of 0.5 µg/ml (Wendling, Piecyk et al. 2017). ONCs were centrifuged for 5 min at 6000g. Phage-containing supernatant was filtered (pore size: 0.20 µm) to remove all bacteria, 10-fold diluted in TM buffer (modified from Sen & Gosh (2005): 50% (v/v) 20 mM MgCl2, 50% (v/v) 50 mM Tris–HCl, pH 7.5) and subsequently stored at 4°C overnight.

In parallel, we initiated six replicate populations from six independent clones of strain K01M1 for each treatment. The treatments comprised a set of 18 populations co-evolving with the filamentous vibriophagesVALGΦ8 at three different salinity conditions: a) constant low (7 Practical Salinity Unit (PSU)), b) constant ambient (15 PSU), and c) fluctuating (starting with 7 PSU on transfer 0 and 1 and then alternating between 7 and 15 PSU every transfer). Another set of 18 populations at the three different salinity treatments but without added phages was used as controls.

Populations were established from 60 μl overnight culture (~5×10^9 CFU/ml) and 300 μl vibriophagesVALGΦ8 suspension (~5×10^8 PFU/ml) in microcosms (30 ml glass container with loose plastic lid) containing 6 ml of liquid medium (medium101: 0.5% (w/v) peptone, 0.3% (w/v) meat extract, 0.7% (w/v) or 1.5% (w/v) NaCl in MilliQ water). Microcosm were incubated at 25 °C and 180 rpm. Every 24 hours, 60 μl of all populations were transferred into fresh microcosms with 6 ml medium to allow continuous growth. Each transfer is equivalent to approximately 7.5 generations, presuming that all populations diluted 1:100 reach the stationary phase after 24 hours, which was the case according to 24-hour growth curves (Supplement S 1).

Phage and bacterial densities were determined on transfer T0, T1, T2, T3, T4 and subsequently, on two consecutive transfers, followed by a transfer with no density measurements. Using this rhythm, in contrast to every 2nd day sampling, allowed us to include both salinity levels of the fluctuating treatment in our measurements. On transfer T0, T2, T3, T4, T6, T10, T12, T16, T22, T29 whole bacterial population samples, phage populations and 24 randomly isolated single colonies from each bacterial population were frozen at -80°C at a final concentration of 33% glycerol.

4.3.3 | Phage and bacterial densities

Bacterial densities

Bacterial densities were determined by plating out 100 μl of a dilution of 10^{-6} or 10^{-7} depending on optical density of the culture on vibrio selective Thiosulfat-Citrat-Bile-Saccharose (TCBS; Fluka Analytica) agar plates. Plates were incubated upside down over night at 25°C and the total number of colonies was counted the following day.

Phage densities

We used spectrophotometry to quantify the prevalence of the filamentous phage using the protocol published on the website of Antibody Design LabsTM (Abdesinglabs 2013). Spectrophotometry is the standard method for quantifying filamentous phages because phage infection does not necessarily result in lysis of bacterial cells. The method is based on the constant relationship between the length of viral DNA and the amount of the major coat protein VIII. Both are major contributors to the absorption in the UV range. The amount of phage particles per ml was calculated according to the following formula:

$$\frac{\text{phages}}{\text{ml}} = \frac{\text{A269} - \text{A320} \times 6 \times 10^{15}}{\text{bp}}$$

where A269 and A320 stand for absorption at 269 and 320 nm (Abdesinglabs 2013). Bp is the genome size of the vibriophagesVALGΦ8 in base pairs, which is 7079 bp (Chibani, Hertel et al. 2019)

After centrifuging 1500 μl of each 24-hour culture at 13,000 g for 2 min, 1200 μl of the supernatant was mixed with 300 μl PEG/NaCl 5× and incubated on ice for 30 min. Subsequently, phage particles were pelleted by two rounds of centrifugation at 13,000 g for 2 min, resuspended in 120 μl TBS (1×) by vortexing and incubated on ice. After one hour, the suspension was cleaned by centrifugation at 13,000 g for 1 min and absorbance was measured at 269 and 320 nm. From the calculated phage particle number, we deducted the average of six blank samples. Blank measurements were conducted with medium101. The quantification limit for this method is 1.3^{12} phage ml^{-1}, which was calculated by adding ten times the standard deviation to the average of the blanks (Shrivastava and Gupta 2011). Below this threshold, the spectrophotometric quantification of filamentous phages is susceptible to inaccuracies.

In addition, we used standard spot assays (Mirzaei and Nilsson 2015) in parallel to determine the presence or absence of phages if PEG values were below the quantification limit. Opaque zones are not necessary caused by lysis and are mainly due to reduced growth rates. Using spot assays allowed us to assess whether the co-evolving phages were able to infect the ancestral K01M1 strain. To do so, we diluted all populations at the end of each transfer 1:100 using medium101 with the respective salinity. Diluted cultures were incubated in 96-well plates at 25 °C for 7 hours. Subsequently, cultures were centrifuged at 2000 g for 2 min and the supernatant was filtered through 0.2 μm filters to remove bacteria. We used TM buffer to dilute phages in 1:10 steps up to 10^{7}. Meanwhile, the overlay agar (0.5% (w/v) peptone, 0.3% (w/v) meat extract, 0.2% (w/v) agar, 1.5% (w/v) NaCl in MilliQ water) was boiled and cooled down to 38°C in a water bath. Afterwards, we poured 5 ml overlay agar containing 1 ml of log-phase growing ancestral K01M1 cultures onto medium101 agar plates. After 30 min, we spotted 4 μl of each dilution onto the overlay agar and incubated the plates overnight at 25 °C before checking for plaques.

4.3.4 | Overnight growth curves of bacterial populations

We monitored the optical density of subcultures to get an impression on small scale dynamics in the populations. Approximately 1 h after clones were picked from single colonies and placed into growth containers with medium101 and 1h after the following transfers: T01, T02, T03, T04, T05, T07, T08, T10, T11, T12 T14, T15, T17, T18, T22, T23, T25, T30, we added a subpopulation of 200 μl to a transparent, flat-bottom 96-well microtitre (Nunclon™) plate and placed it in a plater reader (TECAN infinite M200), where optical density measurements were taken every 20 min at 600 nm (OD_{600}) for 23 hours. Plates were shaken for 10 seconds at 200 rpm prior to each measurement.

4.3.5 | Measuring phage-resistance

We tested bacterial resistance against the ancestral vibriophagesVALGΦ8 by measuring its ability to inhibit growth of evolved clones using a reduction in bacterial growth assay (RBG) in liquid culture (adapted from Poullain, Gandon et al. 2008, Wright, Friman et al. 2018) and modified according to Wendling *et al*. (2018). Twenty-four random colonies of each infected population and twelve random colonies of each control population from transfer T0, T2, T3, T4, T6, T10, T12, T16, T22 and T29 were revived from cryo-stocks. In a few cases the number of tested clones was below 24 due to lower numbers of colony forming units (CFU) on the TCBS agar plates during the evolution experiment.

The RBG-assay was conducted in 96-well microtitre plates containing 120 μl medium101 (15 PSU) to which we added 15 μl of exponentially growing bacteria (~5×10^{8} CFU ml^{-1}) and 15 μl of the ancestral vibriophagesVALGΦ8 (~5×10^{9} PFU ml^{-1}). In addition, we assessed reference bacterial growth by adding 15 μl TM-buffer instead of phages to the bacterial culture. We measured absorbance at 600 nm using an automated plate reader directly after adding the bacteria to medium101 containing the phages (t0) and again after 18 hours (t18) of static incubation at 25°C (S2). The reduction in bacterial growth imposed by vibriophagesVALGΦ8 on clone j, was calculated according to the following formula:

$$RBGj = \frac{OD_{600}\,(t = 18h) - OD_{600}\,(t = 0h)\ (\mathrm{VALG\Phi8, j})}{OD_{600}\,(t = 18h) - OD_{600}\,(t = 0h)\ (Control\ j)}$$

where OD_{600} is the optical density. In a previous study with the same *Vibrio* bacteria-phage system, we observed a bimodal histogram of all RBG values with a local minimum at RBG = 0.82 and concluded that values above 0.82 indicate little or no phage-imposed cost to bacterial growth (Wendling, Goehlich et al. 2018). In this study, we considered clones to be phage resistant if RGB values were above 0.82.

4.3.6 | Frequency of resistant, phage-infected clones

In a previous study (Wendling, Chibani et al. unpublished data), we found two mechanisms contributing to bacterial resistance against the co-evolving filamentous vibriophagesVALGΦ8: (1) resistance was achieved either by superinfection exclusion resulting from the presence of the co-evolving phage in the bacteria cell or (2) resistance was acquired by another, so far unidentified mechanism. To quantify the frequency of co-evolving strains that acquired resistance by superinfection exclusion, we used PCR with a primer pair (Forward primer: TGGAAGTGCCAAGGTTTGGT; Reverse primer: GAAGACCAGGTGGCGGTAAA) that specifically targets a unique region in the co-evolving vibriophagesVALGΦ8. Overnight cultures of the same clones that were used in the RBG assay (see 2.5) were diluted 1:10 with sterile water and frozen at -20°C to disrupt bacterial cell walls. PCR was conducted using the standard protocol for the Thermo Scientific™ DreamTaq™ DNA Polymerase, followed by gel electrophoresis using QIAxcel Advanced System™. PCR-bands at a length of 1.4 kbp were interpreted as presence of phages in the bacterial cell. The absence of a PCR product in phage resistant clones was interpreted as resistance by an unidentified mechanism.

4.3.7 | Cost of resistance

To determine the cost of phage resistance, we selected one resistant phage-infected bacterial clone (PCR-positive) (n = 19) and one resistant non-infected clone (PCR negative) (n = 17) from transfer six as well as one clone from each control population (n = 16). In one 7 PSU population, we found only phage infected resistant clones. Therefore, we used two of them and no uninfected clone, resulting in the unbalanced number of PCR positive and negative clones. We chose transfer six because it is the last time point of the experiment in which at least one of the 24 picked clones of the co-evolving population was either PCR positive or PCR negative. In the control populations (n = 16), we did not assay clones from populations 3 (7 PSU) and population 15 (fluctuating conditions), which were contaminated with phages during the experiment. Selected clones were used for both whole genome sequencing and phenotypic assays measuring (a) bacterial growth rate and phage production. We revived clones from cryo-cultures by incubating them over night in medium101 in the salinity they were selected at after the 6th transfer. Clones from fluctuating conditions were incubated at 15 PSU because they grew in 15 PSU medium on transfer six. The protocols for both assays are described in the following sections.

Absolute Growth rate of single clones

All selected clones were picked from cryo-stocks and regrown in triplicated overnight cultures (ONC). Two μl of ONC was added to 198 μl medium101 in a 96 well plate. Bacterial growth of all clones was assessed in 15 PSU and 7 PSU medium. Optical density of cultures was measured every 20 min for 24 hours using an automated plate reader (TECAN infinite M200).

Phage production of single clones

All overnight clones were diluted 1:100 and incubated in 15 ml Falcon tubes containing 6 ml medium101 with the respective salinity the clones were selected at during the evolution experiment. Clones evolved at fluctuating salinity were incubated at 15 and 7 PSU. After 24-hour incubation at 25 °C and 180 rpm, phage density was measured using spectrophotometry following PEG precipitation as described in section 2.3.2.

4.3.8 | Whole genome sequencing of evolved clones

In order to determine the genetic basis of the observed resistance mechanism, we sequenced the genomes of the same clones (2.7.), which were used for the fitness assays, i.e. one phage-resistant PCR-negative clone and one phage-resistant, PCR-positive clone per co-evolving population and one phage-susceptible clone from each control population at transfer six. DNA for sequencing was isolated from cultures grown in medium101 for 16 h at 25 °C and 180 rpm. High molecular weight DNA was extracted using DNeasy Blood & Tissue Kit (Qiagen, Hilden, Germany).

Sequencing was done using an Illumina 2500 device. The quality of the reads was evaluated with the program FastQC Version 0.11.5. Illumina reads of each sampled clone were assembled using Spades version 3.14.0 (Bankevich, Nurk et al. 2012). In-silico PCR (http://insilico.ehu.eus) on assembled contigs as template and infecting phage-specific primers was used to confirm the empirical PCR results and the presence of the infecting phage in each clone. To identify mutations conferring resistance against the phage we used *breseq* Variant Report pipeline (version 0.35.0) (Deatherage and Barrick 2014). Paired reads were mapped to the annotated reference genome of ancestral K01M1 (GenBank accession number: CP017889.1, CP017890.1) assembled from Pacbio and Illumina sequences using Unicycler (Wick, Judd et al. 2017). Variants that occurred in all replicates were discarded as they represent differences between the reference genome and the ancestral genotype used in the experiment.

4.3.9 | Statistical analyses

All statistics were performed in the R 3.5.1 statistical environment (RCoreTeam 2020). We excluded the contaminated control populations P3 & P15 from all further analyses.

If not otherwise stated we used Maximum Likelihood estimation in linear mixed effect models and tested significance using ANOVA type marginal for models with interaction, or ANOVA type sequential in models with no interaction. We initially included all interaction terms in the models before reducing each model by sequentially removing non-significant interactions according to Akaike Information Criterion (AIC) (Akaike 1976). Post-hoc tests were carried out using TukeyHSD (package: multcomp (Hothorn, Bretz et al. 2020)) or estimated marginal means (package: emmeans (Lenth, Singmann et al. 2020) for generalized least square models.

Bacteria and phage dynamics

We analysed bacteria and phage dynamics over time using generalised least square (gls) models (package: nlme4 (Bates, Machler et al. 2015)). The models were fitted using *PhageEvEx* (presence/absence) and *SalinityEvEx* (7 PSU, 15 PSU, or fluctuating) as fixed effects, and *Transfer* as integer. Weight *varIdent(form=~1|Transfer)* was introduced to account for heterogeneous variances over time and the term (*corAR1(0.6, form=~1|Day*) for autocorrelation. The model suggests a significant interaction between *PhageEvEx*, *Transfer* and *SalinityEvEx* for bacteria dynamics (gls: $F_{1,665} = 5.2$, $p = .006$;S 3) and a significant interaction between *PhageEvEx* and *Transfer* for phage dynamics (gls: $F_{1,678} = 3.3$, $p < .039$; S 4). We thus divided the data set in co-evolving populations and control populations (without phages) to test for the effect of *SalinityEvEx* and *Transfer* on bacteria and phage dynamics. In order to compare the decrease in phage particles over time between the different salinities, we applied an additional gls model comprising the transfers T3 to T9.

Reduction in bacterial growth assay

Bacterial resistance as a ratio of susceptible and resistant clones was analysed using a generalized linear mixed model (glmer – package lme4 (Bates, Machler et al. 2015)) with a binomial error distribution, *SalinityEvEx* (7 PSU, 15 PSU, fluctuating), *PhageEvEx* (presence/absence) as fixed effects, *Transfer* as integer and *Population* as random effect. The model suggests a significant interaction between *PhageEvEx* and *Transfer* (glmer: $\chi^2_2 = 9.8$, $p = .004$, S 5a). Control populations (without phages) were thus excluded from further analyses to test for the effect of *SalinityEvEx* and *Transfer* on phage-resistance evolution.

Resistance mechanism

The proportion of resistant clones carrying vibriophagesVALGΦ8 in the co-evolving populations was analysed as a ratio of resistant phage-infected (PCR positive) vs. resistant non-infected (PCR negative) clones using a generalized linear mixed model (glmer – package lme4 (Bates, Machler et al. 2015) with a binomial error distribution. SalinityEvEx (7 PSU, 15 PSU, fluctuating) and Transfer were assigned as fixed effects and Population as random effect.

Fitness assays

Bacterial growth curves were analysed in R using the package Grofit (Kahm, Hasenbrink et al. 2010) to estimate the maximum slope μ (growth rate) and the maximum bacterial growth A (yield), which is equivalent to the carrying capacity in the stationary phase. To determine differences in bacterial growth rate (μ) and growth yield (A) of selected assay clones at 15 PSU and 7 PSU in the follow-up growth assay of the evolution experiment, we applied a Welch's two sample t-test. To do so, we divided the dataset in *SalinityAssay* 15 PSU and 7 PSU (S6a).

Furthermore, we split the dataset in clones evolved at 15 PSU, 7 PSU and fluctuating to identify differences between controls and resistant clones evolved at respective salinities and the ancestral strain. We applied two orthogonal contrasts for each *SalinityEvEx* and each *SalinityAssay* because the experimental design was not fully factorial, i.e. the ancestral strain, evolved controls (populations without phages) and phage-resistant clones (non-infected/infected) constitute different hierarchical levels. The hierarchical levels and contrasts are the following: C1) Non-evolved (ancestral) strain vs. evolved clones, i.e. controls and co-evolved resistant clones, and C 2) Evolved non-resistant control clones and co-evolved resistant clones, comprised of non-infected resistant clones (PCR negative) and phage-infected clones (PCR positive). A third contrast (C3) was used to identify differences between growth rates of resistant non-infected clones (PCR negative) and resistant infected clones (PCR positive). Two additional contrasts for each assay-salinity were used to test for growth difference between CS1: clones evolved at 15 PSU vs. clones evolved at 7 PSU and fluctuating conditions and CS2: clones evolved at 7 PSU vs. fluctuating conditions.

For phage production, we applied the same contrasts as above (S6). Contrast analyses were followed by fitting linear mixed effect models (lmer – package lme4) with bacterial growth μ, maximum bacterial growth A or phage production as dependent variables. As fixed effects, we used *SalinityEvEx* (7 PSU, 15 PSU, fluctuating) and the phenotypic *resistance type* (phage infected/ phage non-infected). Day of the assays was included as random effect because fitness assays were conducted in four blocks and replicates of each clone were not evenly distributed across blocks.

Correlation between the number of cell forming units and the proportion of resistance / infected cells throughout the evolution experiment.

We performed a spearman-rank correlation using the function ggscatter (package: ggpubr (Kassambara 2019) to test for correlations between the number of cell-forming units (CFU) and the proportion of resistant clones as well as for correlations between the number of cell forming units and the proportion of infected clones, respectively. Data from the following transfers were included into the correlation analyses T02, T03, T04, T06, T10, T12, T16, T22 and T29.

4.3.10 | Mathematical modelling

We modelled the dynamics of the three different bacterial populations, i.e. non-resistant clones (*B*), resistant phage-infected clones (*I*) and resistant non-infected clones (*R*) as well as the phage population (*V*) for each salinity treatment in batch cultures with limiting resource (*N)* by the following system of differential equations:

$$\frac{dN}{dt} = -c\,(g_B(N)B + g_I(N)(I + IR) + g_R(N)R)$$

$$\frac{dB}{dt} = (1-m)\,(g_B(N)B - \Phi BV)$$

$$\frac{dI}{dt} = (1-m)\,(g_I(N)I + \Phi BV)$$

$$\frac{dR}{dt} = g_R(N)R + mg_B(N)B$$

$$\frac{dIR}{dt} = g_I(N)IR + mg_I(N)I$$

$$\frac{dV}{dt} = ß(I + IR) - dV$$

Resource consumption and bacterial growth rate was modelled by a type-specific Monod term of the form $g_i(N) = \frac{a_i N}{H+N}$,

with $i = B, I, R$ or IR depending on whether it is the ancestor *B*; a resistant, phage-infected clone *I*; a non-infected, resistant clone (*R*) or a resistant, phage-infected clone carrying also the 2nd additional resistance mechanism (*IR)*.

Here i is the maximum growth rate (mgr) of the respective bacterial clone. The

efficiency of resource conversion into bacterial biomass (c), and the resource concentration (H) at which half of the maximal growth rate is attained, are assumed to be the same for all clones.

Viruses (*V*) infect non-resistant ancestral bacteria (*B)* following a mass action law with adsorption rate (*f*), reflecting that increasing densities of either bacteria or viruses lead to higher encounter rates and thus more infections. Infection of a bacterial cell transforms cells into a resistant, phage-infected clone (*I)*, which actively produces new viral particles (*V*) with a phage production rate (*ß*). Additionally, both ancestral bacteria (*B)* and phage-infected clones (*I)* can acquire a mode of resistance (*R* & *IR*), which renders them completely resistant.

Phage-infected clones *(I + IR)* have a reduced maximum growth rate compared to resistant, non-infected clones and the ancestor (*B*), so that $a_{RI} = a_I < a_R < a_B$ (Table 1). All bacterial types grow until resources (*N*) are depleted, but bacteria-virus interactions continue to occur as long as there are sensitive bacteria and viruses left. After a certain time t_{max} a portion of the entire community is transferred to fresh medium and the process restarts.

Table 1: Parameter values of mathematical model and their biological meaning

Parameter	Biological meaning	Value
a_B	maximum growth rate (mgr) of ancestor *B*	15 PSU: 0.5 (h^{-1}), 10 PSU: 0.35 (h^{-1}), 7 PSU: 0.3 (h^{-1})
aR	mgr of resistant, non-infected clones *R*	0.95 × *a*B (h^{-1})
aI	mgr of resistant, phage-infected clones *I*	0.7 × *aB* (h^{-1})
aIR	mgr of resistant, phage-infected, mut clones IR	0.7 × aB (h^{-1})
H	bacterial half-saturation constant	0.01 (μg ml^{-1})
c	bacterial conversion efficiency	10^{-6}
f	phage adsorption rate	10^{-8} (h^{-1})
ß	phage production rate	15 phages/cell h^{-1}
d	phage decay rate	0.1 (h^{-1})
m	mutation rate	10^{-8}

4.3.11 | Validation of model parameters

For model validation and to gain a better understanding of bacterial growth and phage production within a transfer cycle of 24 hours, we closely monitored two infected clones from transfer six, one evolved at 7 PSU and one evolved at 15 PSU as well as the ancestral strain K01M1 and strain K04M1 from which the co-evolving vibriophagesVALGΦ8 had been originally isolated. To do so, three replicate overnight cultures of each clone were diluted 1:100 and incubated in falcon tubes containing 15 ml medium101. We monitored phage production (using PEG precipitation and spot assays), optical density of bacterial population at 600 nm (OD_{600}) and number of cell forming units (CFU) at the start of the incubation (time point, TP0), after one hour (TP1) and then every 2 hours until TP17 and again at TP24. CFU and phage density (measured by spot assays and PEG precipitation) were quantified as described above.

In order to achieve a higher number of replicates compared to the previous assay and a better understanding of the number of VALGΦ8 phages released per infected clone, we measured the number of phage particles, using spot assays (plaque forming units (PFU)) and the number of cell forming units (CFUs) after a six hours growth assay.

To do so, we selected the six PCR positive clones used for sequencing plus four additional PCR positive clones per salinity treatment, i.e. 15 & 7 PSU. All clones were revived from cryo-cultures grown overnight in the respective media, in which it evolved, i.e. 15 PSU and 7 PSU medium101, and subsequently diluted 1:100 with the same medium. We measured CFU and PFU directly after the dilution step and after six hours of shaking incubation at 180 rpm and 25 °C.

CFU was determined by plating diluted cultures onto TCBS agar plates, which were incubated overnight at 25 °C. For the determination of PFU, we used standard spot assays, as described in section 2.4. This time, by reducing the incubation time of bacteria added to the overlay agar by 1 hour, we were able to obtain single plaques.

4.4 | Results

4.4.1 | Bacteria and phage dynamics

Bacterial recovery after phage infection takes longer at 7 PSU

Six replicate *Vibrio alginolyticus* populations were propagated for 30 serial transfers (i.e. approximately 240 generations) in the presence or absence of a filamentous phage vibriophagesVALGΦ8 at three different salinity treatments: ambient (15 PSU), low (7 PSU) and fluctuating between 15 and 7 PSU.

Bacterial population densities measured as the number of cell forming units (CFU) differed significantly between populations that co-evolved with the phage and control populations (significant interaction between *PhageEvEx*:*Transfer* in generalised least square model (gls): ($F_{1,665} = 5.2, p = .006$; Figure 2 & S 3). Therefore, we split the data set into control (without phage) and infected populations (with phage) to further investigate the effect of salinity on phage-resistance evolution.

In the absence of a co-evolving phage, bacterial population densities differed significantly between salinity treatments (significant *SalinityEvEx*:*Transfer* interaction in gls: $F_{1,313} = 3.7, p = .026$; Table S **7**). At 15 PSU and in the fluctuating treatment population densities remained similar across 30 transfers (no significant *Transfer* effect in gls: 15 PSU: $F_{1,117} = 0.3, p = .574$; CFU, mean ± s.d.: $6.3\times10^{9} \pm 2.2\times10^{9}$; fluctuating: $F_{1,101} = 1.9, p = .164$; CFU: $5.4\times10^{9} \pm 2.1\times10^{9}$). However, at 7 PSU population densities doubled (significant *Transfer* effect in gls: $F_{1,95} = 10.0, p = .002$) from the early stage of the experiment i.e. transfer 1 (T1) - T3 ($3.0\times10^{9} \pm 1.6\times10^{9}$) to the late phase, i.e. T25 - T29 (CFU: $6.3\times10^{9} \pm 1.4\times10^{9}$;), indicating adaptive evolution to the 7 PSU treatment.

In the presence of the phage, temporal bacterial population densities differed significantly between salinity treatments (significant *SalinityEvEx*:*Transfer* effect in gls: $F_{2,346} = 3.6, p = .030$; Table S 8). After adding phages to the microcosms at T1, the density of all bacterial populations decreased by one order of magnitude relative to T0. While this crash in population size in response to the phage occurred in all salinities, we observed a significant salinity-time interaction with regard to (1) time point of lowest population size and (2) time point of recovery. Bacteria co-evolved at 15 PSU had the lowest population size at T2 (6.90×10^{8} CFU ± 2.1×10^{8}), populations at fluctuating conditions at T3 (7.83×10^{8} CFU) and populations growing at 7 PSU at T4 (1.45×10^{8}). At 15 PSU and fluctuating conditions bacterial populations recovered to starting densities at T7 and T6 respectively. However, at 7 PSU, recovery took twice as long (T12).

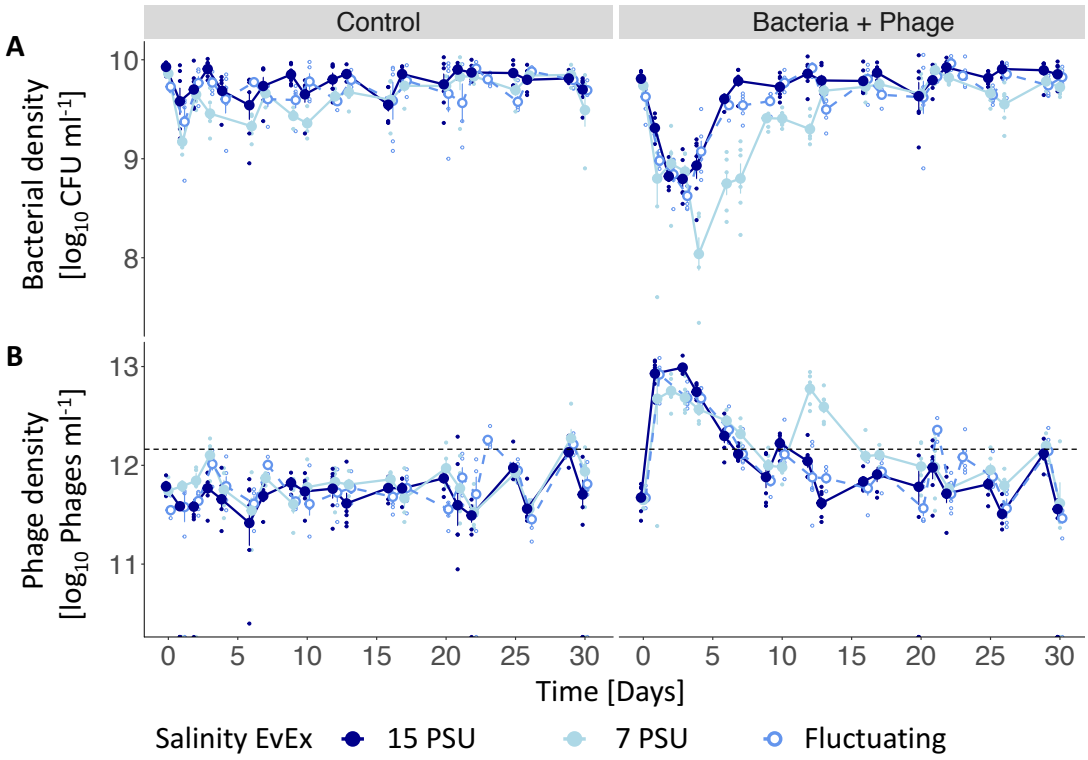

Figure 2: Bacterial and phage dynamics. (A) Bacterial densities are shown as colony forming units (CFU ml^{-1}) and (B) Phage densities as phage particles measured by PEG precipitation (Phages ml^{-1}) over 30 days/transfers (x-axis) in the absence of a co-evolving phage (left) and in the presence of a co-evolving phage (right). Individual replicate populations are represented by small dots (n=6) and means by larger points (± s.e.). Colours represent the salinity level during the evolution experiment (dark blue: 15 PSU, light blue: 7 PSU, blue and dashed line: fluctuating). The black, dashed, horizontal line in panel (B) indicates the quantification limit for phage concentrations.

Filamentous phages persist longer at 7 PSU

Phage densities differed significantly between co-evolving populations and control populations (significant *PhageEvEx:Transfer* interaction in gls model: $F_{1,678} = 3.3$, $p < .039$; S 4). Quantified phage particles in control populations resulted from a low productivity of the resident vibriophagesVALGΦ6 of the K01M1 strain. These, however, mainly remained below the quantification limit throughout the experiment, except for fluctuating populations at transfer T23 and for 7 PSU populations at T29. We thus split the data set into control (without phage) and infected populations (with phage) to further investigate the effect of salinity on the temporal dynamics of the coevolving phage.

After adding the filamentous vibriophagesVALGΦ8 at transfer 1 (T1) to the bacterial populations, phage concentrations reached levels higher than 5.0×10^{12} PFU ml^{-1} (Figure 1). While this initial peak in phage densities was visible in all salinities, phage dynamics were

also affected by salinity (significant interaction between *SalinityEvEx:Transfer* in generalised least square model (gls) for T3-T9: $F_{2,354} = 6.0$, $p = .004$; Table S **9**). At 7 PSU and in fluctuating conditions phage densities decreased from T1 onwards. However, at 15 PSU phage densities first increased for three days to 7.3×10^{13} m PFU/ml before they also started to decrease (Figure 1). While phage concentrations remained below the detection limit at 15 PSU and in fluctuating conditions, at 7 PSU, phage densities reached a second peak between T10 and T12 with concentrations similar to T1. Afterwards, phage concentration remained below the quantification limit until the end of the experiment.

Phages are produced in all co-evolving populations at all time points

In order to find support that increased phage-densities in the coevolving treatments were caused by the coevolving vibriophagesVALGΦ8 and not the resident vibriophagesVALGΦ6, bacterial populations were grown in new medium of the respective salinity for 7 hours and the supernatant was spotted on the ancestral K01M1 strain. As the ancestral K01M1 carries the resident vibriophagesVALGΦ6 it is immune to superinfection by phages particles of this kind and only the co-evolving vibriophagesVALGΦ8 is able to cause clearing zones of reduced bacterial growth (Wendling, Piecyk et al. 2017). Furthermore, spot assays are much more sensitive to low phage densities compared to optical measurements using PEG precipitation. Throughout the experiment, all co-evolving populations produced VALGΦ8 phage particles causing opaque zones of reduced growth zones, regardless of salinity (Figure S10).

Spotting the supernatant of control populations, which only contained the resident ancestral phage of K01M1, did not result in clear plaques, except in populations P3 and P15, indicating contamination with the coevolving vibriophagesVALGΦ8. Both populations were excluded from the analyses.

4.4.2 | Bacterial resistance evolution and prevalence of phage-infected clones

Bacterial resistance acquisition is delayed at 7 PSU

In the absence of the co-evolving phage, we observed a small proportion of clones that were resistant to the co-evolving vibriophagesVALGΦ8 (0.67 ± 2.83%) in all salinities. In contrast, a rapid increase in resistant clones occurred in populations exposed to the co-evolving phage (significant *Transfer*:*PhageEvEx* effect in generalised linear mixed effect model (glmer): $\chi^2_2 = 9.8, p < .008$; S 5). Subsequently, statistics include only phage infected populations to further investigate the effect of salinity on the presence of resistant clones.

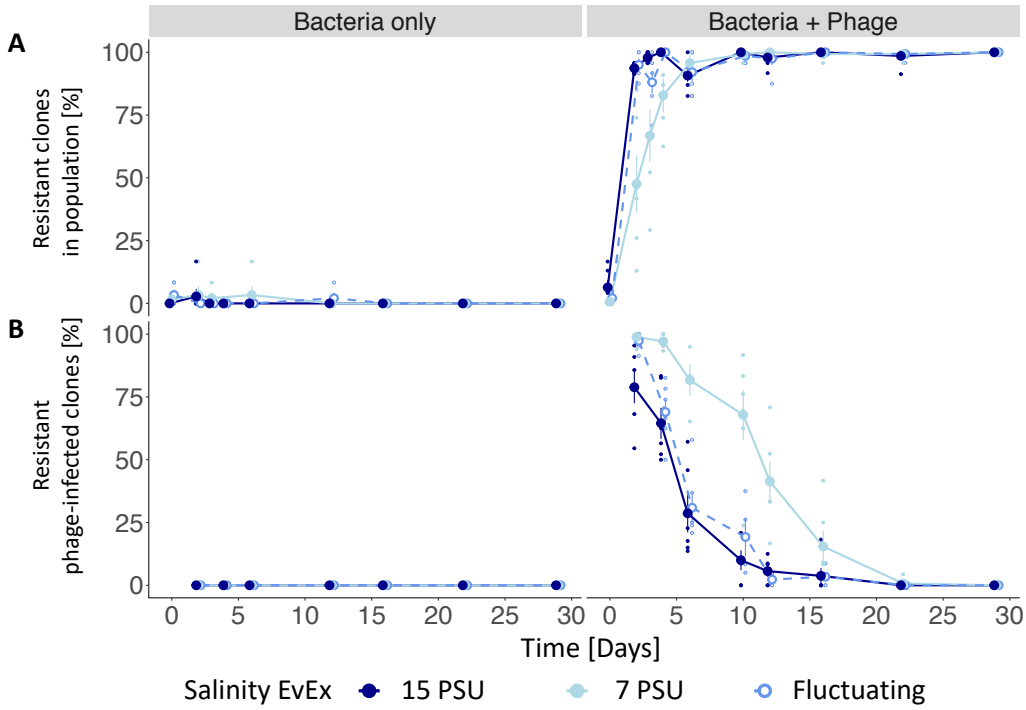

Figure 3: Bacterial resistance (A) and percentage of phage-infected clones on the total number of resistant clones (B). Resistance of bacterial clones was tested against the ancestral bacteriophage VALGΦ8 (throughout the 30-day/transfer evolution experiment. The proportion of phage resistant clones carrying the VALGΦ8 decreased over time. Single replicates (n=24) are indicated by small dots and means by larger points (± s.e.). Colours represent salinity levels during the evolution experiment (dark blue: 15PSU, light blue: 7PSU, blue and dashed line: fluctuating).

After 48 hours at 15 PSU and fluctuating conditions, 95% of 24 tested clones per population acquired resistance to the ancestral genotype of the coevolving phage. At 7 PSU, it took the bacteria until day 6, and thus approximately 25 - 30 generations longer, to reach a similar frequency of resistant clones per population as in the other two salinity treatments

(significant *Transfer*:*SalinityEvEx* effect in generalised linear mixed effect model (glmer): $\chi^2_2 = 9.7, p = .008$; S 10). At fluctuating conditions, resistance decreased again to 88% at T3, when exposed to low saline conditions, whereas 15 PSU populations had an average of 98% resistant clones at the same time. Afterwards, fluctuating and 15 PSU populations followed very similar patterns. In both salinity treatments 100% of the clones were resistant against the ancestral phage at T4. In 7 PSU, resistance was fixed in five out of six populations at T10 and eventually in all populations at T29.

Resistant phage-infected clones remain longer at 7 PSU

Resistance to the filamentous vibriophagesVALGΦ8 can emerge (1) through the presence of the co-evolving phage inside the bacterial host, i.e. superinfection exclusion or (2) through another, so far un-identified, mechanisms that confers resistance in the absence of vibriophagesVALGΦ8 (Wendling et al. unpublished data). To investigate which resistance form is present in the populations we determined the proportion of phage-resistant bacterial cells (determined in 3.2.1) that carried the co-evolving vibriophagesVALGΦ8 at different time points of the experiment using PCR. PCR-positive clones were subsequently termed as resistant infected clones, and PCR negative clones were termed as resistant non-infected clones. Forty-eight hours (T2) after adding the phages (i.e. ~15 bacteria generations) the majority of resistant clones carried the phage in all salinities.

From T4 onwards, the proportion of phage infected clones in the 15 PSU and the fluctuating treatment declined at the same rate, while simultaneously, clones with another resistance form started to increase. At T12, phage-infected clones were outcompeted by resistant non-infected clones in three out of six populations at 15 PSU and fluctuating conditions and persisted at low frequencies in the remaining three populations (15 PSU: 10.2 ±2.6%; Fluctuating: 4.6 ±1.3%). In contrast, at 7 PSU, phage-infected, resistant clones remained significantly longer in the populations (significant *SalinityEvEx:Transfer* interaction in generalised linear mixed effect model (glmer): $\chi^2_2 = 32.0, p < .001$; S 11). This suggests that selection against phage-infected clones is relaxed at 7 PSU compared to 15 PSU and the fluctuating treatment.

Recovery of bacterial populations starts after the decline of phage-infected clones

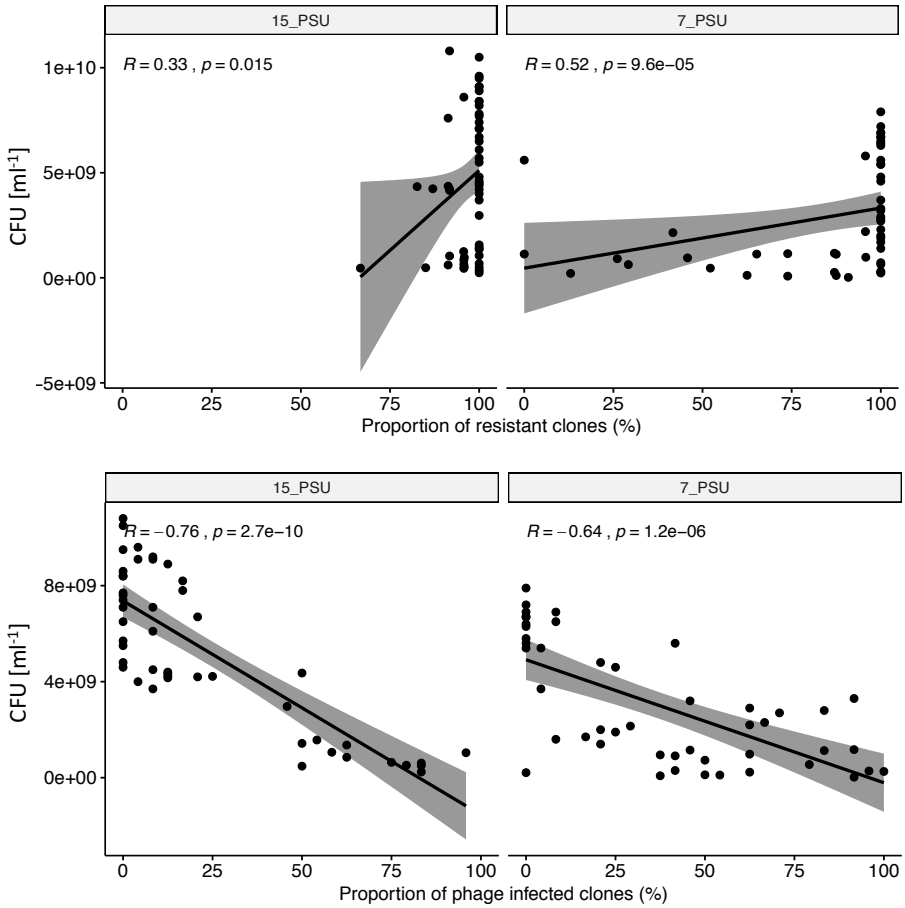

Figure 4: Recovery in bacterial density is driven by resistance evolution and the disappearance of phage-infected clones.
Number of cell forming units (CFU) on the y-axis is correlated either with the proportion of resistant clones (upper panel) or with the proportion of phage-infected cells (lower panel). The right panel shows the data from transfer 2 to 29 of populations evolved at 15 PSU, the left panel the populations evolved at 7 PSU.

To identify whether bacterial recovery is driven by the prevalence of the co-evolving phage and thus superinfection exclusion, we correlated bacterial densities with the proportion of resistant clones as well as with phage-infected clones only. The slope in the correlation between CFU and proportion of phage-infected clones is steeper (15 PSU: - 0.76, $p < .001$; 7 PSU: R = - 0.64, $p < .001$; Figure 4) compared to the slop in the graph correlating CFU and the proportion of resistant clones (15 PSU: R = 0.33, $p < .015$; 7 PSU: R = 0.52, $p < .001$). This suggest that bacterial recovery is rather driven by the appearance of the 2nd

resistant mechanism and the loss of phage-infected clone than by the overall presence of resistance. Furthermore, the wide range of bacterial density in the population, when 100% of clones are resistant supports this hypothesis (Figure 4). In both correlations, the majority of data points are either at 100% resistant clones or 0% phage infected clones. To decrease zero inflation, i.e. we only plotted the proportion of resistant clones for T2-T12 and the proportion of phage-infected clones for the T2-T22 (Figure S 12). Reducing zero inflation confirms the previously observed patterns.

4.4.3 | Whole genome sequencing

We sequenced one resistant non-infected clone (PCR negative) and one resistant phage-infected clone (PCR positive) from each of the 18 populations (six per salinity treatment) that co-evolved with a phage and one clone from each control population to determine the genetic basis of the observed resistance mechanisms. In-silico PCR confirmed the presence and absence of the empirical PCRs with some exceptions. Statistics of follow up assays are based on PCR results obtained in the lab.

We identified mutations in secretion system II specific to phage infected treatments, most of them were in the same region as in a different co-evolution experiment involving the same *Vibrio* strain and the same filamentous phage (Wendling, Chibani et al. unpublished data). The final analysis and visualisation are still in progress.

4.4.4 | Fitness costs of phage resistance

To determine whether the observed phage-resistance mechanisms come with a fitness cost we measured (a) bacterial growth rates as a proxy for bacterial fitness and (b) phage production. Fitness assays were conducted using the ancestral strain K01M1, and the 54 sequenced clones which include one phage-infected and one non-infected resistant clone per co-evolving population as well as one clone from each of the control populations.

Phage infections reduces bacterial growth in all salinities

We measured bacterial growth rate (μ) for all clones in 15 PSU as well as in 7 PSU. The ancestral strain grew significantly slower in 7 PSU (mean ± s.d.) (0.044 $\Delta OD_{600}\,h^{-1}$ ± 0.008) compared to 15 PSU (0.101 $\Delta OD_{600}\,h^{-1}$ ± 0.006; Welch Two Sample t-test $t_{(1.8)} = 8.1$, $p = .02$). Similarly, all evolved clones had a lower growth rates at 7 PSU (0.062 $\Delta OD_{600}\,h^{-1}$ ± 0.007) compared to 15 PSU (0.106 $\Delta OD_{600}\,h^{-1}$ ± 0.009; Welch two sample t-test, $t_{(249.4)} = 44.2$, $p < .001$).

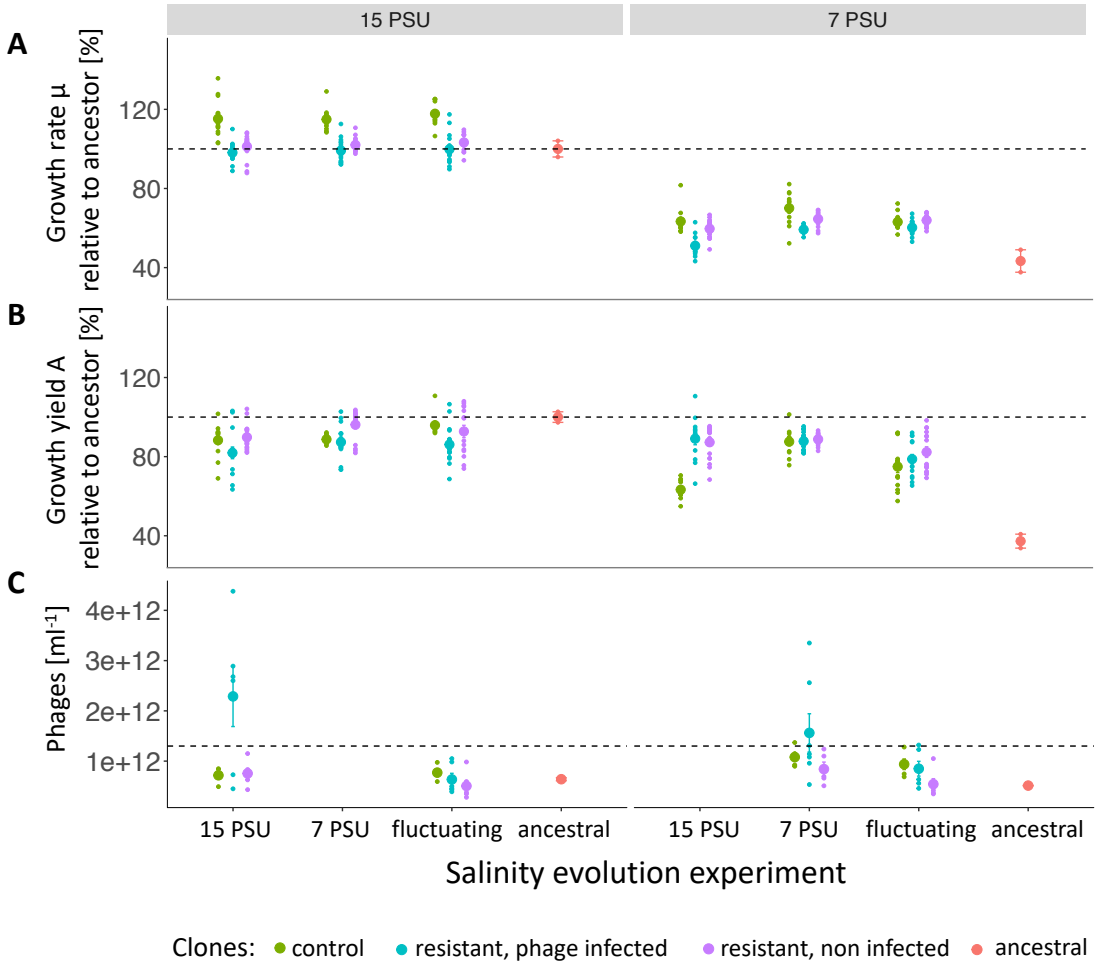

Figure 5: Mean bacterial growth (A), maximum yield (B) and phage production (C) were measured of individual clones from transfer 6 at 15 PSU (left panel) and at 7 PSU (right panel). Mean growth rates μ [% of $\Delta OD_{600}\,h^{-1}$] (A) and growth yield A [% of max OD_{600}] (B) are shown relative to the ancestral strain growing at 15 PSU (y-axis), which is indicated by the dashed line. Number of phage particles (y-axis) were measured after a growth period of 24 hours (C). The dashed line represents the determined quantification limit for the phage concentration using the spectrophotometric measurement. Data are grouped according to the salinity the clones experienced during the evolution experiment (x-axis). Colours specify the clone type: control populations (green), resistant, infected clones (blue), resistant, non-infected clones (purple) and ancestral K01M1 strain (red). A graph with growth data of single clones based on in-silico PCR is attached in the supplement (Figure S 16).

All evolved clones, including controls and co-evolved resistant clones, grew faster than the ancestral strains, when growth rate was measured at 7 PSU (Contrast 1 Salinity EvEx/Salinity assay ($C1_{All/7}$; $t(132) = 4.3, p < .001$; Table S 13) but not at 15 PSU ($C1_{All/15}$; $t(134) = 1.3, p < .191$). Clones evolved at 7 PSU (0.064 $\Delta OD_{600} h^{-1} \pm 0.007$) & fluctuating conditions (0.063 $\Delta OD_{600} h^{-1} \pm 0.004$) grew faster when growth rate was measured at 7 PSU than clones evolved at 15 PSU (0.058 $\Delta OD_{600} h^{-1} \pm 0.008$; Contrast S Saliniy EvEx 15 PSU/ Saliniy EvEx 7 PSU & fluctuating ($CS_{15/7\&fluc}$): $t(131) = -5.0, p < .001$; Table S14), supporting the observed adaptive evolution to 7 PSU (Figure 1). Importantly, adaptive evolution to 7 PSU did not come at a cost for growth at 15 PSU ($CS_{15/7\&fluc}$: $t(133) = 0.2, p = .865$).

Table 2: Comparison of growth performance. Average growth rates μ [$\Delta OD_{600} h^{-1}$] and growth yield A [max OD_{600}] of resistant phage-infected and non-infected clones are compared in the media they evolved, i.e. 15 PSU and 7 PSU. Data are based on 24-hour growth curves of single clones isolated at transfer 6 and visualized in Figure 5.

Salinity EvEx & Growth Assay	15 PSU		7 PSU	
	μ	A	μ	A
Non-infected resistant clone	0.102	1.042	0.065	1.030
Infected resistant clone	0.099	0.951	0.059	1.019
Growth of infected relative to non-infected clone (%)	96.9	91.2	91.7	98.8

Phage production is highest in phage-infected clones evolved at 15 PSU

Statistics of this section need to be interpreted with care because assessed phage concentrations are mostly below the quantification limit and thus prone to inaccuracy. The amount of produced phage particles per clone did neither differ between the ancestral strain and all evolved clones (Orthogonal contrast $C1_{All/15\&7}$ $t(70) = 1.7, p = 0.082$; Table S **17**) nor between non-resistant controls and resistant clones (Orthogonal contrast $C2_{All/15\&7}$ $t(74) = -0.8, p = .416$). The number of phages released by resistant clones is affected by the resistance type (significant *resistance type* effect in linear mixed effect model; $\chi^2_1 = 15.5, p < .001$) i.e. resistant, phage-infected clones produced significantly more phages (1.4×10^{12} phages $ml^{-1} \pm 1.1\times10^{12}$) than resistant, non-infected clones (6.5×10^{11} phages $ml^{-1} \pm 2.8 \times10^{11}$). Phage

production of coevolved clones was also modulated by salinity (significant *SalinityEvEx* effect in linear mixed effect model; $\chi^2_2 = 11.6$, $p < .004$; Table S 18). Clones co-evolved at 15 PSU produced most phage particles (1.5×10^{12} phages $ml^{-1} \pm 1.2\times10^{12}$) followed by coevolved clones from 7 PSU (1.3×10^{12} phages $ml^{-1} \pm 8.5\times10^{11}$) and fluctuating conditions (7.0×10^{11} phages $ml^{-1} \pm 3.9\times10^{11}$).

Intriguingly, the number of released phages varies strongly between phage-infected clones, regardless of the salinity treatment during coevolution, e.g. from 5.3×10^{11} to 3.4×10^{12} at 15 PSU and 4.5×10^{11} to 4.4×10^{12} at 7 PSU. This suggest that phage production is modulated on an individual level for each bacterial cell, not only by salinity but by other cellular mechanisms.

4.4.5 | Mathematical model

We applied a parameterized, mathematical model to better understand the effect of salinity on the ecological and evolutionary dynamics in our filamentous phage *Vibrio* bacteria system. The model includes data obtained from the evolution experiment, additional assays as well as the literature (Table 1). In particular, we wanted to know what is driving the delayed appearance and prolonged presence of resistant, phage-infected clones at 7 PSU.

The number of phage-infections was directly correlated with the frequency of phage-bacteria encounter (Figure 6). As the *V. alginolyticus* strain K01M1 grew faster at 15 PSU compared to 7 PSU, bacterial density increased more rapidly at 15 PSU. Higher bacterial density resulted in a higher frequency of phage-bacteria interaction and phage-infected bacterial clones. Phage-infected clones produced even more phages. This dynamic may explain why the fraction of phage-infected clones was lower at 7 PSU compared to the 15 PSU treatment at the beginning of the evolution experiment.

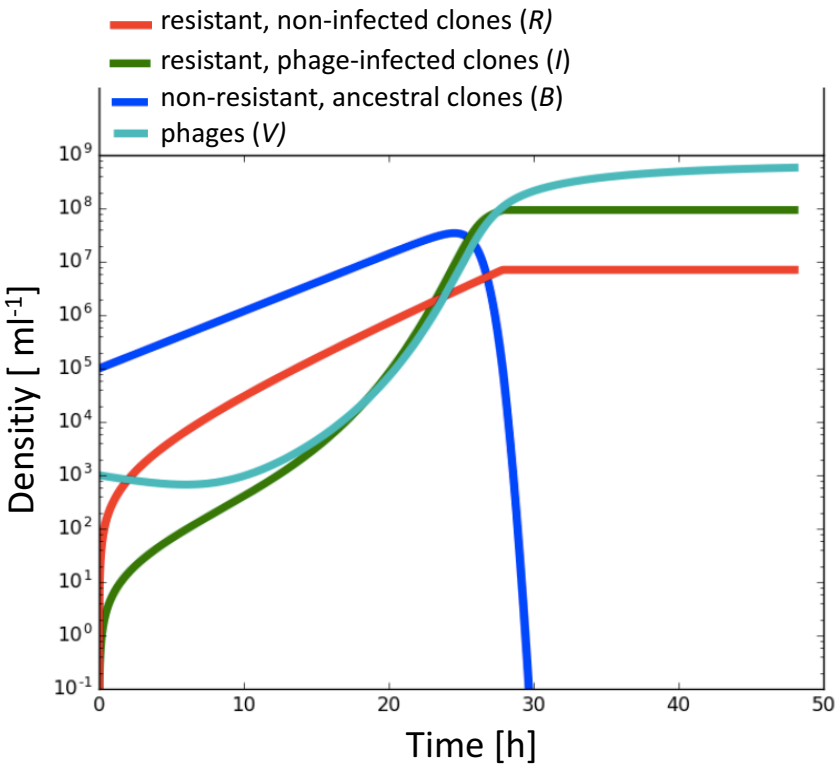

Figure 6: Modelled bacteria and phage dynamics. Density [ml^{-1}] (y-axis) of non-resistant clones (blue), resistant, phage infected (red) and resistant, non-infected clones (green) are displayed over the time course of the first 48 hours (x-axis) in 15 PSU populations.

The model suggests that resistant, non-infected clones appeared already within the first hour of the experiment (Figure 6). However, phage infections occurred at a higher rate than the rise of resistant, non-infected clones, especially toward the end of the first growth cycle (transfer), when bacterial densities of the ancestral strain are still high. Therefore, resistant, phage-infected clones outnumbered resistant, non-infected clones by one to two orders of magnitude making it unlikely to detect them by testing 24 clones. Over several transfers however, resistant, non-infected clones gradually replace phage-infected clones owing to their higher growth rate (Figure 7). Eventually, resistant, non-infected clones outcompete phage-infected clones. As in the experiment, resistant phage-infected clones are outcompeted about five to ten transfers earlier at 15 PSU compared to 7 PSU. This confirms that the model is able to capture the observed population dynamics in the evolution experiment.

In summary, the model suggests that the delayed occurrence and prolonged presence of phage-infected clones at 7 PSU is due to the lower bacterial growth rate which is accompanied by a reduced phage production in the population per time.

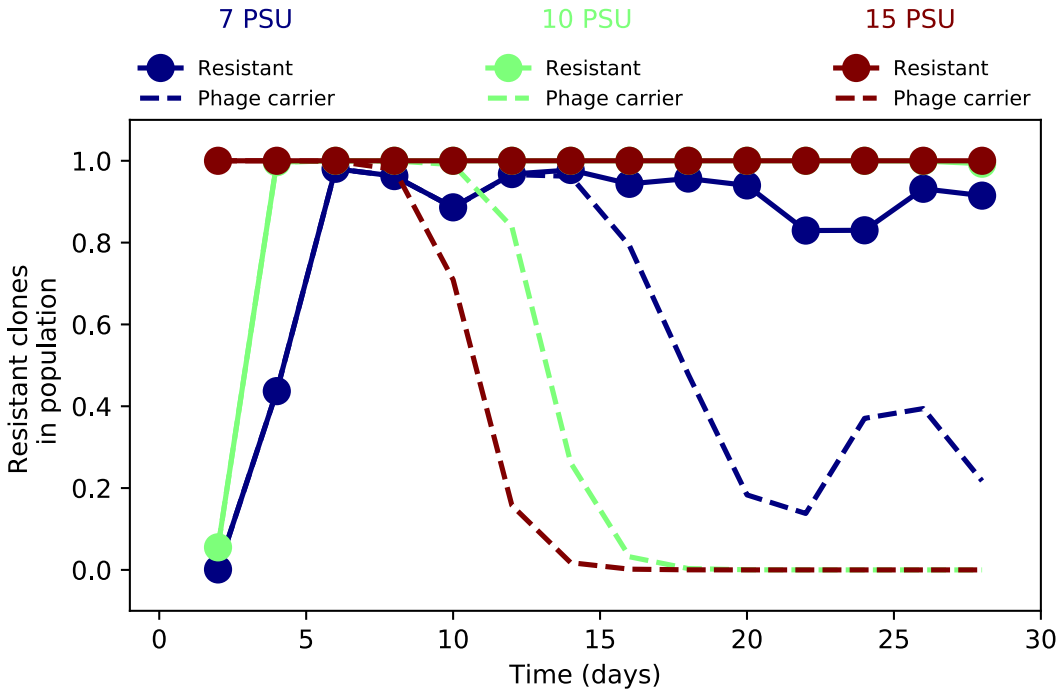

Figure 7: Proportion of resistant clones and phage-infected clones in populations modelled for different salinities. Higher phage production and associated costs for phage production at higher salinities resulted in faster gain of resistance and loss of phage-infected clones in bacterial populations.

4.5 | Discussion

Filamentous phages are recognized for their cooperative lifestyle (Hay and Lithgow 2019) providing various genes, which are potentially beneficial for their bacterial host (Mai-Prochnow, Hui et al. 2015). In this study, we investigated the effect of different salinity scenarios on the cost and benefits of filamentous phages for the bacterial host on evolutionary time scales.

In contrast to their cooperative reputation, filamentous phages used in this study significantly reduced growth of bacterial population shortly after first encounter. This reduction in population growth and size can be caused by phage-induced bacterial death (Kuo, Chiang et al. 1994, Kuo, Yang et al. 2000, Webb, Lau et al. 2004, Rice, Tan et al. 2009) prolonged bacterial generation time due to higher cost of replication (Roy and Mitra 1970, Kuo, Tan et al. 1991) or a combination of both. Based on our observations, we cannot exclude that the reduced population growth is caused by phage induced cell death in a fraction of bacteria cells within a population. An indicator that filamentous phages cause cell death are small-colony variants (Webb, Lau et al. 2004), which we observed on TCBS

agar plates used to determine the number of CFU. Additionally, parabolic bacterial growth curve after Mitomycin C exposure suggests a Mitomycin C induced mortality (Hüttmann 2013), which is characteristic for temperate phages switching from a lysogenic to a lytic cycle (Refardt and Rainey 2010). However, spot assays never resulted in clear plaques, which are typical for bacterial lysis (Jensen, Hair et al. 2015). Instead, vibriophagesVALGΦ8 caused zones of reduced growth resulting in opaque plaques, characteristic for chronically released filamentous phages (Kuo, Yang et al. 2000). Furthermore, genomic analysis of vibriophagesVALGΦ8 (Chibani, Hertel et al. 2019) revealed no toxin-antitoxin systems (Yamaguchi, Park et al. 2011), which when present in filamentous phages, can cause bacterial mortality upon removal of plasmids (Johnson, Strom et al. 1996) or phages (Lehnherr, Maguin et al. 1993, Webb, Lau et al. 2004) from the bacterial host.

Within one to two transfers (see also Wendling, Chibani et al. unpublished data) or after four transfers at reduced salinity more than 80% of bacterial clones gained resistance through superinfection exclusion, a mechanism of an established virus preventing a secondary infection by the same or a closely related phage (Berngruber, Weissing et al. 2010, Folimonova 2012). In our experiment and in previous studies using the same study system (Wendling, Piecyk et al. 2017, Wendling, Goehlich et al. 2018, Goehlich, Roth et al. 2019) we defined bacteria being resistant against phage infection, if the exposure of the ancestral vibriophagesVALGΦ8 does not reduce bacterial growth under the given conditions. However, phage infection without growth rate reduction may still occur.

To explain the delay in the lower number of resistant, phage-infected clones at transfer 2 and 3 in 7 PSU compared to the fluctuating and the 15 PSU treatment, we applied a mathematical model. The model suggests that due to the reduced bacterial growth rate the chance for phage-bacteria encounters is lower at 7 PSU in the initial state of the first 24-hour growth period (T1). This results in a lower frequency of phage infections and thus in a lower number of phage-producing bacteria cells.

In summary, the model suggests that the delayed occurrence and prolonged presence of phage-infected clones at 7 PSU is due to the lower bacterial growth rate which is accompanied by a reduced phage production in the population per time.

Bacterial resistance gained by the infecting phage did not result in recovery of bacterial density (Figure 2 & Figure 3). Instead, the number of CFU is lowest, when the majority of bacteria cells are infected by the phage (Figure 4). The recovery of bacterial populations is

driven by appearance of a 2nd resistance mechanism, which potentially is associated with a mutation in the secretion system II. When the 2nd resistance mechanism is present in about 50% of bacterial cells, population densities regain similar values to the controls.

This is in line with growth characteristics measured for resistant phage-infected and non-infected clones, where we found that vibriophagesVALGΦ8 infected clones had lower maximum growth values than non-infected clones (Figure 5) and with previous studies suggesting reduced bacterial growth rates due to increased replications cost after infection by filamentous phages (Ahmad, Askora et al. 2014). The reduction in growth confirms that infections by filamentous phage are not necessarily beneficial for the bacterial host.

Rapid evolution of phage resistance has been extensively documented using lytic phages (Buckling and Rainey 2002). In our study and the study from Wendling et al, (unpublished data) bacteria also gained resistance against filamentous phages within 20 generations at 15 PSU. The resistance mechanism increased bacterial fitness resulting in the loss of phage-infected clones within 100 generations at 15 PSU and fluctuation conditions. At 7 PSU, the evolution and the increase in frequency of the 2nd resistance mechanism is slowed down. Resistant, non-infected clones only start to outcompete phage-infected clones after transfer four and eventually become fixed at transfer 22 suggesting reduced selection for the phage-independent resistant mechanisms at low saline conditions.

The delay in resistance evolution and the prolonged existence of resistance phage-infected clones suggests that at 7 PSU selection for the 2nd resistance mechanism is lower. Both observations can be explained by the reduced bacterial growth rates leading to a lower encounter rate between phages and bacteria, especially in the first two transfers of the experiment. Furthermore, the higher difference in growth rate between resistant infected and resistant, non-infected clones (Table 2) at 15 PSU suggest that resistant, infected clones are more competitive at 7 PSU. Bacterial resource allocation towards phage production can be a major factor driving reduced bacterial growth rates (Ahmad, Askora et al. 2014). Assessing phage production of single clones from transfer six suggests that phage production per time is indeed higher at 15 PSU compared to 7 PSU in a growing population (Figure 5). However, the ratios of plaque forming units / cell forming units does not reveal a clear trend of increased phage production per individual bacteria cell because the increased number of phages is potentially caused by the faster increasing number of phage-infected bacterial clones at 15 PSU. Furthermore, we find a strong variation in phage production between the single clones of each salinity treatment suggesting that production is modulated on an

individual level and may change over the time course of the evolution experiment. Considering that we have several million cells in a population and a strong variation in phage production among individual infected cells, it is difficult to conclude, whether the average cost of phage production differs at respective salinity levels. Our model suggests that high phage production and associated cost thereof, may indeed be a driver for fast resistance evolution and reduced presence of phage-infected cells over the time course of the evolution experiment at 15PSU. The model also indicates that the cost of phage-infection is most likely to be higher than obtained from single clone growth curves of resistant, phage-infected and resistant, non-infected clones. In the modelled scenario phage-infected clones are only quickly outcompeted by non-infected clones when phage infection causes a growth rate reduction of about 20% compared to resistant, non-infected clones. Considering the shaking environments during the evolution experiment and the static low volume incubation during growth curves measurements, it seems possible that strains perform differently and that growth differences are underestimated.

In our experiment, we could not find evidence for beneficial traits of filamentous phages for *V. alginolyticus* bacteria. We concluded that in our interaction the cost of phage infection outweighs the benefits for the bacteria under the given conditions which can be considered as optimal for bacterial growth. Manipulating further environmental parameters, such as temperature, nutrient or pH, may completely change the outcome of this interaction. The costs of carrying filamentous phages may for example be even higher under nutrient limitation (Bull, Molineux et al. 1991) or the phage might replicate in lower frequency to ensure bacterial survival, if opportunities for horizontal transfers are limited, as shown for phage M13 (Bull, Molineux et al. 1991, Shapiro, Williams et al. 2016).

Under natural conditions, such as the ocean or within a host, selection regimes are expected to be radically different from a fully nutritious laboratory medium, resulting in different evolutionary outcomes of species interactions (Hernandez and Koskella 2019). In the marine environment fluctuation of resources, abiotic conditions and predation impose additional selection on bacteria and phage evolution. Here, the introduction of accessory genes by the phage or positive effects on the host gene expression and metabolism may become more relevant to adapt to novel or changing conditions, e.g. for the deep-sea bacterium *Shewanella piezotolerans* (Jian, Xu et al. 2012, Jian, Xiao et al. 2013, Jian, Xiong et al. 2016) and in arctic *Pseudoalteromonas* strains (Yu, Chen et al. 2015).

During infection of eukaryotic host, virulence factors transferred by the phage may

become more relevant giving infected strains an advantage over resistant non-infected strains (Waldor and Mekalanos 1996, Davis and Waldor 2003, Ilyina 2015). For example motility was reduced after the evolution of phage resistance against lytic phages (Leon and Bastias 2015), which is irrelevant in a shaking falcon tube but may be very relevant during host infection (Josenhans and Suerbaum 2002) or movement to nutrient resources in the open water (Stocker and Seymour 2012).

Bacterial resistance evolution against lytic phages and phage fitness indeed depend on environmental conditions (Harrison, Laine et al. 2013, Wright, Brockhurst et al. 2016, Ferris, Wright et al. 2020). Fine grain environmental heterogeneity in nutrient supply lowered bacterial growth and density, and resulted in reduced coevolutionary arms races dynamics (Harrison, Laine et al. 2013). Low resource conditions further increased the risk of phage extinction (Wright, Brockhurst et al. 2016) which may be the opposite if phages introduce new metabolic pathways, e.g. cyanophages introducing a photosystem (Lindell, Sullivan et al. 2004, Lindell, Jaffe et al. 2005).

Comparing natural vs. laboratory environments may give highly contrasting results Hernandez & Koskella (2019). While bacteria in their natural plant environment remained susceptible towards lytic phages throughout an experiment, the same phage caused fast resistance evolution under *in vitro* conditions. So far it is unknown, whether fast resistance evolution of bacterial strains against filamentous phages can be observed in more natural settings and how this resistance evolution is shaped by a changing environment. Considering the importance of phages in the acquisition of virulence traits, it is highly relevant to understand resistance evolution and phage infections in more natural settings and how the picture may change in times of climate change. Only by comparing natural vs. laboratory conditions, we can shed light on the trajectories of phage-bacteria coevolutionary dynamics in the real world (Hernandez and Koskella 2019).

4.6 | Conclusion

Our study shows how shifts in environmental conditions can affect growth of bacteria which directly influences abundance of phages in the microbial community. This in turn affects the selection for phage-resistant bacteria. The environment also modulates the presence of phage-infected clones in a population emphasizing the importance of the environment for the cost and benefits of filamentous phage. The results emphasis the importance of integrating environmental factors when studying species interactions and

encourages future research projects to design experiments aiming for more natural settings.

Acknowledgments

We thank Kim-Sara Wagner for her support in the laboratory. We also thank Mathias Wegner and Rebekka Wolfensberger for the opportunity and the support to use the QIAxcel Advanced System™ at the Alfred Wegener Institute.

Funding

This study was supported by two grants of the Deutsche Forschungsgemeinschaft: WE 5822/1-1 within the priority programme SPP1819 and the Cluster of Excellence 80 "The Future Ocean" given to CCW and OR. Furthermore, this study was supported by funding from the European Research Council (ERC) under the European Union´s Horizon 2020 research and innovation program (Grant agreement No: 755659 – acronym: MALEPREG). HG received career and financial support from the Max Planck Research School and the Integrated School of Ocean Sciences.

Ethical statement

No ethical approval was required.

Conflict of interest

We have no competing interests.

Author contribution

HG, CCW and OR devised the study; HG conducted the experiments with support from KT, VM. HG did the follow up assays with the help of VM and KT. HG analyzed the data and drafted the manuscript with input from CW and OR. CC, HL and JR analyzed the genomic data. MS made the mathematical model with support from HG and CCW. HG wrote the manuscript with input from all authors.

4.7 | Supplement

S 1: Overnight growth curves of whole populations during the evolution experiment

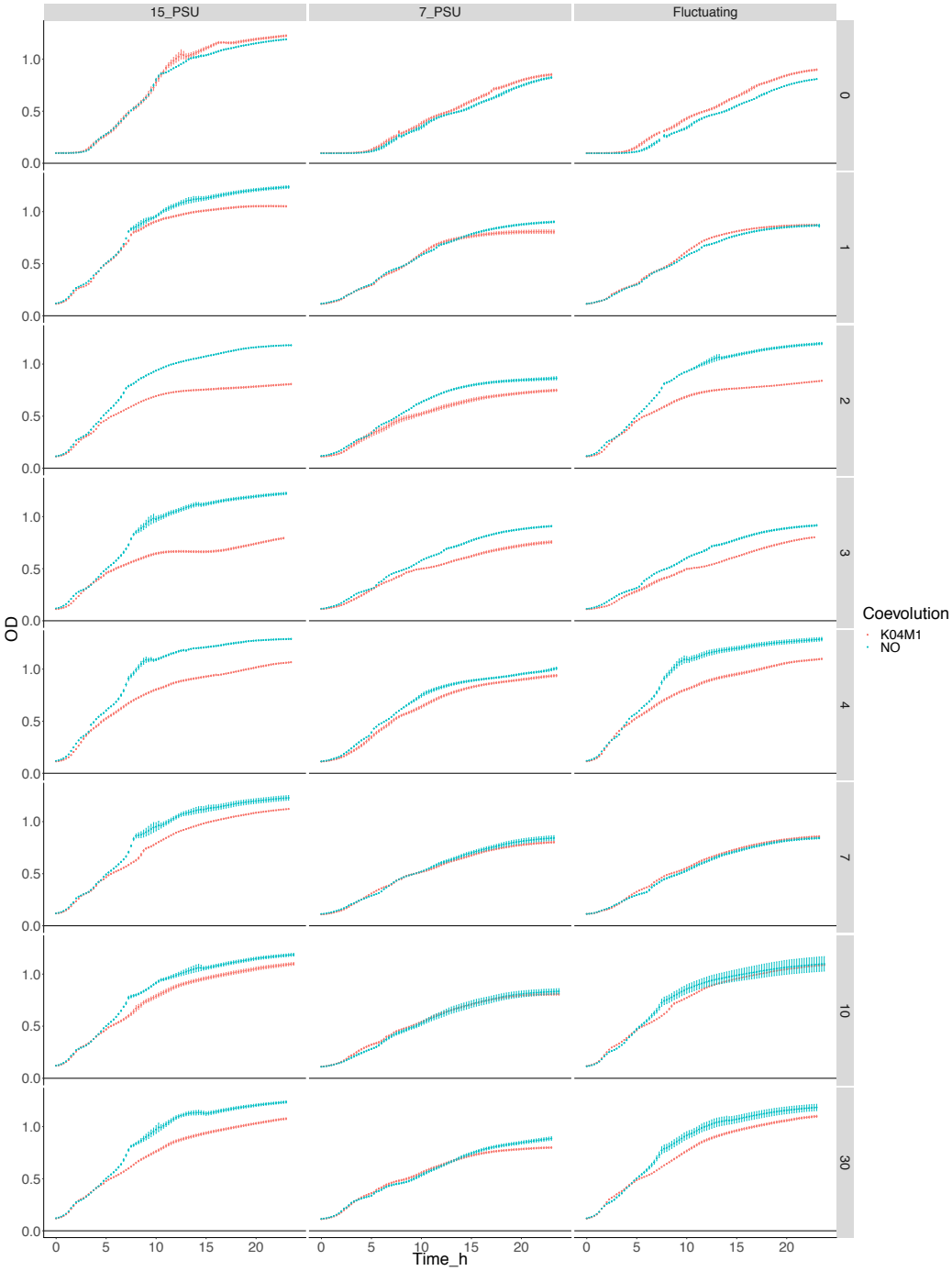

Figure S1: Overnight growth curves of whole populations
The optical density of all replicate populations (x-axis) are presented over a time course of 23 hours (y-axis) with error bars indicating standard error. Each panel row shows the growth curve for a specific transfer. Each panel column represents the salinity the bacteria evolved in, i.e. 15 PSU, 7 PSU or fluctuating conditions. The colours of the growth curve indicate whether poplations were evolving without (blue) or with phage (red)

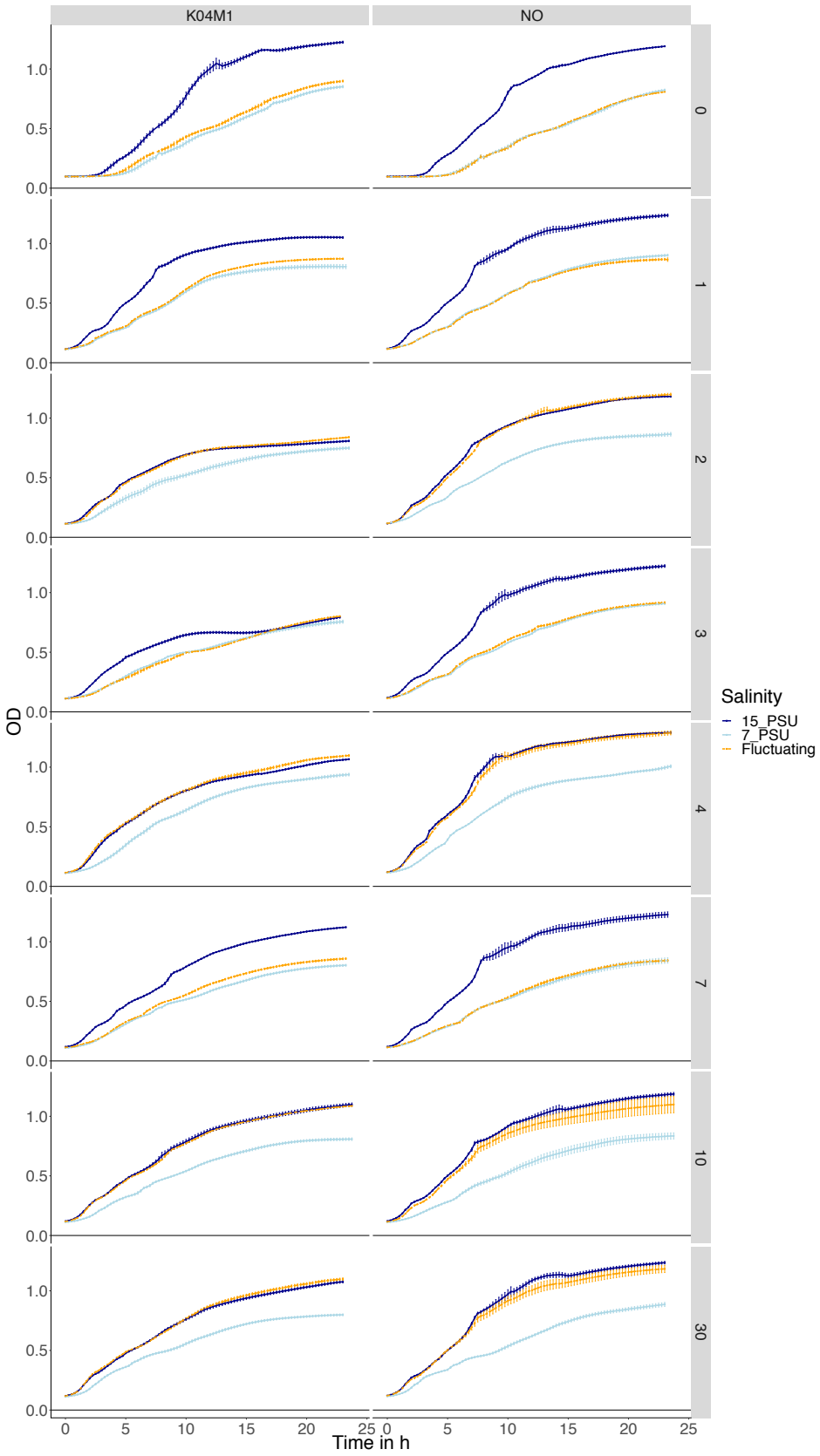

Figure S1a: Overnight growth curves of whole populations
This figure presents the same data as in Figure S1 but with an emphasis on comparison between different salinities.

S 2: Settings for plate reader Thermo Scientific, Multiscan Spectrum 1500 used for OD measurement of RBG assay

Optical density of bacteria growing in 96 well plates (transparent, flat bottom) was measured at 600 nm at the beginning of the RBG assay (T0) and after 18h (T18). Prior each measurement the plate was shaken for 10 seconds at 200 rpm followed by 10 seconds of stasis.

S 3: Analysis of Variance Table (Type marginal – F-statistics) for overall generalised least square model (gls) of Cell forming units (CFU). Degrees of freedom: 665 total; Residuals 653.

	numDf	F-value	p value
Intercept	1	22.0	< 0.001
PhageEvEx	1	51.4	< 0.001
SalinityEvEx	2	3.3	0.039
Transfer	1	83.2	< 0.001
PhageEvEx:Transfer	1	36.7	< 0.001
PhageEvEx:SalinityEvEx	2	3.0	0.048
Salinity_EvEx:Transfer	2	1.0	0.089
PhageEvEx:SalinityEvEx:Transfer	2	5.2	**0.006**

S 4: Analysis of Variance Table (Type marginal – F-statistics) for overall generalised least square model (gls) of Viron dynamics in evolution experiment. Degrees of freedom: 665 total; Residuals 653.

	numDf	F-value	p value
Intercept	1	48652.4	< 0.001
PhageEvEx	1	51.2	< 0.001
SalinityEvEx	2	0.4	0.670
Transfer	1	30.4	< 0.001
PhageEvEx:Transfer	1	**28.9**	**< 0.001**
PhageEvEx:SalinityEvEx	2	0.5	0.633
Salinity_EvEx:Transfer	2	1.0	0.394
PhageEvEx:SalinityEvEx:Transfer	2	2.0	0.132

S 4a: Analysis of Variance Table (Type marginal – F-statistics) for simplified overall generalised least square model (gls) of viron dynamics in evolution experiment. Model simplification of model above according to AIC. Degrees of freedom: 678 total; Residuals 670.

	numDf	F-value	p value
Intercept	1	78052.4	< 0.001
PhageEvEx	1	64.0	< 0.001
SalinityEvEx	2	8.5	< 0.001
Transfer	1	43.2	< 0.001
PhageEvEx:Transfer	1	39.7	< 0.001
PhageEvEx:SalinityEvEx	2	3.3	**0.039**

S 5: Analysis of Deviance Table (Type II Wald chisquare tests) for generalised mixed effect model (glmer) of resistance (Reduction in bacteria growth assay (RBG). Testing Number of observations: 303. Binonmial error distribution.

	Df	Chisq	p value
Transfer	1	62.8	< 0.001
SalinityEvEx	2	6.2	0.046
PhageEvEx	1	174.9	< 0.001
Transfer:SalinityEvEx	2	9.7	0.008
Transfer:PhageEvEx	1	7.8	0.005
SalinityEvEx:PhageEvEx	2	8.3	0.016
Transfer:SalinityEvEx:PhageEvEx	2	0.4	0.838

S 5a: Analysis of Deviance Table (Type II Wald chisquare tests) for reduced generalised mixed effect model (glmer) of resistance (Reduction in bacteria growth assay (RBG). Testing Number of observations: 303. Binonmial error distribution.

	Df	Chisq	p value
Transfer	1	62.8	< 0.001
SalinityEvEx	2	6.1	0.047
PhageEvEx	1	176.6	< 0.001
Transfer:SalinityEvEx	2	9.8	**0.008**
Transfer:PhageEvEx	1	8.1	**0.004**
SalinityEvEx:PhageEvEx	2	8.9	**0.011**

S 6: Statistical design for contrasting growth rates and phage productions of the ancestral and evolved clones.

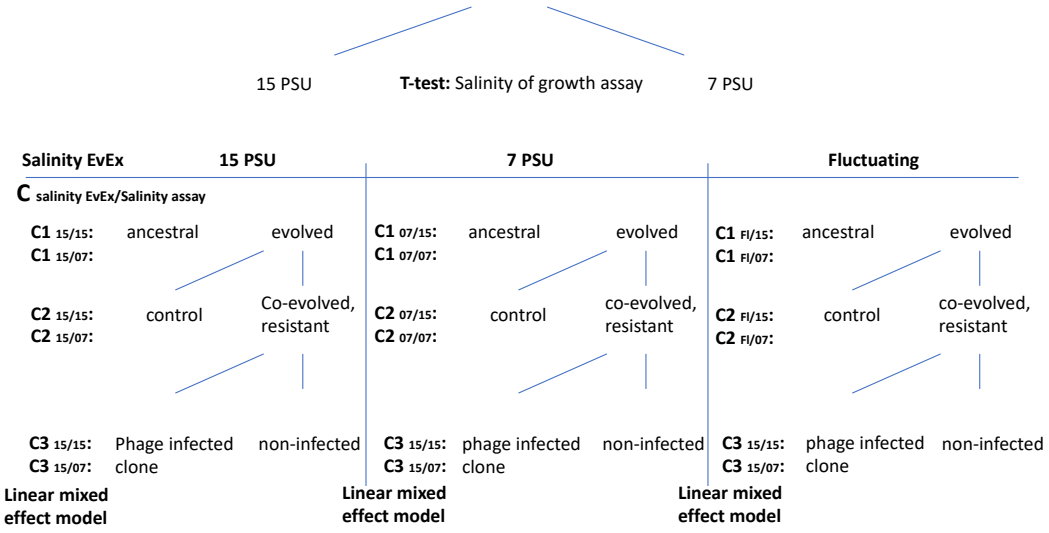

Figure S6a: Statistical design for contrasting growth rate of the ancestral and evolved clones. T-test was used to compare growth rates at 15 PSU and 7 PSU (assay salinity). Subsequently, contrasts were applied to compare growth rates of the ancestral clone with evolved clones (C1), control clones with co-evolved, resistant clones (C2), and resistant phage-infected clones with non-infected clones (C3). First subscipt indicates the salinity treatment (i.e. 15 PSU, 7 PSU, Fluctuating). Second subscript indicates the salinity of the growth assay (i.e. 15 PSU and 7 PSU). Eventually, we applied a linear mixed effect model with *SalinityEvEx* (7 PSU, 15 PSU, fluctuating) and the phenotypic *resistance type* (phage infected/ phage non-infected) as fixed factors.

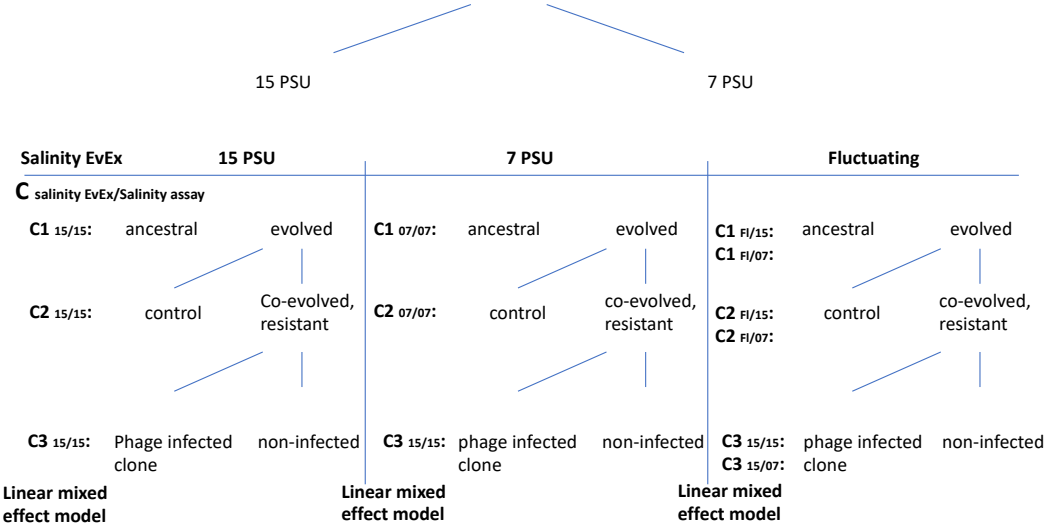

Figure S6b: Statistical design for phage production of the ancestral and evolved clones. contrasts were applied to compare growth rates of the ancestral clone with evolved clones (C1), control clones with co-evolved, resistant clones (C2), and resistant phage-infected clones with non-infected clones (C3). First subscipt indicates the salinity treatment (i.e. 15 PSU, 7 PSU, Fluctuating). Second subscript indicates the salinity of the growth assay (i.e. 15 PSU and 7 PSU). Eventually, we applied a linear mixed effect model with *SalinityEvEx* (7 PSU, 15 PSU, fluctuating) and the phenotypic *resistance type* (phage infected/ phage non-infected) as fixed factors.

Table S 7: Analysis of Variance Table (Type marginal – F-statistics) for generalised least square model (gls) of Cell forming units (CFU) using control populations only. Degrees of freedom: 313 total; Residuals 307

	numDf	F-value	p value
Intercept	1	211.4	< 0.001
SalinityEvEx	2	10.9	< 0.001
Transfer	1	0.1	0.712
SalinityEvEx:Transfer	2	3.7	**0.026**

Table S 8: Analysis of Variance Table (Type marginal – F-statistics) for generalised least square model (gls) of Cell forming units (CFU) using co-evolving populations only. Degrees of freedom 352 total; Residuals 346.

	numDf	F-value	p value
Intercept	1	11.7	< 0.001
SalinityEvEx	2	1.7	0.193
Transfer	1	121.6	< 0.001
SalinityEvEx:Transfer	2	3.6	**0.030**

Table S 9: Analysis of Variance Table (Type marginal – F-statistics) for generalised least square model (gls) of virons dynamics in evolution experiment. Dataset includes only co-evevolving populations from T3-T09. Degrees of freedom: 354 total; Residuals 348.

	numDf	F-value	p value
Intercept	1	1116222.7	< 0.001
SalinityEvEx	2	8.7	< 0.001
Transfer	1	1.1	< 0.001
SalinityEvEx:Transfer	2	6.0	**0.004**

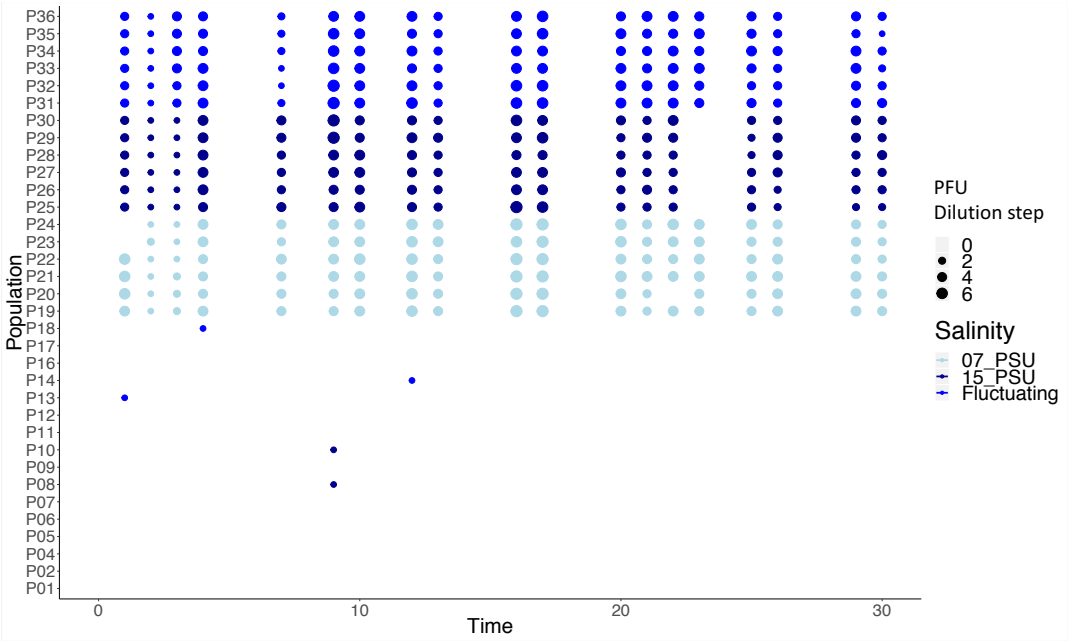

Figure S10: Quantification of phages using standard spot assays. Spot assays with the supernatant of each population were performed during the evolution experiment. Population P01 to P18 are control populations and populations P19 to P36 are coevolving populations. Size of circle indicates the dilution step until phages were visible when spotted on the ancestral K01M1 strain. Colours represent salinity level during evolution experiment (dark blue: 15 PSU, light blue: 7 PSU, blue: fluctuating) Populations P3 and P15 were removed due to contamination.

S 10: Analysis of Deviance Table (Type II Wald chisquare tests) for generalised mixed effect model (glmer) of resistance (Reduction in bacteria growth assay (RBG) using only infected populations. Number of observations: 172. Binonmial error distribution.

	Df	Chisq	p value
Transfer	1	64.6	< 0.001
SalinityEvEx	2	7.3	0.026
Transfer:SalinityEvEx	2	9.7	**0.008**

S 11: Analysis of Deviance Table (Type II Wald chisquare tests) for generalised mixed effect model (glmer) of resistance mode (PCR) using only infected populations. Number of observations: 128. Binonmial error distribution.

	Df	Chisq	p value
Transfer	1	489.9	< 0.001
SalinityEvEx	2	80.4	< 0.001
Transfer:SalinityEvEx	2	32.0	**< 0.001**

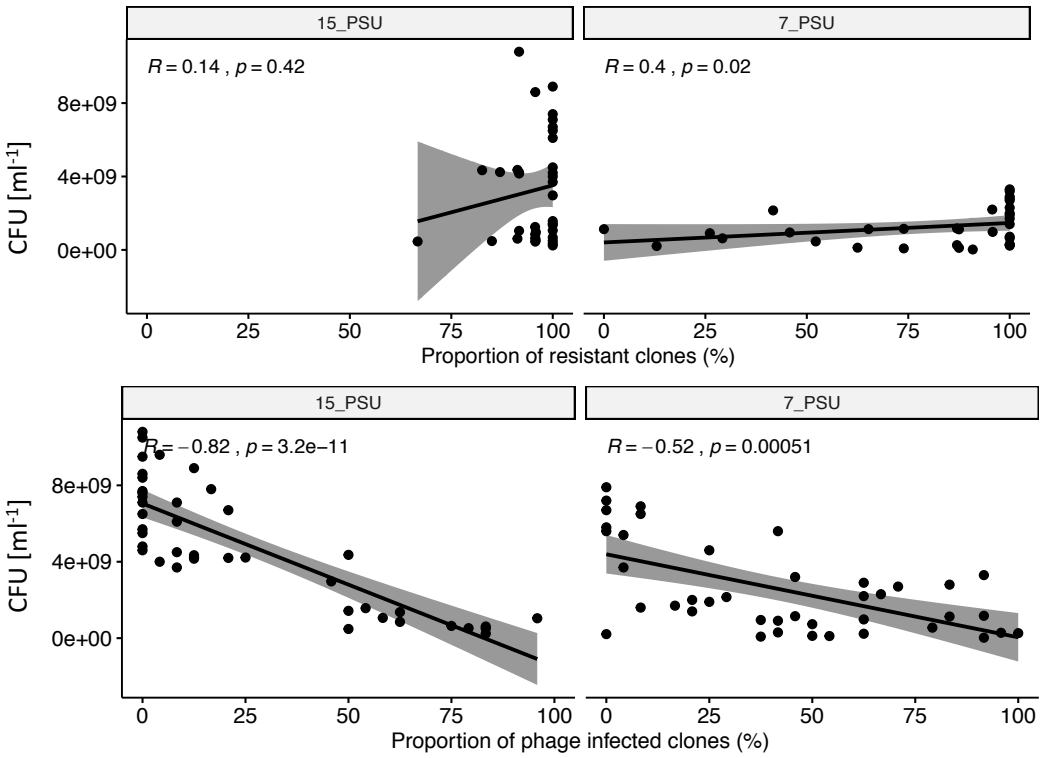

Figure S 12: Recovery in bacterial density is driven by resistance evolution and the disappearance of phage-infected clones. Number of cell forming units (CFU) on the y-axis is correlated either with the proportion of resistant clones (upper panel) or with the proportion of phage-infected cells (lower panel). To decrease zero inflation, i.e. we only plotted the proportion of resistant clones for T2-T12 (upper panels) and the proportion of phage-infected clones for the T2-T22 (lower panels).

Table S 13: Orthogonal contrast of growth rates. Comparision of growth rates μ for single clones achieved in follow up growth assays of the evolution experiment. C1 contrasts ancesteral strain and all evolved clones. C2 contrasts, non-resistant control clones and co-evolved resistant clones, C3 contrasts resistnt phage infected and resistant phage non-infected clones. Salinity EvEx is the salinity during the evolution experiment and salinity assay is the salinity during the growht assay.

Contrast	Salinity EvEx (PSU)	Salinity assay (PSU)	Estimate	Std Error	t value	p value
C1	All	15 & 7	0.0031	0.0029	1.0	0.297
C1	All	15	0.0014	0.0011	1.3	0.191
C1	15	15	0.0012	0.0012	75.5	0.318
C1	7	15	0.0013	0.0009	1.3	0.145
C1	Fluct	15	0.0017	0.0011	1.5	0.143
C1	All	7	0.0045	0.0010	4.3	**< 0.001**
C1	15	7	0.0036	0.0010	3.5	**0.001**
C1	7	7	0.054	0.0009	5.8	**< 0.001**
C1	Fluc	7	0.0048	0.0006	7.0	**< 0.001**
C2	All	15 & 7	0.0037	0.0010	3.6	**< 0.001**
C2	All	15	0.0051	0.0003	13.5	**< 0.001**
C2	15	15	0.0052	0.0006	1.0	**< 0.001**
C2	7	15	0.0048	0.0006	8.5	**< 0.001**
C2	Fluct	15	0.0055	0.0008	7.1	**< 0.001**
C2	All	7	0.0020	0.0003	5.2	**< 0.001**
C2	15	7	0.0029	0.0006	4.5	**< 0.001**
C2	7	7	0.0054	0.0009	5.9	**< 0.001**
C2	Fluc	7	0.0003	0.00004	0.8	0.415
C3	All	15 & 7	0.0036	0.0024	1.5	0.127
C3	All	15	-0.0016	0.0006	-2.7	**0.007**
C3	15	15	-0.0015	0.0011	-1.3	0.195
C3	7	15	-0.0014	0.0009	-1.6	0.112
C3	Fluct	15	-0.0021	0.0012	-1.8	0.079
C3	All	7	-0.0030	0.0006	-4.9	**< 0.001**
C3	15	7	-0.0050	0.0010	-5.0	**< 0.001**
C3	7	7	-0.0027	0.0008	-3.1	**0.004**
C3	Fluc	7	-0.0018	0.0006	-27	**0.010**

Table S 14: Orthogonal contrast of growth rates. Comparision of growth rates μ for single clones achieved in follow up growth assays of the evolution experiment. Contrast CS1 compares growth rates of all clones evolved at 15 PSU with clones evolved in the 7 PSU and fluctuating conditions. Contrast CS2 compared clones evolved at 7 PSU with clones evolved at fluctuating conditions. The contrast includedes clones of the evolved non-resistant controls and the co-evolved resistant clones.

Contrast	Salinity assay (PSU)	Estimate	Std Error	t value	p value
CS1	15	0.0001	0.0005	0.2	0.865
CS2	15	0.0001	0.0010	0.6	0.531
CS1	7	-0.0020	0.0003	-5.0	**< 0.001**
CS2	7	-0.0007	0.0007	-1.1	0.271

Table S 15: Analysis of Deviance Table (Type II Wald chisquare tests) for linear models of 24 h single clones growth assay. μ and A represent the two determined growth characteristics. Salinity EvEx is the salinity during the evolution experiment and salinity assay is the salinity during the growth assay.

	Salinity EvEx (PSU)	Salinity assay (PSU)	Factor	Chisq	Df	*p*
μ	All	15	Salinity EvEx	1.0	2	0.597
			Resistance type	8.7	1	**0.003**
			Salinity EvEx: Resistance type	0.3	2	0.879
μ	All	7	Salinity EvEx	5.4	2	0.066
			Resistance type	59.7	1	**< 0.001**
			Salinity EvEx: Resistance type	10.6	2	**0.005**
A	All	15	Salinity EvEx	2.5	2	**0.282**
			Resistance type	14.9	1	**< 0.001**
			Salinity EvEx: Resistance type	0.4	2	0.802
A	All	7	Salinity EvEx	1.3	2	0.535
			Resistance type	0.5	1	0.471
			Salinity EvEx: Resistance type	5.8	2	0.054

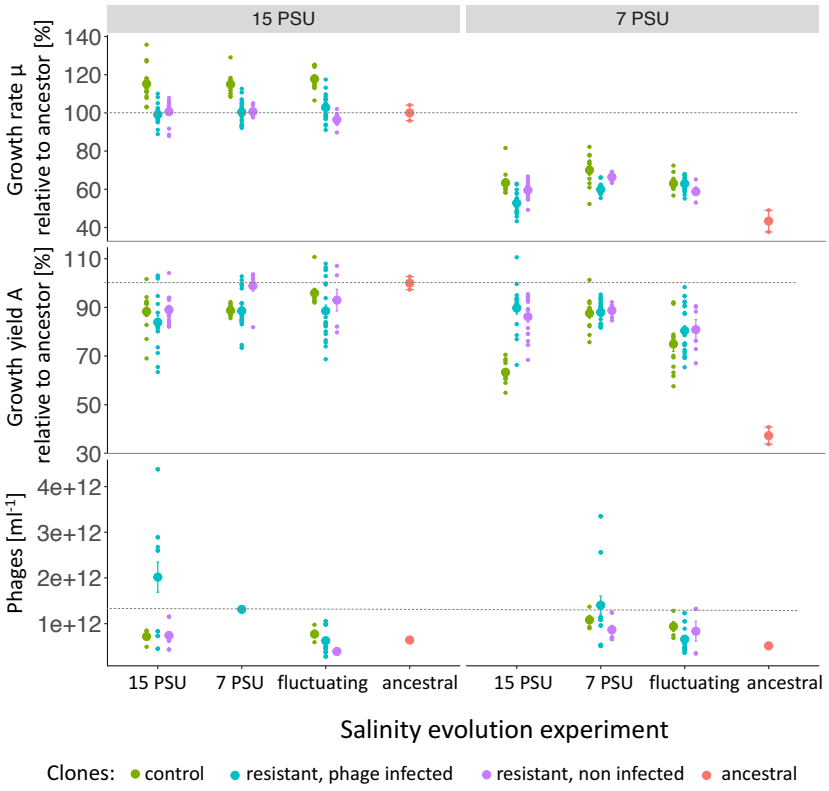

Figure S 16*:* **Mean bacterial growth (top), maximum yield (middle) and phage production** were measured of individual clones from transfer 6 at 15 PSU (left panel) and at 7 PSU (right panel). Mean growth rates μ [% of ΔOD_{600} h^{-1}] and growth yield A [% of max OD_{600}] are shown relative to the ancestral strain growing at 15 PSU (y-axis), which is indicated by the dashed line. Number of phage particles (y-axis) were measured after a growth period of 24 hours. The dashed line represents the determined quantification limit for the phage concentration using the spectrophotometric measurement. Data are grouped according to the salinity the clones experienced during the evolution experiment (x-axis). Colours specify the clone type based on in-silco PCR: control populations (green), resistant, infected clones (blue), resistant, non-infected clones (purple) and ancestral K01M1 strain (red).

Table S 17: Orthogonal contrast of phage production. Comparision of growth rates phage production for single clones measured in in follow up growth assays of the evolution experiment. C1 contrasts ancesteral strain and all evolved clones. C2 contrasts, non-resistant control clones and co-evolved resistant clones, C3 contrasts resistant phage infected and resistant phage non-infected clones. Salinity EvEx is the salinity during the evolution experiment [PSU] and salinity assay is the salinity during the growth assay [PSU].

Contrast	Salinity EvEx	Salinity assay	df	Estimate	Std Error	t value	p value
C1	15	15	18	1.5e+12	1.1e+11	1.4	0.176
C1	7	7	17	1.6e+11	8.6e+10	1.9	0.080
C1	Fluc	15	17	2.9e+09	3.0e+10	0.1	0.924
C1	Fluc	7	18	9.3e+10	4.4e+10	2.1	**0.048**
C2	15	15	18	-2.6e+11	1.3e+11	-2.0	0.056
C2	7	7	17	-4.0e+10	1.1e+11	-0.4	0.722
C2	Fluc	15	17	9.1e+10	3.8e+10	2.4	**0.029**
C2	Fluc	7	18	6.1e+10	5.2e+10	1.1	0.261
C3	15	15	18	7.6e+11	2.2e+11	3.4	**0.003**
C3	7	7	17	3.6e+11	1.8e+11	2.0	0.065
C3	Fluc	15	17	7.1e+10	6.2e+10	1.1	0.267
C3	Fluc	7	18	2.5e+11	9.1e+10	2.8	**0.013**

Table S 18: Analysis of Deviance Table (Type II Wald chisquare tests) for linear models of 24h single clones phage production assay. Salinity EvEx is the salinity [PSU] during the evolution experiment and salinity assay is the salinity [PSU] during the growth assay.

Factor	Chisq	Df	*p*
Salinity EvEx	11.6	2	**0.003**
Resistance type	13.5	1	**< 0.001**
Salinity EvEx: Resistance type	5.8	2	0.054

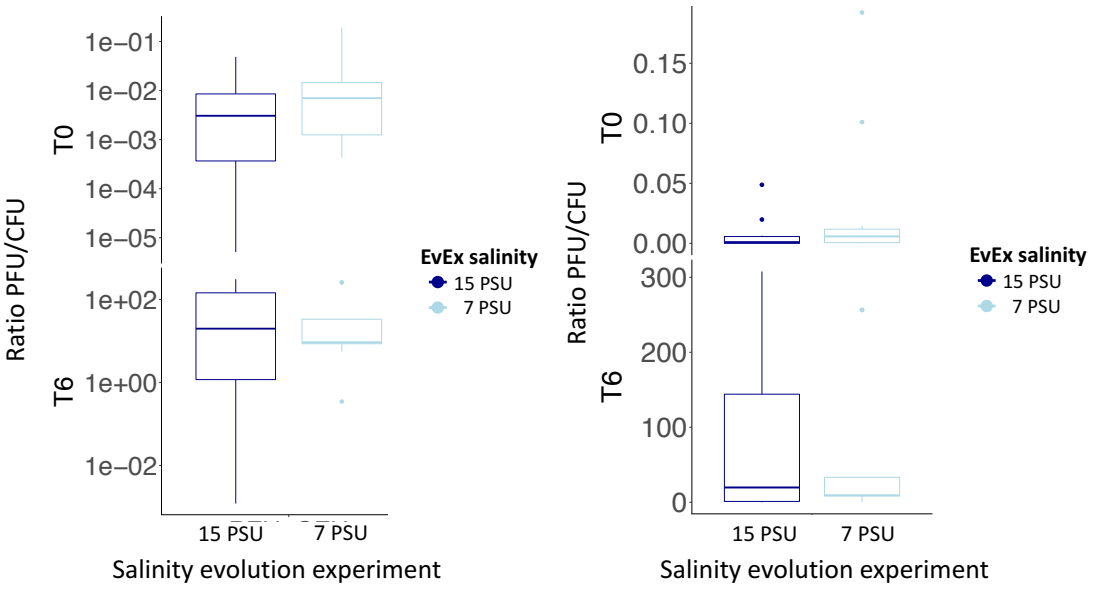

Figure S 19: Ratio plaque forming units / cell forming units

Phage infected clones carrying the added phage VALGΦ8 were incubated for 6 hours. We measured CFU as well as PFU on the ancestral K01M1 *Vibrio* strain at the beginning (T0) and after six hours (T6). Clones were incubated at the same salinity level, in which they evolved, i.e. 15 PSU (dark blue) and 7 PSU (light blue). The upper panel shows the pfu/cfu ratio at the beginning of the assay and the lower panel after 6 h.

5 | Chapter IV

Pipefish locally adapted to low salinity in the Baltic Sea retain phenotypic plasticity to cope with ancestral salinity levels.

Henry Goehlich[1,*], Linda Sartoris[1,2], Kim-Sara Wagner[1], Carolin C. Wendling[1,3], Olivia Roth[1]

In Frontiers in Ecology and Evolution (2021)

[1] Parental Investment and Immune Dynamics, Marine Evolutionary Ecology, GEOMAR Helmholtz Centre for Ocean Research, Kiel, Germany
[2] current address: Social Immunity Group, Institute of Science and Technology, Austria
[3] current address: Institute of Integrative Biology, ETH Zürich, Zürich, Switzerland

5.1 | Abstract

Genetic adaptation and phenotypic plasticity facilitate the invasion of new habitats and enable organisms to cope with a rapidly changing environment. In contrast to genetic adaptation that spans multiple generations as an evolutionary process, phenotypic plasticity allows acclimation within the life-time of an organism. Genetic adaptation and phenotypic plasticity are usually studied in isolation, however, only by including their interactive impact, we can understand acclimation and adaptation in nature. We aimed to explore the contribution of adaptation and plasticity in coping with an abiotic (salinity) and a biotic (*Vibrio* bacteria) stressor using six different populations of the broad-nosed pipefish *Syngnathus typhle* that originated from either high or low saline environments. We hypothesized that wild *S. typhle* populations are locally adapted to the salinity and prevailing pathogens of their native environment, and that short-term acclimation of parents to a novel salinity may aid in buffering offspring phenotypes in a matching environment. To test these hypotheses, we exposed all wild caught animals, to either high or low salinity, representing native and novel salinity conditions and allowed animals to mate. After male pregnancy, offspring was split and each half was exposed to one of the two salinities and infected with *Vibrio alginolyticus* bacteria that were evolved at either of the two salinities in a fully reciprocal design. We investigated life history traits of fathers (offspring survival, offspring size) and expression of 47 target genes in mothers and offspring.

Pregnant males originating from high salinity exposed to low salinity were highly susceptible to opportunistic fungi infections resulting in decreased offspring size and number. In contrast, no signs of fungal infection were identified in fathers originating from low saline conditions suggesting that genetic adaptation has the potential to overcome the challenging conditions of low salinity. Genetic adaptation increased survival rates of juveniles from parents in lower salinity (in contrast to those from high salinity). Juvenile gene expression indicated patterns of local adaptation, trans-generational plasticity and developmental plasticity. The results of our study suggest that pipefish locally adapted to low salinity retain phenotypic plasticity, which allows them to also cope with ancestral salinity levels and prevailing pathogens.

Keywords

Transgenerational plasticity, genetic adaptation, local adaptation, phenotypic plasticity, Baltic Sea, climate change, salinity, Syngnathidae

5.2 | Introduction

Genetic adaptation and phenotypic plasticity (Chevin, Lande et al. 2010) facilitate the invasion of new habitats and permit coping with the consequences of global climate change (Brierley and Kingsford 2009, Poloczanska, Brown et al. 2013, Urban 2015). Genetic adaptation is a multigenerational process spreading in the population over the rise and fixation of novel mutations (Chatterjee, Pavlogiannis et al. 2014), or over selection on standing genetic variation and shifts in allele frequency (Barrett and Schluter 2008, Eizaguirre, Lenz et al. 2012, Torda, Donelson et al. 2017). In contrast, phenotypic plasticity is an individual trait that enables organisms of one genotype to show multiple, alternative phenotypes in response to biotic or abiotic conditions (West-Eberhard 1989). The environment influences the phenotype (Chevin, Lande et al. 2010) and elicits changes in gene expression, which can then impact individual development, morphology, physiology and behavior (Angers, Castonguay et al. 2010). Phenotypic responses can occur within the life-time of an organism (reversible and developmental plasticity) or persist across one or several generations (trans-generational plasticity).

Trans-generational plasticity (TGP) is the non-genetic inheritance of an alternative phenotype by transferring nutrients, hormones, proteins or epigenetic marks from the parent to the offspring generation (Sunday, Calosi et al. 2014). The impact of TGP may differ among species, life stages and abiotic conditions (Uller, Nakagawa et al. 2013, Laland, Uller et al. 2014) as well as the biotic interaction partners (e.g. parasite type or strain) (Beemelmanns and Roth 2016, Beemelmanns and Roth 2016, Beemelmanns and Roth 2017, Roth, Beemelmanns et al. 2018). TGP can be adaptive and result in increased offspring performance when environmental conditions of parental and offspring generations match (Sunday, Calosi et al. 2014). This has been shown for instance in wild Atlantic silversides exposed to ocean acidification (Murray, Malvezzi et al. 2014) or in three-spine sticklebacks exposed to heat stress (Shama and Wegner 2014). However, TGP can also induce negative carry-over effects (Eriksen, Bakken et al. 2006, Marshall 2008), e.g. increased mortality in the early life stages of sticklebacks upon changes in salinity levels (Heckwolf, Meyer et al. 2018). Adaptive phenotypic plasticity allows organisms to survive and reproduce in a novel environment but was suggested to slow down genetic adaptation by buffering against the effects of natural selection (Kelly 2019).Whether TGP is enhancing or constraining adaptation is still debated and may depend on various factors such as species, traits or the level of current environmental variability and predictability (Reed, Waples et al. 2010, Lind,

Zwoinska et al. 2020).

The interactive contribution of genetic adaptation and phenotypic plasticity in invading new habitats and coping with climate change has been rarely addressed, instead, the two mechanisms were mainly studied in isolation (Gienapp, Teplitsky et al. 2008). However, to depict and understand biological responses to climate driven environmental changes, we need models (Donelson, Sunday et al. 2019) and experiments (Kelly 2019) addressing such mechanisms simultaneously. An approach to study the interaction between genetic adaptations and phenotypic plasticity are space-for-time experiments (Blois, Williams et al. 2013, Kelly 2019), where organisms living along a natural gradient can serve as a prediction for how organisms can cope with future environmental conditions (Reusch, Dierking et al. 2018).

Even though salinity shifts are predicted to have strong implications for coastal populations (Meier, Kjellstrom et al. 2006, Andersson, Meier et al. 2015, Kniebusch, Meier et al. 2019), the main focus of climate change research still lies on warming and acidification studies (but see DeFaveri and Merila 2014, Hasan, DeFaveri et al. 2017, Heckwolf, Meyer et al. 2018). Changing ocean salinity will have major impacts on coastal and polar ecosystems (Gibson and Najjar 2000, Loder, van der Baaren et al. 2015), because of the overriding effects on the physiology of aquatic organisms (Morgan and Iwama 1991, Velasco, Gutierrez-Canovas et al. 2019), comprising metabolism, growth, development, immunity and reproduction in teleost fishes (Haddy and Pankhurst 2000, Boeuf and Payan 2001). Osmoregulation enables marine organisms to acclimate to different salinity levels but consumes up to 50% of the fish's total energy budget (Boeuf and Payan 2001). High energy demand for osmoregulation results in metabolic trade-offs (DeWitt, Sih et al. 1998), which makes genetic adaptation to novel salinities important.

The Baltic Sea is particularly prone to future reductions in salinity due to little water exchange with the North Sea and river runoffs from the surrounding countries. Increased precipitation in the northern part may cause a decrease by up to 30% in surface salinity by the end of the century (Meier, Kjellstrom et al. 2006, Andersson, Meier et al. 2015). Already today, the Baltic Sea is characterized by a strong salinity gradient ranging from 30 PSU in the transition to the North Sea to an almost freshwater environment in the north-eastern parts making it an ideal setting for space for time experiments (Blanquart and Gandon 2013, Heckwolf, Meyer et al. 2018). The stability of the salinity gradient (Janssen, Schrum et al. 1999, Hinrichs, Jahnke-Bornemann et al. 2019), the energetic cost of both, osmoregulation

(Boeuf and Payan 2001) and phenotypic plasticity (DeWitt, Sih et al. 1998), promote genetic adaptation in teleost fishes towards different salinity levels in the Baltic Sea (DeFaveri and Merila 2014, Berg, Jentoft et al. 2015, Guo, DeFaveri et al. 2015, Guo, Li et al. 2016). If salinity levels in the new environment are relatively stable, genetic assimilation was suggested to result in reduced plasticity and more adaptive genotypes (Angers, Castonguay et al. 2010). Adaptation to the low salinity conditions of the Baltic Sea and the isolation from the Atlantic source population is also accompanied by a loss of genetic diversity (Johannesson and Andre 2006, Holmborn, Goetze et al. 2011). Therefore, adaptation to low salinity may result in reduced osmoregulatory plasticity, such as changes in kidney morphology and gene expression (Hasan, DeFaveri et al. 2017), and thus hamper the ability to cope with further salinity fluctuations. TGP may not be sufficient to buffer the negative impacts of salinity change (Heckwolf, Meyer et al. 2018), in particular if salinity is subject to strong fluctuations and if populations are locally adapted. However, increased selection due to negative carry-over effects may facilitate rapid adaptation but may also reduce genetic variation, which raises the risk of extinction (Heckwolf, Meyer et al. 2018). Unclear remains whether strong selection for genetic adaptation to low saline environments generally resulted in a reduction of phenotypic plasticity or whether, alternatively, animals have evolved different strategies to cope with salinity changes.

A suitable organism to study the interactive contribution of genetic adaptation and phenotypic plasticity is the sex-role reversed broad-nosed pipefish *Syngnathus typhle* (Syngnathidae, Teleostei). *S. typhle* inhabits a wide range of waters with different salinity levels along the European coastline from the Black Sea in Eastern Europe to the Mediterranean Sea and from the Eastern Atlantic to the north of the Baltic Sea (Wilson and Veraguth 2010). TGP in response to immune and temperature challenges has been demonstrated in broad-nosed pipefish in numerous studies (Beemelmanns and Roth 2016, Beemelmanns and Roth 2017, Roth and Landis 2017) as well as the impairing effect of low salinity on the immune system (Birrer, Reusch et al. 2012). Beyond the direct impact of salinity changes on organisms and populations (genotype x environment interaction, GxE), salinity shifts may increase or decrease the virulence of parasites and pathogens (genotype x genotype x environment interaction, GxGxE) (Stockwell, Purcell et al. 2011, Hall, Vettiger et al. 2013, Poirier, Listmann et al. 2017) and alter co-evolutionary dynamics between host and pathogens (Mostowy and Engelstadter 2011, Molnar, Kutz et al. 2013, Brunner and Eizaguirre 2016, Kutzer and Armitage 2016).

The abundance and virulence of opportunistic and omnipresent marine pathogens, such as several strains of the *Vibrio* bacteria clade (Baker-Austin, Trinanes et al. 2017) are modulated by salinity and temperature (Chen, Li et al. 2011, Oberbeckmann, Wichels et al. 2011, Baker-Austin, Trinanes et al. 2017). *Vibrio alginolyticus* frequently infects pipefish in the Baltic Sea (Roth, Keller et al. 2012) and is known to cause higher mortality in artemia and herring at low salinity (Dayma, Raval et al. 2015, Poirier, Listmann et al. 2017). Increases in bacterial virulence are evoked due to a combination of phenotypic changes, including bacterial biofilm formation (Dayma, Raval et al. 2015, Kim and Chong 2017) and the expression of bacterial motility and virulence factors (Hase and Barquera 2001). We hypothesized that genetic adaptation of the pipefish to local salinity and the prevailing pathogens may compensate for the previously observed drop of immunological activity in case of exposure to decreasing salinities (Birrer, Reusch et al. 2012, Poirier, Listmann et al. 2017) and, hence, has the potential to reduce the negative impact of pathogens like *Vibrio* bacteria (Roth, Keller et al. 2012).

To explore how pipefishes have genetically adapted to long-term salinity changes and how this adaptation influences their phenotypic plasticity to cope with short-term shifts in salinity, we compared the potential of pipefish originating from either high or low salinity environments to react towards salinity shifts with developmental and trans-generational plasticity. Furthermore, we investigated how adaptation and acclimation of the pipefish host and the bacterial *Vibrio* pathogen to high and low salinity changes the host-pathogen interaction. We tested the following hypotheses: 1) *S. typhle* populations are genetically adapted to the salinity in their local habitat, 2) adaptive trans-generational plasticity in matching parental and offspring salinity results in enhanced juvenile survival and matching gene expression pattern in the parental and offspring generation, 3) *S. typhle* populations locally adapted to low salinity have reduced phenotypic plasticity and are not able to cope with ancestral salinity levels, and 4) bacterial virulence is higher at low salinity.

To investigate how *S. typhle* have adapted towards their local salinity and local pathogens in the past (genetic adaptation) and to assess their consecutive acclimation potential (phenotypic plasticity) towards salinity shifts and their immune response towards a bacterial infection, we collected six *S. typhle* populations in the Baltic Sea. Fish were collected at three sampling sites with high saline conditions and at three sampling sites with low saline conditions. In a laboratory aquaria experiment, animals were exposed to either their native salinity (high or low respectively) or the salinity of the other three populations

(novel salinity). Upon successful male pregnancy, offspring were exposed to either native or novel salinity conditions, in a fully reciprocal design. Subsequently, juvenile fish were injected with a *V. alginolyticus* strain that evolved for 90 days either at low or high salinity in the laboratory. In addition to life history traits and mortality, we investigated the expression of 47 target genes involved in (i) general metabolism, (ii) immune response, (iii) gene regulation (DNA and histone modification) and (iv) osmoregulation.

5.3 | Material and Methods

The parental *Syngnathus typhle* generation was caught in seagrass meadows of six sampling sites along the German coastline of the Baltic Sea in spring 2017 (Figure 1 & Table 1). Three sampling sites are characterized by relatively high salinity conditions (14 - 17 PSU; high salinity origin; H) and three sampling sites by relatively low salinity conditions (7 - 11 PSU; low salinity origin, L; Table 1). Salzhaff was assigned the category low because salinity drops are common after rainfall accompanied with freshwater discharge due to enclosed morphology of the inlet. Therefore, pipefish in Salzhaff are likely to be exposed to salinity levels below 10 PSU. A minimum of 30 non-pregnant males and 30 females were caught snorkeling with hand nets at each sampling site at depths ranging between 0.5 and 2.5 m. At each sampling site, water temperature and salinity were measured from water collected about 1 m below the surface using a salinometer (WTW Cond 330i).

Table 1: Pipefish sampling sites with coordinates, sampling date and ambient salinity and water temperature.

Sampling sites (Abbreviation)	GPS Coordinates	Salinity (PSU)	Salinity (Category)	Water Temperature (°C)
Flensburg Fjord Westerholz (Flens)	54° 49’14 N 9° 40’26 E	17	High	15
Kiel Fjord Falckensteiner Strand (Falck)	54° 23'26 N 10° 11'33 E	14	High	10-11
Orth Bay Fehmarn (Fehm)	54°26'55 N 11° 3'19 E	15	High	13
Salzhaff Werder (Salz)	54° 1'35 N 11° 3'57 E	10-11	Low	14
Wieker Bodden Wiek (RuegN)	54° 37'20 N 13° 16'56 E	8	Low	18
Strelasund Grabow (RuegS)	54° 13'32 N 13° 24'25 E	7	Low	12

Pipefish were transported in large aerated coolers to the aquaria facilities of the GEOMAR (Westshore) in Kiel (Germany). Females and males were separated and kept in groups of 5-7 per 80-liter tank resulting in a total number of 36 tanks. These tanks were connected to two independent circulating water systems containing either high saline (15 PSU; n = 18) or low saline water (7 PSU, n = 18) and equipped with artificial seagrass. Pipefish from high salinity origins were kept at 15 PSU (Baltic Sea water) and those from low salinity origins at 7 PSU (Baltic Sea water, diluted with deionized water and tap water (ratio 2:1:1) to keep the water alkalinity constant). The water temperature throughout the experiment was 18° C and illumination was set to a 16:8 h day and night cycle. Pipefish adults were fed twice a day with frozen and occasionally with live mysids.

After pipefish were acclimated to laboratory conditions for at least two days, half of the individuals from each sampling site were gradually acclimated to the novel salinity over four days. Each day, tanks were briefly connected to the 15 PSU or the 7 PSU circulating system to either increase or decrease the salinity by 1.5 to 2 PSU. The other half of the fish remained in their native salinity. Apart from the salinity adjustment, all 36 tanks remained disconnected from the circulation system during the time of salinity acclimation. Subsequently, four to six randomly chosen males and four to six females originating from the same sampling site and acclimated to the same salinity, were placed together in one of the 36 tanks connected to circulating water systems of either high or low acclimation salinity (Figure 1). During mating and male pregnancy, fish maintenance and aquaria set-up remained as previously described.

One week after mating, pipefish males started to show signs of infection with a fungus growing inside and on the brood pouch. Three weeks after mating, we visually assessed and photographically documented the prevalence of fungus.

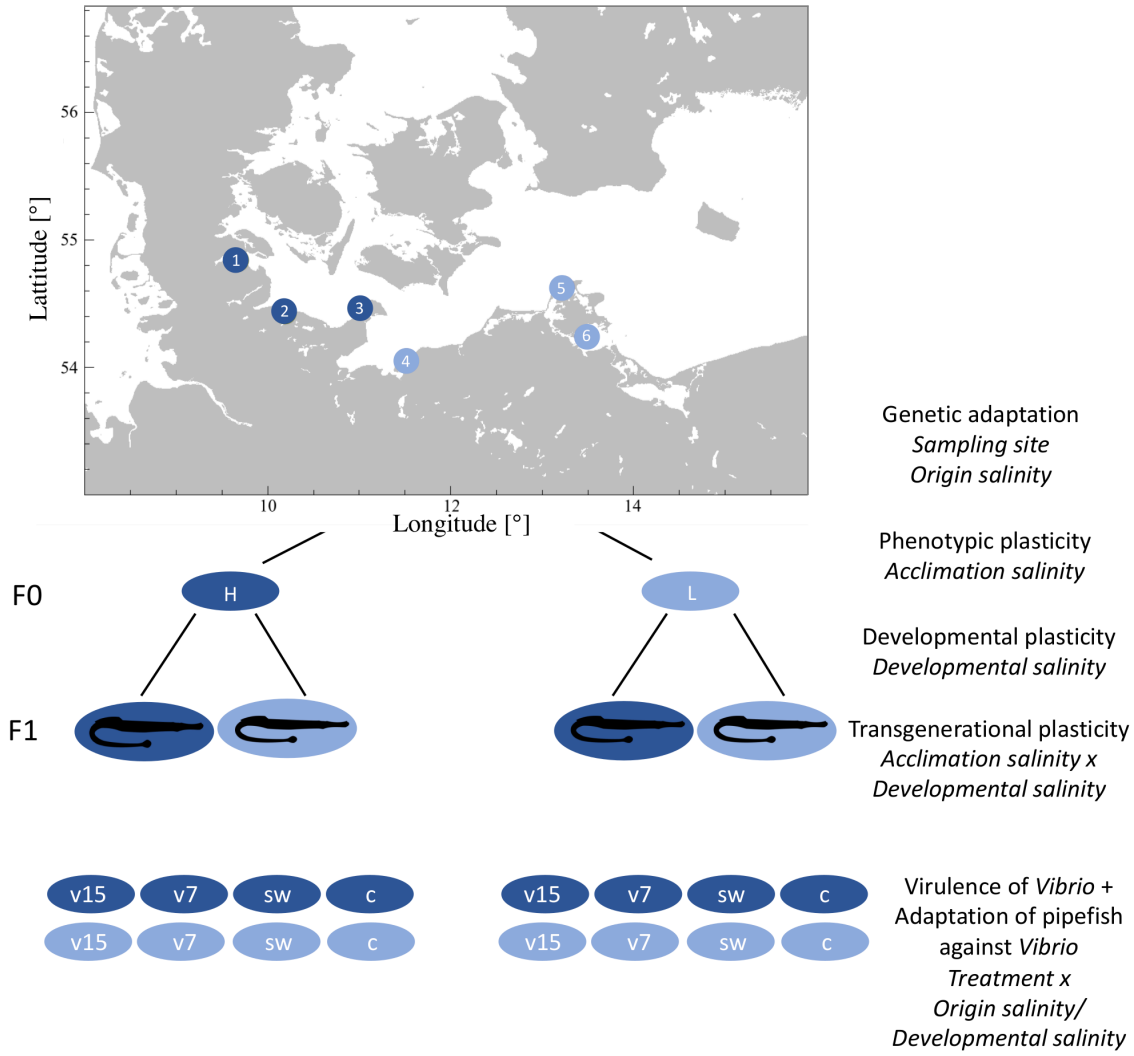

Figure 8: Fully reciprocal experimental design

We sampled pipefish along the Baltic Sea coast, at three sampling sites from a relatively high saline environment (high origin salinity: 14 - 17 PSU; dark blue circles; subsequently labeled as italic H): 1) Flensburg Fjord, 2) Falckenstein Strand and 3) Fehmarn and three sampling sites with a relatively low salinity level (low origin salinity: 7 - 11 PSU; light blue circles; subsequently labeled as italic L): 4) the Salzhaff and 5) Ruegen North and 6) Ruegen South. In the laboratory males and females were kept separately and acclimated to the opposing salinity (acclimation salinity: 15 PSU (H, dark blue), 7 PSU (L, light blue)) or their respective native salinity. Subsequently, males and females were allowed to mate and pregnant males were kept at constant conditions. Half of the F1 generation was either exposed to high (h) or low (l) salinity within 24h after birth (developmental salinity). Ten days post hatch juveniles were injected with *Vibrio alginolyticus* evolved at 15 PSU (v15) or at 7 PSU (v7), sham injected with sterile seawater (W) or left naive (C) (treatment). Label in italic on the right side correspond to the factors that were considered in the statistical models.

5.3.1 | Sampling of adult pipefish for target gene expression & population genetics

Four days after mating, females were removed from the tanks and immediately euthanized using anesthetic tricaine methane sulfonate (MS-222, 500 mg/L). We measured standard body length and total weight and removed the gills to store them in RNAlater at 4° C overnight and subsequently at -80° C. Fin clips were taken and placed in 96% Ethanol for population genetic analysis.

5.3.2 | Population genetics using microsatellites

DNA isolation & preparation

Genomic DNA was isolated from fin clips of F0 female pipefish using the DNeasy 96 Blood & Tissue Kit (Qiagen, Venlo, Netherlands) following the manufacturer's protocol. All samples were incubated and eluted twice to obtain a higher extraction yield. A subset of the isolated genomic DNA was quantified using NanoDrop (Spectrometer; Peqlab, Erlangen, Germany) and visually evaluated by gel electrophoresis on a 1.2% agarose gel (GelRed nucleic acid stain, Lambda DNA/HindIII Marker and 1kb DNA marker (Invitrogen; Thermo Fisher Scientific, Germany)).

All 144 *S. typhle* samples were genotyped for 11 microsatellite loci, with a minimum of 20 individuals per sampling site. Genotyping was performed in three pooled reactions, each containing 3-4 primer pairs that were designed on an expressed sequence tag (EST) library of *S. typhle* (**Pool A**: Sy_ty_1, Sy_ty_4, Sy_ty_6, Sy_ty_7; **Pool B**: Sy_ty_11, Sy_ty_22, Sy_ty_23; **Pool C**: Sy_ty_16, Sy_ty_17, Sy_ty_21, Sy_ty_24 (Jones, Rosenqvist et al. 1999, Roth, Keller et al. 2012)). Microsatellites and the associated primer pairs and the Multiplex PCR protocol can be found in GenBank under accession numbers JQ598279–JQ598290. Primers had an initial concentration of 5 pmol and were color labeled with either Hex green or Fam blue to allow differentiation during fragment analysis. In a 10 μl reaction, several loci were amplified simultaneously from 1 μl of extracted DNA using 5 μl of the Multiplex PCR Master Mix (Qiagen) and varying amounts of the pooled primer mixes (Pool A: 1.75 μl, Pool B: 0.75 μl, Pool C: 1.5 μl). Three negative controls (ddH_2O) were added onto each 96-well plate.

Capillary electrophoresis and fragment analysis were performed using the 3130xl Genetic Analyzer (Applied Biosystems/Thermo Fisher Scientific). A loading mix containing

8.75 µl HiDi Formamide and 0.25 µl GeneScan 350 ROX dye Size Standard (Applied Biosystems/Thermo Fisher Scientific) was added to 1 µl of each PCR product. Prior to the fragment run, samples were denatured in a thermo cycler for 2 min at 90° C.

Microsatellite analysis

Raw fragment data were scored using the GeneMarker Genotyping Software (Liu et al. 2011). The software displays allele frequency panels that identify the alleles for each locus in each sample, thus provides an overview of whether individuals are homozygous or heterozygous for certain alleles at a locus. Additionally, the raw data were screened using the Microsatellite Data Checking Software Micro-Checker (Van Oosterhout et al. 2004). Micro-Checker identifies genotyping errors caused by non-amplified null-alleles that either appear due to mutations in the primer binding regions or generally occur in fragment analysis because PCR shows greater efficiency in longer sequences. GENETIX (Belkhir et al. 2004) was used to describe the level to which the genotype frequency differed from the expected Hardy-Weinberg equilibrium (HWE) frequency by calculating a global F_{ST} value as a correlation of inbreeding in the substructure vs. in the entire population. For completeness, pairwise F_{ST} values were calculated to display distances between pairs of haplotypes and a F_{IS} value was calculated as a correlation of inbreeding vs. random mating within the population. Although GENETIX has a greater statistical power, the population structure within the multi-locus genotype data was further investigated by the STRUCTURE Software for Population Genetics Inference (Pritchard et al. 2000). Based on the Bayesian clustering method, STRUCTURE creates an admixture model, which provides likelihood scores for each individual of belonging to a certain population. The model was tested with varying numbers of expected populations ranging from a minimum of two (high salinity vs. low salinity) to a maximum of six (number of sampling stations). Visualization of the population clustering was performed using the PHYLogeny Inference Package PHYLIP (Felsenstein 1989). PHYLIP provides a pipeline of programs to randomize comparisons, create randomized trees, which are then assembled to a final phylogeographic tree that is based on the most frequent combinations found within the randomized trees. As the retrieved fragment data did not provide any lineage data that allows to draw conclusions with regard to a common ancestor, we created an unrooted phylogeographic tree.

5.3.3 | Canditate gene expression of females

To assess local adaptation to salinity and the potential of *S. typhle* to cope with novel salinity conditions, we selected candidate genes from three different functional categories, i.e. (i) immune response, (ii) metabolism and (iii) gene regulation (DNA and histone modification) (Supplement 1 (Table S1)). Immune genes were further subdivided into innate, adaptive and complement system genes and gene regulation genes into activating and silencing genes.

RNA extraction and reverse transcription

RNA was extracted from gill tissue of adult pipefish that was stabilized in RNAlater using the RNeasy® Universal Tissue kit (QIAGEN, Venlo, Netherlands). Tissue samples were homogenized by adding a 5 mm stainless steel bead into each collection tube and placing them into a homogenizer shaking for two times 30 seconds at 25 Hertz. Thereafter, we followed the manufacturer's protocol "Purification of Total RNA from Animal Tissues Using Spin Technology". RNA concentration (extraction yield) and purity of the samples were checked by spectrophotometry (NanoDrop ND-1000 Spectrometer; Peqlab, Erlangen, Germany). Protein contamination was quantified using the adsorption ratio of 260/280 nm (target > 2.0) and the ratio 260/230 nm (target > 1.8) was used to detect organic contamination. A fixed amount of RNA (300 ng/sample = 50 ng/μl) was then reverse transcribed into cDNA using the QuantiTect Reverse Transcriptase kit (QIAGEN, Venlo, Netherlands).

Preamplification of cDNA and candidate gene expression

For each sample, 1.4 μl target cDNA was pre-amplified with 0.5 μl primer pool mix of all 48 genes (500 nM), 2.5 μl TaqMan PreAmp Master Mix (Applied Biosystems, Waltham, MA, USA) and 0.7 μl H2O (10 min at 95° C, 14 cycles: 15 sec at 95° C followed by 4 min at 60° C). Afterwards, the PCR product was diluted 1:10 with low TE buffer (10 mM Tris, 0.1 mM EDTA, pH 8). The sample mix for the 96.96 Dynamic ArrayTM IFCs chips contained 3.1 μl pre-amplified and diluted PCR product, 3.55 μl SsoFast-EvaGreen Supermix with Low ROX (Bio-Rad Laboratories, Hercules, CA, USA) and 0.37 μl 20 x DNA Binding Dye Sample Loading Reagent (Fluidigm) per sample. The assay mix for the chip contained 0.7 μl primer pair mix (50 μM), 3.5 μl Assay Loading Reagent (Fluidigm) and 2.8 μl low TE buffer per primer pair. Chips were loaded with 5 μl sample mix and 5 μl

assay mix. To measure gene expression, the chips were placed into the BioMark system (Fluidigm, South San Francisco, CA, 15 USA) applying the 'GE fast 96x96 PCR+Melt v2.pcl' protocol (Fluidigm). Each of the chips contained two technical replicates per sample and gene, two no-template controls (H2O), one control for gDNA contamination (-RT) and one between plate control.

5.3.4 | Juvenile infection experiment

Experimental design and treatment groups

Within the first 24 hours after birth, half of the juveniles from each clutch was exposed to native salinity conditions and half to novel salinity conditions in a fully reciprocal design. Juveniles were fed twice a day with freshly hatched, nutrient enriched (Aqua Biotica orange+TM) *Artemia salina* nauplii. Siblings were kept together in one non-aerated 1.5 l tank, of which one third of the water was exchanged daily. Once a day, left-over food was removed using single-use pipettes and mortality was documented.

Ten days post-hatch, juveniles received one of the four following treatments: i) no injection (c), ii) sham injection of autoclaved seawater with the equivalent salinity, i.e. 15 or 7 PSU (sw) or iii) injection of *Vibrio alginolyticus* strain K01M1, which evolved for 90 days under laboratory condition either at 15 (v15) or 7 PSU (v7) (Goehlich, Roth et al., unpublished data). 2 μl of sterile seawater with or without bacteria was injected in the ventral part of the juveniles, using a MonojectTM insulin syringe (Coviden) with a sterile 30 Gauge needle. Subsequently, all juvenile siblings with the same treatment were placed in one 500 ml Kautex bottle containing seawater with the respective salinity of the 1.5 l tanks. Survival of juveniles was documented for six days and fish maintenance was according to the procedure described for 1.5 l tanks. One day post infection, one juvenile from each treatment (Kautex bottle) was euthanized and decapitated to assess expression of candidate genes. Standard body length was measured and whole-body samples were stored in RNAlater overnight at 4° C and subsequently at -80° C.

Characterization and evolution of Vibrio alginolyticus strain used for injection

The *Vibrio alginolyticus* strain K01M1 used for injection of pipefish juveniles was isolated from a healthy pipefish caught in the Kiel Fjord (Roth, Keller et al. 2012) and fully sequenced (Chibani, Roth et al. 2020). The strain was evolved for 90 days either at 15 or 7

PSU (medium 101: 0.5% (w/v) peptone, 0.3% (w/v) meat extract, 1.5% (w/v) or 0.7% (w/v) NaCl in Milli-Q deionized water) (Goehlich, Roth et al., unpublished data). We used the same strain and evolved it at two different salinities to ensure that salinity is the only driver for differences in bacterial virulence, which can potentially also be influence by the presence of filamentous phages (Waldor and Mekalanos 1996, Ilyina 2015, Chibani, Hertel et al. 2019).

After 90 days the bacterial populations were diluted and plated onto *Vibrio* selective Thiosulfate-Citrate-Bile-Saccharose (TCBS) agar plates (Fluka AnalyticalTM). The next day, single colonies from each plate were picked and grown overnight in medium 101 with the respective salinity. Subsequently, cultured bacteria were stored at -80°C as 33% glycerol stocks. For the infection experiment, part of the glycerol stocks were plated onto TCBS agar and one clone was grown in a 50 ml Falcon tube containing 30 ml medium 101 in the respective salinity for 24 hours, at 25 °C with shaking at 230 rpm. Overnight cultures were centrifuged for 20 min at 2000 rpm. The supernatant was discarded and the cell pellet was resuspended in 3 ml sterile seawater (7 or 15 PSU respectively) to achieve similar bacterial densities of $5*10^{10}$ ml^{-1}.

Juvenile gene expression

We measured gene expression of juveniles to assess the effect of (a) genetic adaptation (i.e. origin salinity) on gene expression, (b) trans-generational effects driven by an interaction between acclimation salinity and developmental salinity and (c) developmental plasticity induced by developmental salinity. Furthermore, we investigated (d) whether virulence differed in *V. alginolyticus* evolved at 15 or 7 PSU and whether juveniles from parents originating from a matching salinity were better adapted to *Vibrio* strains evolved at the respective salinity. Therefore, we selected genes from three functional categories, namely (i) immune response (ii), general metabolism (iii) gene regulation (DNA and histone modification) as described above for female pipefish *S. typhle* (Section 2.4). Compared to female gene expression, eleven genes from the categories (i)-(iii) were replaced by osmoregulation genes (iv). We selected osmoregulatory genes from teleost studies (S 2) and designed specific primers with Primer3Web (Koressaar and Remm 2007, Untergasser, Cutcutache et al. 2012) (S 3). RNA extraction and quantification of gene expression were conducted as described before with the following modifications due to a higher RNA yield: the fixed amount of RNA that was reverse transcribed into cDNA was 400 ng/sample (67

ng/μl) instead of 300 ng/sample (50 ng/μl) and pre-amplified cDNA was diluted 1:10 and instead of 1:20.

5.3.5 | Statistics

All statistical analyses and visualizations were performed in the R 3.6.1 environment (RCoreTeam 2020).

Life history traits

We used two-way ANOVAs to assess size and weight differences between adults as well as differences in clutch size and in total length between juveniles at 10 days post-hatch. Fixed factors included *origin salinity* (Salinity at sampling sites of origin two levels: *High* or *Low*), *acclimation salinity* (High or Low), *sex* of the pipefish (male or female) and the *sampling site* (Flens, Fehm, Falck, Salz, RuegN or RuegS) nested in *origin salinity*. ANOVA of clutch size additionally included the average body length of males exposed to a given treatment. Homogeneity of variances was tested by Fligner test and normal distribution of data by using the Cramer-von Mises normality test. The clutch size was square root transformed to achieve normal distribution of residuals.

We performed two spearman-rank correlations using the function ggscatter (package: ggpubr) to test for 1) correlation between the total length of adult pipefish and the salinity measured at the sampling site on the day of capture as well as 2) between clutch size and average male size of sampling site. The clutch size of males originating from high salinity and acclimated to low salinity conditions was removed from the correlation due to fungus infection. Post-hoc tests were carried out using Tukey's "honest significant difference" (TukeyHSD, package: multcomp) (Hothorn, Bretz et al. 2020).

Gene expression of parental generation & juveniles

From the Fluidigm output data, mean cycle time (Ct) and standard deviation (SD) for each of the two technical replicates were calculated. Expression measurements with a coefficient of variation (CV; CV = SD/Ct) larger than 4% were excluded from the study (Bookout and Mangelsdorf 2003). For females, the combination of HDAC1 and HDAC3 were identified as the optimal reference genes (geNorm V < 0.15 (Vandesompele, De Preter et al. 2002)) with high reference target stability (geNorm M ≤ 0.5), based on 155 samples (S

5) and 34 target genes in *Qbase+3.0* (Biogazelle; Hellemans, Mortier et al. 2007).
In the analyses of juvenile gene expression one osmoregulation gene (15% NAs) and 36 samples were excluded from the study due to failed reactions on the Fluidigm chip in at least one of the duplicates. Samples with more than 10% excluded genes were omitted from the analysis, as many missing Ct values are indicative for insufficient sample quality. Remaining missing Ct values were substituted by the mean Ct for the given gene calculated from all other samples, as subsequent analyses are sensitive to missing data. Based on 559 samples and 47 target genes, the reference genes ASH and HDAC1 were selected using the same criteria as for pipefish females. From the geometrical mean of the two reference genes –ΔCt values were calculated to quantify relative gene expression.

Origin salinity (*high* or *low*), *acclimation salinity* (high or low) and *developmental salinity* (high or low) were defined as fixed factors, whereas *sampling site* (Flens, Fehm, Falck, Salz, RuegN or RuegS) was nested within *origin salinity*. A Permutational Multivariate Analysis of Variance (PERMANOVA) was applied to gene expression (–ΔCt values) of all samples and target genes for each factor and every interaction of the fixed factors. The PERMANOVA (package 'vegan', function 'adonis' in R (Oksanen, Blanchet et al. 2019)) was based on Euclidean distance matrixes with 1000 permutations (Beemelmanns and Roth 2016). A post-hoc analysis of variance (ANOVA) for every gene was applied; though, to account for multiple testing, only factors and factor interactions identified as significant by the PERMANOVA were considered. To visualize similarity/dissimilarity in gene expression among treatment groups, we performed PCAs (package: 'ade4', function: 'dudi.pca' and 's.class'(Dray and Dufour 2007)). To visualize significant differential gene expression among groups in heatmaps (package: 'NMF', function 'aheatmap'), –ΔΔCt values for each gene were calculated as follows (Yuan, Reed et al. 2006):

$$-\Delta\Delta\mathrm{Ct} = \varnothing - \Delta\mathrm{Ct}\ \text{all samples} - \varnothing - \Delta\mathrm{Ct}\ \text{specific group}$$

Mortality of juveniles within the first 10 days and post-infection

Ten days post-hatch endpoint mortality of juveniles was analyzed as a ratio of "alive" vs "dead" fish using a generalized linear model (package: lme4, function: glm) with binomial error and the following fixed factors: *Origin salinity* (*High* or *Low*), *acclimation salinity* (High or Low) and *developmental salinity* (high or low) and the *sampling site* nested

in *origin salinity*. Significance was tested using ANOVA type two partial sums of squares, and models were simplified using Akaike information criterion (AIC) (Akaike, 1976). Post-hoc tests were carried out using Tukey's honest significant difference (TukeyHSD, package: multcomp, function: glht (Hothorn, Bretz et al. 2020)).Endpoint mortality of juveniles used in the infection experiment was analyzed as described above including *infection treatment* (control (c), sea water injection (sw), *Vibrio* 7 PSU (v7) and *Vibrio* 15 PSU (v15) injection) as an additional factor.

5.4 | Results

5.4.1 | Pipefish population structure

Allele frequencies obtained at 11 microsatellite loci of pipefish sampled at six sampling sites along the German Baltic Sea coastline indicated gene flow or recently isolated populations with no or very little divergence on neutral genetic markers. The findings are based on a Bayesian clustering method using the software STRUCTURE (Figure 2), global fixation index (F_{ST}) of 0.002 and pairwise F_{ST} (S 5).

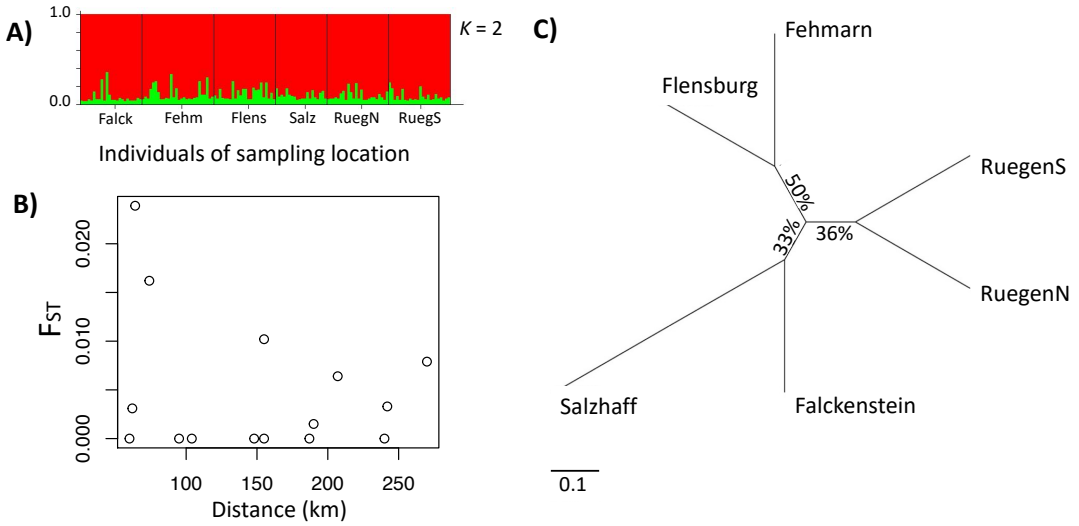

Figure 9: Population structure of pipefish in the southern Baltic Sea

A: STRUCTURE software results based on 11 microsatellite loci. Each individual is represented by a vertical line, which is colored according to the assigned groups (K = 2). **B:** Plotting pairwise F_{ST}s (y-axis) against distance between sampling sampling sites (x-axis) does not reveal isolation by distance (waterway). **C:** Unrooted phylogeographic PHYLIP tree. Distances indicate the relative divergence of microsatellite loci in pipefish between sampling sites. Scale bar represents nucleotide substitutions per site.

Overall, the pairwise F_{ST} were low for all comparisons and with the exception of Flackenstein-Fehmarn (F_{ST} = 0.024) and Falckenstein-Flensburg (F_{ST} = 0.016) pairwise comparisons had a $F_{ST} \leq 0.01$ (S 5). Populations with no differentiation on neutral markers are an ideal setting to study local adaptation because it enables us to observe phenotypic differences caused by genes under selection rather than differences caused by drift and isolation.

5.4.2 | Life history traits, fungus infection and gene expression of parental generation

Pipefish adults from low saline environment have a smaller body size

We found an interaction in the total length of adult pipefish between *origin salinity* and *acclimation salinity* (ANOVA $F_{1,320} = 7.4$, $p < 0.01$) indicating that parental *acclimation salinity* negatively affects growth of adult pipefish depending on the *origin salinity*. There was a trend that adults from high *origin salinity* grew slower at low *acclimation salinity* compared to high *acclimation salinity* (Tukey HSD, *H*H - *H*L: p = 0.085; S 6b), whereas *acclimation salinity* did not affect size of pipefish from low *origin salinity* (Tukey HSD, *L*L - *L*H: p = 0.535). Furthermore, all pairwise comparisons suggest that pipefish from high *origin salinity* are in general larger than pipefish from low *origin salinity* (Tukey HSD, *L*L - *H*H: $p < 0.001$, *L*L - *H*H: $p < 0.001$, *L*H - *H*L: $p < 0.001$). The significant factor *sampling site*, which was nested in *origin salinity* (ANOVA $F_{4,320} = 11.2$, $p < 0.01$) indicates that individuals from Salzhaff were larger compared to individuals from Ruegen North and Ruegen South but did not differ from pipefish caught at the high *origin salinity* (Tukey HSD, Salz - RuegN: $p < 0.001$; Salz - RuegS: $p < 0.001$; S 6c).

The correlation between the salinity at the sampling site and the size of the adults, i.e. length (Figure 3 B) and weight (Figure S6) suggest that pipefish from low *origin salinity* were smaller. The total length and weight in these plots are not corrected for age, which has not been assessed. However, pipefish are usually all in the same age cohort when they are caught in spring. Most of them were born the summer before and reached sexual maturity around the time of catching.

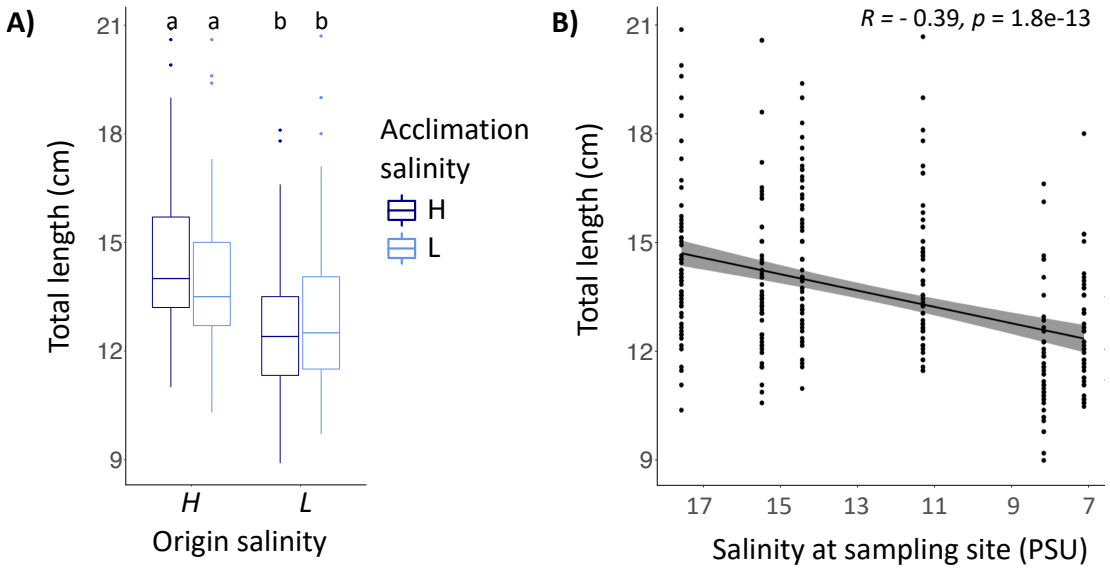

Figure 10: Body length of adult pipefish (A) correlated with salinity at the sampling site (B)

A: The total length of pipefish is shown for both salinity categories (high - 15 PSU, low -7 PSU). Colors indicate whether the parental generation was acclimated to a high (H, dark blue) or to low saline environment (L, light blue). **B:** The total length of pipefish after acclimation correlated with the salinity measured at the sampling site using spearman rank correlation. Grey bar indicates 95% confidence interval.

Pipefish from high saline environments were more susceptible to fungus infection when exposed to low saline conditions

Visible fungus infections of the brood pouch occurred in almost half of the pipefish males (47%) caught at high *origin salinity* and kept at low *acclimation salinity* (Figure 4). Fungus infections ranged from mild infections in the brood pouch not affecting clutch size to a complete loss of the offspring. Males from a high *origin salinity* that remained at high *acclimation salinity* as well as males from the low *origin salinity* had no symptoms of fungus infection regardless of the *acclimation salinity*.

Figure 11: Brood pouch fungus infections were present in 47 % of fathers from high salinity origin kept at low acclimation salinity. Pipefish from low *origin salinity* independent of *acclimation salinity* and pipefish from high *origin salinity* kept at high *acclimation salinity* did not show any signs of fungus infection (A). In males caught at high *origin salinity* and kept at low *acclimation salinity* fungi infections ranged from mild (B) to extreme (C) resulting in the complete loss of eggs and offspring.

Clutch size

Males from a high *origin salinity* kept at high *acclimation salinity* had the largest clutch size (*H*H, mean ± s.d., 41.8, ± 23.4, Tukey TSD; S 7b) followed by males from low *origin salinity* kept at high salinity (*L*H, 27.8 ± 13.2) or low salinity (*L*L, 25.2 ± 16.9), which corresponds to the lower body size at low salinity (Figure 3). Pipefish from high *origin salinity* exposed to low *acclimation salinity* were frequently infected by a brood pouch fungus which reduced the clutch size (*H*L 19.4 ± 15.2; Tukey TSD, *H*L-*H*H, $t = -4.8$, $p < 0.001$;S 7b). In contrast, *acclimation salinity* did not affect clutch size of parents from low *origin salinity* (Tukey TSD, *L*L-*L*H, $t = -0.4$, $p = 0.976$; S 7b) This divergent patterns caused a o*rigin salinity*:*acclimation* salinity interaction (ANOVA $F_{1,109} = 9.0$, $p = 0.003$; S 7a). Higher clutch size, was in general driven by a larger total body length of male pipefish (Spearman rank correlation, $R = 0.43$, $p < 0.001$; Figure 5)

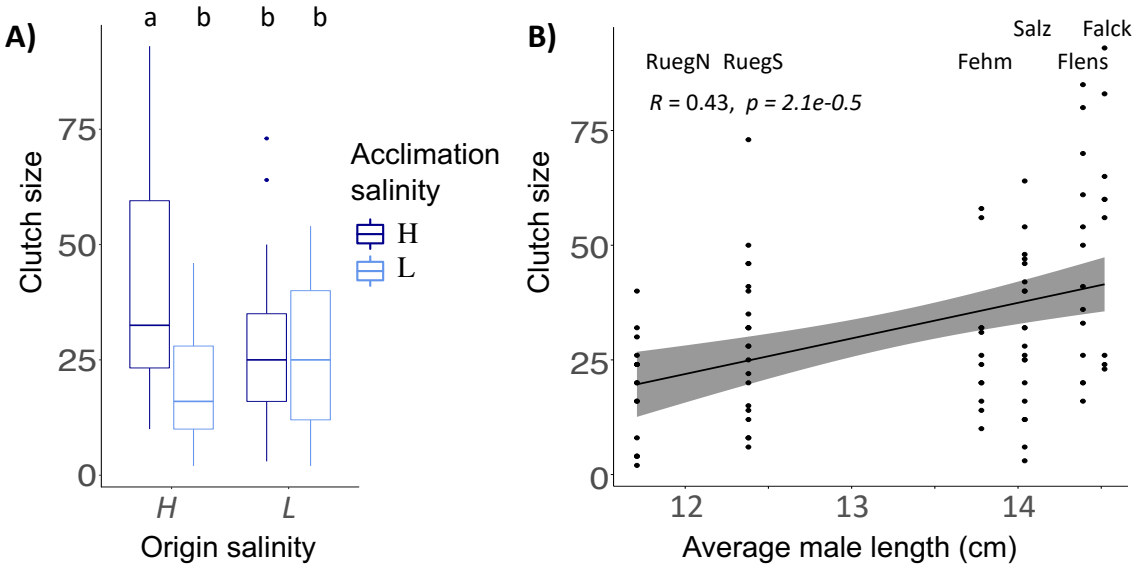

Figure 12: Parental life history traits

A: Number of juveniles (clutch size) is shown for pipefish with high (*H*) or low (*L*) *salinity origin*. Color indicates *acclimation salinity* in the lab (H: 15 PSU - dark blue and L: 7 PSU - light blue). Different letters indicate significant differences (Tukey's HSD, $p < 0.05$). **B:** Clutch size correlated positively with the average size of male pipefish from each sampling site. The *sampling sites* are presented above the data points. The grey bar along the regression line indicates the 95% confidence interval. A more detailed figure visualizing the differences between the single origins can be found in the supplement (S 7c).

Two immune genes are upregulated in females from a high origin salinity

Origin salinity had an impact on the expression of immune genes in female pipefish (PERMANOVA, *immune* $F_{1,146} = 3.1$, $p = 0.010$; S 8), in particular of the innate immune system (PERMANOVA, *innate* $F_{1,146} = 4.0$, $p = 0.002$). *Lectin protein type I* (*Lecpt1*), a pathogen recognition receptor, and *chemokine 7* (*ck7*), a gene encoding a protein responsible for chemotaxis in blood cells, were upregulated in pipefish from high *origin salinity* in contrast to low *origin salinity* females. Low *acclimation salinity* caused a slight upregulation in the expression of histone modification gene *histone deacetylase 6-like* (*hdac6*) (PERMANOVA, *silencing* $F_{1,146} = 2.9$, $p = 0.044$).

5.4.3 | Survival and gene expression patterns of juveniles

Juveniles from low origin salinity parents have higher survival rates and are smaller

In the first ten days after hatching, patterns of juvenile survival suggest an *origin salinity*:*acclimation salinity* interaction (GLM, $\chi^2_1 = 6.1$, $p = 0.031$; S 9a). Whereas, survival of juveniles from parents continuously exposed to the same salinity (Tukey HSD, *L*L - *H*H: $z = -3.4$, $p = 0.783$; S 9b) or non-matching *origin* and *acclimation salinity* did not differ (*L*L - *L*H: $z = -4.7$, $p = 0.842$; *H*H - *H*L: $z = -2.1$, $p = 0.148$), juveniles from high *origin salinity* parents exposed to high *acclimation salinity* in the lab (*L*L) had higher survival rates compared to juveniles from high *origin salinity* exposed to low *acclimation salinity* (Tukey HSD, *L*L - *H*L: $z = -3.4$, $p = 0.043$; S 9b). The *origin salinity:sampling site* effect suggest that patterns at single sampling sites differ. In particular, Flensburg offspring exposed to high *developmental salinity* had reduced survival rates, when parents were acclimated to low instead of high salinity (Tukey's HSD; Hh - Lh: $z = -4.4$, $p = 0.046$; S 9b). Following the same pattern of non-matching *acclimation salinity*, Ruegen South offspring exposed to low *developmental salinity* had reduced survival, when parents were kept at high *acclimation salinity* (Tukey HSD; Hl - Ll: $z = 5.8$, $p < 0.001$). This suggests that exposure of parents to novel salinities can negatively impact juvenile survival when juveniles experience salinity conditions, which did not match parental *acclimation salinity*.

Overall higher survival at high *developmental salinity* compared to low *developmental salinity* (*developmental salinity*, GLM, $\chi^2_1 = 192.8$, $p = 0.031$; Figure 6; S 9a) indicates that low salinity imposes a stress on pipefish juveniles regardless of the *salinity origin*. An exception are juveniles from Ruegen North (*sampling site*, GLM, $\chi^2_4 = 24.1$, $p < 0.001$; S 9a) where juvenile survival was not affected by *developmental salinity* (GLM, $\chi^2_1 = 0.1$, $p = 0.766$)

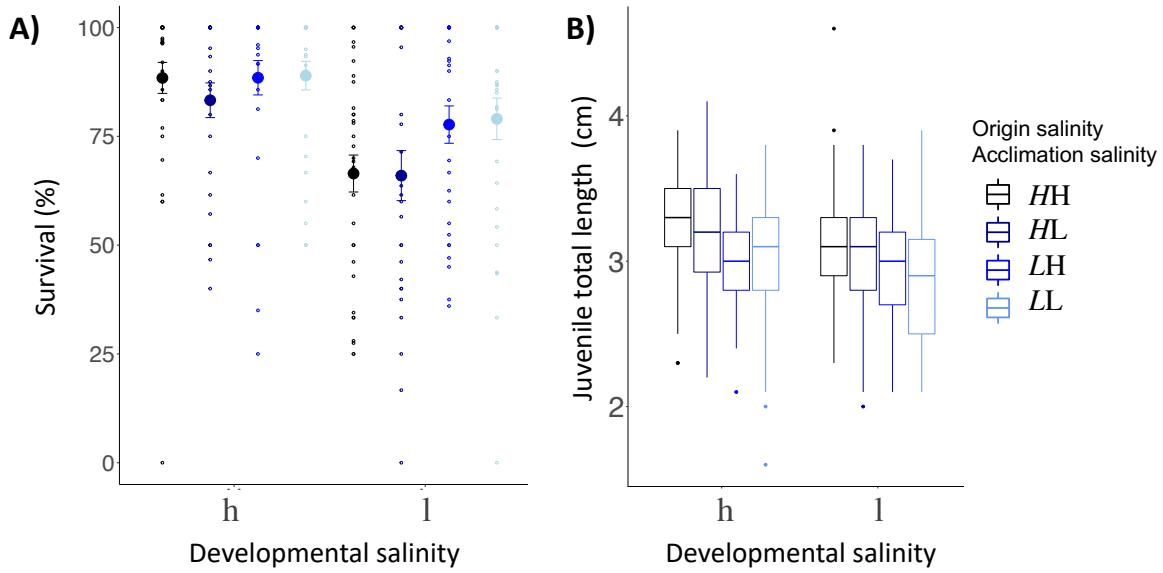

Figure 13: Juvenile life history parameters (A) survival rate (%), (B) body length (cm)
A: The percentage of juveniles surviving the first 10 days post-hatch (%) are plotted on the y-axis. The x-axis indicates the *developmental salinity* after hatching (h – high/15 PSU, l – low/7 PSU). Italic letters and colors specify the *origin salinity* of the parental generation (*H*: 15 PSU, black & dark blue; *L*: 7 PSU blue & light blue). The 2nd letter indicates the *acclimation salinity* in the lab (H: 15 PSU, black and blue; L: 7 PSU, dark & light blue). **B:** Juvenile size (cm) 10 days post hatch is plotted on the y-axis. Labelling and color code correspond to Panel A.

Ten days after hatching, juveniles from high *origin salinity* were larger (3.18 cm ± 0.37, n = 408) than juveniles from low *origin salinity* sampling sites (2.95 cm ± 0.37, n = 405) (*origin salinity*, ANOVA $F_{1,782} = 86.2$, $p < 0.001$; S 10). While *acclimation salinity*, i.e. mating and male pregnancy, had no effect on size of juveniles (*acclimation salinity*, ANOVA $F_{1,782} = 2.2$, $p < 0.136$), low *developmental salinity* reduced offspring size (*developmental salinity*, ANOVA $F_{1,782} = 17.4$, $p < 0.001$) suggesting are stressful for pipefish offspring and reduce growth rates.

Juvenile survival is reduced after injections and at low salinity

Ten days post hatch, juvenile pipefish were challenged either with *Vibrio alginolyticus* bacteria evolved at 15 PSU, 7 PSU, autoclaved seawater (sham injection) or not treated at all (control) and survival was measured six days post infection, i.e. approximately 16 days post hatch. Non-challenged control groups had the highest survival rates (Mean ± s.d.; 83.0% ± 32.2; Figure 7). The injection itself decreased survival of juveniles by at least 10%

in all salinity treatments combined, regardless whether seawater (66.9% ± 38.2), *Vibrio* evolved at 15 PSU (73.0% ± 36.8) or 7 PSU (66.7% ± 38.6) was administered. *Vibrio* strains evolved at 15 PSU caused a higher mortality in juveniles from high *origin salinity* regardless of *acclimation salinity* compared to juveniles from low *origin salinity* with low parental *acclimation salinity* (*origin salinity* x *acclimation salinity* x *treatment,* GLM, $\chi^2_1 = 13.0$, p = 0.005; S 11; Tukey HSD; *L*Lv15 - *H*Hv15: z = -3.4, p = 0.046; *L*Lv15 - *H*Lv15: z = -3.5, p = 0.038). When fathers from low *origin salinity* were exposed to high *acclimation salinity* these positive effects on offspring survival were lost (Tukey's HSD, *L*Hv15 - *H*Hv15 z = -1.5, p = 0.971). This suggests that mis-matching salinity levels between the parental and juvenile generation can lead to reduced survival rates and that juveniles of fathers from low salinity levels have higher survival rates compared to juveniles of fathers from high salinity.

Juvenile survival was in general higher in high *developmental salinity* conditions (71.1% ± 36.7) compared to low *developmental salinity* conditions (58.6% ± 36.7) (GLM, *developmental salinity,* $\chi^2_1 = 40.2$, p = 0.031) suggesting that low salinity levels are a stressful environment for pipefish development. An adaptation to low salinity may result in an increased fitness as juveniles from low *origin salinity* fathers (69.8% ± 40.1) had in general a higher survival rate compared to juveniles from high *origin salinity* fathers (60.6% ±37.7).

An effect of *sampling site* nested in *origin salinity* (GLM, $\chi^2_4 = 39.5$, p < 0.001; S 11) indicates that survival patterns for each sampling site within the *origin salinity* categories are diverse. The statistical diversity may be a result of the high variation in survival rates within a single treatment, which sometimes ranged from 0 - 100%. Combining the survival rates of all three sample sites of one *origin salinity* resulted in more robust and conclusive results.

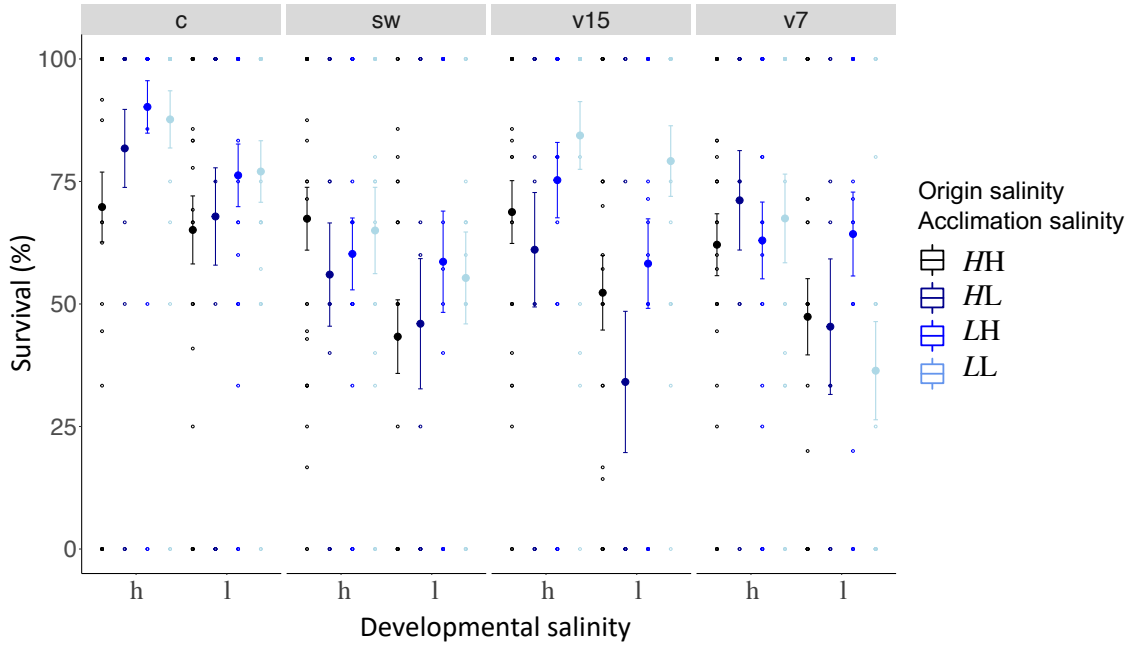

Figure 14: Juvenile survival six days post infection

Juvenile survival six days post infection is plotted on the y-axis. The x-axis indicates the *developmental salinity* (h - high/15 PSU, l - low/7PSU). Italic letters and colors specify the *origin salinity* of the parental generation (*H*: 15 PSU, black & dark blue; *L*: 7 PSU blue & light blue). The 2nd letter and colors indicate the *acclimation salinity* in the lab (H: 15 PSU, black and blue; L: 7 PSU, dark & light blue). Each *treatment* is represented by one panel, i.e. control (c) or injection with seawater (sw), *Vibrio* strain evolved at 15 PSU (v15), or at 7 PSU (v7).

5.4.1 | Matching parental acclimation and juvenile developmental salinity results in similar juvenile gene expression patterns of adaptive immune genes

An *origin salinity* effect indicates that gene expression of juvenile differs depending on the salinity they originate from (PERMANOVA, *all genes; origin salinity* $F_{1,523} = 4.2$, $p = 0.003$). Such signs of genetic adaptation were found in genes associated with the innate immune system (PERMANOVA, *innate,* $F_{1,523} = 9.2$, $p = 0.001$) and with osmoregulation (PERMANOVA, *osmo*, $F_{1,523} = 4.1$, $p = 0.003$; Figure 8, Table 2). Single ANOVAs suggested that this effect was driven by five genes. Whereas the pathogen reception recognition gene *lectin protein type II* (*lectpt2*) was higher expressed in parents from low *origin salinity*, the expression of the following genes was upregulated in juveniles from high *origin salinity* parents: *immunoglobulin light chain* (*IgM*; pathogen recognition), *heat shock protein 70 kDa* (*hsp70;* osmotic stress response); *voltage gated potassium channel* (*kcnh8;* cell volume regulation), *prolactin (prl;* ion uptake promotion and ion secretion inhibition). The genetically induced upregulation of osmoregulatory genes suggests an adaptation to low salinity levels.

Juvenile gene expression did not provide further evidence for genetic adaptation, tested as an interaction between *origin salinity* and *acclimation salinity* (PERMANOVA, *all genes* $F_{1,523} = 0.5$, $P = 0.858$). Trans-generational plasticity could also not be detected in the interaction between *acclimation salinity* and *developmental salinity* (PERMANOVA, *all genes* $F_{1,523} = 0.6$, $P = 0.730$).

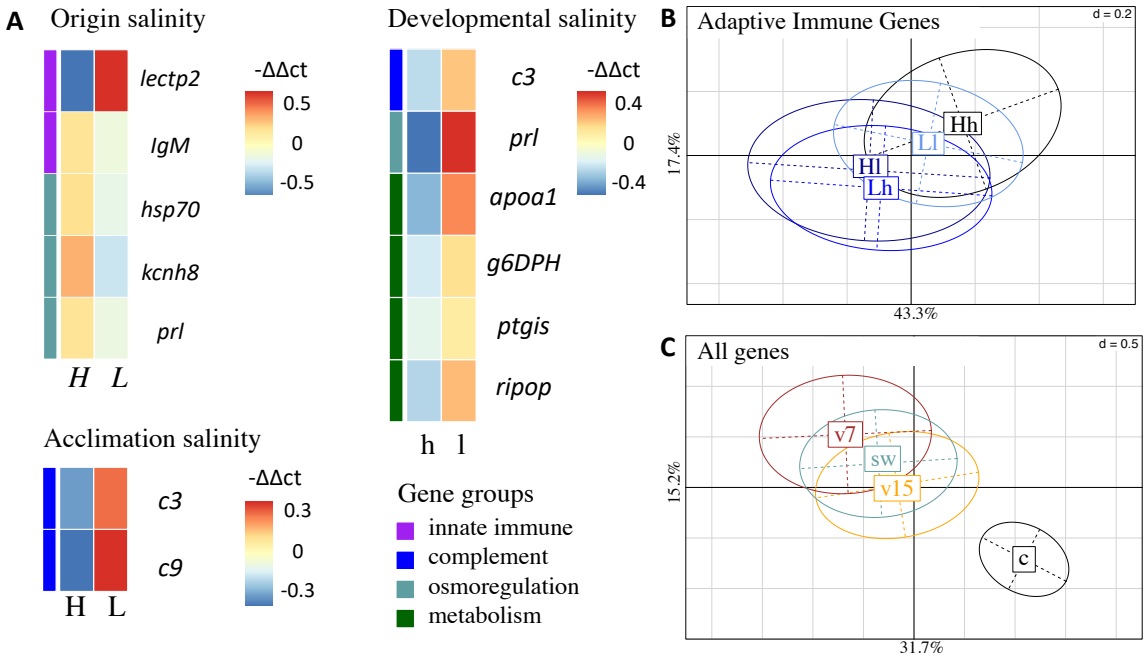

Figure 15: Gene expression patterns of juveniles

A: Non-hierarchical gene expression heatmap for genes showing differential expression (-ΔΔCt) in response to *origin salinity*, *acclimation salinity* or *developmental salinity*. Genes are sorted by gene groups which are assigned with different colors (purple: innate immune system, blue: complement system, turquoise: osmoregulation, green: metabolism).

B: Principal component analysis (PC1: 43.3%; PC2: 17.4%) of adaptive immune genes for significant interaction between parental *acclimation salinity* (H – high (15 PSU), L – low (7 PSU)) and *developmental salinity* (h, l). Four out of seven adaptive immune gene were upregulated (S 4), when parental *acclimation salinity* and juvenile *developmental salinity* did not match, i.e. Hl and Lh, compared to a matching *acclimation* and *developmental salinity*, i.e. Hh and Ll (PERMANOVA, *adaptive* $F_{1,523} = 2.6$, $p = 0.034$). The confidence ellipse explains 20 % of the variability.

C: Principal component analysis (PC1: 31.7%; PC2: 15.2%) of gene expression patterns caused by juvenile *treatment*, i.e. injection with *Vibrio alginolyticus* evolved at 15 PSU (v15, orange), *V. alginolyticus* evolved at 7 PSU (v7, brown), sham injection with seawater (sw, bluegreen) or untreated control (c, black). The confidence ellipse explains 20 % of the variability.

Table 2: PERMANOVA results of juvenile gene expression: A PERMANOVA was applied to gene expression (-ΔCt values) of all 558 samples for all genes (47), immune genes comprised of the innate, adaptive and complement genes, as well as genes involved in metabolism, osmoregulation and epigenetics, e.g. methylation or histone modification. Results are based on Euclidian distance matrices with 1000 permutations. Significant p-values are in bold and marked with a *.

		All genes		**Immune**		**Innate**		**Adaptive**		**Complement**		**Metabolism**		**Osmoreg**		**Epigentics**	
	df	F Model	Pf(>F)	F Model	Pf(>F)	F Model	Pf(>F)	F Model	Pf(>F)	F Model	Pf(>F)	F Model	Pf(>F)	F Model	Pf(>F)	F Model	Pf(>F)
Origin salinity (Origin sal)	1	**4.2**	**0.003***	5.2	**0.001***	**9.2**	**0.001***	1.4	0.21	2.3	0.098	1.5	0.203	**4.1**	**0.003***	0.7	0.508
Acclimation salinity Acclim sal)	1	1.5	0.15	1.6	0.129	1.2	0.277	0.5	0.715	**4.6**	**0.014***	1.1	0.326	1	0.411	2.6	0.578
Developmental salinity (Devo sal)	1	**3.2**	**0.005***	**2.5**	**0.034***	1.7	0.136	1.3	0.234	**3.3**	**0.028***	**4.2**	**0.020***	**6.4**	**0.001***	1.2	0.298
Treatment (Treat)	3	**11.3**	**0.001***	**13.9**	**0.001**	**17.5**	**0.001***	**16.8**	**0.001***	**6.3**	**0.001***	**2.5**	**0.025***	**9.1**	**0.001***	**3.2**	**0.005***
Origin sal:Acclim sal	1	0.5	0.858	0.4	0.93	0.3	0.91	0.7	0.582	0.6	0.535	0.2	0.908	0.8	0.525	1.6	0.182
Origin sal:Devo sal	1	0.6	0.73	0.6	0.783	0.6	0.663	0.6	0.642	0.3	0.74	0.3	0.798	1.2	0.265	0.5	0.672
Acclim sal:Devo sal	1	1.6	0.141	1.8	0.088	2.1	0.639	**2.6**	**0.034***	1.3	0.26	0.8	0.436	1.2	0.311	2.2	0.093
Origin sal:Treat	3	1.1	0.289	1.2	0.255	0.9	0.502	0.6	0.782	1.5	0.19	2.1	**0.037***	0.7	0.796	0.6	0.762
Acclim sal:Treat	3	0.6	0.933	0.4	0.995	0.3	0.999	0.8	0.633	0.3	0.947	0.9	0.503	0.9	0.526	0.5	0.881
Devo sal:Treat	3	0.8	0.675	0.9	0.603	0.8	0.671	1.1	0.336	0.6	0.722	0.9	0.453	0.8	0.678	0.6	0.815
Origin sal:sampling site	4	**2.9**	**0.001***	**3.1**	**0.001***	**3.5**	**0.001***	**3.2**	**0.001***	**2.2**	**0.036***	**2.3**	**0.023***	**2.1**	**0.005***	**3.7**	**0.003***
Origin sal:Acclim sal:Devo sal	1	1.2	0.251	1	0.372	1.3	0.221	1.1	0.354	0.3	0.809	1.4	0.214	0.7	0.633	2.2	0.089
Origin sal:Acclim sal:Treat	3	0.8	0.725	0.8	0.705	0.7	0.805	0.9	0.513	1	0.42	0.9	0.498	0.8	0.669	0.9	0.482
Origin sal:Devo sal:Treat	3	0.9	0.604	0.6	0.877	0.5	0.917	0.4	0.953	0.6	0.72	1.2	0.28	1.1	0.307	0.9	0.465
Acclim sal:Devo sal:Treat	3	0.9	0.534	0.9	0.582	0.8	0.618	1.3	0.202	1.1	0.37	0.7	0.628	0.8	0.665	0.9	0.541
Origin sal:Aacclim sal:Devo sal: Treat	3	0.6	0.933	0.5	0.983	0.5	0.956	0.5	0.912	0.4	0.918	0.6	0.718	0.9	0.507	0.7	0.664
Residuals	523																
Total	558																

Exposing parents to low *acclimation salinity* led to an expression induction of two genes in juveniles (PERMANOVA, *complement; acclimation salinity* $F_{1,523} = 4.6$, $p = 0.014$). Both genes are associated with the complement system*: Complement component 3* (c3, complement system activation) and *Complement component 9* (*c9*, membrane attack complex). In addition to this parental effect a trans-generational effect was observed as a *parental acclimation salinity* : *developmental salinity* interaction effect on adaptive immune gene expression (PERMANOVA, *adaptive* $F_{1,523} = 2.6$, $p = 0.034$). Gene expression was lower in four out of seven adaptive immune genes when *acclimation salinity* and *developmental salinity* were matching compared to non-matching conditions (S 12): *Human immunodeficiency virus type l enhancer* 2 (*hivep2*, transcription factor, MHC enhancer binding*)* and *3* (*hivep3;* transcription factor, MHC enhancer binding*), B-cell receptor-associated protein (becell.rap31*, T- and B-cell regulation activity) and *immunoglobulin light chain* (*igM;* antigen/pathogen recognition). The reduction in gene expression of immune genes can hint at a reduced stress level in offspring fish when parents are acclimated to the same salinity as their offspring.

Developmental plasticity allows juveniles to quickly respond to present salinity levels. Low *developmental salinity* resulted in higher expression of six gens. *Complement component 3 (c3)* is involved in the complement system (PERMANOVA, *comple; developmental salinity* $F_{1,523} = 4.6$, $p = 0.014$; Figure 8, Table 2), *prolactin* (*prl*, ion uptake promotion and ion secretion inhibition) is associated with osmoregulation (PERMANOVA, *osmo; developmental salinity* $F_{1,523} = 3.3$, $p = 0.028$) and *apolipoprotein A1* (*apoa1,* antimicrobial activity*), glucose 6 phosphate dehydrogenase* (*g6DPH*, pentose phosphate pathway)*, prostaglandin I2 Synthase* (*ptgis,* Lipid and fatty acid metabolism), *ribosomal protein* (*ripop*, Translation process) are related to the metabolism (PERMANOVA, *meta; developmental salinity* $F_{1,523} = 4.6$, $p = 0.014$).

Finally, we wanted to test whether genetic background, i.e. *origin salinity*, *acclimation salinity* of the parents and the *developmental salinity* influenced the ability of juveniles to cope with infections of the opportunistic pathogen *V. alginolyticus*, which evolved in the lab at either 15 or 7 PSU. However, we found no interaction between any salinity regime of parents or juveniles interacting with gene expression after juvenile infection. An injection, regardless of the component, i.e. autoclaved seawater, *V. alginolyticus* evolved at 15 PSU or 7 PSU caused similar changes in gene expression patterns that could only be differentiated

from the untreated control group. In 24 genes injections caused a higher gene expression (PERMANOVA, *all genes;* $F_{3,523} = 11.3$, $p = 0.001$; S 13), including genes from all groups. In five genes, injections caused a lower gene expression compare to the control group. Using post-hoc tests on ANOVAs of single genes, we found no differences in gene expression between the three injection treatments.

In the present study we investigated the role of genetic adaptation and phenotypic plasticity as well as their interaction on the ability of the broad-nosed pipefish *Syngnathus typhle* to cope with changes in salinity levels. *S. typhle* is a marine teleost, which originally invaded from the North Sea into the Baltic Sea (Wilson and Veraguth 2010). The brackish salinity environment in the Baltic Sea imposes osmoregulatory stress on marine animals and is thus assumed to be an important driver for genetic divergence and adaptation to local condition (Berg, Jentoft et al. 2015, Guo, DeFaveri et al. 2015, Johannesson, Le Moan et al. 2020). Here, we focused on six pipefish populations from the Baltic Sea, out of which three originated from a rather high saline environment (14 - 17 PSU), and three from a low saline environment (7 - 11 PSU). By taking the two salinity regimes into account, our experiment permitted to test both for local adaptation and for phenotypic plastic acclimation to different salinities.

S. typhle caught in the Baltic Sea high salinity environments (14 - 17 PSU) were smaller (14.2 cm) than those populating the marine realm with more than 28 PSU (mean size animals caught between 28 and 36 PSU: 18.7 cm (Rispoli and Wilson 2008) or 15.5 cm (Gurkan and Taskavak 2007), but larger than those sampled in Baltic Sea low salinity environments (mean size in this study: 12.8 cm; pipefish sampled at 5.5 PSU around Askö (Sweden): 14.5 cm (Rispoli and Wilson 2008). This suggests that osmoregulation is costly (Rolfe and Brown 1997, Boeuf and Payan 2001) and that the negative impact of low salinity can potentially not be fully compensated through local adaptation This implies that trade-offs for osmoregulation reduce growth rates, which ultimately correspond to a decreased fitness. Studies of other marine teleosts that originated from fully marine environments, e.g. sticklebacks and cod, suggested that high growth rates at intermediate salinity levels (10 - 20 PSU) are possible, especially when close or slightly above isosmotic levels (Dutil, Lambert et al. 1997, Imsland, Foss et al. 2001, Heckwolf, Meyer et al. 2018).

In this and a previous study (Nygard, Kvarnemo et al. 2019), the parental phenotype correlated with the body weight or length of the offspring. The heritability of morphological traits was suggested to be lower for ectotherms than for endotherms (Mousseau and Roff 1987). However, body size of pipefish females is known to correlate with egg size, and larger fathers were shown to give birth to embryos of an induced size (Nygard, Kvarnemo et al. 2019). To this end, both the parental body size and a resource-allocation trade off imposed by an increased energy demand for osmoregulation can explain the reduced embryonal growth in the low saline environment (Boeuf and Payan 2001). In the here presented survival experiment, juveniles from low origin salinity parents survived better compared to high origin salinity parents, independent of the parental acclimation salinity, developmental salinity and exposure to *Vibrio* bacteria. We thus suggest two alternative parental care strategies: large broad-nosed pipefish parents can invest in larger clutch and offspring size, while small parents may rather invest in survival (Nygard, Kvarnemo et al. 2019) via genetically determined gene expression patterns.

Such genetically determined gene expression patterns that are inherited from generation to generation, can be indicative signs for local adaptation (Larsen, Schulte et al. 2011, Fraser 2013, Heckwolf, Meyer et al. 2020). Females from high origin salinity had an induced baseline innate immune gene expression compared to females originating from low salinity environment. This induced innate immune gene expression pattern was inherited to their offspring: juveniles from animals caught from high saline environments generally had an induced expression of innate immune genes. We suggest that the observed induction of innate immune genes in pipefish originating from high saline origins is indicative for the existence of sufficient resources allowing to keep the innate immune response at a high baseline level. This can result in a faster and stronger and eventually more effective immune response. In contrast, pipefish from low origin salinity may rather suffer stress induced by the above stated resource allocation trade-off, which decreases the resources available for the innate immune system.

Under stress, animals are more susceptible to infections with pathogens, which may turn opportunistic pathogens into causative agents of deadly diseases (Boyett, Bourne et al. 2007, Poirier, Listmann et al. 2017, Sullivan and Neigel 2018). Furthermore, low saline environments have been suggested to select for increased pathogenic virulence, e.g. due to changes in gene expression (Hase and Barquera 2001) and biofilm formation (Dayma, Raval et al. 2015). This is in line with the observed brood pouch infections during pregnancy that

massively impacted fathers adapted to a high origin salinity but exposed to low acclimation salinity. Their clutch sizes at birth were reduced and their offspring were smaller. Fathers caught at low origin salinity (*L*L & *L*H) did not show signs of brood pouch infection, which gives support for our hypothesis that these animals were locally adapt to low saline environments and the associated pathogens. An adaptation to potentially more virulent infections at low saline conditions was also found in our experiment: juveniles infected with *Vibrio* bacteria survived better when the parents were caught at low originated from low saline environments.

Juveniles are expected to have advantages when exposed to the same environment as their parents (Sunday, Calosi et al. 2014, Roth, Beemelmanns et al. 2018). An interaction of the parental acclimation salinity and the juvenile developmental salinity is generally interpreted as an indicator for trans-generational plasticity (Uller, Nakagawa et al. 2013, Heckwolf, Meyer et al. 2018). In contrast to previous experiments focusing on trans-generational plasticity and immune priming in pipefish (Beemelmanns and Roth 2016, Beemelmanns and Roth 2017, Roth and Landis 2017), the adaptive trans-generational plastic effects identified in this study were limited. Even though survival of juveniles was higher in matching parental acclimation and developmental salinity, the effect was driven by the genetic adaptation and not the parental acclimation. The same applied for juvenile growth, which was imposed both by origin salinity and by the developmental salinity, but not by acclimation salinity. However, parental acclimation shifted expression of genes involved in complement and adaptive immune systems. As such, parental acclimation to low salinity (main effect) induced the expression of genes of the complement system. Non-matching parental acclimation and developmental salinity (interaction) upregulated genes of the adaptive immune system compared to matching parental acclimation and developmental salinity. In contrast to the above discussed upregulation of innate immune genes, an upregulation of the complement and adaptive immune system is indicative for a clear response towards prevailing parasites and pathogens, due to the specificity of the adaptive immune system (Janeway 2005). The complement system links the innate to the specific adaptive immune system. Their joint induction could give evidence for a shift in the microbial pathogen community in non-matching environments to which the specific arm of the immune system has to react. However, final support would enquire the genotyping of the microbial pipefish gut community.

The limited presence of trans-generational plasticity gives only partial support for our hypotheses and is in strong contrast to previous experiments performed with the same model system, where the genetic background was mostly ignored and experiments focused only on one population (Roth, Keller et al. 2012, Beemelmanns and Roth 2016, Beemelmanns and Roth 2017, Roth and Landis 2017). The here performed experiment allows us to at least partially disentangle genetic adaptation and trans-generational plasticity and suggests that selection imposed by genetic adaptation is a lot stronger than the impact of trans-generational plasticity. To this end, the unexpected limited identification of trans-generational plastic effects could indicate that we are generally overestimating trans-generational plasticity in experiments that ignore genetic background, as genetic adaptation is intermingled with the phenotypic plastic components. Alternatively, we have potentially not identified all present signs of trans-generational plasticity in this experiment as the populations are too distinct due to their history of genetic adaptation hindering the identification of trans-generational plastic effects. By taking the genetic adaptation into account, we suggest that the probability to identify existing phenotypic plastic effects is lower, as the impact of phenotypic plastic effects is weaker than the impact of genetic differences among populations.

Populations that invaded a new habitat are under strong selection for genetic adaptation towards the novel environmental condition. They go through a bottleneck, which results in populations that are diverged from their ancestral populations (Johannesson, Le Moan et al. 2020) and are characterized by a reduced genetic diversity (Johannesson and Andre 2006). In another study this reduced genetic diversity as a consequence of genetic adaptation negatively impacted the individual phenotypic plasticity of sticklebacks populating low salinity regions of the Baltic Sea (DeFaveri and Merila 2014, Hasan, DeFaveri et al. 2017). In a stable salinity environment, we would thus expect that genetic adaptation had resulted in reduced phenotypic plasticity and lower performance in the ancestral environment (DeWitt, Sih et al. 1998, Schneider and Meyer 2017). In contrast to our expectation, juvenile survival of parents from low salinity origins was not reduced at high developmental salinity suggesting that genetic adaptation towards low salinity conditions did not result in a reduction of phenotypic plasticity. Along the same line, the smaller size of juveniles from parents originating from low salinity environments is no indicator for reduced plasticity either. The smaller phenotype (at the same age) was more likely a result of the reduced parental size (Nygard, Kvarnemo et al. 2019), which can be an adaptation to low salinities

caused by shifts in allele frequencies (McGuigan, Nishimura et al. 2011). The strong salinity fluctuations in the coastal environments across the Baltic Sea (Bock and Lieberum 2017) most likely selected against the loss of phenotypic plasticity.

The isosmotic level of many marine fish is equivalent to around 12 PSU (Schaarschmidt, Meyer et al. 1999) or a couple of units higher, depending on the ambient salinity conditions (Quast and Howe 1980, Partridge, Shardo et al. 2007). This suggests that the here applied high salinity treatment is rather hyper- to isosmotic, whereas the low salinity treatment is hypoosmotic. The hormone prolactin is involved in many metabolic pathways in vertebrates and highly relevant for fish in hypoosmotic conditions as it prevents the loss of ions and the uptake of water. Both mechanisms are crucial in hypoosmotic conditions to maintain homeostasis (McCormick 2001, Manzon 2002, Breves, McCormick et al. 2014). In our study, prolactin (*prl*) was the gene with the strongest upregulation in juveniles at low developmental salinity conditions underlining the ability of pipefish to quickly respond to prevailing salinity conditions. Similar patterns in the upregulation of prolactin in marine fish have been identified in black porgy *Acanthopagrus schlegelii* (Tomy, Chang et al. 2009) and rainbow trout *Oncorhynchus mykiss* (Prunet, Avelia et al. 1990). This implies that higher *prl* expression under low salinity conditions could be indicative for adaptive developmental plasticity and suggest that juvenile fish are able to cope with short term salinity changes.

Some strains of the species *Vibrio alginolyticus* have been shown to become more virulent under low saline conditions (Dayma, Raval et al. 2015, Poirier, Listmann et al. 2017). Drivers for this increased virulence can be trade-offs in the host (Birrer, Reusch et al. 2012, Poirier, Listmann et al. 2017), a phenotypic response of the bacteria (Hase and Barquera 2001, Dayma, Raval et al. 2015) or a genetic adaptation of the bacteria to low salinity (Brown, Cornforth et al. 2012). Under low saline condition, we thus expected strong selection for immunological adaptation towards the prevailing pathogens that potentially resulted in a higher tolerance or a more effective immune defense against *Vibrio* bacteria. In line with this expectation, we found that pipefish offspring from parents caught at low salinity origin survived better when exposed to *Vibrio* bacteria than offspring from parents caught at high saline origins. This suggests that local adaptation to low saline conditions allows pipefish to allocate sufficient resources towards their immune system for fighting *Vibrio* infections. To this end, we found support for our hypothesis that increased *Vibrio* virulence in marine host organism can result from resource allocation tradeoffs towards osmoregulation, impairing the host's immune system (Birrer, Reusch et al. 2012).

The bacteria used in this experiment were previously evolved at the respective high (V15: 15 PSU) or low (V7: 7 PSU) Baltic Sea salinity condition. If genetic adaptation of bacteria to low salinity induces their virulence, we would have expected that the bacteria evolved at 7 PSU (V7) are more virulent, in particular for the pipefish offspring from parents originating from high saline locations. In contrast to our expectation, we have identified that v15 caused a higher mortality in juveniles originating from a high saline environment than in juveniles coming from low salinity origin and low parental salinity acclimation, while the impact of v7 was not differentiable across all groups. Gene expression measurements were not appropriate to answer the question of induced virulence and a corresponding stronger host immune response against bacteria evolved at low or high salinity depending on pipefish local salinity adaptation. Instead, the injury imposed by the injection had the strongest impact on the gene expression pattern. As such, gene expression of sham-injected animals was not distinguishable from those injected either with v7 or v15. This is an unexpected limitation of our study, however, given that impact of *Vibrio* bacteria on pipefish mortality could have been identified, we are assuming that we have not chosen the time point when reactions towards *Vibrio* infection would have been best mirrored in the gene expression patterns but rather the timepoint when inflammation or stress upon the injection could be assessed. Bearing these limitations in mind, we suggest that the increased virulence of the *V. alginolyticus* strain is mainly driven by trade-offs impairing the pipefish's immune system. A deficiency that can potentially be overcome by local adaptation.

The here identified patterns have to be interpreted with care. Due to the unintended brood pouch infection that negatively affected 47% of the pregnant males originating from high saline conditions and parentally acclimated at low saline conditions, we are dealing with distinct selection intensities on the different treatment groups (Roth, Beemelmanns et al. 2018). In the treatment affected by the brood pouch fungus (Origin Salinity: *H*, Acclimation salinity: L) multiple clutches have at least been partially lost and potentially all infected fathers were suffering stress levels that can seriously confound the results from this study. The brood pouch fungus has severely impacted offspring development such that only the strongest will have survived. Addressing life history traits in the offspring and their gene expression will thus in the *H*L group only be done in the strongest animals, which does not resemble the original cohort, and makes interpretation of the data in the offspring generation difficult. We are aware of this limitation and have been taking this into account when interpreting our data.

5.5 | Conclusion

After the last glacial maximum, broad-nosed pipefish have successfully populated the low salinity areas of the Baltic Sea. The results of our study suggest that the components of this success story are a mixture of genetic adaptation and the maintenance of a high degree of phenotypic plasticity of locally adapted pipefish enabling them to deal with present and ancestral salinity levels and even with re-occurring salinity fluctuations. Pipefish individuals with suitable alleles for low salinity conditions can inhabit low saline environments. The adaptation and adjustment of life history strategies to lower salinity also enable pipefish to cope with prevailing pathogens such as *Vibrio* bacteria or aquatic fungi. Pipefish of the species *S. typhle* inhabiting the Baltic Sea are thus expected to be well prepared for predicted further drops in salinity, which is also underlined by the fact that already now they inhabit areas in the northern part of the Baltic Sea with salinity levels below 5 PSU.

Acknowledgments

We are grateful for the help of Kristina Dauven, Andreas Ebner, Janina Röckner and Paulina Urban for fish collection in the field and fish maintenance. Furthermore, we thank Fabian Wendt for setting up the aquaria system. We thank Tatjana Liese, Paulina Urban, Jakob Gismann and Thorsten Reusch for support with DNA extraction and analysis of pipefish population structure. The authors acknowledge support of Isabel Tanger, Agnes Piecyk, Jonas Müller, Grace Walls, Sebastian Albrecht, Julia Böge and Julia Stefanschitz for their support in preparing cDNA and running of Fluidigm chips. A special thank goes to Diana Gill for general lab support, ordering materials and just being the good spirit of our molecular lab, to Till Bayer for bioinformatics support and to Melanie Heckwolf for fruitful discussion and feedback on the manuscript. H.G. is very grateful for inspirational office space with ocean view provided by Lisa Hentschel and family. This manuscript has been released as a pre-print at https://biorxiv.org/cgi/content/short/2020.11.12.379305v1 (Goehlich, Sartoris et al. 2020).

Funding

This project was funded by a DFG grant [WE 5822/ 1-1] within the priority programme SPP1819 given to CCW and OR, and a DFG grant [349393951] to OR. Furthermore, this study was supported by funding from the European Research Council (ERC) under the European Union´s Horizon 2020 research and innovation program (Grant agreement No: 755659 – acronym: MALEPREG). HG received career and financial support from the Max Planck Research School.

Ethical statement

Experimental work was conducted in agreement with the German animal welfare law and approved by the Ministerium für Energiewende, Landwirtschaft, Umwelt, Natur und Digitalisierung under permission MELUR V 312–7224.121-19 (67–5/13), “komparative Vergleichsstudie von Immunantwort-Transfer von Eltern zu Nachkommen in Fischarten mit extremer Brutpflege”)

Conflict of interest

The authors declare that the research was conducted in the absence of any commercial or financial relationships that could be construed as a potential conflict of interest.

Author contribution

O.R. and H.G. designed the study with input from C.C.W. H.G., K.W., O.R. collected fish in the field, conducted the experiment and sampled the fish. L.S. designed the primers. L.S., H.G. and K.W. did the molecular lab work. H.G., L.S., O.R and K.W. analyzed the data. H.G., L.S. and O.R. wrote the manuscript with input from all others.

Data archiving

Data is available at the PANGEA database: https://doi.pangaea.de/10.1594/PANGAEA.926923.

5.6 | Supplement

Supplement 1: Table S 1: Name and function of target genes used to study gene expression. Listed are all target genes from four different functional categories: general metabolism, immune response (adaptive and innate), gene regulation (acetylation and methylation) and osmoregulation. The column 'Organism' specifies, whether the gene was targeted in female (f) or juvenile (juv) samples.

Gene	Organism	Category	Gene name	Function	Reference
BROMO	juv, f	epigenetic/ activation	Histone acetyltransferase	Histone acetylation	Beemelmanns & Roth 2016
MYST	juv	epigenetic	Histone acetyltransferase	Histone acetylation	Beemelmanns & Roth 2016
Bcell.rap	juv	adaptive	B-cell receptor-associated protein	T- and B-cell regulation activity	Roth et al. 2012
CD45	juv	adaptive	CD45 (Leukocyte common antigen)	T-cell and B-cell antigen receptor signalling	Beemelmanns & Roth 2016
HIVEP2	juv	adaptive	Human immunodeficiency virus type I enhancer 2	Transcription factor, V(D)J recombination, MHC enhancer binding	Beemelmanns & Roth 2016
HIVEP3	juv	adaptive	Human immunodeficiency virus type I enhancer 3	Transcription factor, V(D)J recombination, MHC enhancer binding	Beemelmanns & Roth 2016
IgM	juv	adaptive	Immunoglobulin light chain	Antigen/pathogen recognition	Beemelmanns & Roth 2016
lymphag75	juv	adaptive	Lymphocyte antigen 75	Antigen recognition	Birrer et al. 2012
aif	juv, f	innate	Allograft inflammation factor	Inflammatory responses, allograft rejection, macrophages activation	Roth et al. 2012
apoa1	juv	innate	Apolipoprotein A1	Antimicrobial activity	Roth et al in prep.
c1	juv	innate	Recognition subcomponent C1q	Antigen-antibody complex formation	Beemelmanns & Roth 2016
c3	juv	innate	Complement component 3	Complement system activation	Birrer et al. 2012
c9	juv	innate	Complement component 9	Membrane attack complex, bacteria lysis	Roth et al. 2012
cf	juv, f	innate	Coagulation factor II	Blood clotting and inflammation response	Birrer et al. 2012
hsp60	juv, f	innate	Heat shock protein 60 kDa	Chaperone, general stress response	Roth et al. 2012
il10	juv	innate	Interleukin 10	Macrophage activity regulation	Birrer et al. 2012
il8	juv	innate	Interleukin 8	Phagocytosis, inflammation	Beemelmanns & Roth 2016

Gene	Organism	Category	Gene name	Function	Reference
kin	juv, f	innate	Kinesin	Intracellular transport	Roth et al. 2012
lectpt2	juv, f	innate	Lectin protein type II	Pathogen recognition receptor	Beemelmanns & Roth 2016
tranfe	juv, f	innate	Transferrin	Bacterial growth prevention	Beemelmanns & Roth 2016
tspo	juv, f	innate	Translocator protein	Inflammatory responses, allograft rejection, macrophage activation	Roth et al. 2012
tyroprot	juv, f	innate & adaptive	Tyroproteinkinase	Cytokine receptor signalling	Beemelmanns & Roth 2016
ddpgly	juv, f	metabolism	Ddp-glycosyltransferase	Metabolizing process (natural glyosidic linkages)	Roth et al. in prep.
g6DPH	juv, f	metabolism	Glucose 6 phosphate dehydrogenase (G6PD)	Metabolizing process (pentose phosphate pathway)	Roth et al. in prep.
ptgis	juv	metabolism	Prostaglandin I2 Synthase	Lipid and fatty acid metabolism	Roth et al. in prep.
ripop	juv, f	metabolism	Ribosomal protein	Translation process	Roth et al. in prep.
TNF	juv	metabolism	Tumor necrosis factor	Lipid metabolism	Roth et al. in prep.
ubi	juv, f	metabolism	Ubiquitin	Regulatory protein labelling for degradation	Birrer, Reusch, et al. 2012
DnMt3B	juv	epigenetic	DNA methyltransferase 3b	De novo methylation	Beemelmanns & Roth 2016
JmicPhD	juv, f	epigenetic/ silencing	Lysine-specific demethylase 5B	Histone demethylation	Beemelmanns & Roth 2016
N6admet	juv	epigenetic/ activation	N(6)- adenine-specific DNA-methyltransferase 2	DNA-methyltransferase	Beemelmanns & Roth 2016
no66	juv,f	epigenetic/ silencing	Lysine-specific histone demethylase NO66	Histone demethylation	Beemelmanns & Roth 2016
TPR	juv, f	epigenetic/ activation	Lysine-specific demethylase 6A	Histone demethylation	Beemelmanns & Roth 2016
aqp3	juv	osmoregulation	Aquaporin 3	Water and small solute channel	This study
atp1a1	juv	osmoregulation	ATPase alpha 1	Na+/K+ transporting	This study
cftr	juv	osmoregulation	Cystic fibrosis transmembrane conductance regulator	Apical membrane anion channel	This study
cldn1	juv	osmoregulation	Claudin 1	Epithelial permeability regulation	This study
hsp70	juv	osmoregulation	Heat shock protein 70 kDa	Osmotic stress response	This study

Gene	Organism	Category	Gene name	Function	Reference
kcnh8	juv	osmoregulation	Voltage gated potassium channel subfamily h member 8	Cell volume regulation	This study
mapk8ip3	juv	osmoregulation	Mitogen-activated protein kinase 8 interacting protein 3	Osmosensing	This study
nkcc2	juv	osmoregulation	Na+/K+ /2Cl cotransporter (Slc12A1)	Ion transport	This study
nr3c1	juv	osmoregulation	Nuclear Receptor Subfamily 3 Group C Member 1	Glucocorticoid receptor	This study
prl	juv	osmoregulation	Prolactin	Ion uptake promotion; ion secretion inhibition	This study
prlr	juv, f	osmoregulation	Prolactin receptor	Prolactin receptor	This study
hdac1	juv	reference/ epigenetic	Histone deacetylase 1-like	Histone deacetylation	Beemelmanns & Roth 2016
hdac3	juv	reference/ epigenetic	Histone deacetylase 3-like	Histone deacetylation	Beemelmanns & Roth 2016
ash	juv	reference/epigenetic/activation	Histone methyltransferase	Histone methyltransferase	Beemelmanns & Roth 2016
calrcul	f	innate	Calreticulin	Chaperone, promotes phagocytosis and clearance of apoptotic cells	Beemelmanns & Roth 2016
ck7	f	innate & adaptive	Chemokine 7	Chemotaxis for leukocytes, monocytes, neutrophils, blood cells	Beemelmanns & Roth 2016
dnmt1	f	epigenetic/ silencing	DNA (cytosine-5)-methyltransferase 1	copies complementary marks of newly replicated DNA, maintenance methylation	Beemelmanns & Roth 2016
dnmt3a	f	epigenetic/ silencing	DNA (Cytosine-5-)-Methyltransferase 3 Alpha	de novo modifications; essential for epigenetic changes based on environmental stress	Beemelmanns & Roth 2016,
hdac6	f	epigenetic/ silencing	Histone deacetylase 6-like	Histone deacetylation (deacetylation lysine residues of core histones)	Beemelmanns & Roth 2016
hemk2	f	epigenetic/ silencing	HemK-methyltransferase family member 2	DNA methyltransferase (N6-methyladenine)	Beemelmanns & Roth 2016,
ik-cytoine	f	adaptive & innate	Ik cytokine(RED-protein)	Inhibits interferon gamma mediated downregulation of MHCII	Beemelmanns & Roth 2016
Intf	F	Innate	Interferon induced transmembrane protein 3	Negative regulation of viral entry into host cell, antiviral response	Beemelmanns & Roth 2016

Supplement 2: Description and selection of osmoregulatory genes

Osmoregulatory target genes were selected based on their function, involvement in adaptation to marine or freshwater environment, and/or inducibility upon salinity stress. The genes aquaporin 3 (*AQP3*), claudin 1 (*CLDN1*) and mitogen-activated protein kinase 8 interacting protein 3 (*MAPK8IP3*) were recently shown to alter their expression in response to different salinity treatments in alewives *Alosa pseudoharengus* (Velotta, Wegrzyn et al. 2017). *AQP3* is a member of transmembrane channel proteins transporting water and small solutes. It plays a major role in osmoregulatory organs such as the gill, kidney, oesophagus and intestine (Cutler, Martinez et al. 2007). *CLDN1* is a cell surface component of tight junction complexes (Paris, Tonutti et al. 2008) and *MAPK8IP3* is involved in osmosensing (Velotta, Wegrzyn et al. 2017). ATPase Na^+/K^+ transporting subunit alpha 1 (*ATP1α1*), cystic fibrosis transmembrane regulator (CFTR), $Na^+/K^+/2Cl^-$ cotransporter (*NKCC*) and heat shock protein 70 kDa (HSP70) were all found to be induced upon salinity changes (Hwang and Lee 2007, Taugbol, Arntsen et al. 2014, Ronkin, Seroussi et al. 2015). ATP1α1, a membrane spanning enzyme active for example in fish gills, actively transports sodium ions (Na^+) out of and potassium ions (K^+) into a cell (Cutler, Martinez et al. 2007, Hwang and Lee 2007). *CFTR* is an apical membrane anion channel secreting Cl^-, and *NKCC2* (NKCC isoform 2; also known as solute carrier family 12 member 1) is an ion cotransporter located in the membrane (Hwang and Lee 2007) Other important ion transporters like voltage gated potassium channel genes regulate cell volume and the subfamily h member 4 (*KCNH4*) gene was shown to be involved in freshwater adaptation in the three-spined stickleback *Gasterosteus aculeatus* (Taugbol, Arntsen et al. 2014). However, as no orthologous for *KCNH4* could be identified in the *S. typhle* genome, the closely related *KCNH8* was selected for this study instead (Gutman, Chandy et al. 2005). Additionally, *ATP1α1, CFTR, KCNH4* were proposed to be under selection in animals exposed to marine-freshwater gradients (Tomy, Chang et al. 2009, Taugbol, Arntsen et al. 2014) showed that expression of the prolactin receptor gene (*PRLR*) was correlated with adaptation to freshwater. Among other functions, the hormone prolactin (*PRL*) regulates water and electrolyte balance by promoting ion intake and inhibiting ion secretion (McCormick 2001, Manzon 2002). Gene nuclear receptor subfamily 3 group C member 1 (*NR3C1*) encodes glucocorticoid receptor, which stimulates ATPase Na^+/K^+ transport and proliferation and differentiation of ion transporting chloride-cells in osmoregulatory organs (Marshall, Cozzi et al. 2005). *NR3C1* expression has also been linked to salinity stress in the euryhaline fish black porgy *Acanthopagrus schlegeli* (Tomy, Chang et al. 2009) (Table S2).

Supplement 3: Design of primers for osmoregulatory genes

Transcripts for (iv) osmoregulatory genes in *S. typhle* were identified by searching for orthologous of candidate genes in transcriptomes from other teleost fish. The transcripts were taken from the NCBI nucleotide database (https://www.ncbi.nlm.nih.gov/nuccore) and using the basic local alignment search tool BLAST (Altschul, Gish et al. 1990). The osmoregulatory candidate genes were identified in the *S. typhle* transcriptome and genome (Haase, Roth et al. 2013, Roth, Solbakken et al. 2020). Additionally, the protein product of the *S. typhle* gene transcript was verified in UniProt (The UniProt Consortium 2017). *S. typhle* specific primer pairs for 11 osmoregulatory genes were designed with Primer3web (version 4.1.0; for parameters see Table S1) and, finally, primer specificity was checked with BLAST against the *S. typhle* genome and transcriptome. Whenever possible, primers were designed to span Exon-Exon boundaries, visualized in alignment viewer and editor AliView (Larsson 2014).

The efficiency of potential primers was tested with quantitative real time polymerase chain reactions (qPCR) in a dilution series (1:10, 1:20, 1:40, 1:80, 1:160, 1:320). Primer specificity was checked again by visual evaluation of the melting curves. Only candidate primer pairs with efficiency between 79 - 106 % and standard curve slope (log quantity vs. threshold cycles) between -3.2 and -4.2 were chosen for the study (Table S3).

Supplement table S3: Osmoregulatory gene primers. Primer sequences and properties of all primers osmoregulatory gene primers used in this study. Hits on scaffold, hit annotation and PCR product sequence can be found in the data archive PANGEA.

Gene	Target	Primer Sequence (forward/reverse)	PCR product length	melting temperature	efficiency [%]
aqp3	Aquaporin 3	CTTCCAGATCCGCAACCTACTG	145	60.74	105.8
		GGCAAAGTTAACCGTCAAGAACA		59.93	
atp1a1	ATPase alpha 1	GCTGGGAAGAGGGAAAGATGAT	170	59.83	85.5
		GGTCGGTTCCGTACTTCCTATG		60.22	
zcldn1	Claudin 1	AACGACAACACCAAAGCTTACG	145	59.97	89.4
		ATGATCTCCACCATGACGTACG		59.97	
mapk8ip3	Mitogen-activated protein kinase 8 interacting protein 3	CACGAAATCAAAGACGCCAAGT	130	60.03	89
		GAAGCTGTTTGTTCTCCGTCAG		59.78	
prl	Prolactin	TGGTTTTGTCCTCTTCCGCTAA	182	59.89	88.6
		GATGTCATTGCCGCCTCTGTA		60.47	
prlr	Prolactin receptor	CGGCTGGATCACACTCATCTAT	188	59.7	83.9
		TTTGGGACTCAGAGCTCCATTC		60.03	
nr3c1	Nuclear Receptor Subfamily 3 Group C Member 1	TCCCGTCAACAGGAAGTCTTTT	163	59.83	73.3
		ACGTTGGCAGTGATAGAAGAGG		60.09	
cftr	Cystic fibrosis transmembrane conductance regulator	AAGTTGGACCTCACTGACGTTT	125	60.09	86.4
		CGCATCAAACTGGGCTTCTTC		60.14	
kcnh8	Voltage gated potassium channel subfamily h member 8	CTCATCTTTGCACTCGTCAACC	181	59.84	79.2
		GCTGGCAGTTAAACAACGACAT		60.03	
hsp70	Heat shock protein 70 kDa	TGAGGGCGTTGATTTCTACACA	124	59.96	81.6
		GCCCTTGTCCATCTTAGCATCT		60.16	
nkcc2	Na+/K+ /2Cl- cotransporter (Slc12A1)	CTTCATCCTACTGGCGGCTATT	145	59.96	98
		CGACTCTTGATTCCTGAAAGCC		59.32	

Supplement 4: Sample size of target gene expression for females

Supplement table S4: Sample size of target gene expression for females, including sampling site, salinity category at origin, salinity acclimation in the lab and number of processed females

Origin	Origin salinity	Acclimation salinity	Number of females
Flensburg	High	High	14
	High	Low	15
Falkenstein	High	High	14
	High	Low	14
Fehmarn	High	High	12
	High	Low	13
Salzhaff	Low	High	12
	Low	Low	15
Ruegen North	Low	High	11
	Low	Low	12
Ruegen South	Low	High	12
	Low	Low	11

Supplement table S5: Pairwise F_{ST} of pipefish from different sampling sites

Comparison	F_{ST}
Falck-Fehm	0.0239
Falck-Flens	0.0162
Falck-Salz	0
Falck-RuegN	0.0064
Falck-RuegS	0
Fehm-Flens	0
Fehm-RueN	0.0102
Fehm-RuegS	0.0015
Fehm-Salz	0.0031
Flens-ReugN	0.0033
Flens-RuegS	0.0079
Flens-Salz	0
RuegN-RuegS	0
RuegN-Salz	0

Supplement 6: Statistics tables and additional graphs for total length and body weight of adult pipefish

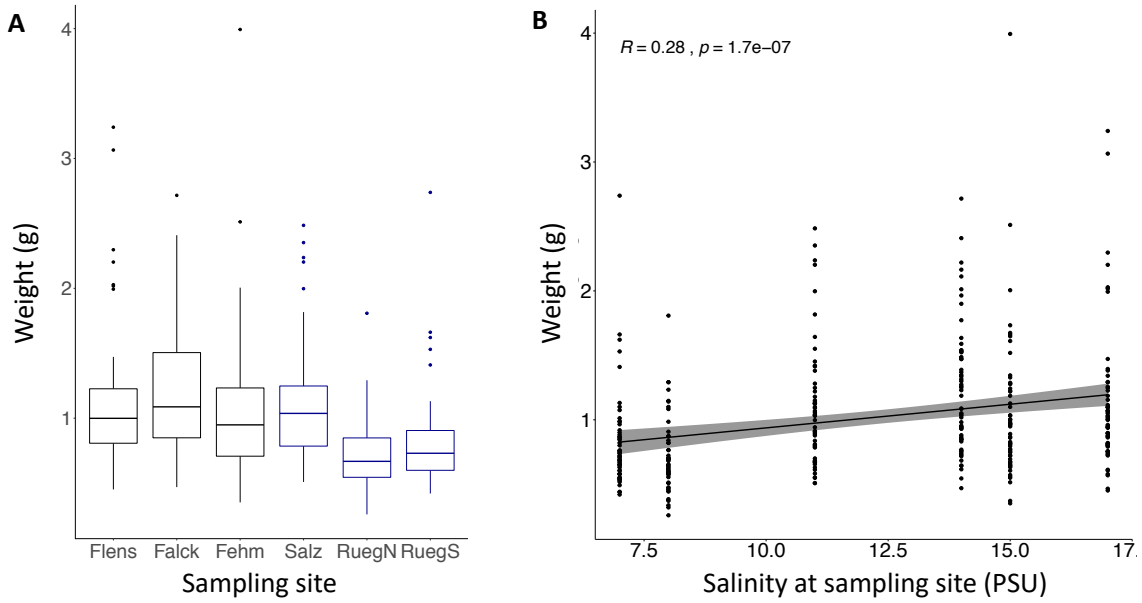

Supplement figure S6: Weight of adult pipefish. The weight of pipefish (y-axis) is plotted for different sampling site (x-axis) (A), and correlated with the salinity at the different sampling sites (B).

Supplement table S6a: Analysis of variance (ANOVA) for length of adult pipefish

Fixed factors are *Sex*, *Origin salinity*, *Acclimation salinity* and *Sampling site* nested in *Origin salinity*.

Full model – Adult length	Df	Sum Sq	Mean Sq	F value	p
Sex	1	8.82	8.824	2.4	0.123
Origin salinity	1	182.00	182.004	49.4	**< 0.001***
Acclimation salinity	1	3.19	3.189	0.9	0.353
Sex: Origin salinity	1	1.44	1.443	0.4	0.531
Sex: Acclimation salinity	1	0.10	0.105	0.0	0.866
Origin salinity:Acclim salinity	1	27.27	27.269	7.4	**0.006***
Origin salinity:Sampling site	4	166.46	41.616	11.3	**< 0.001***
Sex: Origin salinity:Acclimation salinity	1	2.52	2.525	0.7	0.409
Residuals	320	1179.79	3.687		

Reduced model	Df	Sum Sq	Mean Sq	F value	p
Origin salinity	1	182.0	182.0	49.4	**< 0.001***
Acclimation salinity	1	3.2	3.2	0.8	0.353
Origin salinity:Acclimation salinity	1	26.7	27.3	7.4	**0.007**
Origin salinity:Sampling site	4	165.0	41.6	11.3	**< 0.001***
Residuals	320	1179.8	3.7		

Supplement table S6b: Post hoc test Tukey HSD for body length of adult pipefish contrasting different salinity histories, i.e. salinity origin and acclimation salinity.

	Estimate	Std. Error	t value	Pr(>|t|)
*H*L – *H*H == 0	-0.72	0.30	-2.3	0.083
*L*H – *H*H == 0	-2.08	0.32	-6.4	**< 0.001***
*L*L – *H*H == 0	-1.66	0.32	-5.2	**< 0.001***
*L*H – *H*L == 0	-1.36	0.32	-4.3	**< 0.001***
*L*L – *H*L == 0	-0.94	0.31	-3.0	**0.014**
*L*L – *L*H == 0	0.41	0.33	1.2	0.583

Supplement table S6c: Post hoc test Tukey HSD for body length of adult pipefish contrasting sampling sites.

	Estimate	Std. Error	t value	Pr(>|t|)
Fehm – Falck == 0	-0.7373	0.3566	-2.067	0.307
Flens – Falck == 0	-0.1271	0.3537	-0.359	0.999
RuegN – Falck == 0	-2.8133	0.3765	-7.471	**< 0.001***
RuegS – Falck == 0	-2.1409	0.3684	-5.811	**< 0.001***
Salz – Falck == 0	-0.4729	0.3666	-1.290	0.790
Flens – Fehm == 0	0.6102	0.3537	1.725	0.516
RuegN – Fehm == 0	-2.0760	0.3765	-5.513	**< 0.001***
RuegS – Fehm == 0	-1.4036	0.3684	-3.810	**0.002***
Salz – Fehm == 0	0.2644	0.3666	0.721	0.979
RuegN – Flens == 0	-2.6862	0.3738	-7.187	**< 0.001***
RuegS – Flens == 0	-2.0138	0.3656	-5.508	**< 0.001***
Salz – Flens == 0	-0.3459	0.3637	-0.951	0.933
ReugS – RuegN == 0	0.6724	0.3877	1.734	0.510
Salz – RuegN == 0	2.3404	0.3860	6.063	**< 0.001***
Salz – RuegS == 0	1.6680	0.3781	4.412	**< 0.001***

Supplement 7: Statistic tables and additional graphs for clutch size

Supplement table S7a: Analysis of variance (ANOVA) for clutch size of adult pipefish Fixed factors are *Origin salinity*, *Acclimation salinity* and *Sampling site* nested in *Origin salinity*.

Full model	Df	Sum Sq	Mean Sq	F value	p
Origin salinity	1	5.0	5.0	2.0	0.160
Acclimation salinity	1	41.2	41.2	15.0	**0.001***
Av male length	1	14.6	14.6	5.8	**0.017***
Origin salinity:Acclimation salinity	1	25.6	25.6	9.0	**0.003***
Origin salinity:Sampling site	2	9.1	4.6	1.8	0.168
Origin salinity:Av male length	1	0.4	0.4	0.1	0.705
Acclimation salinity:Av male length	1	1.3	1.3	0.5	0.474
Origin sal: Acclim sal:Av male length	1	31.7	31.7	12.6	**0.001***
Residuals	109	273.6	2.5		

Supplement table 7b: Post hoc test Tukey HSD for clutch size of adult pipefish salinity histories. The italic letter represents the origin salinity (*H* - High, *L* - Low) and the second letter indicates the salinity level in the lab (H - High, L - Low).

	Estmate Std.	Error	t value	p
***H*L - *H*H == 0**	-22.4	4.6	-4.8	**< 0.001***
***L*H - *H*H == 0**	-14.0	4.5	-3.1	**0.010***
***L*L - *H*H == 0**	-16.5	4.5	-3.6	**0.003***
*L*H - *H*L == 0	8.4	4.8	1.7	0.512
*L*L - *H*L == 0	5.8	4.8	1.2	0.762
*L*L - *L*H == 0	-2.5	4.7	-0.5	0.976

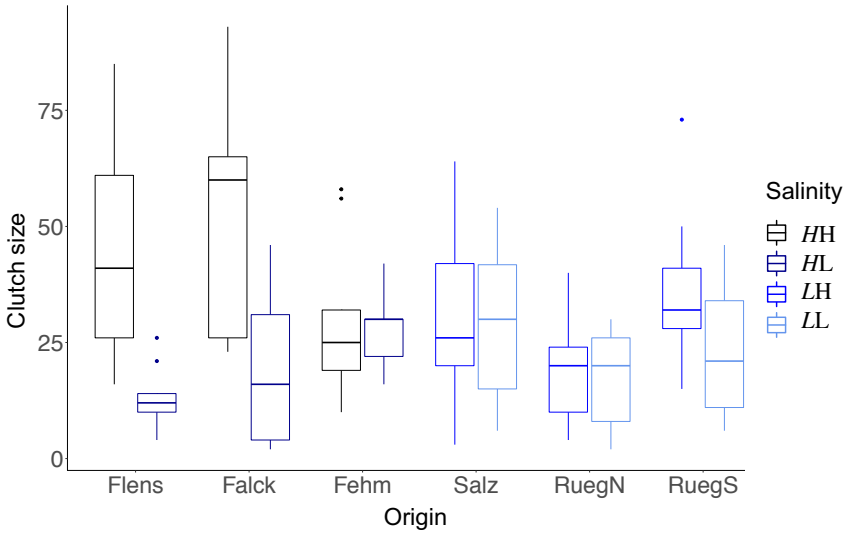

Supplement Figure 7c: Clutch size is reduced at low salinity for all sampling sites Number of juveniles (clutch size) is shown for pipefish from different origins (sampling site). Italic letters and colors indicate the salinity level at the origin of (*H*: 15 PSU, black & dark blue; *L*: 7 PSU blue & light blue). The 2nd letter indicates the salinity during breeding in the lab (H: 15 PSU, black and blue; L: 7 PSU, dark & light blue).

6 | SYNTHESIS & PERSPECTIVE

6.1 | Synthesis

In order to understand whether and how species can adapt to ongoing climate change, we need to move beyond studying individual organisms and integrate coevolutionary approaches in our research repertoire (Northfield and Ives 2013). This is, because natural selection may act differently on each of the interacting species, creating co-evolutionary dynamics that can lead to shifts in species abundance or even drive extinctions (Vandvik, Skarpaas et al. 2020) Imbalances between two coevolving species may be buffered or further amplified by the intervention of a third agent. Understanding these complex dynamics on ecological and evolutionary time scales is essential to predict the direction towards which ecosystems are moving and their resilience upon climate change.

The overall goal of this thesis is to study the effects of salinity changes as predicted under climate change scenarios in the Baltic Sea in a complex tripartite species interaction comprising filamentous phages, *Vibrio* bacteria and the pipefish *Syngnathus typhle*. While filamentous phages engage in inter-species relationships that lie on a continuum between mutualism and parasitism, the *Vibrio* strains considered in this study are opportunistic pathogens experiencing distinct selection regimes outside and inside the pipefish host.

In **Chapter I**, we selected a variety of *Vibrio* strains from multiple clades and their temperate phages to assess the potential phage mediated gene transfer facilitated by filamentous or other temperate phages between *Vibrio* clades and strains. We found that across distantly related clades, infections are predominantly restricted to modules of the same clade. Infections across clades do occur in low frequency suggesting that transfer of genetic material is possible across different *Vibrio* clades, which can contribute to the spread of prophage-encoded virulence factors in marine *Vibrio* communities (Castillo, Kauffman et al. 2018). The detected nested infections patterns within the modules are hypothesized to result from gene for gene coevolution (Lenski and Levin 1985), which were also described for lytic phages and bacteria (Flores, Meyer et al. 2011, Weitz, Poisot et al. 2013, Fortuna, Barbour et al. 2019).

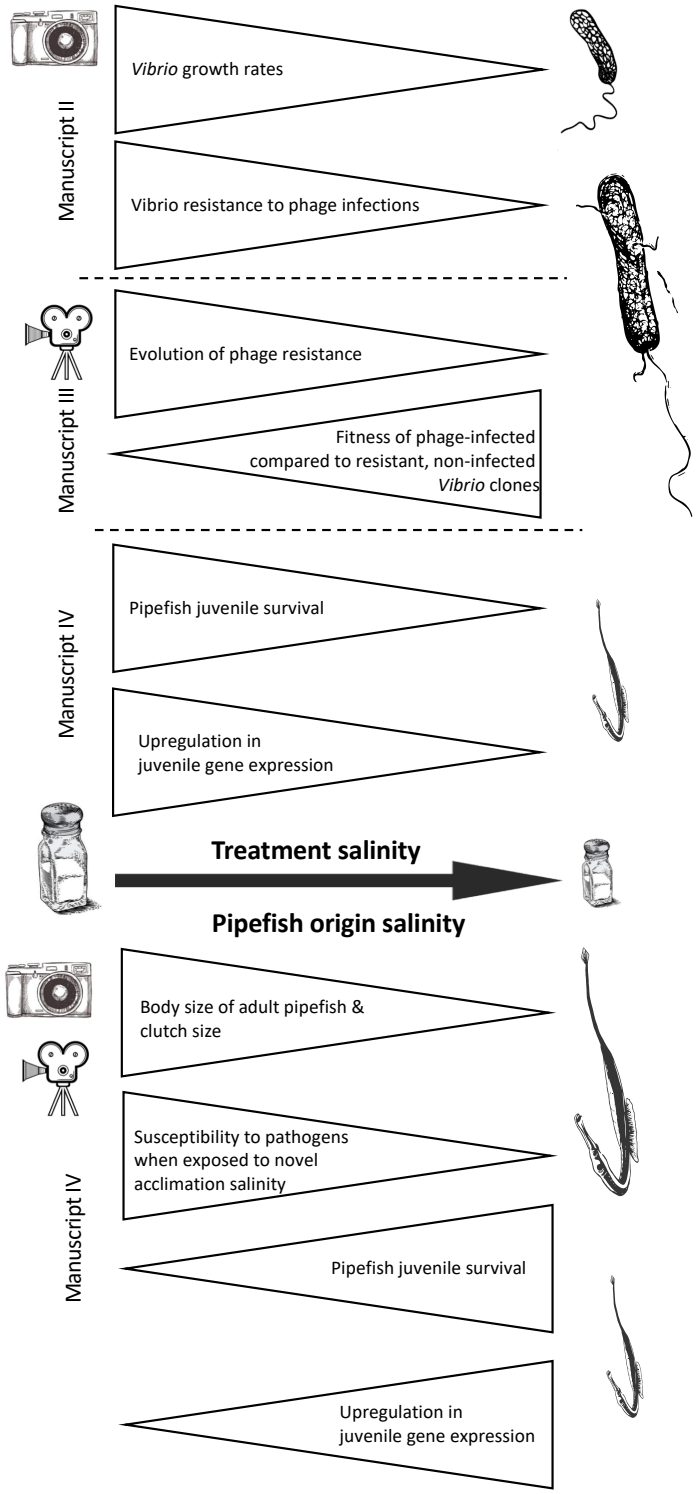

Figure 1: Impact of salinity on study organisms

Figure summarizes the results of the PhD thesis. Large side of the triangle states that the observed pattern, trait or dynamic is stronger/higher at the respective salinity.

Climate change is predicted to lead to salinity changes that have the potential to influence infections patterns and modulate the cost and benefits of phage infections. In **Chapter II**, we explored infection patterns between temperate phages and *Vibrio* strains within the *Vibrio alginolyticus* clade at three different salinity levels. While a drop from 15 PSU to 11 PSU only slightly decreased *V. alginolyticus* growth rates and increased the cost of phage infection imposed on the bacterial host, a salinity level of 7 PSU significantly increased the number of bacterial strains negatively impacted by phage infections. To the best of our knowledge, this is the first study showing that abiotic conditions (here salinity) influence bacterial resistance to filamentous phages, a predominant group of phages in the oceans (Castillo, Kauffman et al. 2018, Hay and Lithgow 2019, Roux, Krupovic et al. 2019). This extends findings from previous work indicating salinity as a driver for phage infection in various lytic phages and bacterial hosts (Kukkaro and Bamford 2009), including lytic phages infecting *Vibrio cholera* (Silva-Valenzuela and Camilli 2019). Based on incubation times of less than 24 hours, infection networks represent only a snapshot of phage bacteria interactions (Chapter I; Chapter II; Poullain, Gandon et al. 2008, Wendling, Piecyk et al. 2017). While these infection networks are useful to assess the potential of gene transfer between bacterial strains and potential genetic models of coevolution (Lenski and Levin 1985, Weitz, Poisot et al. 2013), they lack insights into eco-evolutionary dynamics between phages and bacteria. This deficit can be solved with experimental evolution (Kawecki, Lenski et al. 2012, Kassen 2019)

In **Chapter III**, I conducted an evolution experiment to investigate how different salinity regimes modulate population size and bacterial resistance evolution. Filamentous phages (derived from *Vibrio alginolyticus*) reduced *Vibrio* bacteria population density by one order of magnitude in all salinity regimes. Taken together, the results of **Chapter I**, **II** and **III** are strongly suggestive of a negative effect of filamentous phages on bacterial population growth despite their cooperative reputation (Hay and Lithgow 2019), which is in line with previous work showing impaired bacterial growth or cell death after infection by filamentous phages (Kuo, Yang et al. 2000, Rice, Tan et al. 2009, Shapiro, Williams et al. 2016). At 15 PSU and fluctuating conditions, bacterial populations quickly recovered to original density levels within only six days, whereas the recovery of bacterial density at 7 PSU took approximately twice as long. This fast retrieve of bacterial population density can be explained by rapid evolution of bacterial resistance, which was delayed at 7 PSU. Together with work by Wendling et al. (unpublished data), **Chapter III** provides the first

empirical evidence for evolution of resistance by bacteria against filamentous phages. Applying a mathematical model, we found that reduced growth rates at low salinity lowered the encounter rates of phages and bacteria in the initial phase of the experiment, which resulted in lower number of infections and reduced selection for resistant clones. At 15 PSU and fluctuating conditions, resistant, phage-infected clones were quickly outcompeted by resistant, non-infected clones. At 7 PSU, phage-infected clones remained approximately twice as long in the bacterial populations due to reduced fitness differences of resistant, phage-infected clones and resistant, non-infected clones. The prolonged presence of resistant, phage-infected clones suggests that low salinity levels may select for phage-infected bacteria. Therefore, the success of filamentous phages is driven by minimizing the cost (virulence) to the bacterial host (Bull, Molineux et al. 1991, Shapiro, Williams et al. 2016, Shapiro and Turner 2018) or even increasing bacterial fitness by providing beneficial genes (Ilyina 2015, Hay and Lithgow 2019). This is in line with kin selection theory, which suggest that selection favours reduced parasite virulence and maximizes inclusive fitness of host and parasite, if cooperating organisms have a high degree of genetic relatedness (Smith 1964, Buckling and Brockhurst 2008). Filamentous phages have a high dependency on the fitness of the bacteria, especially, if the main transmission mode is vertical (instead of horizontal). Predominant vertical transmission is suggested to turn parasites into mutualists (Yamamura 1993, Frank 1996) and resulted in reduced phage virulence in a previous experiment (Bull, Molineux et al. 1991). In our experiment, we could not find sufficient evidence for reduced horizontal transmission (i.e. lower phage production) because of the high variability in non-lethal phage release through the bacterial cell wall by different phage-infected clones of the same treatment released. To achieve more robust result and detect potentially differences in phage production at different salinities, it would require more experiments assessing the Cell Forming Units to Plaque Forming Units. Ideally the assays would include clones from different transfers to uncover whether phage production is reduced over time. A reduction in phage production would reduce the costs for the bacterial cell and may either be a result of phage adaptation lowering the virulence for the bacterium or an adaptation by the bacteria hampering phage production.

I suggest that the faster evolution of resistance at 15 PSU compared to 7 PSU and the extended presence of the phage-infected clones are an example of how changes in environmental conditions may move species interactions from rather antagonistic (15 PSU, and fluctuating conditions) with rapid resistance evolution (Red Queen effect) to more

mutualistic interactions (7 PSU), where slower resistance evolution favours cooperation (Red King effect (Bergstrom and Lachmann 2003, Gao, Li et al. 2015, Veller, Hayward et al. 2017)). This is in line with a theoretical model which predicts that Red King dynamics of slow evolution become more successful when both interacting species gain benefits from an interaction (Gao, Li et al. 2015). In the filamentous phage – bacteria system, the benefits of an interaction for both organisms can depend on their surrounding biotic and abiotic environment. For example, toxins encoded in filamentous phages, which are present in the genome of *Vibrio cholerae* (Waldor and Mekalanos 1996, Faruque and Mekalanos 2012), may be costly in the water column but boost the fitness of bacteria and are selected for in the digestive system of the human host. Here, the effect of the toxin results in water inflow into the small intestine and flushes out the competitive microbial community (Holmgren 1981, Nelson, Harris et al. 2009). The now available niches can be used by the *V. cholerae,* which in turn increases the fitness of the infecting filamentous phages.

If changing environmental conditions (outside the host) favour an enhanced transfer of virulence factors by filamentous phages (**Chapter II**) and a fitness benefit of phage-infected bacteria (**Chapter III**), the likelihood for phage-induced bacterial diseases in eukaryotic host is suggested to grow under present climate change scenarios. More virulent *Vibrio* bacteria combined with evidence for emerging *Vibrio* abundance under current climate change scenarios may reshape the distribution and dynamics of *Vibrio* infections (Baker-Austin, Trinanes et al. 2013, Baker-Austin, Trinanes et al. 2017). The chance for disease outbreaks also depends on the capability of host organisms to cope with their abiotic and biotic environment, for example via genetic adaptation, transgenerational plasticity and developmental plasticity (Roth, Keller et al. 2012, Sunday, Calosi et al. 2014, Roth, Beemelmanns et al. 2018, Kelly 2019).

In **Chapter IV**, I explored the ability of a eukaryotic host, namely the pipefish *Syngnathus typhle*, to cope with reduced salinity levels through genetic adaptation, transgenerational plasticity and developmental plasticity. Further, I studied whether virulence of associated opportunistic pathogens increased at low salinity. To address that, we conducted the first multigenerational pipefish study comprising replicated sampling locations for each salinity level and an opportunistic pathogen evolved at the respective salinity. The results suggest that pipefish are locally adapted to salinity conditions and the ambient pathogen community in the Baltic Sea. Considering their common marine ancestry, low salinity populations retained their ability to deal with salinity levels and pathogens

characteristic of the highest saline environment treatment (15 PSU). This confirms previous work on sticklebacks showing that rapid adaptation to low salinities is possible via selection (McGuigan, Nishimura et al. 2011, Heckwolf, Meyer et al. 2018) and that transgenerational plasticity can aid this process through epigenetic regulation (Heckwolf, Meyer et al. 2020). In contrast to previous studies raising single species under optimal and pathogen free conditions in filtered sea water (Heckwolf, Meyer et al. 2018), this study integrated complex multispecies interactions, including the natural microbial community of the Kiel fjord and a *Vibrio* strain evolved at 15 and 7 PSU. Adaptation to local pathogens (Roth, Keller et al. 2012, Piecyk, Roth et al. 2019) and transgenerational immune priming enable organisms to cope with present pathogens (Beemelmanns and Roth 2016, Beemelmanns and Roth 2016, Beemelmanns and Roth 2017, Roth, Beemelmanns et al. 2018). However, if shifts towards low salinity levels are occurring on short time scales, recourse allocations toward osmoregulation impairs the pipefish's immune system (Bowden 2008, Birrer, Reusch et al. 2012) and can result in harmful fungus infections as seen in **Chapter IV**. In a similar way, recourse allocations towards osmoregulation resulting in an impaired immune system may have cause higher *Vibrio* virulence at low salinity levels (Poirier, Listmann et al. 2017). Based on the results of **Chapter IV**, we found no evidence that low salinity outside the host selects for more virulent *Vibrio* strains. Despite adaptation of fish to low salinity conditions, low salinity constitute a challenging environment for all pipefish from all sampling sites as implied by the smaller adult size, reduced clutch size, juvenile survival and growth rates. This confirms other studies of marine fish showing reduced growth with increasing divergence between treatment or environmental salinity conditions and isosmotic salinity levels of the fish (Boeuf and Payan 2001).

The findings of **Chapter IV** are consistent with the evidence emerging from **Chapter II** and **III**. All studies indicate that each member of the coevolutionary complex examined here suffers from a rapid reduction in salinity (Figure 1): bacteria face reduced growth rates (**Chapter II** and **III**), while the eukaryotic host endures impaired immune function (**Chapter IV**). The negative impact of the altered environment is magnified by the addition of an additional organism: bacteria suffer more from phage infections (**Chapter II**), resistance evolution and the regain of original populations densities is delayed (**Chapter III**) and pipefish suffer from fungus infection while their juveniles exhibit higher mortality after *Vibrio* infections (**Chapter IV**).

Chapter III and **IV** show that changing environmental conditions in combination with threatening pathogens can be overcome on evolutionary time scales via bacterial resistance evolution and local adaptation to salinity conditions. However, if changes in the environment are rapid and cause strong reduction in population size or genetic diversity (Johannesson and Andre 2006, Johannesson, Le Moan et al. 2020), organisms may not be able to adapt to novel environmental conditions and associated pathogens. Failure in adaptation may result in unpredictable extinctions because of unexpected or understudies species interactions (Vandvik, Skarpaas et al. 2020).

Climate change studies using a single species and one or two environmental factors, provide important insights in mechanisms involved in adaptation to environmental conditions induced by anthropogenic climate change (Gazeau, Parker et al. 2013, Schlüter, Lohbeck et al. 2014, Shama and Wegner 2014, Heckwolf, Meyer et al. 2018, Heckwolf, Meyer et al. 2020). However, the results of my PhD suggest that conclusions drawn studies taking study organism out of their ecological context fail to capture fundamental interactions between host, mutualists and parasites that shape each individual species' fitness. The implication is that projecting future species trajectories without accounting for their reciprocal interactions during environmental change will severely constrain our ability to predict the future of any one species in a rapidly changing ocean.

The more I learn, the more I realize, I don't know. The more I realize, I don't know, the more I want to learn.

Albert Einstein.

6.2 | Perspective

The novelty of my approach, considering the role of mutually interacting players in the fate of environmental change, was bound to raise at least as many new questions as it succeeded to answer.

The results emerging from **Chapter I** and **Chapter II** point to an important role of filamentous phages in significantly reducing bacterial growth and infecting a wide range of bacteria of the same clade and across phylogenetically related clades. However, it remains to be investigated whether those bacteria not showing reduced growth rates after exposure to filamentous phages are in fact resistant or the impact of filamentous phages on bacterial

growth is below the sensitivity of the experiment. An approach using a subset of phages and bacterial strains with sequenced genomes (Chibani, Hertel et al. 2019, Chibani, Roth et al. 2020) and repeating the pairwise infection assay with subsequent PCR of single clones targeting the phage sequence has the potential to test whether the phenotypically observed resistance is confirmed by genomic evidence.

An important issue raised by the work in **Chapter II** is whether a physical or molecular mechanism prevents a filamentous phage from entering the bacterial cell or whether the cost of phage infection increases with reduced salinity, such that infections become detectable with the reduction in bacterial growth assay used in **Chapter I and II**. The questions can be answered by a PCR, as described above. If the infection patterns are consistent at all salinities, droplet digital PCR with fluorescent probes (Morella et al 2018) would allow to characterize the effects of salinity on the adsorption rate of filamentous phages on the bacterial cell wall and on phage production. NaCl concentration affects the ionic strength of the media, which in turn could influence adsorption rates of the phage onto the bacterial cell wall (Kukkaro and Bamford 2009). The adsorption rate may be especially relevant at low bacteria and phage density. Furthermore, environmental factors affecting the condition of the bacterial cell are known to influence lysis-lysogeny decisions in temperate phages (Refardt and Rainey 2010, Bednarz, Halliday et al. 2014). As a consequence, the phage production rate of filamentous phages may also be determined by the physiological state of the bacterial cell, which directly influences the energetic cost for the cell. Both low adsorption rates followed by delayed infections and low phage production rates causing low costs for the bacterial cell can cause a failure by the Reduction in Bacterial Growth Assay in detecting phage infection.

In a more natural setting, the phage production rate may be crucial for the fitness of filamentous phages and may depend on biotic and abiotic conditions. In low nutrient environments with a high number of diverse bacteria, the resources for bacterial growth and the number of susceptible hosts are limited. Increasing phage production at the cost of reduced bacterial growth may be only a successful strategy, if the number of susceptible hosts is high, otherwise the reduced host fitness will result in reduced phage fitness as seen in the experiment of **Chapter III**. Some temperate phages with lysogenic and lytic lifecycles use small-molecule communication system to coordinate lysis-lysogeny decisions (Erez, Steinberger-Levy et al. 2017, Stokar-Avihail, Tal et al. 2019). If the number of already phage-infected bacterial cells is high phages tend to decide to choose the dormant lysogenic

cycle (Erez, Steinberger-Levy et al. 2017). Whether filamentous phages can actively regulate their production and release through the bacterial cell wall depending on biotic and abiotic conditions remains so far unexplored.

That salinity is indeed an important driver for ecological dynamics in filamentous phage -bacteria populations clearly emerges from the results of **Chapter III.** However, small glass containers with nutrient rich media are far from conditions representing a natural environment with complex biotic and abiotic interactions. To understand the fitness costs and benefits of the evolution of bacterial resistance and infections by filamentous phages, we need to move from rather artificial environments to more natural settings (Wagner and Rajkov 2019). Previous studies showed very strong divergence in the lab and experiments in natural settings, e.g. resistance evolution of bacteria exposed to lytic phages occurred only in liquid media but not in the lab (Hernandez and Koskella 2019) or survival of gammarids during heatwaves was much higher in the Kiel outdoor benthocosms than in the lab (Paiva et al, unpublished data). Our model system is well suited to examine how an additional biotic partner, here, the eukaryotic final host *Syngnathus typhle* pipefish, may promote or constrain rapid bacterial resistance evolution against filamentous phages and how filamentous phage may increase bacterial fitness by providing beneficial virulence genes to the bacteria. In a future serial passage experiment with a filamentous phage and a susceptible *V. alginolyticus* strain through the gut of the pipefish, the influence of the host immune system and the microbiome on co-evolutionary dynamics can be assessed in a natural environment. Performing the experiment at 15 PSU and 7 PSU, will give insights if an impaired immune system (Birrer, Reusch et al. 2012, Manuscript IV) selects for less virulent strains. The proposed experiment, will provide further insights about co-evolutionary dynamics in close to nature setting. In contrast to the lab experiment (**Chapter III)** the host's immune system may select for more virulent bacterial strains carry additional virulence genes introduced by the phage and against the evolution of phage resistance which has been associated with reduced virulence in the host (Heierson, Sidén et al. 1986, Leon and Bastias 2015, Wendling, Piecyk et al. 2017).

The salinity gradient of the Baltic Sea offers the opportunity for field studies of *S. typhle* individuals at various salinity conditions ranging from almost fully marine environment in the seagrass meadows of western Sweden to salinity levels below 5 PSU in the south of Finland. Conducting a comparative RNAseq analysis of specific organs, e.g. brain and head kidney, from individuals would allow us to further explore genes involved in local

adaptation to salinity. Sequencing *Vibrio* spp. isolates from the gut microbiome of the pipefish along the salinity gradient and the ambient seawater could tell us if the pipefish's immune system and salinity are selecting for *Vibrio* strains with specific genes encoded by filamentous phages and other mobile elements. Examining the presence of viral genes in the genome of the bacteria can give us insights on the potential fitness advantage conferred by filamentous phages in particular environments and therefore help clarify their position in the mutualist-parasite continuum of species interactions. Experiments supporting those genomic analyses could include measuring pair-wise bacteria-phage infection patterns, gene expression of viral genes and virulence of isolated bacteria through infection experiments with eukaryotic hosts paired with analyses of host and bacterial gene expression and immunological measurements. Combining genomics with well-defined experiments would provide mechanistic insights into functional implications of filamentous phage encoded genes and their role in marine *Vibrio* communities.

Besides a decrease in salinity (Vuorinen, Hanninen et al. 2015), the organisms of the Baltic Sea are facing many more stressors, including a rapid warming of water temperature, reduced levels of oxygen and elevated levels of nutrients (Reusch, Dierking et al. 2018). However, this may be the perfect mixture for *Vibrio* bacteria to strive as their growth rates and abundance increases at elevated temperatures (Singleton, Attwell et al. 1982, Oberbeckmann, Wichels et al. 2011) and as facultative anaerobe organisms they are suited to grow in oxygen depleted waters (Youngren-Grimes, Grimes et al. 1988). Therefore, it is not surprising that *Vibrio* bacteria are considered as winners in a changing ocean (Baker-Austin, Trinanes et al. 2013, Baker-Austin, Trinanes et al. 2017). Bearing in mind that the ocean is full of phages having the potential to kill the winner (Avrani, Schwartz et al. 2012) or supply *Vibrio* bacteria with additional weapons (Obeng, Pratama et al. 2016, Harrison and Brockhurst 2017), we need further research to disentangle how climate change is driving life in our future ocean.

"Gentlemen, it is the microbes who will have the last word"

Louis Pasteur

6.3 | Concluding remarks

In recent years, the development of new analytical and molecular methods as well as affordable high throughput sequencing enabled us to deepen our knowledge about evolutionary processes and molecular mechanisms driving the adaptation of organisms to their biotic and abiotic environment. Step by step, we are unraveling the complex processes involved in shaping the biodiversity on our planet as we see it today. However, current human activities and anthropogenic climate change are altering ecosystems at an ever-accelerating speed resulting in species extinctions around the globe. Current research is addressing the yet unsolved question if organisms will be able to cope with these severe challenges and what the future ocean may look like.

The results of this thesis provide further evidence that rapidly changing environmental conditions, in particular lowered salinity levels, are not only hampering individual species but also alter interactions between species and their coevolutionary dynamics. We learned that filamentous phages can be detrimental to *Vibrio* bacteria and may only be cooperative in a selective environment. Whether the future ocean will be an environment selecting for enhanced cooperation between *Vibrio* bacteria and filamentous phages still needs to be explored. The research also showed that organisms, i.e. *Vibrio* bacteria and pipefish, are able to adapt to changing environmental conditions but biotic interactions or ideally ecosystem approaches need to be considered when making predictions about the performance of species in a future ocean.

There is no doubt that life will find its way in a changing ocean. The question is, what we want the ocean to look like for the fascinating organisms in the water, for us and for future generations.

7 | REFERENCES

Abdesinglabs. (2013). "Quantification of Bacteriophage by Spectrophotometry." Retrieved 15.02.2016, 2016.

Agrawal, A. and C. M. Lively (2002). "Infection genetics: gene-for-gene versus matching-alleles models and all points in between." Evolutionary Ecology Research **4**(1): 79-90.

Ahmad, A. A., A. Askora, T. Kawasaki, M. Fujie and T. Yamada (2014). "The filamentous phage XacF1 causes loss of virulence in Xanthomonas axonopodis pv. citri, the causative agent of citrus canker disease." Frontiers in Microbiology **5**: 11.

Akaike, H. (1976). "An information criteron (AIC)." Math Sci **14**: 5-7.

Albaret, J. J., M. Simier, F. S. Darboe, J. M. Ecoutin, J. Raffray and L. T. de Morais (2004). "Fish diversity and distribution in the Gambia Estuary, West Africa, in relation to environmental variables." Aquatic Living Resources **17**(1): 35-46.

Ali, M., A. R. Nelson, A. L. Lopez and D. A. Sack (2015). "Updated global burden of cholera in endemic countries." PLoS neglected tropical diseases **9**(6): e0003832-e0003832.

Allen, L. Z., J. P. McCrow, K. Ininbergs, C. L. Dupont, J. H. Badger, J. M. Hoffman, M. Ekman, A. E. Allen, B. Bergman and J. C. Venter (2017). "The Baltic Sea Virome: Diversity and Transcriptional Activity of DNA and RNA Viruses." Msystems **2**(1): 16.

Almeida-Neto, M., P. Guimaraes, P. R. Guimaraes, R. D. Loyola and W. Ulrich (2008). "A consistent metric for nestedness analysis in ecological systems: reconciling concept and measurement." Oikos **117**(8): 1227-1239.

Altschul, S. F., W. Gish, W. Miller, E. W. Myers and D. J. Lipman (1990). "BASIC LOCAL ALIGNMENT SEARCH TOOL." Journal of Molecular Biology **215**(3): 403-410.

Andersson, A., H. E. M. Meier, M. Ripszam, O. Rowe, J. Wikner, P. Haglund, K. Eilola, C. Legrand, D. Figueroa, J. Paczkowska, E. Lindehoff, M. Tysklind and R. Elmgren (2015). "Projected future climate change and Baltic Sea ecosystem management." Ambio **44**: S345-S356.

Angers, B., E. Castonguay and R. Massicotte (2010). "Environmentally induced phenotypes and DNA methylation: how to deal with unpredictable conditions until the next generation and after." Molecular Ecology **19**(7): 1283-1295.

Anthony, K. R. N., D. I. Kline, G. Diaz-Pulido, S. Dove and O. Hoegh-Guldberg (2008). "Ocean acidification causes bleaching and productivity loss in coral reef builders." Proceedings of the National Academy of Sciences of the United States of America **105**(45): 17442-17446.

Antonovics, J., J. Bergmann, S. Hempel, E. Verbruggen, S. Veresoglou and M. Rillig (2015). "The evolution of mutualism from reciprocal parasitism: more ecological clothes for the Prisoner's Dilemma." Evolutionary Ecology **29**(5): 627-641.

Antonovics, J., M. Boots, D. Ebert, B. Koskella, M. Poss and B. M. Sadd (2013). "The origin of specificity by means of natural selection: evolved and nonhost resistance in host-pathogen interactions." Evolution **67**(1): 1-9.

Assmy, P., V. Smetacek, M. Montresor, C. Klaas, J. Henjes, V. H. Strass, J. M. Arrieta, U. Bathmann, G. M. Berg, E. Breitbarth, B. Cisewski, L. Friedrichs, N. Fuchs, G. J. Herndl, S. Jansen, S. Kragefsky, M. Latasa, I. Peeken, R. Rottgers, R. Scharek, S. E. Schuller, S. Steigenberger, A. Webb and D. Wolf-Gladrow (2013). "Thick-shelled, grazer-protected diatoms decouple ocean carbon and silicon cycles in the iron-limited Antarctic Circumpolar Current." Proceedings of the National Academy of Sciences of the United States of America **110**(51): 20633-20638.

Atkinson, M. J. and P. Cuet (2008). "Possible effects of ocean acidification on coral reef biogeochemistry: topics for research." Marine Ecology-Progress Series **373**: 249-256.

Aung, K., Y. J. Jiang and S. Y. He (2018). "The role of water in plant-microbe interactions." Plant Journal **93**(4): 771-780.

Avrani, S., D. A. Schwartz and D. Lindell (2012). "Virus-host swinging party in the oceans: Incorporating biological complexity into paradigms of antagonistic coexistence." Mobile genetic elements **2**(2): 88-95.

Axelrod, R. and W. D. Hamilton (1981). "The evolution of cooperation." Science **211**(4489): 1390-1396.

Baker-Austin, C., J. D. Oliver, M. Alamo, A. Ali, M. K. Waldor, F. Qadri and J. Martinez-Urtaza (2018). "Vibrio spp. infections." Nature Reviews Disease Primers **4**: 19.

Baker-Austin, C., J. Trinanes, N. Gonzalez-Escalona and J. Martinez-Urtaza (2017). "Non-Cholera Vibrios: The Microbial Barometer of Climate Change." Trends in Microbiology **25**(1): 76-84.

Baker-Austin, C., J. A. Trinanes, N. G. H. Taylor, R. Hartnell, A. Siitonen and J. Martinez-Urtaza (2013). "Emerging Vibrio risk at high latitudes in response to ocean warming." Nature Climate Change **3**(1): 73-77.

Balcázar, J. L., N. M. Lee, J. Pintado and M. Planas (2010). "Phylogenetic characterization and in situ detection of bacterial communities associated with seahorses (Hippocampus guttulatus) in captivity." Systematic and Applied Microbiology **33**(2): 71-77.

Bankevich, A., S. Nurk, D. Antipov, A. A. Gurevich, M. Dvorkin, A. S. Kulikov, V. M. Lesin, S. I. Nikolenko, S. Pham, A. D. Prjibelski, A. V. Pyshkin, A. V. Sirotkin, N. Vyahhi, G. Tesler, M. A. Alekseyev and P. A. Pevzner (2012). "SPAdes: A New Genome Assembly Algorithm and Its Applications to Single-Cell Sequencing." Journal of Computational Biology **19**(5): 455-477.

Barletta, M., A. Barletta-Bergan, U. Saint-Paul and G. Hubold (2005). "The role of salinity in structuring the fish assemblages in a tropical estuary." Journal of Fish Biology **66**(1): 45-72.

Barrett, R. D. H. and D. Schluter (2008). "Adaptation from standing genetic variation." Trends in Ecology & Evolution **23**(1): 38-44.

Bart, R. (2019). "Dissecting the Disease Triangle: Hosts, pathogens and the environment." Molecular Plant-Microbe Interactions **32**(10): 50-50.

Bates, D., M. Machler, B. M. Bolker and S. C. Walker (2015). "Fitting Linear Mixed-Effects Models Using lme4." Journal of Statistical Software **67**(1): 1-48.

Beckett, S. J., C. A. Boulton and H. T. Williams (2014). "FALCON: a software package for analysis of nestedness in bipartite networks." F1000Res **3**: 185.

Beckett, S. J., C. A. Boulton and H. T. P. Williams (2014). "FALCON: a software package for analysis of nestedness in bipartite networks." F1000Res **3**.

Bednarz, M., J. A. Halliday, C. Herman and I. Golding (2014). "Revisiting Bistability in the Lysis/Lysogeny Circuit of Bacteriophage Lambda." Plos One **9**(6): 9.

Beemelmanns, A. and O. Roth (2016). "Bacteria-type-specific biparental immune priming in the pipefish Syngnathus typhle." Ecology and Evolution **6**(18): 6735-6757.

Beemelmanns, A. and O. Roth (2016). "Biparental immune priming in the pipefish Syngnathus typhle." Zoology **119**(4): 262-272.

Beemelmanns, A. and O. Roth (2017). "Grandparental immune priming in the pipefish Syngnathus typhle." Bmc Evolutionary Biology **17**: 14.

Berg, P. R., S. Jentoft, B. Star, K. H. Ring, H. Knutsen, S. Lien, K. S. Jakobsen and C. Andre (2015). "Adaptation to Low Salinity Promotes Genomic Divergence in Atlantic Cod (Gadus morhua L.)." Genome Biology and Evolution **7**(6): 1644-1663.

Bergstrom, C. T. and M. Lachmann (2003). "The Red King effect: When the slowest runner wins the coevolutionary race." Proceedings of the National Academy of Sciences of the United States of America **100**(2): 593-598.

Berngruber, T. W., F. J. Weissing and S. Gandon (2010). "Inhibition of Superinfection and the Evolution of Viral Latency." Journal of Virology **84**(19): 10200-10208.

Betts, A., O. Kaltz and M. E. Hochberg (2014). "Contrasted coevolutionary dynamics between a bacterial pathogen and its bacteriophages." Proceedings of the National Academy of Sciences of the United States of America **111**(30): 11109-11114.

Beumer, A. and J. B. Robinson (2005). "A broad-host-range, generalized transducing phage (SN-T) acquires 16S rRNA genes from different genera of bacteria." Applied and Environmental Microbiology **71**(12): 8301-8304.

Bille, E., J. Meyer, A. Jamet, D. Euphrasie, J. P. Barnier, T. Brissac, A. Larsen, P. Pelissier and X. Nassif (2017). "A virulence-associated filamentous bacteriophage of Neisseria meningitidis increases host-cell colonisation." Plos Pathogens **13**(7).

Birrer, S. C., T. B. H. Reusch and O. Roth (2012). "Salinity change impairs pipefish immune defence." Fish & Shellfish Immunology **33**(6): 1238-1248.

Blanquart, F. and S. Gandon (2013). "Time-shift experiments and patterns of adaptation across time and space." Ecology Letters **16**(1): 31-38.

Blois, J. L., J. W. Williams, M. C. Fitzpatrick, S. T. Jackson and S. Ferrier (2013). "Space can substitute for time in predicting climate-change effects on biodiversity." Proceedings of the National Academy of Sciences of the United States of America **110**(23): 9374-9379.

Bock, G. and C. Lieberum (2017). Neobiota in ausgewählten Häfen der schleswig-holsteinischen Ostsee, Landesamtes für Landwirtschaft, Umwelt und ländliche Räume des Landes Schleswig-Holstein.

Boeuf, G. and P. Payan (2001). "How should salinity influence fish growth?" Comparative Biochemistry and Physiology C-Toxicology & Pharmacology **130**(4): 411-423.

Bookout, A. L. and D. J. Mangelsdorf (2003). "Quantitative real-time PCR protocol for analysis of nuclear receptor signaling pathways." Nuclear receptor signaling **1**: e012-e012.

Bordenstein, S. R., C. Paraskevopoulos, J. C. D. Hotopp, P. Sapountzis, N. Lo, C. Bandi, H. Tettelin, J. H. Werren and K. Bourtzis (2009). "Parasitism and Mutualism in Wolbachia: What the Phylogenomic Trees Can and Cannot Say." Molecular Biology and Evolution **26**(1): 231-241.

Bourne, D., Y. Iida, S. Uthicke and C. Smith-Keune (2008). "Changes in coral-associated microbial communities during a bleaching event." Isme Journal **2**(4): 350-363.

Bowden, T. J. (2008). "Modulation of the immune system of fish by their environment." Fish & Shellfish Immunology **25**(4): 373-383.

Boyd, R. and P. J. Richerson (1992). "Punishment allows the evolution of cooperation (or anything else) in sizable groups." Ethology and Sociobiology **13**(3): 171-195.

Boyett, H. V., D. G. Bourne and B. L. Willis (2007). "Elevated temperature and light enhance progression and spread of black band disease on staghorn corals of the Great Barrier Reef." Marine Biology **151**(5): 1711-1720.

Bravetti, A. and P. Padilla (2018). "An optimal strategy to solve the Prisoner's Dilemma." Scientific Reports **8**: 6.

Breves, J. P., S. D. McCormick and R. O. Karlstrom (2014). "Prolactin and teleost ionocytes: New insights into cellular and molecular targets of prolactin in vertebrate epithelia." General and Comparative Endocrinology **203**: 21-28.

Brierley, A. S. and M. J. Kingsford (2009). "Impacts of Climate Change on Marine Organisms and Ecosystems." Current Biology **19**(14): R602-R614.

Brockhurst, M. A., A. Buckling and P. B. Rainey (2005). "The effect of a bacteriophage on diversification of the opportunistic bacterial pathogen, Pseudomonas aeruginosa." Proceedings of the Royal Society B-Biological Sciences **272**(1570): 1385-1391.

Brockhurst, M. A., A. D. Morgan, P. B. Rainey and A. Buckling (2003). "Population mixing accelerates coevolution." Ecology Letters **6**(11): 975-979.

Broman, E., C. Raymond, C. Sommer, J. S. Gunnarsson, S. Creer and F. J. A. Nascimento (2019). "Salinity drives meiofaunal community structure dynamics across the Baltic ecosystem." Molecular Ecology **28**(16): 3813-3829.

Bronstein, J. L. (2001). "The costs of mutualism." American Zoologist **41**(4): 825-839.

Bronstein, J. L. (2009). "The evolution of facilitation and mutualism." Journal of Ecology **97**(6): 1160-1170.

Brown, D. M. Cornforth and N. Mideo (2012). "Evolution of virulence in opportunistic pathogens: generalism, plasticity, and control." Trends in Microbiology **20**(7): 336-342.

Brown, B. L., R. P. Creed, J. Skelton, M. A. Rollins and K. J. Farrell (2012). "The fine line between mutualism and parasitism: complex effects in a cleaning symbiosis demonstrated by multiple field experiments." Oecologia **170**(1): 199-207.

Brown, S. P., D. M. Cornforth and N. Mideo (2012). "Evolution of virulence in opportunistic pathogens: generalism, plasticity, and control." Trends in Microbiology **20**(7): 336-342.

Brown-Jaque, M., W. Calero-Caceres and M. Muniesa (2015). "Transfer of antibiotic-resistance genes via phage-related mobile elements." Plasmid **79**: 1-7.

Brunner, F. S. and C. Eizaguirre (2016). "Can environmental change affect host/parasite-mediated speciation?" Zoology **119**(4): 384-394.

Bruno, J. F. (2015). "MARINE BIOLOGY The coral disease triangle." Nature Climate Change **5**(4): 302-303.

Brussow, H., C. Canchaya and W. D. Hardt (2004). "Phages and the evolution of bacterial pathogens: From genomic rearrangements to lysogenic conversion." Microbiology and Molecular Biology Reviews **68**(3): 560-+.

Brzuszkiewicz, E., H. Bruggemann, H. Liesegang, M. Emmerth, T. Oschlager, G. Nagy, K. Albermann, C. Wagner, C. Buchrieser, L. Emody, G. Gottschalk, J. Hackert and U. Dobrindt (2006). "How to become a uropathogen: Comparative genomic analysis of extraintestinal pathogenic Escherichia coli strains." Proceedings of the National Academy of Sciences of the United States of America **103**(34): 12879-12884.

Buckling, A. and M. A. Brockhurst (2008). "Kin selection and the evolution of virulence." Heredity **100**(5): 484-488.

Buckling, A. and P. B. Rainey (2002). "Antagonistic coevolution between a bacterium and a bacteriophage." Proceedings of the Royal Society B-Biological Sciences **269**(1494): 931-936.

Bull, J. J., I. J. Molineux and W. R. Rice (1991). "Selection of benevolence in a host-parasite system." Evolution **45**(4): 875-882.

Burgener, E. B., J. M. Sweere, M. S. Bach, P. R. Secor, N. Haddock, L. K. Jennings, R. L. Marvig, H. K. Johansen, E. Rossi, X. Cao, L. Tian, L. Nedelec, S. Molin, P. L. Bollyky and C. E. Milla (2019). "Filamentous bacteriophages are associated with chronic Pseudomonas lung infections and antibiotic resistance in cystic fibrosis." Science Translational Medicine **11**(488).

Calosi, P., P. De Wit, P. Thor and S. Dupont (2016). "Will life find a way? Evolution of marine species under global change." Evolutionary Applications **9**(9): 1035-1042.

Capela, D., M. Marchetti, C. Clerissi, A. Perrier, D. Guetta, C. Gris, M. Valls, A. Jauneau, S. Cruveiller, E. P. C. Rocha and C. Masson-Boivin (2017). "Recruitment of a Lineage-Specific Virulence Regulatory Pathway Promotes Intracellular Infection by a Plant Pathogen Experimentally Evolved into a Legume Symbiont." Molecular Biology and Evolution **34**(10): 2503-2521.

Castillo, D., K. Kauffman, F. Hussain, P. Kalatzis, N. Rørbo, M. F. Polz and M. Middelboe (2018). "Widespread distribution of prophage-encoded virulence factors in marine *Vibrio* communities." Scientific Reports **8**(1): 9973.

Cattano, C., J. Claudet, P. Domenici and M. Milazzo (2018). "Living in a high CO2 world: a global meta-analysis shows multiple trait-mediated fish responses to ocean acidification." Ecological Monographs **88**(3): 320-335.

Chakraborty, S., A. K. Mukhopadhyay, R. K. Bhadra, A. N. Ghosh, R. Mitra, T. Shimada, S. Yamasaki, S. M. Faruque, Y. Takeda, R. R. Colwell and G. B. Nair (2000). "Virulence genes in environmental strains of *Vibrio cholerae*." Applied and Environmental Microbiology **66**(9): 4022-4028.

Chamberlain, S. A., J. L. Bronstein and J. A. Rudgers (2014). "How context dependent are species interactions?" Ecology Letters **17**(7): 881-890.

Chappelka, A. H. and N. E. Grulke (2016). "Disruption of the 'disease triangle' by chemical and physical environmental change." Plant Biology **18**: 5-12.

Chatterjee, K., A. Pavlogiannis, B. Adlam and M. A. Nowak (2014). "The Time Scale of Evolutionary Innovation." Plos Computational Biology **10**(9): 7.

Chen, M. X., H. Y. Li, G. Li and T. L. Zheng (2011). "Distribution of *Vibrio alginolyticus*-like species in shenzhen coastal waters, China." Brazilian Journal of Microbiology **42**(3): 884-896.

Chevin, L. M., R. Lande and G. M. Mace (2010). "Adaptation, Plasticity, and Extinction in a Changing Environment: Towards a Predictive Theory." Plos Biology **8**(4): 8.

Chibani, C. M., R. Hertel, M. Hoppert, H. Liesegang and C. C. Wendling (2019). "Closely related *Vibrio alginolyticus* strains encode an identical repertoire of prophages and filamentous phages." bioRxiv: 859181.

Chibani, C. M., O. Roth, H. Liesegang and C. C. Wendling (2020). "Genomic variation among closely related *Vibrio alginolyticus* strains is located on mobile genetic elements." (- 1): - 354.

Chomicki, G., E. T. Kiers and S. S. Renner (2020). "The Evolution of Mutualistic Dependence." Annual Review of Ecology, Evolution, and Systematics.

Cobey, S. (2014). "Pathogen evolution and the immunological niche." Annals of the New York Academy of Sciences **1320**(1): 1-15.

Cognetti, G. and F. Maltagliati (2000). "Biodiversity and adaptive mechanisms in brackish water fauna." Marine Pollution Bulletin **40**(1): 7-14.

Cole, V. J., L. M. Parker, S. J. O'Connor, W. A. O'Connor, E. Scanes, M. Byrne and P. M. Ross (2016). "Effects of multiple climate change stressors: ocean acidification interacts with warming, hyposalinity, and low food supply on the larvae of the brooding flat oyster Ostrea angasi." Marine Biology **163**(5): 17.

Cooper, M. D. and M. N. Alder (2006). "The Evolution of Adaptive Immune Systems." Cell **124**(4): 815-822.

Crozier, L. G. and J. A. Hutchings (2014). "Plastic and evolutionary responses to climate change in fish." Evolutionary Applications **7**(1): 68-87.

Cutler, C. P., A.-S. Martinez and G. Cramb (2007). "The role of aquaporin 3 in teleost fish." Comparative Biochemistry and Physiology Part A: Molecular & Integrative Physiology **148**(1): 82-91.

Das, B. (2014). "Mechanistic insights into filamentous phage integration in *Vibrio cholerae*." Frontiers in Microbiology **5**.

Davies, E. V., C. Winstanley, J. L. Fothergill and C. E. James (2016). "The role of temperate bacteriophages in bacterial infection." Fems Microbiology Letters **363**(5): 10.

Davis, B. M. and M. K. Waldor (2003). "Filamentous phages linked to virulence of *Vibrio cholerae*." Current Opinion in Microbiology **6**(1): 35-42.

Dayma, P., I. H. Raval, N. Joshi, N. P. Patel, S. Haldar and K. H. Mody (2015). "Influence of low salinity stress on virulence and biofilm formation potential in *Vibrio alginolyticus*, isolated from the Gulf of Khambhat, Gujarat India." Aquatic Living Resources **28**(2-4): 99-109.

Deatherage, D. E. and J. E. Barrick (2014). "Identification of mutatuions in laboratory-evolved microbes from next-generation sequencing data using breseq." Mehtods in Molecular Biology **1151**(1940-6029 (Electronic)): 165-188.

Decaestecker, E., S. Gaba, J. A. M. Raeymaekers, R. Stoks, L. Van Kerckhoven, D. Ebert and L. De Meester (2007). "Host-parasite 'Red Queen' dynamics archived in pond sediment." Nature **450**(7171): 870-U816.

DeFaveri, J. and J. Merila (2014). "Local adaptation to salinity in the three-spined stickleback?" Journal of Evolutionary Biology **27**(2): 290-302.

DeWitt, T. J., A. Sih and D. S. Wilson (1998). "Costs and limits of phenotypic plasticity." Trends in Ecology & Evolution **13**(2): 77-81.

Dobrindt, U., B. Hochhut, U. Hentschel and J. Hacker (2004). "Genomic islands in pathogenic and environmental microorganisms." Nature Reviews Microbiology **2**(5): 414-424.

Doebeli, M. and N. Knowlton (1998). "The evolution of interspecific mutualisms." Proceedings of the National Academy of Sciences of the United States of America **95**(15): 8676-8680.

Donelson, J. M., J. M. Sunday, W. F. Figueira, J. D. Gaitan-Espitia, A. J. Hobday, C. R. Johnson, J. M. Leis, S. D. Ling, D. Marshall, J. M. Pandolfi, G. Pecl, G. G. Rodgers, D. J. Booth and P. L. Munday (2019). "Understanding interactions between plasticity, adaptation and range shifts in response to marine environmental change." Philosophical Transactions of the Royal Society B-Biological Sciences **374**(1768): 14.

Dormann, C., B. Gruber and J. Fründ (2008). "Introducing the bipartite Package: Analysing Ecological Networks." R News **8**(2): 8-11.

Dormann, C. F. and R. Strauss (2014). "A method for detecting modules in quantitative bipartite networks." Methods in Ecology and Evolution **5**(1): 90-98.

Dray, S. and A.-B. Dufour (2007). "The ade4 Package: Implementing the Duality Diagram for Ecologists." Journal of Statistical Software **22**(4).

Dutil, J. D., Y. Lambert and E. Boucher (1997). "Does higher growth rate in Atlantic cod (Gadus morhua) at low salinity result from lower standard metabolic rate or increased protein digestibility?" Canadian Journal of Fisheries and Aquatic Sciences **54**: 99-103.

Dy, R. L., C. Richter, G. P. C. Salmond and P. C. Fineran (2014). Remarkable Mechanisms in Microbes to Resist Phage Infections. Annual Review of Virology, Vol 1. L. W. Enquist. Palo Alto, Annual Reviews. **1:** 307-331.

Ebert, D. and P. D. Fields (2020). "Host-parasite co-evolution and its genomic signature." Nature Reviews Genetics: 15.

Eiler, A., M. Johansson and S. Bertilsson (2006). "Environmental influences on *Vibrio* populations in northern temperate and boreal coastal waters (Baltic and Skagerrak Seas)." Applied and Environmental Microbiology **72**(9): 6004-6011.

Eizaguirre, C., T. L. Lenz, M. Kalbe and M. Milinski (2012). "Rapid and adaptive evolution of MHC genes under parasite selection in experimental vertebrate populations." Nature Communications **3**: 621.

Engelstadter, J. (2015). "Host-Parasite Coevolutionary Dynamics with Generalized Success/Failure Infection Genetics." American Naturalist **185**(5): E117-E129.

Erez, Z., I. Steinberger-Levy, M. Shamir, S. Doron, A. Stokar-Avihail, Y. Peleg, S. Melamed, A. Leavitt, A. Savidor, S. Albeck, G. Amitai and R. Sorek (2017). "Communication between viruses guides lysis-lysogeny decisions." Nature **541**(7638): 488-493.

Eriksen, M. S., M. Bakken, A. Espmark, B. O. Braastad and R. Salte (2006). "Prespawning stress in farmed Atlantic salmon Salmo salar: maternal cortisol exposure and hyperthermia during embryonic development affect offspring survival, growth and incidence of malformations." Journal of Fish Biology **69**(1): 114-129.

Faruque, S. M. and J. J. Mekalanos (2012). "Phage-bacterial interactions in the evolution of toxigenic *Vibrio cholerae*." Virulence **3**(7): 556-565.

Feldman, C. R., A. M. Durso, C. T. Hanifin, M. E. Pfrender, P. K. Ducey, A. N. Stokes, K. E. Barnett and E. D. Brodie (2016). "Is there more than one way to skin a newt? Convergent toxin resistance in snakes is not due to a common genetic mechanism." Heredity **116**(1): 84-91.

Fenn, K. and M. Blaxter (2006). "Wolbachia genomes: revealing the biology of parasitism and mutualism." Trends in Parasitology **22**(2): 60-65.

Ferris, C., R. Wright, M. A. Brockhurst and A. Best (2020). "The evolution of host resistance and parasite infectivity is highest in seasonal resource environments that oscillate at intermediate amplitudes." Proceedings of the Royal Society B-Biological Sciences **287**(1927): 9.

Fineran, P., N. Petty and G. Salmond (2009). Transduction: Host DNA Transfer by Bacteriophages. The Encyclopedia of Microbiology, Schaechter, M., Ed.; Elsevier.

Flajnik, M. F. and M. Kasahara (2010). "Origin and evolution of the adaptive immune system: genetic events and selective pressures." Nature reviews. Genetics **11**(1): 47-59.

Flores, C. O., J. R. Meyer, S. Valverde, L. Farr and J. S. Weitz (2011). "Statistical structure of host-phage interactions." Proceedings of the National Academy of Sciences of the United States of America **108**(28): E288-E297.

Flores, C. O., J. R. Meyer, S. Valverde, L. Farr and J. S. Weitz (2011). "Statistical structure of host–phage interactions." Proceedings of the National Academy of Sciences **108**(28): E288.

Flores, C. O., S. Valverde and J. S. Weitz (2013). "Multi-scale structure and geographic drivers of cross-infection within marine bacteria and phages." Isme Journal **7**(3): 520-532.

Flyg, C., K. Kenne and H. G. Boman (1980). "Insect pathogenic properties of Serratia marcescens: phage-resistant mutants with a decreased resistance to Cecropia immunity and a decreased virulence to Drosophila." Journal of general microbiology **120**(1): 173-181.

Folimonova, S. Y. (2012). "Superinfection Exclusion Is an Active Virus-Controlled Function That Requires a Specific Viral Protein." Journal of Virology **86**(10): 5554-5561.

Forterre, P. and D. Prangishvili (2009). "The Great Billion-year War between Ribosome- and Capsid-encoding Organisms (Cells and Viruses) as the Major Source of Evolutionary Novelties." Natural Genetic Engineering and Natural Genome Editing **1178**: 65-77.

Fortuna, M. A., M. A. Barbour, L. Zaman, A. R. Hall, A. Buckling and J. Bascompte (2019). "Coevolutionary dynamics shape the structure of bacteria-phage infection networks." Evolution **73**(5): 1001-1011.

Francis, M. E., M. L. King and A. A. Kelvin (2019). "Back to the Future for Influenza PreimmunityLooking Back at Influenza Virus History to Infer the Outcome of Future Infections." Viruses-Basel **11**(2): 21.

Frank, S. A. (1992). "A kin selection model for the evolution of virulence." Proceedings of the Royal Society B-Biological Sciences **250**(1329): 195-197.

Frank, S. A. (1994). "Kin selection and virulence in the evolution of protocells and parasites." Proceedings of the Royal Society B-Biological Sciences **258**(1352): 153-161.

Frank, S. A. (1996). "Models of parasite virulence." Quarterly Review of Biology **71**(1): 37-78.

Fraser, H. B. (2013). "Gene expression drives local adaptation in humans." Genome Research **23**(7): 1089-1096.

Frelat, R., A. Orio, M. Casini, A. Lehmann, B. Merigot, S. A. Otto, C. Sguotti and C. Mollmann (2018). "A three-dimensional view on biodiversity changes: spatial, temporal, and functional perspectives on fish communities in the Baltic Sea." Ices Journal of Marine Science **75**(7): 2463-2475.

Friman, V. P., T. Hiltunen, M. Jalasvuori, C. Lindstedt, E. Laanto, A. M. Ormala, J. Laakso, J. Mappes and J. K. H. Bamford (2011). "High Temperature and Bacteriophages Can Indirectly Select for Bacterial Pathogenicity in Environmental Reservoirs." Plos One **6**(3).

Fuhrman, J. A. (1999). "Marine viruses and their biogeochemical and ecological effects." Nature **399**(6736): 541-548.

Gandon, S., A. Buckling, E. Decaestecker and T. Day (2008). "Host-parasite coevolution and patterns of adaptation across time and space." Journal of Evolutionary Biology **21**(6): 1861-1866.

Gao, L., Y. T. Li and R. W. Wang (2015). "The shift between the Red Queen and the Red King effects in mutualisms." Scientific Reports **5**: 9.

Gao, W., B. P. Howden and T. P. Stinear (2018). "Evolution of virulence in Enterococcus faecium, a hospital-adapted opportunistic pathogen." Current Opinion in Microbiology **41**: 76-82.

Garcia, J. and A. Traulsen (2019). "Evolution of coordinated punishment to enforce cooperation from an unbiased strategy space." Journal of the Royal Society Interface **16**(156): 8.

Gazeau, F., L. M. Parker, S. Comeau, J. P. Gattuso, W. A. O'Connor, S. Martin, H. O. Portner and P. M. Ross (2013). "Impacts of ocean acidification on marine shelled molluscs." Marine Biology **160**(8): 2207-2245.

Gibson, J. R. and R. G. Najjar (2000). "The response of Chesapeake Bay salinity to climate-induced changes in streamflow." Limnology and Oceanography **45**(8): 1764-1772.

Gienapp, P., C. Teplitsky, J. S. Alho, J. A. Mills and J. Merila (2008). "Climate change and evolution: disentangling environmental and genetic responses." Molecular Ecology **17**(1): 167-178.

Girjatowicz, J. P. and M. Swiatek (2016). "Salinity variations of the surface water at the southern coast of the Baltic Sea in years 1950-2010." Continental Shelf Research **126**: 110-118.

Goehlich, H., O. Roth, M. Sieber, J. Rajkov, K. Trübenbach, C. M. Chibani, H. Liesegang and C. Wendling Low salinity slows down resistance evolution of *Vibrio alginolyticus* against a filamentous phage.

Goehlich, H., O. Roth and C. C. Wendling (2019). "Filamentous phages reduce bacterial growth in low salinities." Royal Society Open Science(12): 191669.

Goehlich, H., L. Sartoris, K. S. Wagner, C. C. Wendling and O. Roth (2020). "Pipefish locally adapted to low salinity in the Baltic Sea retain phenotypic plasticity to cope with ancestral salinity levels." bioRxiv: 2020.2011.2012.379305.

Gomez, P. and A. Buckling (2011). "Bacteria-Phage Antagonistic Coevolution in Soil." Science **332**(6025): 106-109.

Guo, B. C., J. DeFaveri, G. Sotelo, A. Nair and J. Merila (2015). "Population genomic evidence for adaptive differentiation in Baltic Sea three-spined sticklebacks." Bmc Biology **13**.

Guo, B. C., Z. T. Li and J. Merila (2016). "Population genomic evidence for adaptive differentiation in the Baltic Sea herring." Molecular Ecology **25**(12): 2833-2852.

Gurkan, S. and E. Taskavak (2007). "Length-weigth relationships for syngnathid fishes of the Aegean Sea, Turkey." Belgian Journal of Zoology **137**(2): 219-222.

Gutman, G. A., K. G. Chandy, S. Grissmer, M. Lazdunski, D. McKinnon, L. A. Pardo, G. A. Robertson, B. Rudy, M. C. Sanguinetti, W. Stühmer and X. Wang (2005). "International Union of Pharmacology. LIII. Nomenclature and Molecular Relationships of Voltage-Gated Potassium Channels." Pharmacological Reviews **57**(4): 473.

Haase, D., O. Roth, M. Kalbe, G. Schmiedeskamp, J. P. Scharsack, P. Rosenstiel and T. B. H. Reusch (2013). "Absence of major histocompatibility complex class II mediated immunity in pipefish, Syngnathus typhle: evidence from deep transcriptome sequencing." Biology Letters **9**(2): 6.

Hacker, J. and J. B. Kaper (2000). "Pathogenicity islands and the evolution of microbes." Annual Review of Microbiology **54**: 641-679.

Haddy, J. A. and N. W. Pankhurst (2000). "The effects of salinity on reproductive development, plasma steroid levels, fertilisation and egg survival in black bream Acanthopagrus butcheri." Aquaculture **188**(1-2): 115-131.

Hague, M. T. J., A. N. Stokes, C. R. Feldman and E. D. Brodie (2020). "The geographic mosaic of arms race coevolution is closely matched to prey population structure." Evolution Letters: 16.

Hague, M. T. J., G. Toledo, S. L. Geffeney, C. T. Hanifin and E. D. Brodie (2018). "Large-effect mutations generate trade-off between predatory and locomotor ability during arms race coevolution with deadly prey." Evolution Letters **2**(4): 406-416.

Hall, A. R., P. D. Scanlan, A. D. Morgan and A. Buckling (2011). "Host-parasite coevolutionary arms races give way to fluctuating selection." Ecology Letters **14**(7): 635-642.

Hall, J. P. J., M. A. Brockhurst and E. Harrison (2017). "Sampling the mobile gene pool: innovation via horizontal gene transfer in bacteria." Philosophical Transactions of the Royal Society B-Biological Sciences **372**(1735).

Hall, M. D., A. Vettiger and D. Ebert (2013). "Interactions between environmental stressors: the influence of salinity on host-parasite interactions between Daphnia magna and Pasteuria ramosa." Oecologia **171**(4): 789-796.

Hamelin, F. M., F. M. Hilker, T. A. Sun, M. J. Jeger, M. R. Hajimorad, L. J. S. Allen and H. R. Prendeville (2017). "The evolution of parasitic and mutualistic plant-virus symbioses through transmission-virulence trade-offs." Virus Research **241**: 77-87.

Hamm, C. E., R. Merkel, O. Springer, P. Jurkojc, C. Maier, K. Prechtel and V. Smetacek (2003). "Architecture and material properties of diatom shells provide effective mechanical protection." Nature **421**(6925): 841-843.

Hampton, H. G., B. N. J. Watson and P. C. Fineran (2020). "The arms race between bacteria and their phage foes." Nature **577**(7790): 327-336.

Harcombe, W. R., A. Betts, J. W. Shapiro and C. J. Marx (2016). "Adding biotic complexity alters the metabolic benefits of mutualism." Evolution **70**(8): 11.

Harrison, E. and M. A. Brockhurst (2017). "Ecological and Evolutionary Benefits of Temperate Phage: What Does or Doesn't Kill You Makes You Stronger." Bioessays.

Harrison, E. and M. A. Brockhurst (2017). "Ecological and Evolutionary Benefits of Temperate Phage: What Does or Doesn't Kill You Makes You Stronger." Bioessays **39**(12): 6.

Harrison, E., A. L. Laine, M. Hietala and M. A. Brockhurst (2013). "Rapidly fluctuating environments constrain coevolutionary arms races by impeding selective sweeps." Proceedings of the Royal Society B-Biological Sciences **280**(1764): 9.

Hasan, M. M., J. DeFaveri, S. Kuure, S. N. Dash, S. Lehtonen, J. Merila and R. J. S. McCairns (2017). "Sticklebacks adapted to divergent osmotic environments show differences in plasticity for kidney morphology and candidate gene expression." Journal of Experimental Biology **220**(12): 2175-2186.

Hase, C. C. and B. Barquera (2001). "Role of sodium bioenergetics in *Vibrio cholerae*." Biochimica Et Biophysica Acta-Bioenergetics **1505**(1): 169-178.

Hay, I. D. and T. Lithgow (2019). "Filamentous phages: masters of a microbial sharing economy." EMBO reports: e47427.

Heath-Heckman, E. A. C., S. M. Peyer, C. A. Whistler, M. A. Apicella, W. E. Goldman and M. J. McFall-Ngai (2013). "Bacterial Bioluminescence Regulates Expression of a Host Cryptochrome Gene in the Squid-*Vibrio* Symbiosis." mBio **4**(2): e00167-00113.

Heckwolf, M. J., B. S. Meyer, T. Doring, C. Eizaguirre and T. B. H. Reusch (2018). "Transgenerational plasticity and selection shape the adaptive potential of sticklebacks to salinity change." Evolutionary Applications **11**(10): 1873-1885.

Heckwolf, M. J., B. S. Meyer, R. Hasler, M. P. Hoppner, C. Eizaguirre and T. B. H. Reusch (2020). "Two different epigenetic information channels in wild three-spined sticklebacks are involved in salinity adaptation." Science Advances **6**(12): 13.

Hede, K. (2014). "Antibiotic resistance: An infectious arms race." Nature **509**(7498): S2-S3.

Heierson, A., I. Sidén, A. Kivaisi and H. G. Boman (1986). "Bacteriophage-resistant mutants of Bacillus thuringiensis with decreased virulence in pupae of Hyalophora cecropia." Journal of Bacteriology **167**(1): 18.

Helenius, L. K., E. Leskinen, H. Lehtonen and L. Nurminen (2017). "Spatial patterns of littoral zooplankton assemblages along a salinity gradient in a brackish sea: A functional diversity perspective." Estuarine Coastal and Shelf Science **198**: 400-412.

Hellemans, J., G. Mortier, A. De Paepe, F. Speleman and J. Vandesompele (2007). "qBase relative quantification framework and software for management and automated analysis of real-time quantitative PCR data." Genome biology **8**(2): R19-R19.

Herlemann, D. P. R., M. Labrenz, K. Jurgens, S. Bertilsson, J. J. Waniek and A. F. Andersson (2011). "Transitions in bacterial communities along the 2000 km salinity gradient of the Baltic Sea." Isme Journal **5**(10): 1571-1579.

Herlemann, D. P. R., D. Lundin, A. F. Andersson, M. Labrenz and K. Jurgens (2016). "Phylogenetic Signals of Salinity and Season in Bacterial Community Composition Across the Salinity Gradient of the Baltic Sea." Frontiers in Microbiology **7**: 13.

Herlemann, D. P. R., J. Woelk, M. Labrenz and K. Jurgens (2014). "Diversity and abundance of "Pelagibacterales" (SAR11) in the Baltic Sea salinity gradient." Systematic and Applied Microbiology **37**(8): 601-604.

Hernandez, C. A. and B. Koskella (2019). "Phage resistance evolution in vitro is not reflective of in vivo outcome in a plant-bacteria-phage system." Evolution: 15.

Herre, E. A., N. Knowlton, U. G. Mueller and S. A. Rehner (1999). "The evolution of mutualisms: exploring the paths between conflict and cooperation." Trends in Ecology & Evolution **14**(2): 49-53.

Herrera, P., L. Schuster, C. Wentrup, L. König, T. Kempinger, H. Na, J. Schwarz, S. Köstlbacher, F. Wascher, M. Zojer, T. Rattei and M. Horn (2020). "Molecular causes of an evolutionary shift along the parasitism–mutualism continuum in a bacterial symbiont." Proceedings of the National Academy of Sciences **117**(35): 21658.

Hinrichs, I., A. Jahnke-Bornemann, A. Andersson, A. Ganske, V. Gouretski, C. Jensen, B. Klein, J. Moller, R. Sadikni and B. Tinz (2019). "The Baltic and North Seas Climatology (BNSC) - A Comprehensive, Observation-Based Data Product of Atmospheric and Hydrographic Parameters." Frontiers in Earth Science **7**: 21.

Hobbs, Z. and S. T. Abedon (2016). "Diversity of phage infection types and associated terminology: the problem with 'Lytic or lysogenic'." Fems Microbiology Letters **363**(7): 8.

Hofmann, G. E., J. P. Barry, P. J. Edmunds, R. D. Gates, D. A. Hutchins, T. Klinger and M. A. Sewell (2010). The Effect of Ocean Acidification on Calcifying Organisms in Marine Ecosystems: An Organism-to-Ecosystem Perspective. Annual Review of Ecology, Evolution, and Systematics, Vol 41. D. J. Futuyma, H. B. Shafer and D. Simberloff. Palo Alto, Annual Reviews. **41:** 127-147.

Holliday, F. G. T. and J. H. S. Blaxter (1960). "The effects of salinity on the developing eggs and larvae of the herring." Journal of the Marine Biological Association of the United Kingdom **39**(3): 591-603.

Holmborn, T., E. Goetze, M. Pollupuu and A. Pollumae (2011). "Genetic species identification and low genetic diversity in Pseudocalanus acuspes of the Baltic Sea." Journal of Plankton Research **33**(3): 507-515.

Holmgren, J. (1981). "Actions of cholera toxin and the prevention and treatment of cholera." Nature **292**(5822): 413-417.

Horabin, J. I. and R. E. Webster (1986). "Morphogenesis of f1 filamentous bacteriophage - increasedexpression of gene-1 inhibits bacterial-growth." Journal of Molecular Biology **188**(3): 403-413.

Horabin, J. I. and R. E. Webster (1988). "An amino-acid seqeunce which directs membrane insertion causes loss of membrane-potential." Journal of Biological Chemistry **263**(23): 11575-11583.

Hothorn, T., F. Bretz, P. Westfall, R. M. Heiberger, A. Schetzenmeister and S. Scheibe (2020). multcomp: Simultaneous Inference in General Parametric Models. https://cran.r-project.org/web/packages/multcomp/index.html, CRAN.

Hu, Y. O. O., B. Karlson, S. Charvet and A. F. Andersson (2016). "Diversity of Pico- to Mesoplankton along the 2000 km Salinity Gradient of the Baltic Sea." Frontiers in Microbiology **7**: 17.

Hutchinson, G. E. (1959). "Homage to Santa Rosalia or why are there so many kinds of animals?" American Naturalist **93**(870): 145-159.

Hwang, P.-P. and T.-H. Lee (2007). "New insights into fish ion regulation and mitochondrion-rich cells." Comparative Biochemistry and Physiology Part A: Molecular & Integrative Physiology **148**(3): 479-497.

Hüttmann, A. (2013). Tackling the root of evolution - What can we learn from a multi-scale infection matrix

of *Vibrios* and associated temperate phages? Master thesis, Christian-Albrechts-University Kiel.

Ilyina, T. S. (2015). "Filamentous Bacteriophages and Their Role in the Virulence and Evolution of Pathogenic Bacteria." Molecular Genetics Microbiology and Virology **30**(1): 1-9.

Imsland, A. K., A. Foss, S. Gunnarsson, M. H. G. Berntssen, R. FitzGerald, S. W. Bonga, E. Von Ham, C. Naevdal and S. O. Stefansson (2001). "The interaction of temperature and salinity on growth and food conversion in juvenile turbot (Scophthalmus maximus)." Aquaculture **198**(3-4): 353-367.

Ina-Salwany, M. Y., N. Al-saari, A. Mohamad, F.-A. Mursidi, A. Mohd-Aris, M. N. A. Amal, H. Kasai, S. Mino, T. Sawabe and M. Zamri-Saad (2019). "Vibriosis in Fish: A Review on Disease Development and Prevention." Journal of Aquatic Animal Health **31**(1): 3-22.

James, T. Y., L. F. Toledo, D. Rodder, D. D. Leite, A. M. Belasen, C. M. Betancourt-Roman, T. S. Jenkinson, C. Soto-Azat, C. Lambertini, A. V. Longo, J. Ruggeri, J. P. Collins, P. A. Burrowes, K. R. Lips, K. R. Zamudio and J. E. Longcore (2015). "Disentangling host, pathogen, and environmental determinants of a recently emerged wildlife disease: lessons from the first 15years of amphibian chytridiomycosis research." Ecology and Evolution **5**(18): 4079-4097.

Janeway, C. (2005). Immunobiology : the immune system in health and disease. New York :, Garland Science.

Janssen, F., C. Schrum and J. O. Backhaus (1999). "A climatological data set of temperature and salinity for the Baltic Sea and the North Sea." Deutsche Jydrpgrafische Zeitschrift(9): 5.

Janzen, D. H. (1980). "When is it coevolution?" Evolution **34**(3): 611-612.

Jeffares, D. C., A. Pain, A. Berry, A. V. Cox, J. Stalker, C. E. Ingle, A. Thomas, M. A. Quail, K. Siebenthall, A. C. Uhlemann, S. Kyes, S. Krishna, C. Newbold, E. T. Dermitzakis and M. Berriman (2007). "Genome variation and evolution of the malaria parasite Plasmodium falciparum." Nature Genetics **39**(1): 120-125.

Jensen, K. (2010). "Punishment and spite, the dark side of cooperation." Philosophical Transactions of the Royal Society B-Biological Sciences **365**(1553): 2635-2650.

Jensen, K. C., B. B. Hair, T. M. Wienclaw, M. H. Murdock, J. B. Hatch, A. T. Trent, T. D. White, K. J. Haskell and B. K. Berges (2015). "Isolation and Host Range of Bacteriophage with Lytic Activity against Methicillin-Resistant Staphylococcus aureus and Potential Use as a Fomite Decontaminant." Plos One **10**(7): 13.

Jian, H. H., X. Xiao and F. P. Wang (2013). "Role of Filamentous Phage SW1 in Regulating the Lateral Flagella of Shewanella piezotolerans Strain WP3 at Low Temperatures." Applied and Environmental Microbiology **79**(22): 7101-7109.

Jian, H. H., L. Xiong, G. P. Xu and X. Xiao (2016). "Filamentous phage SW1 is active and influences the transcriptome of the host at high-pressure and low-temperature." Environmental Microbiology Reports **8**(3): 358-362.

Jian, H. H., J. Xu, X. Xiao and F. P. Wang (2012). "Dynamic Modulation of DNA Replication and Gene Transcription in Deep-Sea Filamentous Phage SW1 in Response to Changes of Host Growth and Temperature." Plos One **7**(8): 9.

Johannesson, K. and C. Andre (2006). "Life on the margin: genetic isolation and diversity loss in a peripheral marine ecosystem, the Baltic Sea." Molecular Ecology **15**(8): 2013-2029.

Johannesson, K., A. Le Moan, S. Perini and C. André (2020). "A Darwinian Laboratory of Multiple Contact Zones." Trends in Ecology & Evolution.

Johnson, E. P., A. R. Strom and D. R. Helinski (1996). "Plasmid RK2 toxin protein ParE: Purification and interaction with the ParD antitoxin protein." Journal of Bacteriology **178**(5): 1420-1429.

Jones, A. G., G. Rosenqvist, A. Berglund and J. C. Avise (1999). "The genetic mating system of a sex-role-reversed pipefish (Syngnathus typhle): a molecular inquiry." Behavioral Ecology and Sociobiology **46**(5): 357-365.

Jones, C. G., J. H. Lawton and M. Shachak (1996). Organisms as Ecosystem Engineers. Ecosystem Management: Selected Readings. F. B. Samson and F. L. Knopf. New York, NY, Springer New York**:** 130-147.

Josenhans, C. and S. Suerbaum (2002). "The role of motility as a virulence factor in bacteria." International Journal of Medical Microbiology **291**(8): 605-614.

Kahm, M., G. Hasenbrink, H. Lichtenberg-Frate, J. Ludwig and M. Kschischo (2010). "grofit: Fitting Biological Growth Curves with R." Journal of Statistical Software **33**(7): 1-21.

Kao, C.-Y., B.-S. Sheu and J.-J. Wu (2016). "Helicobacter pylori infection: An overview of bacterial virulence factors and pathogenesis." Biomedical Journal **39**(1): 14-23.

Kao, C. Y., W. H. Lin, C. C. Tseng, A. B. Wu, M. C. Wang and J. J. Wu (2014). "The complex interplay among bacterial motility and virulence factors in different Escherichia coli infections." European Journal of Clinical Microbiology & Infectious Diseases **33**(12): 2157-2162.

Kassambara, A. (2019). ggpubr: 'ggplot2' Based Publication Ready Plots. https://cran.r-project.org/web/packages/ggpubr/index.html.

Kassen, R. (2019). "Experimental Evolution of Innovation and Novelty." Trends in Ecology & Evolution **34**(8): 712-722.

Kauffman, K. M., F. A. Hussain, J. Yang, P. Arevalo, J. M. Brown, W. K. Chang, D. VanInsberghe, J. Elsherbini, R. S. Sharma, M. B. Cutler, L. Kelly and M. F. Polz (2018). "A major lineage of non-tailed dsDNA viruses as unrecognized killers of marine bacteria." Nature **554**: 118.

Kawecki, T. J., R. E. Lenski, D. Ebert, B. Hollis, I. Olivieri and M. C. Whitlock (2012). "Experimental evolution." Trends in Ecology & Evolution **27**(10): 547-560.

Kelly, M. (2019). "Adaptation to climate change through genetic accommodation and assimilation of plastic phenotypes." Philosophical Transactions of the Royal Society B-Biological Sciences **374**(1768): 10.

Kiers, E. T. and M. G. A. van der Heijden (2006). "Mutualistic stability in the arbuscular mycorrhizal symbiosis: Exploring hypotheses of evolutionary cooperation." Ecology **87**(7): 1627-1636.

Killingback, T. and M. Doebeli (2002). "The continuous prisoner's dilemma and the evolution of cooperation through reciprocal altruism with variable investment." American Naturalist **160**(4): 421-438.

Kim, L. H. and T. H. Chong (2017). "Physiological Responses of Salinity-Stressed *Vibrio* sp and the Effect on the Biofilm Formation on a Nanofiltration Membrane." Environmental Science & Technology **51**(3): 1249-1258.

Kim, S., T. D. Lieberman and R. Kishony (2014). "Alternating antibiotic treatments constrain evolutionary paths to multidrug resistance." Proceedings of the National Academy of Sciences of the United States of America **111**(40): 14494-14499.

Kimes, N. E., C. J. Grim, W. R. Johnson, N. A. Hasan, B. D. Tall, M. H. Kothary, H. Kiss, A. C. Munk, R. Tapia, L. Green, C. Detter, D. C. Bruce, T. S. Brettin, R. R. Colwell and P. J. Morris (2012). "Temperature regulation of virulence factors in the pathogen *Vibrio coralliilyticus*." Isme Journal **6**(4): 835-846.

Kniebusch, M., H. E. M. Meier and H. Radtke (2019). "Changing Salinity Gradients in the Baltic Sea As a Consequence of Altered Freshwater Budgets." Geophysical Research Letters **46**(16): 9739-9747.

Koonin, E. V. and V. V. Dolja (2013). "A virocentric perspective on the evolution of life." Current Opinion in Virology **3**(5): 546-557.

Koressaar, T. and M. Remm (2007). "Enhancements and modifications of primer design program Primer3." Bioinformatics **23**(10): 1289-1291.

Koskella, B., D. M. Lin, A. Buckling and J. N. Thompson (2012). "The costs of evolving resistance in heterogeneous parasite environments." Proceedings of the Royal Society B-Biological Sciences **279**(1735): 1896-1903.

Koskella, B. and S. Meaden (2013). "Understanding Bacteriophage Specificity in Natural Microbial Communities." Viruses-Basel **5**(3): 806-823.

Kukkaro, P. and D. H. Bamford (2009). "Virus-host interactions in environments with a wide range of ionic strengths." Environmental Microbiology Reports **1**(1): 71-77.

Kuo, M. Y., M. K. Yang, W. P. Chen and T. T. Kuo (2000). "High-frequency interconversion of turbid and clear plaque strains of bacteriophage f1 and associated host cell death." Canadian Journal of Microbiology **46**(9): 841-847.

Kuo, T. T., C. C. Chiang, S. Y. Chen, J. H. Lin and J. L. Kuo (1994). "A long lytic cycle in filamentous phage Cf1tv infecting *Xanthomonas campestris* pv. *citri*." Archives of Virology **135**(3-4): 253-264.

Kuo, T. T., M. S. Tan, M. T. Su and M. K. Yang (1991). "Complete nucleotide-sequence of filamentous phage CF1c from *Xanthomonas-campestris pv citri*." Nucleic Acids Research **19**(9): 2498-2498.

Kurihara, H. (2008). "Effects of CO2-driven ocean acidification on the early developmental stages of invertebrates." Marine Ecology Progress Series **373**: 275-284.

Kutzer, M. A. M. and S. A. O. Armitage (2016). "Maximising fitness in the face of parasites: a review of host tolerance." Zoology **119**(4): 281-289.

Labrie, S. J., J. E. Samson and S. Moineau (2010). "Bacteriophage resistance mechanisms." Nature Reviews Microbiology **8**(5): 317-327.

Lages, M. A., M. Balado and M. L. Lemos (2019). "The Expression of Virulence Factors in *Vibrio anguillarum* Is Dually Regulated by Iron Levels and Temperature." Frontiers in Microbiology **10**: 11.

Laine, A. L. (2009). "Role of coevolution in generating biological diversity: spatially divergent selection trajectories." Journal of Experimental Botany **60**(11): 2957-2970.

Laland, K., T. Uller, M. Feldman, K. Sterelny, G. B. Muller, A. Moczek, E. Jablonka and J. Odling-Smee (2014). "Does evolutionary theory need a rethink? - POINT Yes, urgently." Nature **514**(7521): 161-164.

Landis, S. H., M. Kalbe, T. B. H. Reusch and O. Roth (2012). "Consistent Pattern of Local Adaptation during an Experimental Heat Wave in a Pipefish-Trematode Host-Parasite System." Plos One **7**(1): 7.

Larsen, P. F., P. M. Schulte and E. E. Nielsen (2011). "Gene expression analysis for the identification of selection and local adaptation in fishes." Journal of Fish Biology **78**(1): 1-22.

Larsson, A. (2014). "AliView: a fast and lightweight alignment viewer and editor for large datasets." Bioinformatics (Oxford, England) **30**(22): 3276-3278.

Lauritano, C., Y. Carotenuto, A. Miralto, G. Procaccini and A. Ianora (2012). "Copepod Population-Specific Response to a Toxic Diatom Diet." Plos One **7**(10): 7.

Leder, E. H., C. Andr, A. Le Moan, M. Topel, A. Blomberg, J. N. Havenhand, K. Lindstrom, F. A. M. Volckaert, C. Kvarnemo, K. Johannesson and O. Svensson (2020). "Post-glacial establishment of locally adapted fish populations over a steep salinity gradient." Journal of Evolutionary Biology: 19.

Leeksl, A., M. dos Santos and S. A. West (2019). "Transmission, relatedness, and the evolution of cooperative symbionts." Journal of Evolutionary Biology **32**(10): 1036-1045.

Lehnherr, H., E. Maguin, S. Jafri and M. B. Yarmolinsky (1993). "Plasmid addiction genes of bacteriophage-P1 - DPC, which causes cell-death on curing of prophage, and PHD, which prevents host death when prophage is retained." Journal of Molecular Biology **233**(3): 414-428.

Leigh, E. G. (2010). "The evolution of mutualism." Journal of Evolutionary Biology **23**(12): 2507-2528.

Lenski, R. E. and B. R. Levin (1985). "Constraints on the coevolution of bacteria and virulent phage - a model, some experiments, and predctions fro natural communities." American Naturalist **125**(4): 585-602.

Lenski, R. E. and B. R. Levin (1985). "Constraints on the Coevolution of Bacteria and Virulent Phage - a Model, Some Experiments, and Predictions for Natural Communities." American Naturalist **125**(4): 585-602.

Lenth, R., H. Singmann, J. Love, P. Buerkner and M. Herve (2020). emmeans: Estimated Marginal Means, aka Least-Squares Means. https://cran.r-project.org/web/packages/emmeans/index.html, CRAN.

Leon, M. and R. Bastias (2015). "Virulence reduction in bacteriophage resistant bacteria." Frontiers in Microbiology **6**: 7.

Levin, B. R. (1988). "Frequency-dependent selection in bacterial-populations." Philosophical Transactions of the Royal Society B-Biological Sciences **319**(1196): 459-472.

Lewis, H. M. and A. J. Dumbrell (2013). "Evolutionary games of cooperation: Insights through integration of theory and data." Ecological Complexity **16**: 20-30.

Li, Y. M., X. X. Liu, K. H. Tang, W. Q. Wang, Y. X. Guo and X. X. Wang (2020). "Prophage encoding toxin/antitoxin system PfiT/PfiA inhibits Pf4 production in Pseudomonas aeruginosa." Microbial Biotechnology: 13.

Lind, M. I., M. K. Zwoinska, J. Andersson, H. Carlsson, T. Krieg, T. Larva and A. A. Maklakov (2020). "Environmental variation mediates the evolution of anticipatory parental effects." Evolution Letters **n/a**(n/a).

Lindell, D., J. D. Jaffe, Z. I. Johnson, G. M. Church and S. W. Chisholm (2005). "Photosynthesis genes in marine viruses yield proteins during host infection." Nature **438**(7064): 86-89.

Lindell, D., M. B. Sullivan, Z. I. Johnson, A. C. Tolonen, F. Rohwer and S. W. Chisholm (2004). "Transfer of photosynthesis genes to and from Prochlorococcus viruses." Proceedings of the National Academy of Sciences of the United States of America **101**(30): 11013-11018.

Loder, J. W., A. van der Baaren and I. Yashayaev (2015). "Climate Comparisons and Change Projections for the Northwest Atlantic from Six CMIP5 Models." Atmosphere-Ocean **53**(5): 529-555.

Mai-Prochnow, A., J. G. K. Hui, S. Kjelleberg, J. Rakonjac, D. McDougald and S. A. Rice (2015). "'Big things in small packages: the genetics of filamentous phage and effects on fitness of their host'." Fems Microbiology Reviews **39**(4): 465-487.

Manzon, L. A. (2002). "The role of prolactin in fish osmoregulation: A review." General and Comparative Endocrinology **125**(2): 291-310.

Marchetti, M., D. Capela, M. Glew, S. Cruveiller, B. Chane-Woon-Ming, C. Gris, T. Timmers, V. Poinsot, L. B. Gilbert, P. Heeb, C. Medigue, J. Batut and C. Masson-Boivin (2010). "Experimental Evolution of a Plant Pathogen into a Legume Symbiont." Plos Biology **8**(1): 10.

Marshall, D. J. (2008). "Transgenerational plasticity in the sea: Context-dependent maternal effects across the life history." Ecology **89**(2): 418-427.

Marshall, W. S., R. R. F. Cozzi, R. M. Pelis and S. D. McCormick (2005). "Cortisol receptor blockade and seawater adaptation in the euryhaline teleost Fundulus heteroclitus." Journal of Experimental Zoology Part A: Comparative Experimental Biology **303A**(2): 132-142.

Mauchline, W. S., B. W. James, R. B. Fitzgeorge, P. J. Dennis and C. W. Keevil (1994). "Growth temperature reversibly modulates the virulence of *Legionella pneumophila*." Infection and Immunity **62**(7): 2995-2997.

Maurelli, A. T. and P. J. Sansonetti (1988). "Identification of a chromosomal gene controlling temperature-regulated expression of *Shigella* virulence." Proceedings of the National Academy of Sciences of the United States of America **85**(8): 2820-2824.

McCormick, S. D. (2001). "Endocrine control of osmoregulation in teleost fish." American Zoologist **41**(4): 781-794.

McFall-Ngai, M., M. G. Hadfield, T. C. G. Bosch, H. V. Carey, T. Domazet-Lošo, A. E. Douglas, N. Dubilier, G. Eberl, T. Fukami, S. F. Gilbert, U. Hentschel, N. King, S. Kjelleberg, A. H. Knoll, N. Kremer, S. K. Mazmanian, J. L. Metcalf, K. Nealson, N. E. Pierce, J. F. Rawls, A. Reid, E. G. Ruby, M. Rumpho, J. G. Sanders, D. Tautz and J. J. Wernegreen (2013). "Animals in a bacterial world, a new imperative for the life sciences." Proceedings of the National Academy of Sciences **110**(9): 3229.

McGuigan, K., N. Nishimura, M. Currey, D. Hurwit and W. A. Cresko (2011). "Cryptic genetic variation and body size evolution in threespine stickleback." Evolution **65**(4): 1203-1211.

Mei, Y. J., C. C. He, Y. C. Huang, Y. Liu, Z. Q. Zhang, X. D. Chen and P. Shen (2015). "Salinity Regulation of the Interaction of Halovirus SNJ1 with Its Host and Alteration of the Halovirus Replication Strategy to Adapt to the Variable Ecosystem." Plos One **10**(4): 12.

Meier, H. E. M., H. C. Andersson, B. Arheimer, T. Blenckner, B. Chubarenko, C. Donnelly, K. Eilola, B. G. Gustafsson, A. Hansson, J. Havenhand, A. Hoglund, I. Kuznetsov, B. R. MacKenzie, B. Muller-Karulis, T. Neumann, S. Niiranen, J. Piwowarczyk, U. Raudsepp, M. Reckermann, T. Ruoho-Airola, O. P. Savchuk, F. Schenk, S. Schimanke, G. Vali, J. M. Weslawski and E. Zorita (2012). "Comparing reconstructed past variations and future projections of the Baltic Sea ecosystem-first results from multi-model ensemble simulations." Environmental Research Letters **7**(3): 8.

Meier, H. E. M., E. Kjellstrom and L. P. Graham (2006). "Estimating uncertainties of projected Baltic Sea salinity in the late 21st century." Geophysical Research Letters **33**(15): 4.

Middelboe, M., A. Hagström, N. Blackburn, B. Sinn, U. Fischer, N. H. Borch, J. Pinhassi, K. Simu and M. G. Lorenz (2001). "Effects of bacteriophages on the population dynamics of four strains of pelagic marine bacteria." Microbial Ecology **42**(3): 395-406.

Mirzaei, M. K. and A. S. Nilsson (2015). "Isolation of Phages for Phage Therapy: A Comparison of Spot Tests and Efficiency of Plating Analyses for Determination of Host Range and Efficacy." Plos One **10**(3): 13.

Moebus, K. (1987). Ecology of marine bacteriophages. Phage ecology. S. Goyal, C. Gerba and G. Bitton. New York, John Wiley & Sons**:** 137-156.

Molnar, P. K., S. J. Kutz, B. M. Hoar and A. P. Dobson (2013). "Metabolic approaches to understanding climate change impacts on seasonal host-macroparasite dynamics." Ecology Letters **16**(1): 9-21.

Morgan, J. D. and G. K. Iwama (1991). "Effects of salinity on growth, metabolism, and ion regulation in juvenile rainbow and steelhead trout (*Oncorhynchus mykiss*) and fall chinook salmon (*Oncorhynchus tshawytscha*)." Canadian Journal of Fisheries and Aquatic Sciences **48**(11): 2083-2094.

Mostowy, R. and J. Engelstadter (2011). "The impact of environmental change on host-parasite coevolutionary dynamics." Proceedings of the Royal Society B-Biological Sciences **278**(1716): 2283-2292.

Mousseau, T. A. and D. A. Roff (1987). "Natural selection and the heritability of fitness components." Heredity **59**(2): 181-197.

Murata, H., S. Nakano, T. Yamanaka, T. Shimokawa, T. Abe, H. Ichida, Y. Hayashi, K. Tahara and A. Ohta (2019). "Conversion from mutualism to parasitism: a mutant of the ectomycorrhizal agaricomycete Tricholoma matsutake that induces stunting, wilting, and root degeneration in seedlings of its symbiotic partner, Pinus densiflora, in vitro." Botany **97**(8): 463-474.

Muthiga, N. A. and A. M. Szmant (1987). "The effects of salinity stress on the rates of aerobic respicartion and photosynthesis in the hermatypic coral *Siderastrea-siderea*." Biological Bulletin **173**(3): 539-551.

Nalepa, C. A. (2020). "Origin of Mutualism Between Termites and Flagellated Gut Protists: Transition From Horizontal to Vertical Transmission." Frontiers in Ecology and Evolution **8**: 15.

Nelson, E. J., J. B. Harris, J. Glenn Morris, S. B. Calderwood and A. Camilli (2009). "Cholera transmission: the host, pathogen and bacteriophage dynamic." Nature Reviews Microbiology **7**(10): 693-702.

Northfield, T. D. and A. R. Ives (2013). "Coevolution and the Effects of Climate Change on Interacting Species." Plos Biology **11**(10): 13.

Nowak, M. A. (2006). "Five rules for the evolution of cooperation." Science **314**(5805): 1560-1563.

Nuismer, S. L., R. Gomulkiewicz and B. J. Ridenhour (2010). "When Is Correlation Coevolution?" American Naturalist **175**(5): 525-537.

Nutman, A. P., V. C. Bennett, C. R. L. Friend, M. J. Van Kranendonk and A. R. Chivas (2016). "Rapid emergence of life shown by discovery of 3,700-million-year-old microbial structures." Nature **537**(7621): 535-+.

Nygard, M., C. Kvarnemo, I. Ahnesjo and I. Braga Goncalves (2019). "Pipefish embryo oxygenation, survival, and development: egg size, male size, and temperature effects." Behavioral Ecology **30**(5): 1451-1460.

Obeng, N., A. A. Pratama and J. D. van Elsas (2016). "The Significance of Mutualistic Phages for bacterial Ecology and Evolution." Trends in Microbiology **24**(6): 440-449.

Oberbeckmann, S., A. Wichels, K. H. Wiltshire and G. Gerdts (2011). "Occurrence of *Vibrio parahaemolyticus* and *Vibrio alginolyticus* in the German Bight over a seasonal cycle." Antonie Van Leeuwenhoek International Journal of General and Molecular Microbiology **100**(2): 291-307.

Ohtomo, Y., T. Kakegawa, A. Ishida, T. Nagase and M. T. Rosing (2014). "Evidence for biogenic graphite in early Archaean Isua metasedimentary rocks." Nature Geoscience **7**(1): 25-28.

Oksanen, J., F. G. Blanchet, R. Kindt, P. Legendre, P. R. Minchin, R. B. O'Hara, G. L. Simpson, P. Solymos, M. H. H. Stevens and H. Wagner. (2019). "vegan: Community Ecology Package. R packae version 2.5-4."

Omstedt, A. and C. Nohr (2004). "Calculating the water and heat balances of the Baltic Sea using ocean modelling and available meteorological, hydrological and ocean data." Tellus Series a-Dynamic Meteorology and Oceanography **56**(4): 400-414.

Papkou, A., C. S. Gokhale, A. Traulsen and H. Schulenburg (2016). "Host–parasite coevolution: why changing population size matters." Zoology **119**(4): 330-338.

Paris, L., L. Tonutti, C. Vannini and G. Bazzoni (2008). "Structural organization of the tight junctions." Biochimica et Biophysica Acta (BBA) - Biomembranes **1778**(3): 646-659.

Partridge, C., J. Shardo and A. Boettcher (2007). "Osmoregulatory role of the brood pouch in the euryhaline Gulf pipefish, Syngnathus scovelli." Comparative Biochemistry and Physiology a-Molecular & Integrative Physiology **147**(2): 556-561.

Pascua, L. L., A. R. Hall, A. Best, A. D. Morgan, M. Boots and A. Buckling (2014). "Higher resources decrease fluctuating selection during host-parasite coevolution." Ecology Letters **17**(11): 1380-1388.

Pavloudi, C., J. B. Kristoffersen, A. Oulas, M. De Troch and C. Arvanitidis (2017). "Sediment microbial taxonomic and functional diversity in a natural salinity gradient challenge Remane's "species minimum" concept." Peerj **5**: 25.

Piecyk, A., O. Roth and M. Kalbe (2019). "Specificity of resistance and geographic patterns of virulence in a vertebrate host-parasite system." BMC Evolutionary Biology **19**(1): 80.

Poirier, M., L. Listmann and O. Roth (2017). "Selection by higher-order effects of salinity and bacteria on early life-stages of Western Baltic spring-spawning herring." Evolutionary Applications **10**(6): 603-615.

Poloczanska, E. S., C. J. Brown, W. J. Sydeman, W. Kiessling, D. S. Schoeman, P. J. Moore, K. Brander, J. F. Bruno, L. B. Buckley, M. T. Burrows, C. M. Duarte, B. S. Halpern, J. Holding, C. V. Kappel, M. I. O'Connor, J. M. Pandolfi, C. Parmesan, F. Schwing, S. A. Thompson and A. J. Richardson (2013). "Global imprint of climate change on marine life." Nature Climate Change **3**(10): 919-925.

Poullain, V., S. Gandon, M. A. Brockhurst, A. Buckling and M. E. Hochberg (2008). "The evolution of specificity in evolving and coevolving antagonistic interactions between a bacteria and its phage." Evolution **62**(1): 1-11.

Prunet, P., M. Avelia, A. Föstier, B. T. Björnsson, G. Boeuf and C. Haux (1990). "Roles of prolactin in salmonids." Progress in Comparative Endocrinology: 547-552.

Quast, W. D. and N. R. Howe (1980). "The osmotic role of the brood pouch in the pipefish *Syngnathus scovelli* " Comparative Biochemistry and Physiology a-Physiology **67**(4): 675-678.

Raihani, N. J. and R. Bshary (2011). "Resolving the iterated prisoner's dilemma: theory and reality." Journal of Evolutionary Biology **24**(8): 1628-1639.

Rakonjac, J. (2012). "Filamentous Bacteriophages: Biology and Applications." eLS.

Rakonjac, J., N. J. Bennett, J. Spagnuolo, D. Gagic and M. Russel (2011). "Filamentous Bacteriophage: Biology, Phage Display and Nanotechnology Applications." Current Issues in Molecular Biology **13**(2): 51-75.

Rakonjac, J., J. N. Feng and P. Model (1999). "Filamentous phage are released from the bacterial membrane by a two-step mechanism involving a short C-terminal fragment of pIII." Journal of Molecular Biology **289**(5): 1253-1265.

Rakonjac, J., M. Russel, S. Khanum, S. J. Brooke and M. Rajic (2017). "Filamentous Phage: Structure and Biology." Recombinant Antibodies for Infectious Diseases **1053**: 1-20.

Ratzke, C., J. Barrere and J. Gore (2020). "Strength of species interactions determines biodiversity and stability in microbial communities." Nature Ecology & Evolution **4**(3): 376-+.

RCoreTeam, R. (2020). R: A language and environment for statistical computing. R Foundation for Statistical Computing. Vienna, Austria. URL https://www.R-project.org/.

Redman, R. S., D. D. Dunigan and R. J. Rodriguez (2001). "Fungal symbiosis from mutualism to parasitism: who controls the outcome, host or invader?" New Phytologist **151**(3): 705-716.

Reed, T. E., R. S. Waples, D. E. Schindler, J. J. Hard and M. T. Kinnison (2010). "Phenotypic plasticity and population viability: the importance of environmental predictability." Proceedings of the Royal Society B-Biological Sciences **277**(1699): 3391-3400.

Refardt, D. and P. B. Rainey (2010). "Tuning a genetic switch: Experimental evolution and natural varaiation of prophage induction." Evolution **64**(4): 1086-1097.

Retel, C., V. Kowallik, W. Huang, B. Werner, S. Künzel, L. Becks and P. G. D. Feulner (2019). "The feedback between selection and demography shapes genomic diversity during coevolution." Science Advances **5**(10): eaax0530.

Retel, C., H. Markle, L. Becks and P. G. D. Feulner (2019). "Ecological and Evolutionary Processes Shaping Viral Genetic Diversity." Viruses-Basel **11**(3): 16.

Reusch, T. B. H. (2014). "Climate change in the oceans: evolutionary versus phenotypically plastic responses of marine animals and plants." Evolutionary Applications **7**(1): 104-122.

Reusch, T. B. H., J. Dierking, H. C. Andersson, E. Bonsdorff, J. Carstensen, M. Casini, M. Czajkowski, B. Hasler, K. Hinsby, K. Hyytiainen, K. Johannesson, S. Jomaa, V. Jormalainen, H. Kuosa, S. Kurland, L. Laikre, B. R. MacKenzie, P. Margonski, F. Melzner, D. Oesterwind, H. Ojaveer, J. C. Refsgaard, A. Sandstrom, G. Schwarz, K. Tonderski, M. Winder and M. Zandersen (2018). "The Baltic Sea as a time machine for the future coastal ocean." Science Advances **4**(5).

Rice, S. A., C. H. Tan, P. J. Mikkelsen, V. Kung, J. Woo, M. Tay, A. Hauser, D. McDougald, J. S. Webb and S. Kjelleberg (2009). "The biofilm life cycle and virulence of Pseudomonas aeruginosa are dependent on a filamentous prophage." Isme Journal **3**(3): 271-282.

Rispoli, V. F. and A. B. Wilson (2008). "Sexual size dimorphism predicts the frequency of multiple mating in the sex-role reversed pipefish Syngnathus typhle." Journal of Evolutionary Biology **21**(1): 30-38.

Rivera-Ingraham, G. A. and J. H. Lignot (2017). "Osmoregulation, bioenergetics and oxidative stress in coastal marine invertebrates: raising the questions for future research." Journal of Experimental Biology **220**(10): 1749-1760.

Rivera-Ingraham, G. A., A. Nommick, E. Blondeau-Bidet, P. Ladurner and J. H. Lignot (2016). "Salinity stress from the perspective of the energy-redox axis: Lessons from a marine intertidal flatworm." Redox Biology **10**: 53-64.

Roemhild, R., C. Barbosa, R. E. Beardmore, G. Jansen and H. Schulenburg (2015). "Temporal variation in antibiotic environments slows down resistance evolution in pathogenic Pseudomonas aeruginosa." Evolutionary Applications **8**(10): 945-955.

Rohwer, F. and R. V. Thurber (2009). "Viruses manipulate the marine environment." Nature **459**(7244): 207-212.

Rolfe, D. F. S. and G. C. Brown (1997). "Cellular energy utilization and molecular origin of standard metabolic rate in mammals." Physiological Reviews **77**(3): 731-758.

Ronkin, D., E. Seroussi, T. Nitzan, A. Doron-Faigenboim and A. Cnaani (2015). "Intestinal transcriptome analysis revealed differential salinity adaptation between two tilapiine species." Comparative Biochemistry and Physiology Part D: Genomics and Proteomics **13**: 35-43.

Roth, O., A. Beemelmanns, S. M. Barribeau and B. M. Sadd (2018). "Recent advances in vertebrate and invertebrate transgenerational immunity in the light of ecology and evolution." Heredity **121**(3): 225-238.

Roth, O., I. Keller, S. H. Landis, W. Salzburger and T. B. Reusch (2012). "Hosts are ahead in a marine host-parasite coevolutionary arms race: innate immune system adaptation in pipefish *Syngnathus typhle* against *Vibrio phylotypes*." Evolution **66**(8): 2528-2539.

Roth, O., I. Keller, S. H. Landis, W. Salzburger and T. B. H. Reusch (2012). "Host are ahead in a marine host-parasite coevolutionary arms race: innate ummune system adapatation in pipefish *Syngnathus typhle* agains *Vibrio* phylotypes." Evolution **66**(8): 2528-2539.

Roth, O. and S. H. Landis (2017). "Trans-generational plasticity in response to immune challenge is constrained by heat stress." Evolutionary Applications **10**(5): 514-528.

Roth, O., M. H. Solbakken, O. K. Tørresen, T. Bayer, M. Matschiner, H. T. Baalsrud, S. N. K. Hoff, M. S. O. Brieuc, D. Haase, R. Hanel, T. B. H. Reusch and S. Jentoft (2020). "Evolution of male pregnancy associated with remodeling of canonical vertebrate immunity in seahorses and pipefishes." Proceedings of the National Academy of Sciences **117**(17): 9431.

Roux, S., M. Krupovic, R. A. Daly, A. L. Borges, S. Nayfach, F. Schulz, A. Sharrar, P. B. M. Carnevali, J. F. Cheng, N. N. Ivanova, J. Bondy-Denomy, K. C. Wrighton, T. Woyke, A. Visel, N. C. Kyrpides and E. A. Eloe-Fadrosh (2019). "Cryptic inoviruses revealed as pervasive in bacteria and archaea across Earth's biomes." Nature Microbiology **4**(11): 1895-1906.

Roy, A. and S. Mitra (1970). "Increased fragility of *Escherichia coli* after infection with bacteriophage M13." Journal of Virology **6**(3): 333.

Russel, M. (1995). "Moving through the membrane with filamentous phages." Trends in Microbiology **3**(6): 223-228.

Ryan, F. P. (2007). "Viruses as symbionts." Symbiosis **44**(1-3): 11-21.

Sachs, J. L. and E. L. Simms (2006). "Pathways to mutualism breakdown." Trends in Ecology & Evolution **21**(10): 585-592.

Sachs, J. L., R. G. Skophammer, N. Bansal and J. E. Stajich (2014). "Evolutionary origins and diversification of proteobacterial mutualists." Proceedings of the Royal Society B-Biological Sciences **281**(1775): 9.

Santander, J. and J. Robeson (2007). "Phage-resistance of Salmonella enterica serovar Enteritidis and pathogenesis in Caenorhabditis elegans is mediated by the lipopolysaccharide." Electronic Journal of Biotechnology **10**(4): 627-632.

Sawabe, T., Y. Ogura, Y. Matsumura, G. Feng, A. R. Amin, S. Mino, S. Nakagawa, T. Sawabe, R. Kumar, Y. Fukui, M. Satomi, R. Matsushima, F. L. Thompson, B. Gomez-Gil, R. Christen, F. Maruyama, K. Kurokawa and T. Hayashi (2013). "Updating the *Vibrio* clades defined by multilocus sequence phylogeny: proposal of eight new clades, and the description of *Vibrio tritonius sp*. nov." Front Microbiol **4**: 414.

Scanlan, P. D. and A. Buckling (2012). "Co-evolution with lytic phage selects for the mucoid phenotype of Pseudomonas fluorescens SBW25." Isme Journal **6**(6): 1148-1158.

Schaarschmidt, T., E. Meyer and K. Jurss (1999). "A comparison of transport-related gill enzyme activities and tissue-specific free amino acid concentrates of Baltic Sea (brackish water) and freshwater threespine sticklebacks, Gasterosteus aculeatus, after salinity and temperature acclimation." Marine Biology **135**(4): 689-697.

Schade, F. M., M. J. Raupach and K. M. Wegner (2016). "Seasonal variation in parasite infection patterns of marine fish species from the Northern Wadden Sea in relation to interannual temperature fluctuations." Journal of Sea Research **113**: 73-84.

Schimanke, S. and H. E. M. Meier (2016). "Decadal-to-Centennial Variability of Salinity in the Baltic Sea." Journal of Climate **29**(20): 7173-7188.

Schlüter, L., K. T. Lohbeck, M. A. Gutowska, J. P. Gröger, U. Riebesell and T. B. H. Reusch (2014). "Adaptation of a globally important coccolithophore to ocean warming and acidification." Nature Climate Change **4**(11): 1024-1030.

Schneider, R. F. and A. Meyer (2017). "How plasticity, genetic assimilation and cryptic genetic variation may contribute to adaptive radiations." Molecular Ecology **26**(1): 330-350.

Scholthof, K. B. G. (2007). "The disease triangle: pathogens, the environment and society." Nature Reviews Microbiology **5**(2): 152-156.

Secor, P. R., L. A. Michaels, K. S. Smigiel, M. G. Rohani, L. K. Jennings, K. B. Hisert, A. Arrigoni, K. R. Braun, T. P. Birkland, Y. Lai, T. S. Hallstrand, P. L. Bollyky, P. K. Singh and W. C. Parks (2017). "Filamentous Bacteriophage Produced by Pseudomonas aeruginosa Alters the Inflammatory Response and Promotes Noninvasive Infection In Vivo." Infection and Immunity **85**(1).

Sen, A. and A. N. Ghosh (2005). "Physicochemical characterization of vibriophage N5." Virology Journal **2**: 4.

Shama, L. N. S. and K. M. Wegner (2014). "Grandparental effects in marine sticklebacks: transgenerational plasticity across multiple generations." Journal of Evolutionary Biology **27**(11): 2297-2307.

Shama, L. N. S. and K. M. Wegner (2014). "Grandparental effects in marine sticklebacks: transgenerational plasticity across multiple generations." Journal of Evolutionary Biology **27**(11): 2297-2307.

Shapiro, J. W. and P. E. Turner (2018). "Evolution of mutualism from parasitism in experimental virus populations." Evolution **72**(3): 707-712.

Shapiro, J. W., E. Williams and P. E. Turner (2016). "Evolution of parasitism and mutualism between filamentous phage M13 and Escherichia coli." Peerj **4**.

Shibasaki, S. (2019). "The evolutionary game of interspecific mutualism in the multi-species model." Journal of Theoretical Biology **471**: 51-58.

Shrivastava, A. and V. Gupta (2011). "Methods for the determination of limit of detection and limit of quantitation of the analytical methods." Chronicles of Young Scientists **2**(1).

Silva-Valenzuela, C. A. and A. Camilli (2019). "Niche adaptation limits bacteriophage predation of *Vibrio cholerae* in a nutrient-poor aquatic environment." Proceedings of the National Academy of Sciences: 201810138.

Singleton, F. L., R. Attwell, S. Jangi and R. R. Colwell (1982). "Effects of temperature and salinity on *Vibrio cholerae* growth." Applied and Environmental Microbiology **44**(5): 1047.

Skarlato, S. O. and I. V. Telesh (2017). "The Development of the Protistan Species-Maximum Concept for the Critical Salinity Zone." Russian Journal of Marine Biology **43**(1): 1-11.

Smith, J. M. (1964). "Group Selection and Kin Selection." Nature **201**(4924): 1145-1147.

Smith, P. A. and F. E. Romesberg (2007). "Combating bacteria and drug resistance by inhibiting mechanisms of persistence and adaptation." Nature Chemical Biology **3**(9): 549-556.

Solomon, S., G. K. Plattner, R. Knutti and P. Friedlingstein (2009). "Irreversible climate change due to carbon dioxide emissions." Proceedings of the National Academy of Sciences of the United States of America **106**(6): 1704-1709.

Stern, A. and R. Sorek (2011). "The phage-host arms race: Shaping the evolution of microbes." Bioessays **33**(1): 43-51.

Stevens, R. B. (1960). Plant Pathology, an Advanced Treatise. NY.

Stocker, R. and J. R. Seymour (2012). "Ecology and Physics of Bacterial Chemotaxis in the Ocean." Microbiology and Molecular Biology Reviews **76**(4): 792-812.

Stockwell, C. A., K. M. Purcell, M. L. Collyer and J. Janovy (2011). "Effects of Salinity on Physa acuta, the Intermediate Host for the Parasite Posthodiplostomum minimum: Implications for the Translocation of the Protected White Sands Pupfish." Transactions of the American Fisheries Society **140**(5): 1370-1374.

Stokar-Avihail, A., N. Tal, Z. Erez, A. Lopatina and R. Sorek (2019). "Widespread Utilization of Peptide Communication in Phages Infecting Soil and Pathogenic Bacteria." Cell Host & Microbe **25**(5): 746-755.e745.

Stolting, K. N. and A. B. Wilson (2007). "Male pregnancy in seahorses and pipefish: beyond the mammalian model." Bioessays **29**(9): 884-896.

Sullivan, T. J. and J. E. Neigel (2018). "Effects of temperature and salinity on prevalence and intensity of infection of blue crabs, Callinectes sapidus, by *Vibrio cholerae*, *V. parahaemolyticus*, and *V. vulnificus* in Louisiana." Journal of Invertebrate Pathology **151**: 82-90.

Sundararaman, S. A., L. J. Plenderleith, W. M. Liu, D. E. Loy, G. H. Learn, Y. Y. Li, K. S. Shaw, A. Ayouba, M. Peeters, S. Speede, G. M. Shaw, F. D. Bushman, D. Brisson, J. C. Rayner, P. M. Sharp and B. H. Hahn (2016). "Genomes of cryptic chimpanzee Plasmodium species reveal key evolutionary events leading to human malaria." Nature Communications **7**: 14.

Sunday, J. M., P. Calosi, S. Dupont, P. L. Munday, J. H. Stillman and T. B. H. Reusch (2014). "Evolution in an acidifying ocean." Trends in Ecology & Evolution **29**(2): 117-125.

Tan, D., L. Gram and M. Middelboe (2014). "Vibriophages and their interactions with the fish pathogen *Vibrio anguillarum*." Applied and environmental microbiology **80**(10): 3128-3140.

Taugbol, A., T. Arntsen, K. Ostbye and L. A. Vollestad (2014). "Small Changes in Gene Expression of Targeted Osmoregulatory Genes When Exposing Marine and Freshwater Threespine Stickleback (Gasterosteus aculeatus) to Abrupt Salinity Transfers." Plos One **9**(9): 9.

Thompson, J. N. (1999). "The evolution of species interactions." Science **284**(5423): 2116-2118.

Thompson, J. N. (2009). "The Coevolving Web of Life." American Naturalist **173**(2): 125-140.

Thrall, P. H., A. L. Laine, M. Ravensdale, A. Nemri, P. N. Dodds, L. G. Barrett and J. J. Burdon (2012). "Rapid genetic change underpins antagonistic coevolution in a natural host-pathogen metapopulation." Ecology Letters **15**(5): 425-435.

Tinsley, C. R., E. Bille and X. Nassif (2006). "Bacteriophages and pathogenicity: more than just providing a toxin?" Microbes and Infection **8**(5): 1365-1371.

Tomy, S., Y. M. Chang, Y. H. Chen, J. C. Cao, T. P. Wang and C. F. Chang (2009). "Salinity effects on the expression of osmoregulatory genes in the euryhaline black porgy Acanthopagrus schlegeli." General and Comparative Endocrinology **161**(1): 123-132.

Torda, G., J. M. Donelson, M. Aranda, D. J. Barshis, L. Bay, M. L. Berumen, D. G. Bourne, N. Cantin, S. Foret, M. Matz, D. J. Miller, A. Moya, H. M. Putnam, T. Ravasi, M. J. H. van Oppen, R. V. Thurber, J. Vidal-Dupiol, C. R. Voolstra, S. Watson, E. Whitelaw, B. L. Willis and P. L. Munday (2017). "Rapid adaptive responses to climate change in corals." Nature Climate Change **7**: 627–636.

Trivers, R. L. (1971). "The Evolution of Reciprocal Altruism." The Quarterly Review of Biology **46**(1): 35-57.

Uller, T., S. Nakagawa and S. English (2013). "Weak evidence for anticipatory parental effects in plants and animals." Journal of Evolutionary Biology **26**(10): 2161-2170.

Untergasser, A., I. Cutcutache, T. Koressaar, J. Ye, B. C. Faircloth, M. Remm and S. G. Rozen (2012). "Primer3--new capabilities and interfaces." Nucleic acids research **40**(15): e115-e115.

Urban, M. C. (2015). "Accelerating extinction risk from climate change." Science **348**(6234): 571-573.

Vandesompele, J., K. De Preter, F. Pattyn, B. Poppe, N. Van Roy, A. De Paepe and F. Speleman (2002). "Accurate normalization of real-time quantitative RT-PCR data by geometric averaging of multiple internal control genes." Genome Biology **3**(7): 12.

Vandvik, V., O. Skarpaas, K. Klanderud, R. J. Telford, A. H. Halbritter and D. E. Goldberg (2020). "Biotic rescaling reveals importance of species interactions for variation in biodiversity responses to climate change." Proceedings of the National Academy of Sciences **117**(37): 22858.

Velasco, J., C. Gutierrez-Canovas, M. Botella-Cruz, D. Sanchez-Fernandez, P. Arribas, J. A. Carbonell, A. Millan and S. Pallares (2019). "Effects of salinity changes on aquatic organisms in a multiple stressor context." Philosophical Transactions of the Royal Society B-Biological Sciences **374**(1764): 9.

Veller, C., L. K. Hayward, C. Hilbe and M. A. Nowak (2017). "The Red Queen and King in finite populations." Proceedings of the National Academy of Sciences of the United States of America **114**(27): E5396-E5405.

Velotta, J. P., J. L. Wegrzyn, S. Ginzburg, L. Kang, S. Czesny, R. J. O'Neill, S. D. McCormick, P. Michalak and E. T. Schultz (2017). "Transcriptomic imprints of adaptation to fresh water: parallel evolution of osmoregulatory gene expression in the Alewife." Molecular Ecology **26**(3): 831-848.

Vermeij, G. J. (1994). "The evolutionary interaction among species - selection, escalation, and coevolution." Annual Review of Ecology and Systematics **25**: 219-236.

Vidal-Dura, A., I. T. Burke, R. J. G. Mortimer and D. I. Stewart (2018). "Diversity patterns of benthic bacterial communities along the salinity continuum of the Humber estuary (UK)." Aquatic Microbial Ecology **81**(3): 277-291.

Vonaesch, P., M. Anderson and P. J. Sansonetti (2018). "Pathogens, microbiome and the host: emergence of the ecological Koch's postulates." FEMS Microbiology Reviews **42**(3): 273-292.

Vuorinen, I., J. Hanninen, M. Rajasilta, P. Laine, J. Eklund, F. Montesino-Pouzols, F. Corona, K. Junker, H. E. M. Meier and J. W. Dippner (2015). "Scenario simulations of future salinity and ecological consequences in the Baltic Sea and adjacent North Sea areas-implications for environmental monitoring." Ecological Indicators **50**: 196-205.

Wagner, K.-S. and J. Rajkov (2019). "Digest: Lab versus nature: Disease resistance evolution differs between environments*." Evolution **73**(12): 2540-2541.

Waldor, M. K. and J. J. Mekalanos (1996). "Lysogenic conversion by a filamentous phage encoding cholera toxin." Science **272**(5270): 1910-1914.

Waskito, L. A., J. Yih-Wu and Y. Yamaoka (2018). "The role of integrating conjugative elements in Helicobacter pylori: a review." Journal of biomedical science **25**(1): 86-86.

Wasmund, N., M. Zalewski and S. Busch (1999). "Phytoplankton in large river plumes in the Baltic Sea." Ices Journal of Marine Science **56**: 23-32.

Webb, J. S., M. Lau and S. Kjelleberg (2004). "Bacteriophage and phenotypic variation in Pseudomonas aeruginosa biofilm development." Journal of Bacteriology **186**(23): 8066-8073.

Weeks, A. R., M. Turelli, W. R. Harcombe, K. T. Reynolds and A. A. Hoffmann (2007). "From parasite to mutualist: Rapid evolution of Wolbachia in natural populations of Drosophila." Plos Biology **5**(5): 997-1005.

Wein, T., D. Romero Picazo, F. Blow, C. Woehle, E. Jami, T. B. H. Reusch, W. F. Martin and T. Dagan (2019). "Currency, Exchange, and Inheritance in the Evolution of Symbiosis." Trends in Microbiology **27**(10): 836-849.

Weitz, J. S., T. Poisot, J. R. Meyer, C. O. Flores, S. Valverde, M. B. Sullivan and M. E. Hochberg (2013). "Phage-bacteria infection networks." Trends in Microbiology **21**(2): 82-91.

Wendling, C. C., F. M. Batista and K. M. Wegner (2014). "Persistence, seasonal dynamics and pathogenic potential of *Vibrio* communities from Pacific oyster hemolymph." Plos One **9**(4).

Wendling, C. C., F. M. Batista and K. M. Wegner (2014). "Persistence, seasonal dynamics and pathogenic potential of *Vibrio* communities from Pacific oyster hemolymph." PloS one **9**(4): e94256-e94256.

Wendling, C. C., C. M. Chibani, H. Goehlich, J. Rajkov, H. Liesegang, O. Roth and B. Michael A. Rapid resistance evolution in *Vibrio* bacteria against filamentous phages.

Wendling, C. C., A. G. Fabritzek and K. M. Wegner (2017). "Population-specific genotype x genotype x environment interactions in bacterial disease of early life stages of Pacific oyster larvae." Evolutionary Applications **10**(4): 338-347.

Wendling, C. C., H. Goehlich and O. Roth (2018). "The structure of temperate phage–bacteria infection networks changes with the phylogenetic distance of the host bacteria." Biology Letters **14**(11).

Wendling, C. C., A. Piecyk, D. Refardt, C. Chibani, R. Hertel, H. Liesegang, B. Bunk, J. Overmann and O. Roth (2017). "Tripartite species interaction: eukaryotic hosts suffer more from phage susceptible than from phage resistant bacteria." BMC Evolutionary Biology **17**: 12.

Wendling, C. C., A. Piecyk, D. Refardt, C. Chibani, R. Hertel, H. Liesegang, B. Bunk, J. Overmann and O. Roth (2017). "Tripartite species interaction: eukaryotic hosts suffer more from phage susceptible than from phage resistant bacteria." BMC Evol Biol **17**(98).

Wendling, C. C., D. Refardt and A. R. Hall (2020). "Fitness benefits to bacteria of carrying prophages and prophage-encoded antibiotic-resistance genes peak in different environments." bioRxiv: 2020.2003.2013.990044.

Wendling, C. C. and K. M. Wegner (2015). "Adaptation to enemy shifts: rapid resistance evolution to local *Vibrio* spp. in invasive Pacific oysters." Proceedings of the Royal Society B-Biological Sciences **282**(1804).

West, S. A., C. El Mouden and A. Gardner (2011). "Sixteen common misconceptions about the evolution of cooperation in humans." Evolution and Human Behavior **32**(4): 231-262.

West-Eberhard, M. J. (1989). "Phenotypic plasticity and the origins of diversity." Annual Review of Ecology and Systematics **20**: 249-278.

Weynberg, K. D., C. R. Voolstra, M. J. Neave, P. Buerger and M. J. H. van Oppen (2015). "From cholera to corals: Viruses as drivers of virulence in a major coral bacterial pathogen." Scientific Reports **5**: 9.

Whitfield, A. K., M. Elliott, A. Basset, S. J. M. Blaber and R. J. West (2012). "Paradigms in estuarine ecology - A review of the Remane diagram with a suggested revised model for estuaries." Estuarine Coastal and Shelf Science **97**: 78-90.

Whittington, C. M. and C. R. Friesen (2020). "The evolution and physiology of male pregnancy in syngnathid fishes." Biological Reviews **95**(5): 1252-1272.

Wick, R. R., L. M. Judd, C. L. Gorrie and K. E. Holt (2017). "Unicycler: Resolving bacterial genome assemblies from short and long sequencing reads." Plos Computational Biology **13**(6): 22.

Wilhelm, S. W. and C. A. Suttle (1999). "Viruses and Nutrient Cycles in the Sea - Viruses play critical roles in the structure and function of aquatic food webs." Bioscience **49**(10): 781-788.

Wilson, A. B. and I. E. Veraguth (2010). "The impact of Pleistocene glaciation across the range of a widespread European coastal species." Molecular Ecology **19**(20): 4535-4553.

Wolinska, J. and K. C. King (2009). "Environment can alter selection in host–parasite interactions." (5): 236.

Wong, M. Y. L., P. M. Buston, P. L. Munday and G. P. Jones (2007). "The threat of punishment enforces peaceful cooperation and stabilizes queues in a coral-reef fish." Proceedings of the Royal Society B-Biological Sciences **274**(1613): 1093-1099.

Woolhouse, M. E. J., J. P. Webster, E. Domingo, B. Charlesworth and B. R. Levin (2002). "Biological and biomedical implications of the co-evolution of pathogens and their hosts." Nature Genetics **32**(4): 569-577.

Wright, R. C. T., M. A. Brockhurst and E. Harrison (2016). "Ecological conditions determine extinction risk in co-evolving bacteria-phage populations." Bmc Evolutionary Biology **16**: 6.

Wright, R. C. T., V. P. Friman, M. C. M. Smith and M. A. Brockhurst (2018). "Cross-resistance is modular in bacteria-phage interactions." Plos Biology **16**(10): 22.

Xie, J., L. Bu, S. Jin, X. Wang, Q. Zhao, S. Zhou and Y. Xu (2020). "Outbreak of vibriosis caused by *Vibrio harvey*i and *Vibrio alginolyticus* in farmed seahorse Hippocampus kuda in China." Aquaculture **523**: 735168.

Xue, K. S. and J. D. Bloom (2020). "Linking influenza virus evolution within and between human hosts." Virus Evolution **6**(1): 11.

Xue, K. S., L. H. Moncla, T. Bedford and J. D. Bloom (2018). "Within-Host Evolution of Human Influenza Virus." Trends in Microbiology **26**(9): 781-793.

Yamaguchi, Y., J. H. Park and M. Inouye (2011). Toxin-Antitoxin Systems in Bacteria and Archaea. Annual Review of Genetics, Vol 45. B. L. Bassler, M. Lichten and G. Schupbach. Palo Alto, Annual Reviews. **45:** 61-79.

Yamamura, N. (1993). "Vertical transmission and evolution of mutalism from parasitism." Theoretical Population Biology **44**(1): 95-109.

Youngren-Grimes, B. L., D. J. Grimes and R. R. Colwell (1988). "Growth of *Vibrio cholerae*, V*ibrio parahaemolyticus*, and *Vibrio vulnificus* Under Strict Anaerobic Conditions." Systematic and Applied Microbiology **11**(1): 13-15.

Yu, Z. C., X. L. Chen, Q. T. Shen, D. L. Zhao, B. L. Tang, H. N. Su, Z. Y. Wu, Q. L. Qin, B. B. Xie, X. Y. Zhang, Y. Yu, B. C. Zhou, B. Chen and Y. Z. Zhang (2015). "Filamentous phages prevalent in Pseudoalteromonas spp. confer properties advantageous to host survival in Arctic sea ice." Isme Journal **9**(4): 871-881.

Yuan, J. S., A. Reed, F. Chen and C. N. Stewart, Jr. (2006). "Statistical analysis of real-time PCR data." BMC bioinformatics **7**: 85-85.

Zemb, O., M. Manefield, F. Thomas and S. Jacquet (2013). "Phage adsorption to bacteria in the light of the electrostatics: A case study using E. coli, T2 and flow cytometry." Journal of Virological Methods **189**(2): 283-289.

Zug, R. and P. Hammerstein (2015). "Bad guys turned nice? A critical assessment of Wolbachia mutualisms in arthropod hosts." Biological Reviews **90**(1): 89-111.

8 | DANKSAGUNG

Mit diesen Worten geht das Abenteuer Doktorarbeit langsam zu Ende. Es war eine unglaubliche Erfahrung mit so einigen unvergesslichen Momenten. Einige werden in den kommenden Zeilen kurz angerissen, andere sind auf Fotos festgehalten oder bleiben einfach in Erinnerung.

Livi, deine Power und dein Machergeist sind einfach ansteckend. Danke für das familiäre Gefühl in deiner Arbeitsgruppe. Symbolisch dafür steht u.a. das Skypen mit Caro bei dir an einem Sonntagabend auf der Couch mit Havanna Cola in der Hand. Dazu kommen intensive Gespräche auf deinem Balkon oder an der Förde, unzählige Pipefishgangaktivitäten sowie deutliche Worte, wenn sie notwendig waren. Besonders geschätzt habe ich den immer nach vorne gerichtetem Blick! Danke auch für die gefühlt unendliche Freiheit bei der Doktorarbeit und deinen Einsatz für mein Wohlbefinden und die Setzung von Grenzen beim Fertigwerden. Deine Kommentare in Manuskripten und die Frage, warum das wichtig ist, haben so manchen Abschnitt auf ein neues Level gehoben. Danke für diese unglaubliche Erkenntnisreise auf so vielen Ebenen!

Caro, vielen Dank für die Möglichkeiten und das Vertrauen das Rapid Adaptation Projekt mit Leben zu füllen. Unvergessen bleiben meine ersten Schritte in R und das Babysitten von *Remmidemmi* bei Euch auf dem bayrischen Lande. Danke, dass du trotz Gründung einer Familie und deiner eigenen Arbeitsgruppe in Zürich immer an meiner Seite warst. Dein kritischer Blick auf die Manuskripte und die konstruktiven Comments habe ich immer sehr geschätzt, genau wie deine direkte Art und unsere Diskussionen über Definitionen, Statistik und Ergebnisse.

Hinrich, vielen Dank für die Möglichkeit meinen allerersten Doktorarbeitsvortag in deiner Arbeitsgruppe zu halten und dabei konstruktives Feedback einzusammeln. Herzlichen Dank auch für deine Zeit, diese Doktorarbeit zu begutachten und der Verteidigung beizusitzen.

Thorsten, danke für das umsichtige Leiten unserer Arbeitsgruppe und das Zusammenhalten der Fäden im Hintergrund, von denen wir gar nix mitbekommen.

Lutz, danke für dein Feedback und deine Fragen bei den TAC Meetings und die Möglichkeit vor deiner Arbeitsgruppe das Design meiner ersten Experimente vorzustellen.

Frank und **Martin,** danke dass Ihr Euch bereit erklärt habt, Mitglieder der Prüfungskommission zu sein und mit euren herausfordernden Fragen wichtige Aspekte beleuchtet und neue Denkansätze gegeben habt.

Kim 🥕**,** es war mir eine Freude dich auf dem Weg deines wissenschaftlichen Aufstiegs zu begleiten: von der frechen und fleißigen Praktikantin über den Status des energie-geladenen *Elite Hiwis* und des sagenhaften *Science Knights* bis hin zur selbständig Wissen schaffenden Doktorandin. Vielen Dank, dass du deinen Schlaf, deine Seele und Sachgegenstände, wie Schuhe und Telefon geopfert hast, um die Experimente zum Erfolg zu führen. Deine Powermusik, positive Energie und reichhaltige Nahrung haben mich in den Labornächten am Leben gehalten und die Roadtrips zu einem Erlebnis werden lassen. Danke, dass du mir aufgezeigt hast, wenn „noch Luft nach oben war“ und du dir die Mühe gemacht hast, „mal drüber nachzudenken“ bis der Endboss kommt... und für die Fitnesseinheiten in der Coronazeit.

Katja, aka *The Maschine*, deine Unterstützung bei der Vorbereitung und Durchführung des Evolutionsexperiments war von unschätzbarem Wert. Vielen Dank für das unermüdliche Pipettieren von unsichtbaren Flüssigkeitsmengen, dein Durchhaltevermögen, dein kritisches Hinterfragen sowie die gute Laune bleiben unvergessen. **Véro**, vielen Dank, dass Du genauso akribisch und zuverlässig die Akkordarbeit im Verlaufe des Evolutionsexperiments übernommen hast.

Kosmas, Melanie & Véro, danke, dass ihr mich in eure Bürofamilie aufgenommen habt, obwohl ich viele Stunden im Doktorandenauffanglager verbracht habe. Danke, für die wissenschaftlichen Diskussionen, Feedback zu und Statistiksessions, das Schmackhaft machen von Kaffee und das Teilen von Obst- und Schokoladungen! **Kosmas**, deine kleinen und großen R Hacks haben mir so einige graue Haare erspart und waren die Grundlage für den ein oder anderen wundervollen Plot. **Mela,** die Diskussion mit dir über lineare Modelle und last Minute Feedback zur Doktorarbeit waren von unschätzbarem Wert.

Das nächste Dankeschön geht an die Doktoranden Familienmitglieder außerhalb des Büros. **Agnes, Felix, Lara, Jamie, Kim, Burkard, Luisa, Janina, Andrea, Isa, Philipp, Marie, Tobi, Hanna, Anabel, Isabel, Thea** und **Kwi**. Danke für die vielen gemeinsamen Stunden auf dem Dach, an der Förde, beim Basteln von Doktorhüten, wissenschaftlichen Austausch und Verbreitung von positiver Energie.

Ein dickes Dankeschön geht auch an alle weiteren Phage-*Vibrio*-Pipefishgang Mitglieder, insbesondere an alle, die tatkräftig bei der Feld- und Laborarbeit mit angepackt haben. **Kristina, Andreas,** aka *Der Ösi*, **Janina**, **Maude**, **Angela**, **Gordon, Kaja, Anna, Merle, Julia S.** und **Linda** eure Unterstützung beim Sammeln von Daten, bei der Fisch- und Bakterienpflege waren wichtige Bausteine und Grundlage für die Doktorarbeit.

Till, danke für die Versorgung mit selbstgebackenen Spezialitäten, für technische Kreativität und codierte Lösungen in allen Lebenslagen.

Isabel, danke für die meisterhafte Einführung in die Welt der Flowcytometrie und der Fluidgm chips und deine Unterstützung beim Auseinandernehmen der Fische.

Agnes, danke für das Überlassen der supersauber Tubes und edlen Pipetten für die Fluidigmchips, vielen intensive Gespräche über die Wissenschaft und das Leben sowie die Freundschaftsyogastunden in den wundervollen Räumen von *Yoga in Kiel*.

Felix, du bist einfach ein Mann für alle Fälle! Danke für deinen ansteckenden, pragmatischen Machergeist, die Möglichkeit hinter der Trave der Welt zu entfliehen und deine selbstgemachten Köstlichkeiten.

Alba, muchas gracias for the nice drawings of our study organisms. They make every presentation and this PhD thesis prettier and more vivid.

Thanks a lot also to all the members of the PhD center! **Richard**, **Isabel**, **Filipa, Atul, Mingshuang, Marie, Ross & Lei** for chocolate & scientific exchange as well as relaxing moments on the balcony.

Ein weiter Dank geht an die Göttinger Fraktion. **Robert Hertel,** dass du mich auf meinen ersten Laborschritten in der mikrobiellen Welt begleitet hast. **Cynthia Chibani & Heiko Liesegang** danke für euren Einsatz beim Entschlüsseln des Genoms unserer Bakterien und Phagen. Danke auch für spannende Diskussionen, Feedback und die Übersetzung des bioinformatischen Codes in die Sprache von normal sterblichen Biologen.

Michael, vielen Dank für die Erstellung der mathematischen Modelle für das Evoultionsexperiment und deine für normalsterbliche Biologen verständlichen Erklärungen.

Thanks goes to the **Hentschel group** for support in machine and manpower. Especially to **Julia Böge** for the flow cytometer magic and your enthusiastic help with the fluidigm chips, **Christina Bayer** for last minute help and to **Martin Jahn** for taking pictures of the *Vibrio* bacteria and lively discussions and feedback on the discussion of the PhD.

Mareike and **Jelena**, thanks a lot for taking over this fascinating project and helping me to get the last practical steps done. Seeing the project in your hands gives me a good gut feeling to move on to the next challenge.
Diana, danke, dass du immer da warst, wenn es im Labor gebrannt oder mein Kopf geraucht hat. Dein Verständnis für Materialschlachten, deine detektivischen Fähigkeiten beim Finden von Reagenzien sowie dein Einsatz beim Pipettenspitzenwettstecken waren von unschätzbarem Wert.

Fabian, ohne dein Wissen über die Fische, Aquarien- und Filtersysteme, dein Humor und die Engelsgeduld hätten die Fische und ich nur halb so viel Freude gehabt. Vielen Dank dafür!

Svend & Conny, vielen Dank, dass ihr die nötige Infrastruktur bereitstellt sowie die Bürokratie übernehmt. Euer Einsatz und eure Geduld im Umgang mit den ständig neuen Herausforderungen und den besonderen Charakteren der Wissenschaftler ist bewundernswert.

Astrid, es war mir immer eine Freude, bei dir Fahrten zu buchen. Genauso groß war allerdings auch die Angst, dass das Fahrtenbuch nicht richtig ausgefüllt sein könnte. Danke, dass Du bei allen Herausforderungen dein Bestes gegeben hast. Egal, ob beim Verschicken von gekühlten Last-minute Paketen, der Suche nach verlorenen CDs oder beim Ausfüllen von Zettelkram.

Cas and **Conny**, thanks a lot for your resonating positive vibes and last-minute feedback on parts of the PhD thesis.

I also want to thank my previous mentors **Ulf Karsten**, **Martin Thiel**, **Jürgen Laudien**, **Joost den Haan**, **Hannah Brocke** and **Michele Pierotti** for their encouragement to peruse a career in science, for sharing their passion for research and being inspiring role models.

Thanks a lot to the Integrated School of Ocean Sciences (ISOS), International Max Planck Research School (IMPRS), the Graduate Center of Kiel University and the DFG for funding, career support and organization of courses.

Thanks a lot **Alexandra Elbakyan's** for you fight for open access to publications. Your life work Sci Hub (https://sci-hub.tw/) was a salvation whenever paper were not available.

Lisa Hentschel & **Familie,** ein ganz herzliches Dankeschön für die Möglichkeit in euerm Haus am Meer abzuschalten und die Seele baumeln zu lassen. Besonders in der Corona Zeit, war die Möglichkeit isoliert an der Doktorarbeit zu schreiben von unschätzbarem Wert. Unzählige Sonnenuntergänge, Baden im Meer von April bis Juni und Skypemeetings auf dem Balkon werden noch lange in Erinnerung bleiben.

Hannes, Paul & **Thomas**, vielen Dank, dass ihr mich ab und zu aus der Doktorarbeitswelt zurück in die Realität geworfen habt, jederzeit ein offenes Ohr hattet und mich auf den Höhen und Tiefen der Abenteuerreise begleitet habt.

Liebe **Eltern**, lieber **Julian**, eure Zuversicht und euer unverwüstlicher Optimismus in allen Lebenslagen vor, während und nach der Doktorarbeit geben mir die Kraft meine Ziele zu erreichen, auch wenn sie manchmal mit einigen Umwegen verbunden sind.

Mia cara **bellissima**, grazie per la tua infinita energia positiva e per la ferma convinzione che i tuoi scimmi completeranno con successo la tesi. Bacione!

9 | EIDESTATTLICHE ERKLÄRUNG

Hiermit bestätige ich, Henry Göhlich, dass die vorliegende Dissertation:

von mir, unter Beratung meiner Betreuer, selbstständig verfasst wurde, nach Inhalt und Form meine eigene Arbeit ist und keine weiteren Quellen und Hilfsmittel als die angegebenen verwendet wurden.

Die vorliegende Arbeit ist unter Einhaltung der Regeln guter wissenschaftlicher Praxis der Deutschen Forschungsgemeinschaft entstanden und wurde weder im Rahmen eines Prüfungsverfahrens an anderer Stelle vorgelegt noch veröffentlicht. Veröffentlichte oder zur Veröffentlichung eingereichte Manuskripte wurden kenntlich gemacht.

Ich erkläre mich einverstanden, dass diese Dissertation an die Bibliothek des GEOMAR Helmholtz Zentrum für Ozeanforschung Kiel und die Universitätsbibliothek der Christian-Albrechts-Universität zu Kiel weitergeleitet wird.

Der wissenschaftliche Grad wurde nicht entzogen.

Kiel, Dezember 2020 ……..……...

Henry Göhlich

10 | DECLARATION OF CONTRIBUTION

Chapter I

Idea:
Carolin C. Wendling

Data acquisition:
Henry Göhlich, Carolin C. Wendling

Data interpretation and manuscript preparation:
Carolin C. Wendling analyzed the data and wrote the paper with support from **Henry Göhlich** and Olivia Roth

Chapter II

Idea:
Henry Göhlich, Carolin C. Wendling, Olivia Roth,

Data acquisition:
Henry Göhlich conducted the experiment

Data interpretation and manuscript preparation:
Henry Göhlich analyzed the data and wrote the manuscript with support from Carolin C. Wendling and Olivia Roth.

Chapter III

Idea:
Henry Göhlich, Olivia Roth, Carolin C. Wendling

Data acquisition:
Henry Göhlich conducted the evolution experiment with support from Katja Trübenbach and Véronique Merten. **Henry Göhlich** did the follow up assays with the help of Véronique Mertens and Kim-Sara Wagner. Cynthia Chibani, Heiko Liesegang and Jelena Rajkov analysed the genomic data. Michael Sieber made the mathematical model with support from **Henry Göhlich** and Carolin Wendling.

Data interpretation and manuscript preparation:
Henry Göhlich analyzed the data and wrote the paper with support from Carolin C. Wendling, Olivia Roth and Michael Sieber.

Chapter IV

Idea:
Henry Göhlich, Olivia Roth

Data acquisition:
Henry Göhlich, Olivia Roth and Kim-Sara Wagner collected fish in the field, conducted the experiment and sampled the fish. Linda Sartoris and Olivia Roth designed the primer. **Henry Göhlich**, Linda Sartoris, Kim-Sara Wagner did the molecular lab work.

Data interpretation and manuscript preparation:
Henry Göhlich, Linda Sartoris, Olivia Roth and Kim-Sara Wagner analyzed the data. **Henry Göhlich** wrote the manuscript with input from all other authors.